Durham E-Theses

Assessing glacier retreat and landform production at the 'debris-charged' snout of Kvíárjökull, Iceland

BENNETT, GEORGINA,LUCY

How to cite:

BENNETT, GEORGINA,LUCY (2010) *Assessing glacier retreat and landform production at the 'debris-charged' snout of Kvíárjökull, Iceland*, Durham theses, Durham University. Available at Durham E-Theses Online: http://etheses.dur.ac.uk/110/

Assessing glacier retreat and landform production at the 'debris-charged' snout of Kvíárjökull, Iceland

Georgina Lucy Bennett

Iceland is a critical location for the study of glacier fluctuations and landform production in response to climate change due to its diverse glacial legacy and its archive of aerial photographs that provide accurately dated records of glacier retreat and landform evolution from 1945. This study focuses on Kvíárjökull, an outlet glacier of the Öræfajökull ice cap in southeast Iceland, recently classified as a 'debris-charged glacier landsystem'. Digital photogrammetry was applied on five sets of aerial photographs from 1945 to 2003 in order to produce Digital Elevation Models from which measurements of morphometric change within the glacier snout and foreland were made. This analysis was combined with field assessments and geomorphological mapping to investigate the evolution of landforms from complex debris transport pathways and the impact of ice marginal dynamics on moraine evolution.

The temporal pattern of retreat of Kvíárjökull correlates with fluctuations in air temperature with a lag of about 10 years compared to other Icelandic glaciers. Ice-marginal pushing during lateral fluctuations of the snout results in the construction of push moraine ridges and the destruction of controlled moraine derived from englacial debris concentrations. Accelerated snout retreat between 1998 and 2003 exceeded the rate of increase in air temperature and is attributed to the growth of proglacial and supraglacial lakes associated with high rates of backwasting. Backwasting of ice cores consumes ridges of high relief, thus, reducing the preservation of controlled moraine ridges. A model for the de-icing of ice-cored moraines is presented in which ice-cores remain in the landscape for up to 83 years after detachment from the glacier snout.

A debris-charged glacier landsystem model is presented in which hummocky moraine complexes comprise three process-sediment-landform associations: chaotic hummocky moraine, with minor elements of linearity resulting from the stagnation of controlled moraine; heavily channelized moraine complexes; and, most prevalent, discontinuous push moraine ridges formed during ice-marginal pushing. A time series of five 1:10,000 geomorphological maps illustrates the evolution of this landsystem and provides an unprecedented record of cryospheric change.

Assessing glacier retreat and landform production at the 'debris-charged' snout of Kvíárjökull, Iceland

Georgina Lucy Bennett

A thesis submitted for the degree of

Master of Science

Department of Geography

Durham University

January 2010

Contents

List of Figures

Fig 2.5 - Schematic model of seasonal push moraine formation at the glacier margin developed by Evans and Hiemstra (2005) based on four Icelandic glaciers. "(1) Situation in late summer at typical Icelandic glacier snout where subglacial processes include lodgement and sliding (A), bedrock and sediment plucking (B), subglacial deformation (C) and ice keel ploughing (D) in a temporally and spatially evolving process mosaic. (2) During early winter, the thin part of the glacier snout freezes onto part of the subglacial till. The till slab that freezes onto the ice sole is likely to be from the more porous A horizon (A). (3) The later winter readvance initiates failure along a decollement plane within the A horizon or at the junction with the more compact B horizon, resulting in the carriage of A horizon till onto the proximal side of the previous year's push moraine. (4) In the early summer, the melt-out of the till slab (A) initiates porewater migration, water escape and sediment flow (small arrows) and sediment extrusion due to glaciostatic and glaciodynamic stresses. (5) The late summer situation

List of Tables

Declaration of Copyright

I confirm that no part of the material presented in this thesis has previously been submitted by me or any other person for a degree in this or any other university. In all cases, where it is relevant, material from the work of others has been acknowledged.

Georgina Lucy Bennett

Department of Geography
Durham University

January 2010

Acknowledgements

1 Introduction, aims and objectives

1.1 Introduction

Glaciers are a key link in the research interface between glacial geomorphology and climatology. The majority of glaciers worldwide have been steadily retreating in response to global warming following the 19th century maximum of the Little Ice Age (LIA) (Grove, 1988) providing an excellent field laboratory in which to investigate the evolution of glacial landforms over short to medium timescales. In modern times, continued global warming has resulted in vast changes on and around glacier snouts (e.g. Etzelmüller 2000; Etzelmüller et al. 2000; Lukas et al. 2005), leading to unprecedented, and in some settings catastrophic, landform collapse and sediment and melt-water mobilization such as glacial lake outburst floods (GLOF's; Nakawo et al. 2000). Furthermore, the cumulative ice loss from the retreat of small glaciers, particularly within the climatically sensitive Arctic region, is expected to make the greatest contribution to sea level rise over the next century, a global hazard of increasing concern (Meier, 1984). For many glaciated regions of the world aerial photographs have been systematically and routinely collected for over half a century thus providing accurately dated records of glacier retreat and ice-cored landform evolution. Recently, the development of sophisticated mapping techniques such as digital photogrammetry has facilitated the quantification of historical changes in glacier snouts and their associated proglacial forelands from historical aerial photograph archives (e.g. Sletten et al. 2001; Lyså & Lønne 2001; Evans & Twigg 2002; Schomacker & Kjær 2007; Fox and Czifersky, 2008). This has allowed scientists to make more accurate, systematic assessments of: a) glacier-climate interactions, rates of glacier retreat and landform de-icing rates; b) glacial process-form relationships; and c) to extend the archive of existing records of glacier retreat. This study addresses each of these themes through the three dimensional modeling and mapping of a glacier snout and foreland in southeast Iceland, where repeated aerial imagery since 1945 facilitates a comprehensive assessment of a rapidly retreating debris-charged ice mass and its associated geomorphology.

1.2 Glacier-climate interactions, rates of glacier retreat and landform de-icing

Glaciers are considered to be one of the most reliable and clear indicators of climate change (e.g. Houghton et al., 1996). They integrate the factors of summer temperature and winter precipitation over large, often mountainous areas, whereas meteorological data is restricted to a single point in space and is often not available for mountainous areas where glaciers are common at all latitudes (Jóhannesson and Sigurdsson, 1998). Observing glacier fluctuation is thus seen as a critical indicator of climate change and furthermore helps to quantify the contribution of glaciers to global sea level rise (Pope et al., 2007).

Icelandic lowland glaciers are typically 'active temperate' owing to their seasonally responsive wet based regime and therefore produce a landform-sediment record that reflects a regional decadal to annual palaeo-climatic signal (Boulton, 1986; Evans, 2003). They therefore serve as good climate records both in terms of variations in ice volume and their landform sediment record. The glacier monitoring programme in Iceland that was started in 1930 has observed that glacial termini variations of outlet glaciers of various sizes have reflected major variations in climate during the last century (Sigurdsson et al., 2007). The generation of digital elevation models (DEMs) from aerial photographs is crucial in extending this record of glacier fluctuations (e.g. Etzelmüller and Sollid, 1997). Sequential DEMs are a vital tool for monitoring glacier surface change, providing an assessment of long-term surface change of glaciers that have never been the subject of long term mass balance studies

Current assessments of global glacier decay focus mainly on ice sheets and non-debris-covered glaciers and associated sea-level rise (e.g. Thomas et al., 2004; Alley et al., 2005; Zwally et al., 2005). Relatively little is known about the effects of a warmer climate on debris-covered and partially debris-covered glaciers and associated dead-ice forelands (Schomacker, 2008). Debris-covered glaciers constitute large proportions of glaciated areas particularly in mountainous regions such as the Himalaya (e.g. Takeuchi et al., 2000), European Alps (D'Agata and Zanutta, 2005; Deline, 2005; Kellerer-Pirklbauer et al., 2008) and Southern Alps of New Zealand (Kirkbride, 1995;

Kirkbride and Warren, 1999; Shulmeister et al., 2009). In many of these regions, the melt-out of debris-covered glaciers and ice-cored moraines create hazards in the form of GLOFs (Clague and Evans, 2000; Nakawo et al. 2000). These typically occur when water dammed behind ice-cored landforms at the glacier snout is released at high pressure under, over, or through the ice-dam with destructive force. Quantitative assessments of the long-term evolution of ice-cored landforms at a debris-charged glacier are needed to further understanding of potential hazards such as GLOFs that may arise from the melting of dead-ice.

The most recent addition to a series of glacier landsystems identified within Iceland is the 'debris-charged glacier' (Evans, 2005) with characteristics of more widely reported 'debris-covered' glaciers (Nakawo et al., 2000). This study furthers understanding of glacier-climate interactions at Kvíárjökull, an outlet glacier of the Öræfajökull ice-cap in southeast Iceland, which is the type-site for the 'debris-charged' glacier (Spedding and Evans, 2002).

1.3 Glacial process-form relationships

Glacier recession has uncovered '*a wealth of sedimentological and geomorphological detail*' within glacier forelands (Evans et al., 1999) thus creating the unique opportunity to link landforms to the climatic and glaciological regime and to increase understanding of links between glacier dynamics and ice-marginal deposition (e.g. Clayton and Moran, 1974; Boulton, 1986; Krüger, 1994; Kjær and Krüger, 2001). Much of this research has focused on establishing process-form relationships at retreating glacier margins (e.g. Krüger, 1994; Evans and Rea, 1999; Evans et al., 1999a) and differentiating glacial terrain through the identification of characteristic suites of landforms and sediments, indicative of specific glacier dynamics and topography, through 'landsystems' (Evans, 2005). The establishment of process-sediment-form relationships and landsystems models at modern Icelandic glaciers has aided assessments of the genesis of landform-sediment assemblages at other glaciers and particularly in the ancient terrestrial glacial record (Boulton and Paul, 1976; Boulton and Eyles, 1979; Eyles, 1983a, b; Benn and Evans, 1998; Evans and Rea, 1999; Evans et al., 1999a; Evans, 2003). The accuracy of reconstructions of palaeo-ice dynamics and

palaeo-climate are dependent on the continual development and refinement of contemporary analogues based on well defined process-form relationships (e.g. Krüger, 1994; Evans and Twigg, 2002).

A number of well-established landsystem models are based on Icelandic glaciers: the plateau ice-field, lowland surging and active temperate (or plateau piedmont) landsystem types (Evans, 2005). Exemplar glaciers of these three landsystem types have been mapped previously as part of a long term surveying and landsystems research programme being conducted by Dr David Evans of Durham University and Dr David Twigg of Loughborough University: Breiðamerkurjökull (active temperate/lowland piedmont) (Evans and Twigg, 2002), þórisjökull (plateau ice field) (Evans et al., 2006a), Tungnaárjökull (plateau ice field) (Evans et al. 2006b) and Brúarjökull (surging glacier) (Evans et al., 2007). These maps provide historical records of glacier retreat and illustrate characteristic landform assemblages. As such they are useful for the visualization of landsystems and reconstructions of ancient glaciated terrain.

The most recent addition to the landsystems models is the 'debris-charged glacier landsystem' (Evans, 2005) based on studies of Kvíárjökull by Spedding and Evans (2002). It is differentiated from the other landsystems based principally on its high debris turnover and 'debris-charged' snout. Supraglacial debris may accumulate from different processes and sediment sources, such as thrusting of subglacial material (Hambrey et al., 1999; Krüger and Aber, 1999; Glasser and Hambrey, 2002; Swift et al., 2006), melt-out of englacial debris bands (Kirkbride and Spedding, 1996; Hambrey et al., 1999; Spedding and Evans, 2002), channel-, and tunnel-fill material (Kirkbride and Spedding, 1996; Spedding and Evans, 2002), crevasse-squeezing of subglacial sediment (Johnson, 1975), meltwater bursts through the crevasse and conduit system (Naslund and Hassinen, 1996; Krüger and Aber, 1999; Roberts et al., 2000); rockfall from surrounding rock walls (Eyles, 1979; 1983a,b,c), or aeolian deposition directly on the glacier surface (Kirkbride, 1995; Krüger and Aber, 1999). The nature and distribution of the debris reflects the sediment source and influences the subsequent modification of the snout by resedimentation (Spedding and Evans, 2002; Evans, 2009).

However, despite the numerous conceptual process-sediment-landform models for the melt-out of debris-covered ice, few quantitative studies of dead-ice melting and moraine evolution associated with glacier retreat of a debris-covered/charged glacier have been carried out (e.g. Østrem, 1959; Pickard, 1984; Bennett et al., 2000; Etzelmüller, 2000; Krüger and Kjær, 2000; Schomacker and Kjær, 2007). Schomacker (2008) proposes that a major challenge for future explorations of dead-ice environments is to obtain long-term records of melt progression, either by repetitive field based monitoring or by remote sensing. Process-form relationships of the evolution of a 'debris-charged' snout into moraine remain unrefined (e.g. Spedding and Evans, 2002; Swift et al., 2006; Evans, 2005, 2009) and at present the landsystem archive lacks a map and a definitive landsystem model of an exemplar glacier of the 'debris-charged' glacier landsystem.

1.4 Aerial photography – an underutilised resource

For much of Iceland there is a large and underutilised historical archive of aerial photography dating back to 1945 and thereby recording temporal evolution of a glacial landscape through the historical period of global warming (e.g. Fig 1.1). This archive is effectively a 'time capsule' of potential three dimensional glacier change measurements (Fox and Cziferszky, 2008). Photogrammetry is a well established technique used by geomorphologists to record topography retrospectively from aerial photographs. The recent automation of photogrammetry has greatly increased the efficiency and ease of terrain model extraction from stereophotography (Baily et al., 2003). A number of studies have demonstrated the potential for using digital photogrammetry to convert long archives of photographs into Digital Elevation Models (DEMs) and to use these to quantify long term morphometric changes in a proglacial setting (e.g. Etzelmüller and Sollid, 1997; Fox and Cziferszky, 2008). Icelandic glaciers are prime subjects for the assessment of glacier retreat and landform de-icing rates associated with climate change and the production of time series of maps to serve as cryospheric climate records and analogues for deglaciated forelands around the world. As yet only for Breiðamerkurjökull does a *time series* of maps exist. Detailed maps for 1945 and 1965 (Howarth and Welch, 1969a,b) and for 1998 (Evans and Twigg, 2002), provide 'snapshots' in time that document the evolution of the glacial foreland

following ice retreat after the Little Ice Age and provide an unrivalled historical record of cryospheric responses to climate change.
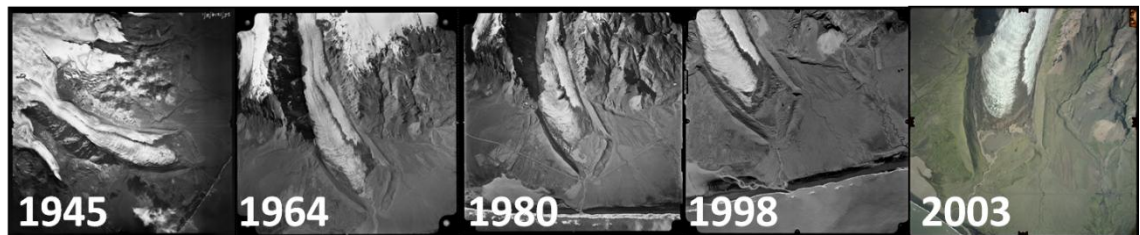
Fig 1.1- Filmstrip of a sample of aerial photographs from the archive of Kvíárjökull

1.5 Aims and Objectives

In view of these wider themes, the overarching aim of this research is to apply digital photogrammetry to convert a historical archive of medium scale aerial photographs into DEMs from which to reconstruct morphometric change occurring within the debris-charged glacial snout and foreland of Kvíárjökull.

1.5.1 Aims

a. Evaluate the links between climate fluctuations, glacier snout fluctuations and landform evolution at a 'debris-charged' glacier.
b. Quantify the de-icing progression of ice-cored landforms in a temperate, maritime climate.
c. Evaluate process-sediment-form relationships in the genesis of hummocky moraine complexes from debris-covered ice.
d. Conduct a reassessment of the landsystem models applied to Kvíárjökull, specifically the 'glaciated valley landsystem' model proposed by Eyles (1983b) and 'debris-charged landsystem' of Evans (2005).

1.5.2 Objectives

a. To establish correlations between glacier snout fluctuations and climate fluctuations, known from meteorological records, so as to establish the climatic signal contained within the landform record.

b. To produce a model of de-icing progression of ice-cored landforms in a temperate, maritime climate.

c. To produce a time series of detailed geomorphological maps of Kvíárjökull documenting the retreat of the glacier and associated changes in the glacier surface, as well as the evolution of the glacial geomorphology within the glacier foreland.

d. To produce a landsystem model for the 'debris-charged landsystem'.

2 Literature review

2.1 Climate-ice interactions

Several studies have correlated Icelandic glacier fluctuations with fluctuations in climate. Jóhannesson and Sigurdsson (1998) and Sigurdsson et al. (2007) inferred trends in Icelandic glacier behaviour in the 20th century to be primarily controlled by variations in summer temperature. According to their mass-balance measurements, variations in summer balance were much greater than those in winter, signifying the importance of summer temperature in the annual mass balance (Sigurdsson et al., 2007). Jóhannesson and Sigurdsson (1998) attributed the extensive rapid glacier retreat that occurred from 1931 to 1960 across Iceland (Fig 2.1) to high summer temperatures in the decades after 1930, and the slowing of this retreat and reversal of the trend of glacier retreat to advance between 1965 and 1970 to climate cooling. Furthermore, they related the timing of the maximum number of advancing glaciers in their sample between 1975 and 1990 to the timing of minimum summer temperature around 1980 (Fig 2.1).
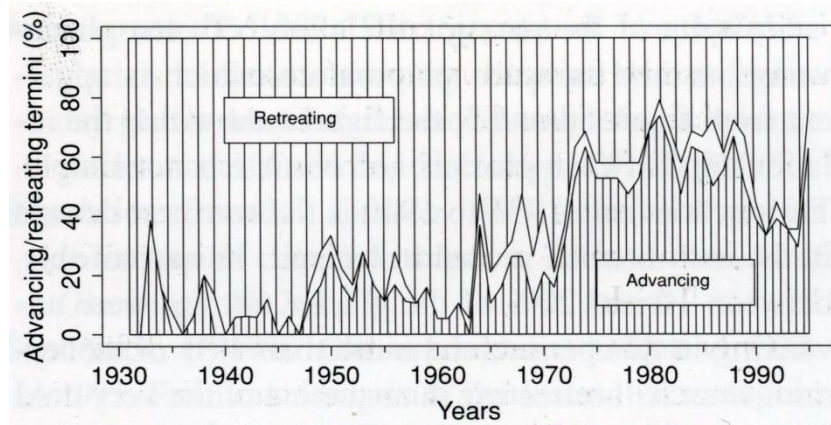
Fig 2.1 - Proportion of advancing and retreating termini of non-surging glaciers in Iceland between 1930/31 to 1994/95. No shading indicates stationary termini. Based on 18 termini. (Source: Jóhannesson and Sigurdsson, 1998).

Despite a rise in temperatures from the mid 1980s, many glaciers continued to advance into the 1990s (Sigurdsson et al., 2007) (Fig 2.1). Iceland is one of the few regions of the world where glaciers were advancing at the end of the 20th century (Dowdeswell et al., 1997). Other regions in which recent glacier advance has been recorded include maritime western Scandinavia (Winkler et al., 1997) and the Southern Alps of New Zealand (Chinn, 1999), suggesting that climate forcing unique to maritime settings may be responsible for this anomalous glacier behaviour. It has been demonstrated that maritime glaciers with higher mass turnovers, such as Kvíárjökull, are more sensitive to fluctuations in precipitation than continental glaciers with low mass turnovers (Nesje et al., 2000; Oerlemans and Reichert, 2000). As such, glacier response to global warming at maritime glaciers is complicated by the influence of ocean-atmospheric oscillations (Nesje et al., 2000; Chinn et al., 2005), such as the North Atlantic Oscillation (NAO), which has been demonstrated to modulate precipitation and temperature in the North Atlantic region, particularly within maritime settings (Nesje et al., 2000). Chinn et al. (2005) suggest that Norway may be considered an example of how global warming can lead to glacier advance, provided that air temperatures do not exceed a critical threshold.

Glacier-climate interactions are further complicated by a number of variables unique to a glacier meaning that climate fluctuations have a delayed impact on snout geometry. The time taken for a glacier to adjust its geometry to a change in mass balance is known as its 'response time' (Jóhannesson et al., 1989; Oerlemans, 2001). Glaciers in the same region may not respond to climate fluctuations synchronously due to their differing response times. Indeed, the response of Icelandic glaciers to fluctuations in air temperature during the 19th century was not synchronous. While 1931 to 1940 was the warmest decade in the instrumental record in Iceland, between 10 and 20% of glacier termini in a sample of 18 glaciers throughout Iceland were advancing in this period (Fig 2.1). Furthermore, more than 40% were still retreating during the very cold summers between 1970 and 1980 (Jóhannesson and Sigurdsson, 1998).

There is still uncertainty regarding the relative importance of air temperature and precipitation variations and the NAO in controlling glacier mass balance and behaviour

in Iceland (Bradwell et al., 2006). The Nordic project Climate and Energy has predicted a warming of 2.8°C by 2071-2100 within the Arctic region (Jóhannesson et al, 2007). Under this scenario the ice cap of Vatnajökull in southern Iceland is predicted to lose 25% of its present volume within half a century (Björnsson and Pálsson, 2008). Long term climate records demonstrate that annual precipitation is increasing with air temperature, particularly in maritime climates (Hanna et al., 2004). The Nordic project Climate and Energy predicts a 6% increase in precipitation by 2071-2100, compared with 1961-1990 levels, associated with 2.8°C of warming (Jóhannesson et al., 2007). It is important to understand how maritime glaciers respond to increases in precipitation relative to temperature so as not to overestimate future glacier ice loss and sea level rise. Ultimately more research is needed on glacier-climate interactions in order to separate the effects of different climatic variables on glacier behaviour within this climatically sensitive region (Bradwell et al., 2006).

2.2 Non-climatic controls on glacier fluctuations

There are several factors other than climate that may disrupt glacier variations and explain the non-synchrony of Icelandic glacier retreat. The most documented is surging, which is dependent on internal glacial forcing rather than external climate forcing. For this reason surging glaciers are excluded from studies on climate induced glacier retreat (Jóhannesson and Sigurdsson, 1992). Other significant factors include geothermal activity (Sturm et al., 1991), proglacial lakes (Sturm et al., 1991; Kirkbride and Warren, 1999), debris on the glacier surface (Kirkbride and Warren, 1999; Kellerer-Pirklbauer et al., 2008) and large rockfalls (Gardner and Hewitt, 1990; Hewitt, 2009; Shulmeister et al., 2009).

The presence of a layer of debris on the glacier surface may influence ablation rates in two ways. Ablation rates may increase with thin debris cover due to decreased albedo compared to the surrounding clean ice. However, above 1 – 2cm in thickness, the debris layer may reduce ablation of underlying ice by protecting it from insolation and radiation (e.g. Mattson et al., 1993; Benn and Evans, 1998: 72-73; Kellerer-Pirklbauer et al., 2008). Debris-covered glaciers may therefore have a muted, delayed or non-existent response to climate forcing, depending on the magnitude and frequency of

that forcing (Thomsen et al., 2000). Studies of partially debris-covered glaciers have found that the insulative properties of a supraglacial debris mantle can have a dramatic effect on the glacier surface velocity, slope and ice thickness (e.g. Kirkbride and Warren, 1999; Thomsen et al., 2000) and that the climatic response of adjacent clean and debris-covered zones of a glacier therefore may differ (e.g. Pelto, 2000; Takaeuchi et al., 2000; Thomsen et al., 2000; Kellerer-Pirklbauer et al., 2008). Debris-covered glacier dynamics are predominantly controlled by the ratio of the supply of debris to the supply of ice at the glacier snout (Shroder et al., 2000; Benn et al., 2003). Glaciers with a high ratio form extensive debris-covers and respond to climate change by thickening and thinning, as lateral movement of their snouts is restricted by the insulative debris cover (Kirkbride, 2000). Conversely, at glaciers with a low ratio, which may either result from a low supply of debris or supply of ice that compensates for a high supply of debris, debris does not accumulate supraglacially but is deposited at the margin. Such glaciers may respond to climate change by frontal advance and retreat, unless constrained by topography or large lateral moraines (Benn et al., 2003).

Landform production and consequently the strength of the climatic signal within the landform record at debris-covered glacier margins is therefore variable, depending both on the ratio of the supply of debris to the supply of ice and the efficiency of the sediment transfer from the glacier margin into the foreland by the glacifluvial system (Benn et al., 2003). Benn et al. (2003) developed a series of conceptual models of landsystem development at valley glaciers associated with the controls on landform production aforementioned (Fig 2.2a-d). Glacier snouts with a large supraglacial debris-cover and inefficient sediment transfer away from the margin stagnate and downwaste to form large tracts of 'hummocky' moraine (Fig 2.2a). Sissons (1974a,b, 1977) interpreted these landforms as the products of widespread glacier stagnation at the termination of the Loch Lomond (Younger Dryas) Stade. Conversely, moraine formation at glacier margins with a limited debris cover involves one or more processes, including pushing, dumping of supraglacial debris, and, if fine-grained saturated sediment is present at the margin, squeezing (Benn and Evans, 1998) and contains a clear climatic signal related to the advance and retreat of the snout (Fig 2.2d). These alternative models of moraine formation are discussed further in section 2.4.
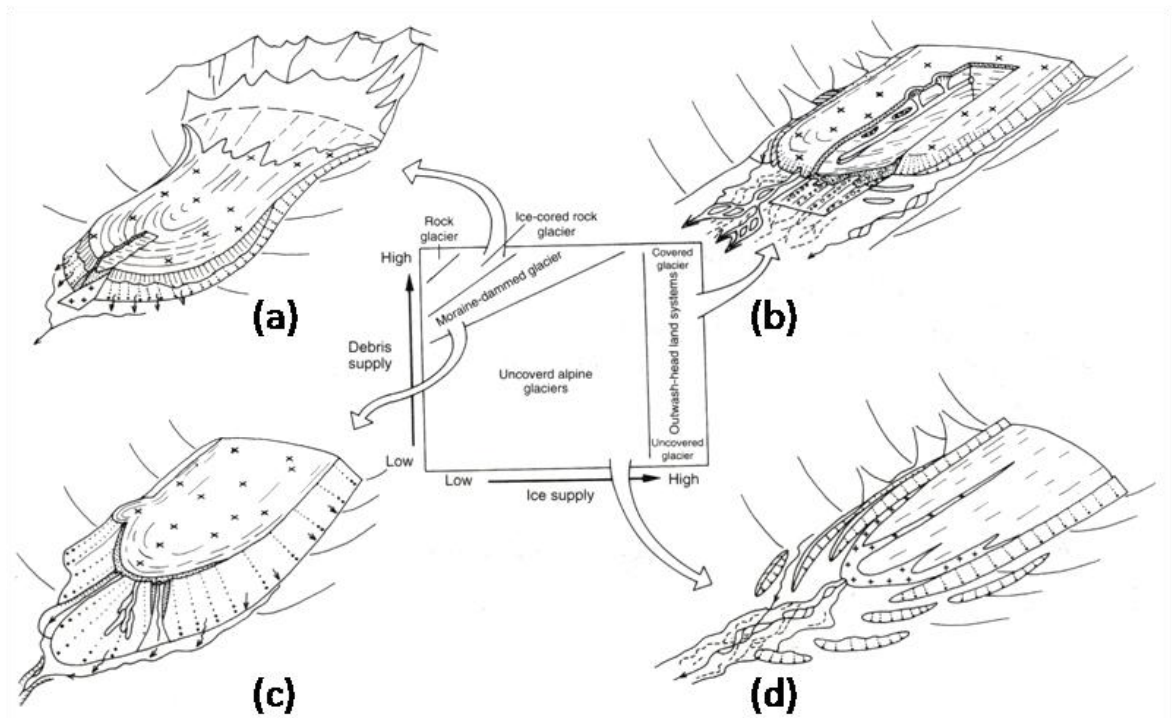
Fig 2.2(a-d) – Continuum of landsystem development at valley glacier termini based on the relative supplies of ice and debris to the glacier margin and the efficiency of the sediment transport system within the glacier foreland.

There is uncertainty regarding whether or not marginal fluctuations of volcanic ice caps are representative of climate fluctuations (Sturm et al., 1991; Bradwell et al., 2006). Volcanic activity may affect glacier behaviour and response to climate in several ways. Volcanic debris cropping out in the ablation zone may lower the albedo considerably and therefore increase the ablation rate. Values of albedo as low as 0.1 are measured for outlets of Vatnajökull covered in volcanic ash, whereas typical values of albedo for pure ice are about 0.4, resulting in an increase in surface ablation of up to 25% (Guðmundsson et al., 2006). Occasionally volcanic debris emitted in an eruption may blanket the ablation area of a glacier, reducing melt and triggering an advance (Sturm et al., 1991). Geothermal heating makes the greatest contribution to ablation by enhancing ice melt along the base of the glacier. Pálsson et al. (2007) estimate that 90% of ablation is due to basal melting in drainage basins within geothermal areas of the Vatnajökull ice cap, whilst ablation due to volcanic ash accounts for 10% of total ablation. Conversely, an increase in basal meltwater pressure may increase basal sliding velocity leading to glacier advance (Sturm et al., 1991; Guðmundsson, 1998; Larsen, 2000). The final way in which volcanic activity may affect glacier behaviour,

related to the last point, is through the production of glacial outburst floods, or jökulhlaups, during or following volcanic eruptions.

While some researchers suggest that glaciers draining volcanic craters should be excluded from studies of investigating glacier climate signals, Sigurdsson et al. (2007) state that *'to be able to evaluate the reaction of a glacier to climate change, each glacier must be analyzed carefully'*. Essentially, Sigurdsson et al. (2007) recognise that all glaciers vary in their response to climate change as a result of their unique local factors. While glaciers undoubtedly respond to large volcanic eruptions, their volcanic setting may be insignificant during times of volcanic stability. More research is needed on volcano-ice interactions to assess whether or not the behaviour of glaciers draining volcanic craters can still be indicative of climate change.

This study assesses the links between debris-cover, glacier-climate interactions and processes of landform production associated with the retreat of a 'debris-charged' glacier with characteristics of a 'debris-covered' glacier.

2.3 Landsystem of Kvíárjökull

Kvíárjökull was originally classified alongside alpine valley glaciers as a 'glaciated valley landsystem' by Eyles (1983b). The main features resulting in this classification were the apparent strong influence of topography on the glacier morphology and perceived dominance of debris from supraglacial sources in the glacial sediment budget and in moraine morphology. Eyle's landsystem model was based on a passive transport model in which debris derived by '*periglacial weathering of valley sides*' is carried in a '*conveyor belt fashion on the glacier surface*' (Eyles, 1983b, p49). Subsequently, Spedding and Evans (2002) found a number of different debris types emerging at the glacier margin that they attributed to a number of different transport pathways, including subglacial and englacial pathways. Based on this finding they rejected the passive transport model and, by implication, the glaciated valley landsystem model for Kvíárjökull. Instead they proposed a new subclass of the glaciated valley landsystem: the 'debris-charged landsystem', distinguished from the former by the complexity of sediment transport pathways through the glacier. Other characteristics they attribute

to the 'debris-charged landsystem' are moderate relief, high debris turnover, and drainage behaviour characteristic of an overdeepened basin.

Evans (2005) re-stated the debris-charged glacier landsystem for glaciers in Iceland but as yet there is no definitive model that illustrates how complex transport pathways are manifest in the landform record. The present study furthers our understanding of the evolution of landforms associated with complex transport pathways in glaciers over a sustained period of glacial retreat and moraine formation, and thus enables the production of a landsystem model for the 'debris-charged glacier' that is a unique addition to the archive and will aid palaeoglaciological reconstructions. The former theme is significant in that Kvíárjökull has been central to conceptual debates: firstly, the occurrence and importance of (a) supercooled meltwater (Roberts et al., 2002; Swift et al 2006) and (b) thrusting (Swift et al., 2006) as modes of debris entrainment and transport; and secondly, the evolution of supraglacial 'controlled' moraine ridges into hummocky moraine (Spedding and Evans, 2002; Evans, 2009). The second point is relevant to the final landsystem signature of Kvíárjökull.

2.4 Moraine formation at Kvíárjökull

Processes of basal sediment entrainment and transport by temperate glaciers are a critical control on the volume and distribution of sediment reaching the glacier margin. Entrainment commonly occurs by the incorporation of a thin layer of sediment onto the basal ice at the glacier bed (Knight, 1997). This layer may form by regelation (Hubbard and Sharp, 1993) and/or diagenesis of englacial ice (Knight and Knight, 1994) but in either case is unlikely to be thicker than tens of millimetres. The glacier snout at Kvíárjökull is 'charged' with large volumes of debris, concentrated within transverse debris bands (Fig 2.3a) (Swift et al., 2006) and thick sequences of debris-rich basal ice (Spedding and Evans, 2002; Swift et al., 2006). Alternative processes of entrainment are required to account for the thickness of this debris-rich basal ice layer. The processes that have received particular attention at Kvíárjökull and at other temperate glaciers are supercooling, tectonic thickening under compressional flow and, related to the latter, thrusting.

Following its discovery at Matanuska glacier, Alaska (Lawson et al., 1998), glaciohydraulic supercooling has been used to explain the occurrence of debris-rich ice sequences at glacier snouts (Strasser et al., 1996; Lawson et al., 1998; Evenson et al., 1999; Knudson et al., 2002; Cook et al., 2006) including those of temperate glaciers (e.g. Roberts et al., 2001). Supercooling refers to the process of freezing that occurs when water ascends a sufficiently steep adverse subglacial slope, such that the pressure melting point rises more rapidly than the water is heated by viscous dissipation (Alley et al., 1998). The elevation and freezing of this water entrains debris, and thus may result in debris rich basal ice and englacial channel fill deposits (Ensminger et al., 1999; Roberts et al., 2002). Evidence both for and against supercooling has been found by Spedding and Evans (2002), Swift et al. (2006). On first appearance the presence of thick sequences of stratified basal ice, englacial channel fill deposits along with a sufficiently steep adverse slope at Kvíárjökull are consistent with supercooling (Spedding and Evans, 2002). On closer inspection of the basal ice Swift et al (2006) found that, whilst the stratification in basal ice sequences at Kvíárjökull is consistant with that at Matanuska glacier formed by supercooling, the basal ice sequences at Kvíárjökull lack any of the features founds at Matanuska, such as channel-like forms and star-shaped aggregates, that are more firm indicators of supercooling. Furthermore, physical analysis of the debris rich ice revealed inconclusive evidence for supercooling (Swift et al., 2006). Based on the finding that ice formed by supercooling should be isotopically heavier than englacial ice (cf. Lawson et al., 1998) some of the sites sampled by Swift et al (2006) were consistent with supercooling, however others were not. Evans (2009) made the point that supercooling may only contribute to debris entrainment above the reverse slope of the overdeepening and therefore does not explain the formation of debris bands up to 500m from the glacier terminus.

An alternative process of entrainment and transport that accounts for thick debris-rich basal ice is thickening of basal ice by folding and/or thrusting (Swift et al., 2006) (Fig 2.3a,b). Several studies have attributed thick debris-rich basal ice at glacier snouts to the thickening of existing basal layers entrained by regelation or diagenesis by deformation (Hambrey and Muller, 1978; Knight, 1989).
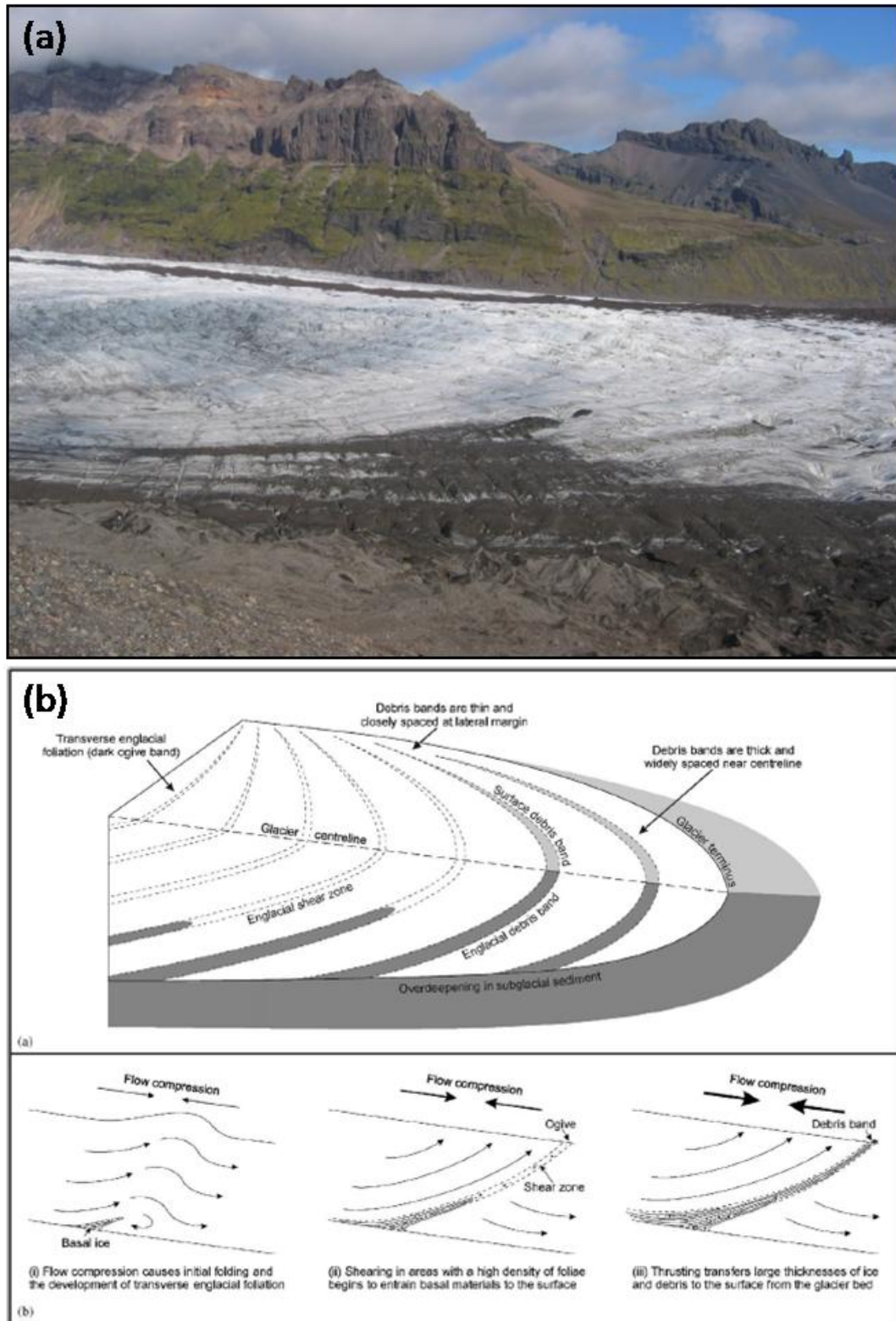
Fig 2.3(a,b) - (a) Photograph of transverse debris bands along the southern snout margin. (b) Model from Swift et al. (2006) showing the elevation of basal sediment by thrusting along shear zones.

Spedding and Evans (2002) advocate the thickening of basal debris by tectonic thickening under compressive ice flow at the base of the ice fall at Kvíárjökull. They also assert that subglacial hydrology associated with the subglacial topography plays a critical role in the development of thick basal ice. Firstly, channel growth at the base of the ice fall is suppressed due to compressive flow, favouring the preservation of basal ice. Secondly, water flow within the overdeepening switches from subglacial to englacial routing, thus preserving basal ice within the overdeepening. Whilst thickening by compression explains the volume of debris reaching the glacier margin, an additional mechanism is required to explain the distribution of debris within transverse englacial bands at many glaciers including Kvíárjökull (Swift et al., 2006).

Transverse debris bands are central to the debate of glacial sediment transfer by thrusting (e.g. Hambrey et al., 1999; Kruger and Aber, 1999; Goodsell et al., 2002, 2005; Swift et al., 2006). Thrusting as a mechanism for elevating basal debris to the glacier surface has mainly been observed at polythermal glaciers (e.g. Alley et al., 1997; Glasser et al., 2003). However, there is recent evidence to suggest that it may occur at temperate glaciers too. Goodsell et al. (2002, 2005) presented evidence for the elevation of basal debris to the glacier surface by thrusting along transverse englacial foliae created by longitudinal flow compression at the base of the ice fall at Haut Glacier D'Arolla in the Swiss Alps. Swift et al. (2006) apply this model of ogive formation to Kvíárjökull on the basis of the arcuate form of the debris bands concordant with transverse supraglacial foliation that occurs downglacier of the icefall. They suggest that longitudinal flow compression results not just in thickening of basal ice but also the elevation of debris by folding, shearing and thrusting along transverse englacial foliae (Fig 2.3b).

Of particular relevance to this research is how complex debris pathways associated with terminal overdeepenings and compressional ice flow are manifest in the landform record and therefore in the debris-charged landsystem. Transverse debris bands melt out at the margin of the glacier to form ice-cored moraine (Fig 2.4a,b) that grades into hummocky moraine in the foreland. The ice-cored moraine has received significant attention in the literature (Spedding and Evans, 2002; Evans, 2009) due to the prevalence of 'controlled' supraglacial linear ridges fed by englacial debris bands (Fig

2.4b). The ice-cored moraine is referred to as 'controlled' moraine for the reason that its morphology is 'controlled' by the pattern of transverse debris bands that melt out on the surface of the glacier (Fig 2.3a). Evans (2009) defines controlled moraine as '*supraglacial debris concentrations that become hummocky moraine upon de-icing and possess clear linearity due to the inheritance of the former pattern of debris-rich folia in the parent ice'.* Kvíárjökull offers a unique opportunity to study the genesis of hummocky moraine from ice-cored 'controlled' moraine at an Icelandic glacier, as hummocky moraine is generally uncommon in the forelands of typically debris poor active temperate glaciers in Iceland (Evans and Twigg, 2002). Refining the process-form relationships involved in the development of hummocky moraine at the margin of a contemporary glacier margin is important for palaeoglaciological reconstructions involving ancient hummocky moraine.
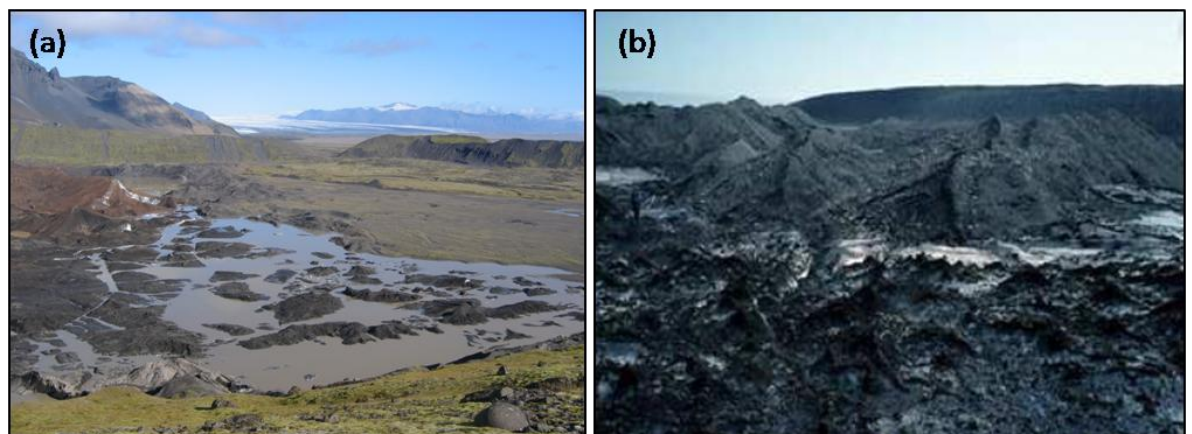
Fig 2.4(a,b) – (a) Ice cored moraine at frontal margin. (b) Linear ridges within ice-cored moraine (source: Evans, 2009)

There has been a reassessment of the processes responsible for the genesis of hummocky moraine in ancient glaciated terrain over the last two decades. Fundamental to this reassessment has been the recognition of linearity or 'control' within apparently chaotic, 'uncontrolled', moraine mound complexes. The recognition of englacial structure in ancient hummocky moraine (Gravenor and Kupsch, 1959; Evans, 2009) has led to the re-interpretation of palaeo-ice dynamics and palaeoclimate in these settings. An example of this is the re-interpretation of the Scottish Younger Dryas landform record. Sissons (1967, 1974a,b, and 1979) initially interpreted tracts of hummocky moraine as representing widespread ice-stagnation. These moraine

complexes have since been re-interpreted as representing incremental 'active' ice retreat on the basis of linearity within the moraine complexes.

Fig 2.5 - Schematic model of seasonal push moraine formation at the glacier margin developed by Evans and Hiemstra (2005) based on four Icelandic glaciers. "(1) Situation in late summer at typical Icelandic glacier snout where subglacial processes include lodgement and sliding (A), bedrock and sediment plucking (B), subglacial deformation (C) and ice keel ploughing (D) in a

temporally and spatially evolving process mosaic. (2) During early winter, the thin part of the glacier snout freezes onto part of the subglacial till. The till slab that freezes onto the ice sole is likely to be from the more porous A horizon (A). (3) The later winter readvance initiates failure along a decollement plane within the A horizon or at the junction with the more compact B horizon, resulting in the carriage of A horizon till onto the proximal side of the previous year's push moraine. (4) In the early summer, the melt-out of the till slab (A) initiates porewater migration, water escape and sediment flow (small arrows) and sediment extrusion due to glaciostatic and glaciodynamic stresses. (5) The late summer situation is again followed by winter freeze-on and marginal stacking of subglacial till produced by the reworking of existing subglacial sediments and fresh materials advected to submarginal locations from up-ice. Repeated reworking of the thin end of submarginal till wedges produces overprinted strain signatures and clast pavements."

Whilst this re-interpretation of the style of deglaciation (active retreat, rather than passive stagnation) is widely accepted, there is debate surrounding the palaeo-ice dynamics responsible for this linearity. This debate is related to the problem of geomorphic equifinality, whereby different processes may result in the same landform. A number of authors interpret linearity as a product of ice-marginal pushing and ice-contact fan accumulation (Bennett and Glasser, 1991; Benn, 1992; Bennett and Boulton, 1993 a, b; Lukas 2003, 2005), whereas others propose englacial thrusting as an alternative, controlled moraine origin for linearity (Hambrey et al., 1997; Bennett et al., 1998). There remains a "push" versus "controlled" debate surrounding Scottish Younger Dryas hummocky moraine. Observations of hummocky moraine formation at modern glacier margins, where final moraine morphology can be linked to the climatic and glaciological processes, are crucial in resolving this debate and in overcoming the problem of geomorphic equifinality.

At Kvíárjökull a similar equifinality problem exists regarding the processes responsible for apparent linearity within hummocky moraine complexes in the glacier foreland. As in Scotland, two separate origins have been proposed for this linearity (Spedding and Evans, 2002; Evans, 2009). The first is a controlled moraine origin based on the recognition of 'controlled' ridges at the present day glacier margin. This origin implicates the processes of thrusting and ogive formation in the linearity of hummocky moraine. The second is the process of ice-marginal pushing/ bulldozing of ice marginal sediments (Spedding and Evans, 2002; Evans, 2009). Bulldozing of ice-marginal sediments, often on an annual basis, is a common process at the margins of outlet

glaciers of Vatnajökull (Fig 2.5) producing distinctive linear ridges (Boulton, 1986; Kruger, 1993, 1995, 1996; Evans and Twigg, 2002; Evans and Hiemstra, 2005). The presence of glacitectonized structures within glacio-fluvial sediments at the margin of Kvíárjökull are indicative of ice-marginal pushing/ bulldozing (Spedding and Evans, 2002). Pro-glacial push moraines therefore provide a clear record of glacier retreat and glacier-climate interactions at glacier margins (e.g. Sharp, 1984; Evans and Hiemstra, 2005) and demonstrate that the glacier is effectively coupled to climate (Evans, 2009).

The melt-out of englacial debris bands however is only indirectly related to climate, in that snout retreat and consequent controlled moraine deposition is controlled by climate. Identifying the relative importance of the 'controlled' and 'pushed' origins for hummocky moraine linearity, therefore, has implications for the interpretation of palaeo ice dynamics from the landform record. Whilst the former origin would imply that the moraine contains a record of englacial structure and processes and an indirect and muted climate signal, the latter origin would constitute a relatively fine-tuned record of palaeoclimate. Determining the relative importance of 'controlled' versus 'pushed' origins for hummocky moraine linearity at Kvíárjökull is therefore pertinent to resolving the genesis and palaeoclimatic significance of ancient landforms such as the Scottish Younger Dryas moraine.

Key to determining the relative importance of a 'controlled' origin in the final landform record at Kvíárjökull and viability of a 'controlled' origin for hummocky moraine in palaeoglaciological reconstructions is the preservation potential of controlled moraine. The preservation of 'controlled' moraine is largely dependent on the intensity and extent of topographic inversion and debris reworking during the melt out of ice cores (e.g. Kjær and Krüger, 2001). Boulton (1972) recognized the importance of de-icing in hummocky moraine evolution in his model of supraglacial moraine development from englacial debris concentrations (Fig 2.6). This model illustrates the gradual lowering of the moraine surface and dissection of moraine ridges by melt-water associated through time. Other research has also highlighted the extensive reworking that occurs at downwasting debris rich glacier snouts and the resulting complexity of glacial sedimentary signatures (e.g. Thomas et al., 1985; Paul and Eyles, 1990; McCarrol and

Harris, 1992; Johnson and Clayton, 2003). This research suggests that the preservation potential of controlled moraine is low.
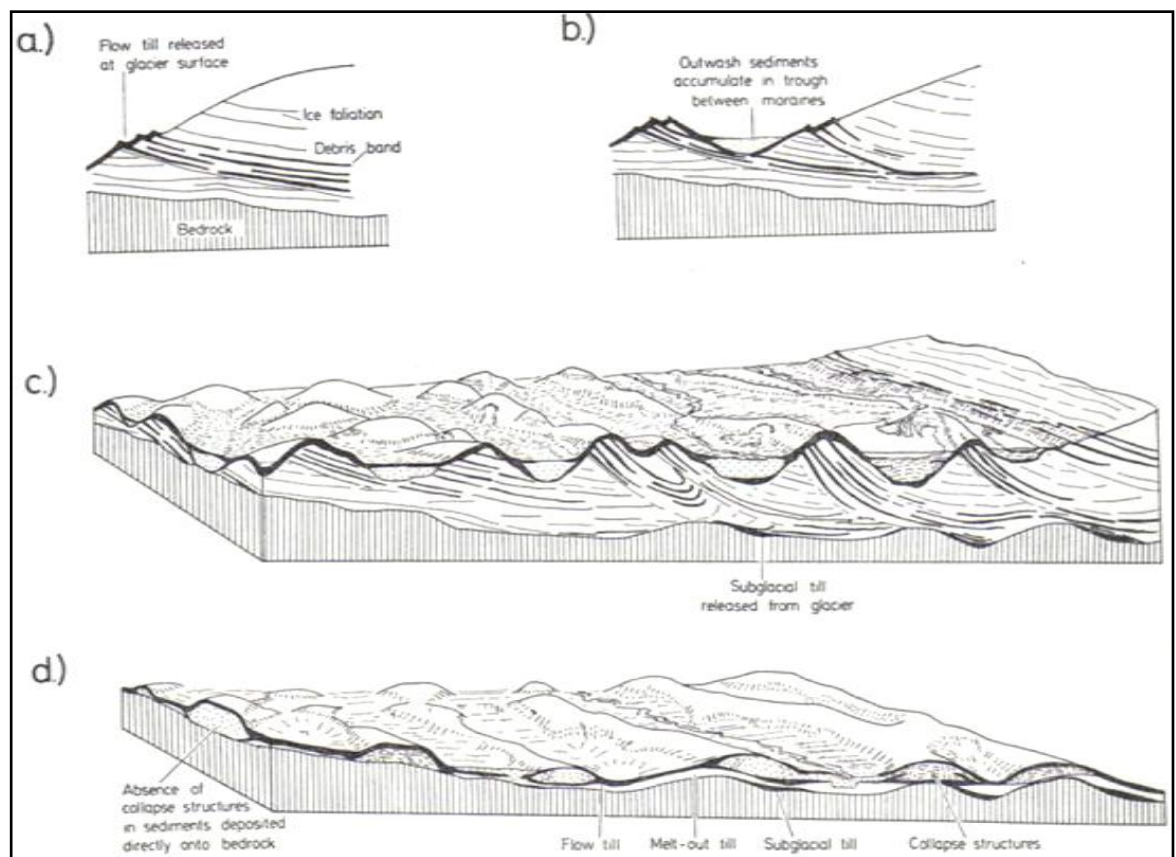
Fig 2.6(a-d) - Process-form model of hummocky moraine evolution from englacial debris concentrations (Boulton, 1972).

Conversely, other authors present evidence for the preservation of 'controlled' moraine. Bennett et al.'s (1998) model of moraine-mound complex evolution at a glacier margin in Svalbard illustrates the lowering of debris thrust bands onto the landscape, uninterrupted by the reworking processes that affect modern glacier snouts (Fig 2.7). Whilst Evans (2009) is sceptical of this model for the reason that it ignores reworking processes he also notes that *'it is not unrealistic to expect debris-charged glacier snouts to produce a landform signature in deglaciated terrains'*. Further research is clearly required to assess the preservation potential of 'controlled' moraine at debris-charged glacier snouts and the viability of a 'controlled' moraine interpretation for ancient hummocky moraine.
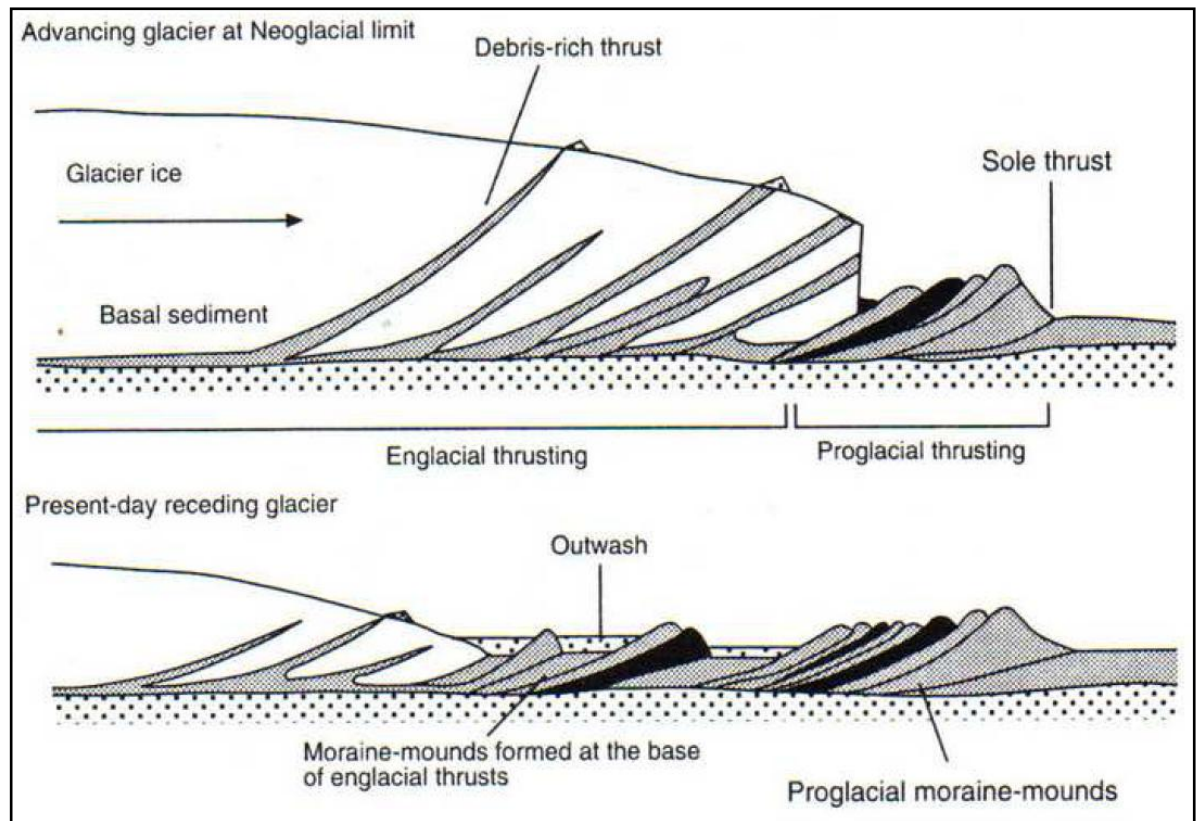
Fig 2.7 - Model for hummocky moraine formation by englacial and proglacial thrusting. Top: Stresses are propagated into the foreland along a basal decollement surface of sole thrust. Bottom: Lowering of englacial debris after ice retreat to form a sequence of stacked moraines with characteristic proximal rectilinear slopes that dip upglacier (Bennett et al., 1998).

Another important consideration with regards to the preservation of 'controlled' moraine is the extent and intensity of ice-marginal pushing. Evans (2009) recognizes the role of pushing in enhancing moraine linearity at Kvíárjökull (Fig 2.8). However, pushing may potentially confuse the 'controlled' moraine signal creating an equifinality problem. Proglacial folding and thrusting underneath a debris cover results in the production of linear ridges around glacier snouts of the Barnes Ice Cap (Evans, 2009). Other authors have also observed proglacial thrust masses buried by supraglacial and outwash deposits (Lønne and Lauritsen, 1996; Waller and Tuckwell, 2005; Yde et al., 2005; Roberts et al., 2009), which document glacitectonic activity rather than processes of debris concentration such as supercooling and englacial thrusting. This highlights the importance of deciphering linearity derived from glacitectonic activity from that derived from englacial debris bands.
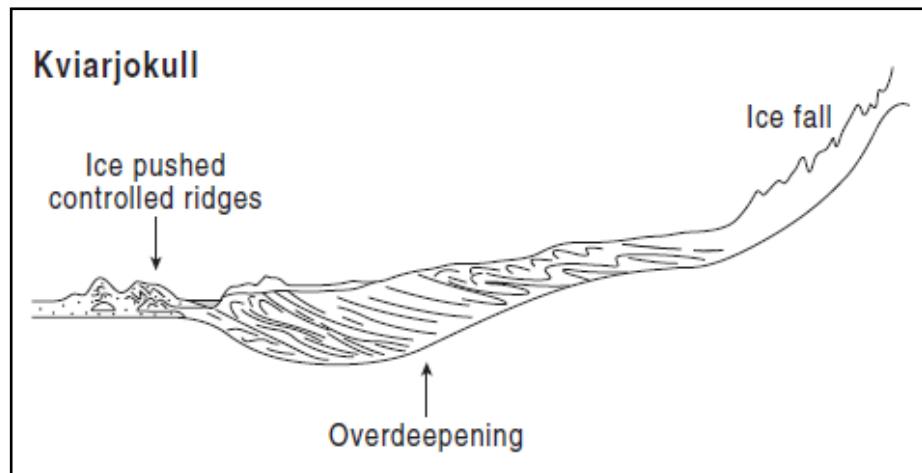
Fig 2.8 – Model of controlled moraine development at Kvíárjökull (Source: Evans, 2009).

Observations of moraine formation at Kvíárjökull (Spedding and Evans, 2002; Evans, 2009) have preliminarily identified an evolutionary continuum of moraine type, from supraglacial linear 'controlled moraine' (Benn and Evans, 1998; Spedding and Evans, 2002; Evans, 2009) fed by debris rich englacial bands (Spedding and Evans, 2002), to hummocky moraine with elements of linearity enhanced by ice-marginal pushing. However, these observations are based on short term investigations of the modern day glacier margin and use of an ergodic approach, which assumes that the process-form relationships observed today have remained unchanged during moraine evolution and therefore that present day glaciological characteristics are representative of those in the past. This study observes and quantifies moraine evolution over a longer time scale, through the use of aerial photography, thus avoiding the pitfalls of an ergodic approach. It also reveals changes in process-form relationships through time, which are related to changes in glaciological characteristics in response to climate fluctuations. This helps to clarify the processes responsible for hummocky moraine linearity.

In summary, this study of long term moraine construction helps to further understanding of the evolution of landforms at a debris-charged glacier terminus. Specifically, it offers insight into the morphological evolution of controlled moraine and hummocky moraine. Two main research questions guide the assessment of the relative importance of englacial processes of debris concentration (tectonic thickening, and thrusting) and ice-marginal pushing in the final landform record:

1) What is the preservation potential of 'controlled' moraine?

2) What is the role of ice-marginal glacitectonic activity in moraine linearity?

Answering these questions at Kvíárjökull offers insight into the viability of determining a 'controlled' versus 'push' origin for ancient moraine fields, such as the Scottish Younger Dryas hummocky moraine. An assessment of the long term landscape evolution through the production of a time series of geomorphological maps enables the development of a comprehensive landsystem model for a 'debris-charged glacier'. The maps and landsystem model serve as an analogue for ancient glacierized hummocky terrain.

3 Location

3.1 Topographic setting of Kvíárjökull

Kvíárjökull (63°55′N, 16°30′W) is an outlet glacier of the Öræfajökull icecap, which coalesces with the Vatnajökull ice cap in southeast Iceland (Fig 3.1).

Fig 3.1 - Location map of Kvíárjökull

The glacier descends from the ice cap at a maximum altitude of 2119m down to the coastal plain at an altitude of about 50m above sea level over a total distance of ~13.5km and has an area of ~25km² (Spedding and Evans, 2002). The glacier descends over an icefall of several hundred meters high (Fig 3.2a) and is bounded on each side by steep volcanic rock walls up to 600m high. It isconstrained in its foreland by a 100m high, latero-frontal Neoglacial moraine ridge (Fig 3.1). This ridge creates 'an enormous amphitheatre' (Thórarinsson, 1956) within which ice marginal complexes of ice-cored and hummocky moraine and outwash sediments are contained (Fig 3.2c). Another distinctive topographic feature is an overdeepening at the base of the ice fall about 50m below sea level, apparent on a ground penetrating radar scan conducted by Spedding and Evans (2002) (Fig 3.3). This would have been carved out by the glacier

when it was at its LIA maximum limit, when the most active outlet glaciers in this region typically excavated their beds down to hard surfaces 200 – 300m below sea level (Björnsson and Pálsson, 2008).
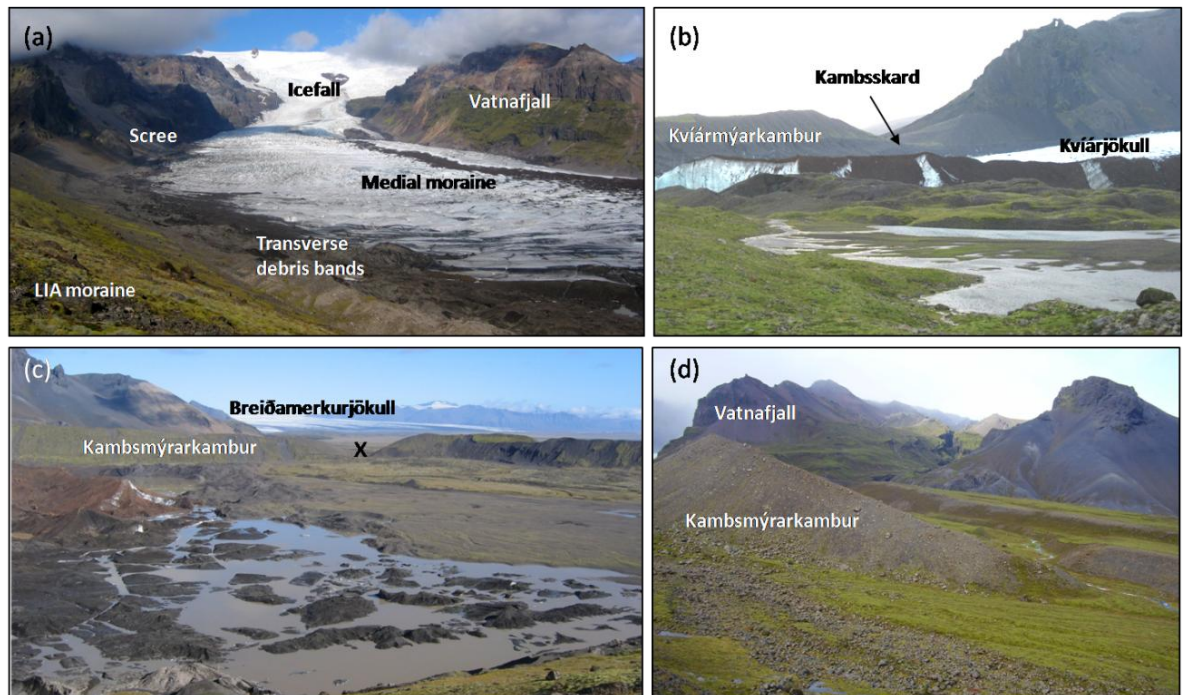
Fig 3.2(a-d) - (a) View upglacier; (b) view of breach in southern lateral moraine; (c) view across foreland with Breiðamerkurjökull to the north; (d) breach in northern lateral moraine (marked as 'x' in (c)).

3.1 Volcanic and geological history

The ice cap of Öræfajökull sits in the crater of the largest active stratovolcano in Iceland (Thórarinsson, 1958). Kvíárjökull has incised a deep valley on the south-eastern flank of Öræfajökull, exposing sequences of tholeiitic basalts, hyaloclastites and volcanic products such as acid lavas as mapped by Stevenson et al. (2006) (Fig 3.4). Volcano-ice interactions have resulted in a number of jökulhlaups during the glacier's history. The volcanic eruptions in 1362 AD and 1728 AD resulted in the production of a large volume of meltwater, much of which was routed down the Kvíárjökull valley in jökulhlaups (Thórarinsson, 1958). The floodwaters incised channels and deposited large outwash fans with large boulders beyond the latero-frontal moraines to both the north and south (e.g. Fig 3.2d). The influence of the volcano on the present day glacier is unknown, though needs to be considered in any assessment of glacier behaviour as

it may disrupt the relationship between glacier behaviour and climate fluctuations (Sturm et al., 1991).
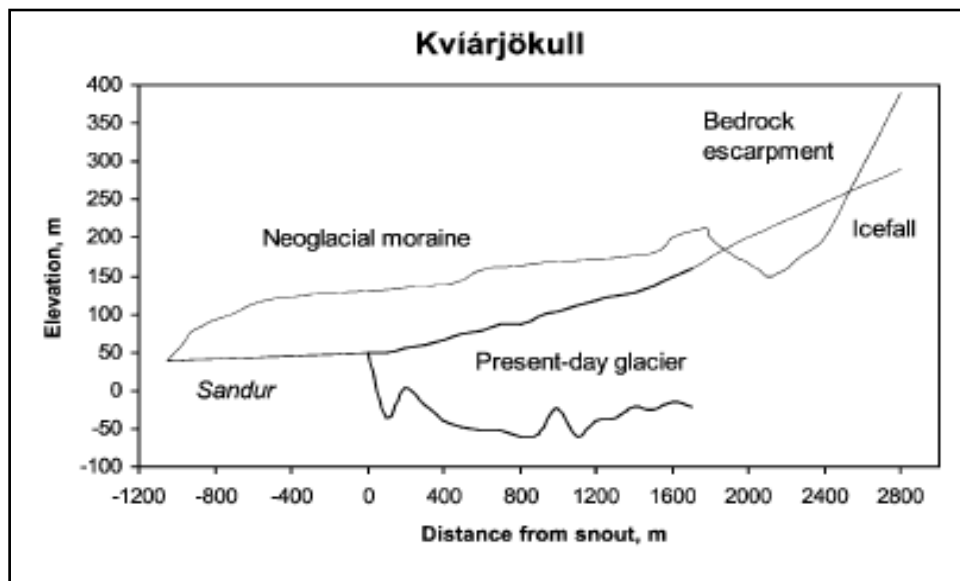
Fig 3.3 - Longitudinal profile of Kvíárjökull's southwestern Neoglacial moraine rampart set against 1996 centerline surface and bed topography. Thick lines depict data obtained by field survey, thin lines data taken from the Icelandic Geodetic Survey sheet 87/88(Öræfajökull) (Spedding and Evans, 2002)
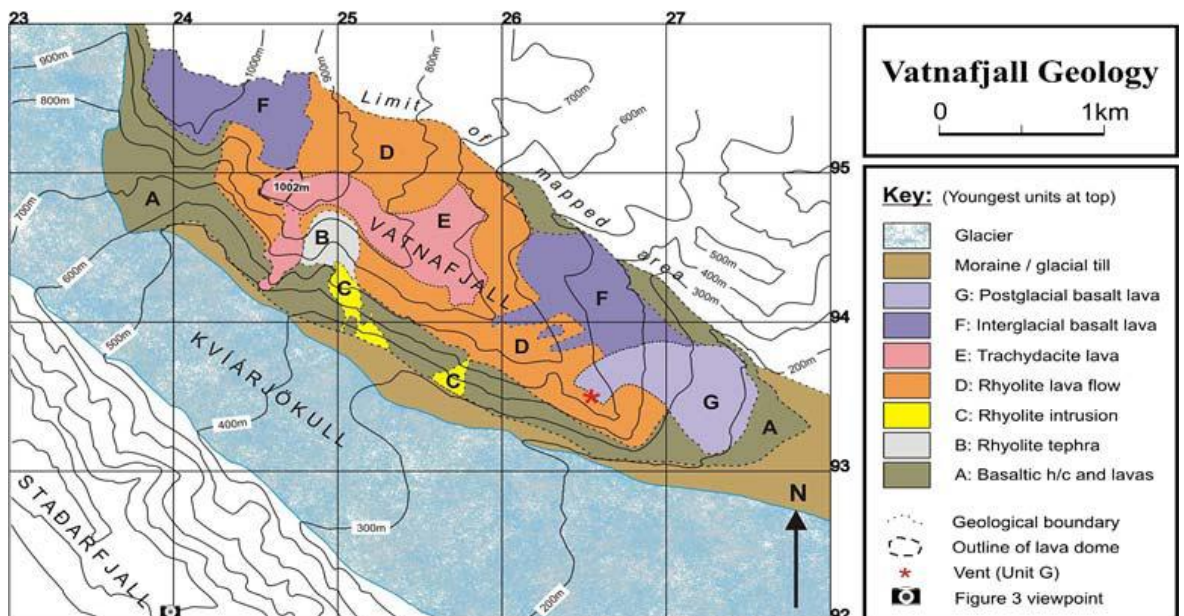
Fig 3.4 - Geological map of Vatnafjall, Öræfajökull, Iceland with contours from Army Map Service (1950). Stevenson et al. (2006)

3.2 Climate

Iceland lies in the North Atlantic Ocean and has a relatively mild oceanic climate with relatively small seasonal variations in temperature (Björnsson and Pálsson, 2008). Frequent cyclones from the North Atlantic bring heavy snowfall to the southern coast where average winter temperature is close to 0°C. On the highest southern slopes of Vatnajökull annual precipitation exceeds 4000-5000mm. Iceland is the only landmass in the North Atlantic Ocean to lie on the latitude of sub polar convergence (Kirkbride and Dugmore, 2008), making its climate sensitive to changes in atmospheric and ocean circulation. Records of average annual summer temperatures (May – September) and winter precipitation totals (October – April) spanning 1949 - 2007 from Fagurhólsmyri meteorological station to the southwest of Kvíárjökull are shown in Fig 3.5Fig 3.6. Temperature fluctuates between ~7°C and ~9.5°C and precipitation between ~800mm and ~1800mm. The 7 year running means show the general trends in temperature and precipitation. Temperature fluctuated from the late 1950s until mid 1980s and has been increasing quite steadily since. Apart from a peak in the early 1960s, precipitation was steady, fluctuating between 1000mm and 1200mm, until 2000 and then increased.
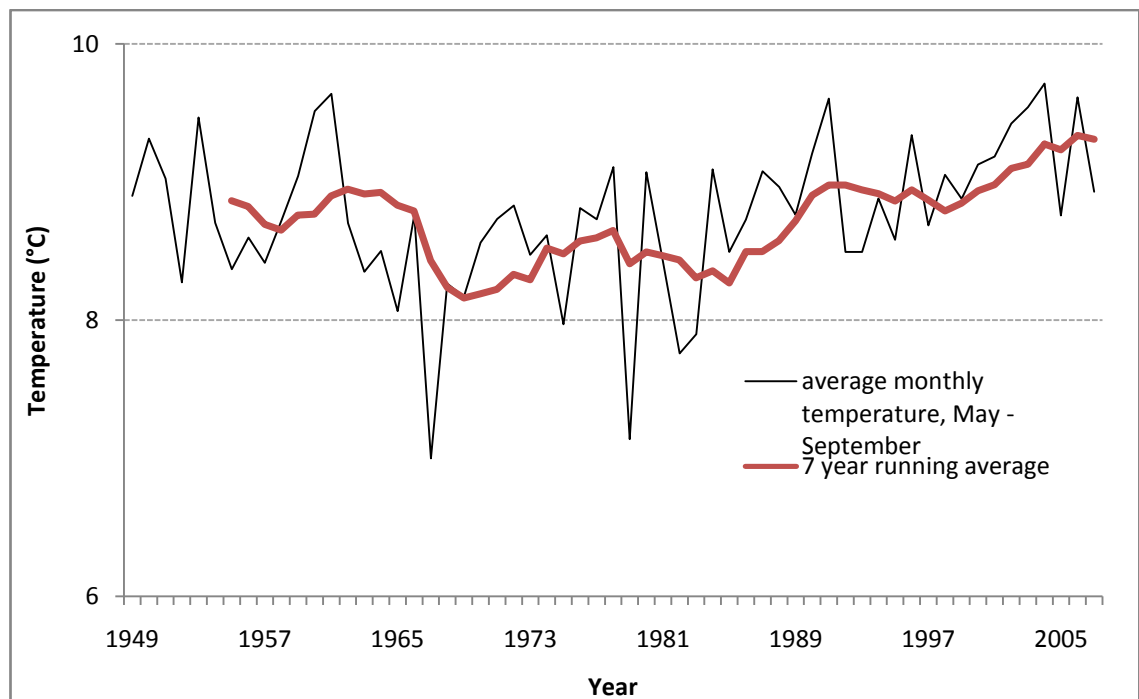
Fig 3.5 - Average monthly summer temperature (May – September) at Fagurhólsmyri, 1949 – 2007 with seven year running mean from 1956.
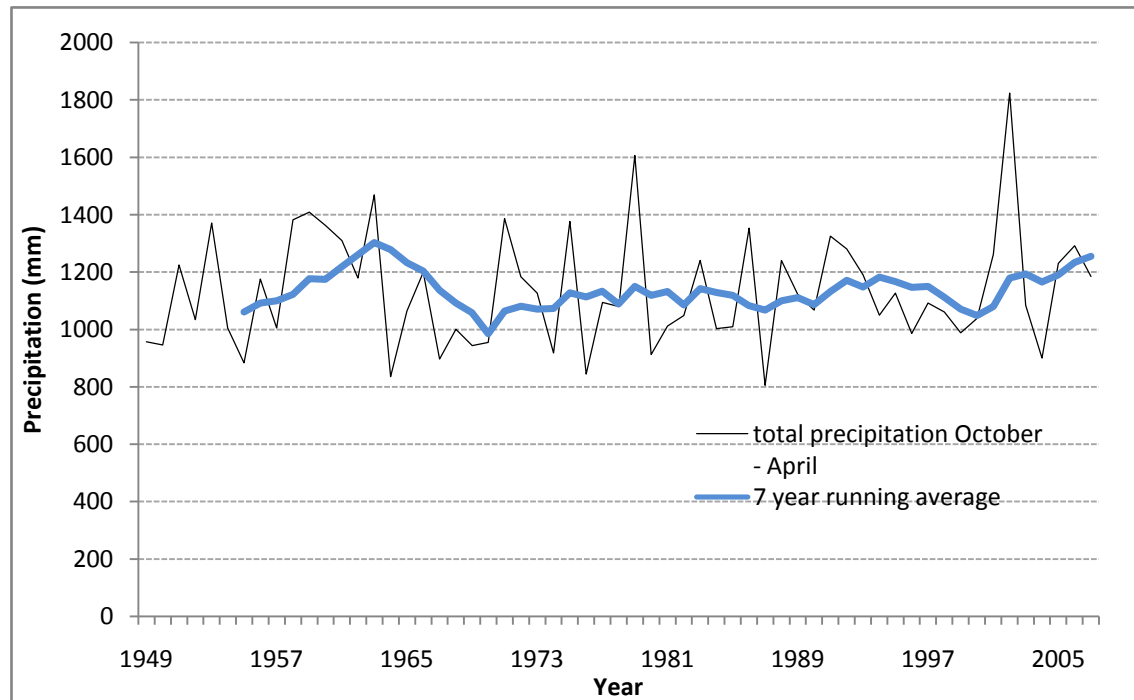
Fig 3.6- Winter precipitation (October to April) at Fagurhólsmyri, 1949 – 2007, with seven year running mean starting in 1956. Data from Icelandic Meteorological Office.

3.3 Glacial history

The historical fluctuations in thickness of ice within Kvíárjökull and the ice cap of Öræfajökull have been inferred from the sequences of volcanic deposits within the Vatnafjall ridge (Fig 3.4). At present, being an interglacial period, ice is restricted to within the summit caldera of Öræfajökull and lies ~600m below the ridge summits, within the Kvíárjökull valley at a thickness of ~50m (Spedding and Evans, 2002). However during glacial stages ice would have been up to 600m thick, filling the valley, leaving just the crest of Vatnafjall above the ice as a nunatak (Stevenson et al. 2006).

Past glacial extent is also recorded by the lateral moraine complex that confines the glacier foreland. This reaches a height of 150m and is thought to have formed during the first period of icecap expansion within the Neoglacial period at around 3200 B.P. (Thórarinsson, 1958; Spedding and Evans, 2002). Such large lateral moraines are exceptional in Iceland and are a dominant feature within the foreland of Kvíárjökull. Spedding and Evans (2002) suggest that their size may be attributed to complex feedback between ice, water and sediment transport. High ice flux during icecap expansion would have resulted in high subglacial erosion rates, the excavation of the overdeepening, steepening of the reverse slope of the overdeepening, rising water

pressures and the formation of englacial channel fills. In turn, the restriction of englacial drainage would have led to the reduced evacuation of sediment by water and therefore increased rates of sedimentation out of the ice. Rockfall debris would have contributed to the restriction of englacial drainage and to sedimentation rates. As the moraines enlarged, ice and water flow would have been restricted, further enhancing sedimentation rates and moraine growth. The development of this moraine complex during the Neoglacial transformed Kvíárjökull from a piedmont glacier tongue similar to many other Icelandic glaciers, including the nearby Fjallsjökull, into the present day constrained glacier snout (Iturrizaga, 2008). The outer extent of this pre-Neoglacial piedmont lobe is recorded by subdued moraines beyond the lateral moraine ridges.

The Little Ice Age (LIA) was the second period of icecap expansion that occurred within the Neoglacial period, beginning in the Middle Ages and terminating at the end of the 19th century. The equilibrium line altitude (ELA) of outlet glaciers of Vatnajökull descended from 1100 to 700m and glaciers advanced up to 15km, excavating their beds to up to 300m below sea level. The lateral moraine complex of Kvíárjökull records several glacial advances during the LIA. An advance in 1870 (Todtmann, 1960) resulted in the moraines being breached at two points by ice (Fig 3.2b,d). The breach named 'Kambsskard' by Thórarinsson (1956) in the southern most lateral moraine (Kvíármýarkambur) is marked by a 50m wide, 250m long tributary tongue basin and several looped moraines. The breach of the northern lateral moraine (Kambsmýrarkambur) is marked by a significant incision of about 100-150m, dividing the lateral moraine into two distinct segments. The lateral moraines were last overridden between 1886 and 1890 (Iturrizaga, 2008) resulting in the deposition of large boulders on the outer slope of Kvíármýarkambur, the southern-most lateral moraine. At its LIA maximum extent at around 1900 AD, Kvíárjökull filled the moraine amphitheatre and was ~3.5km² greater in extent that at present.

During the 1890s, a general glacier recession in Iceland commenced, though retreat at Kvíárjökull did not commence until the end of this decade (Spedding and Evans, 2002). The rate of glacier retreat in Iceland was particularly rapid after 1930, slowing after 1940 in response to cooler summer climate, and becoming rapid after 1985 (Jóhannesson and Sigurdsson, 1998). Present day margin retreat rates are as high as

~100 m a^{-1}.. At Kvíárjökull nested lateral moraines have been constructed against the inner lateral moraine slopes by successively less extensive advances following the LIA maximum, and within the foreland several moraine ridges record more recent glacier oscillations, on which this study focuses. Moraine crests older than 1977 have been mapped and dated by Evans et al. (1999b) using lichenometric and Schmidt hammer dating techniques (Fig 3.7).
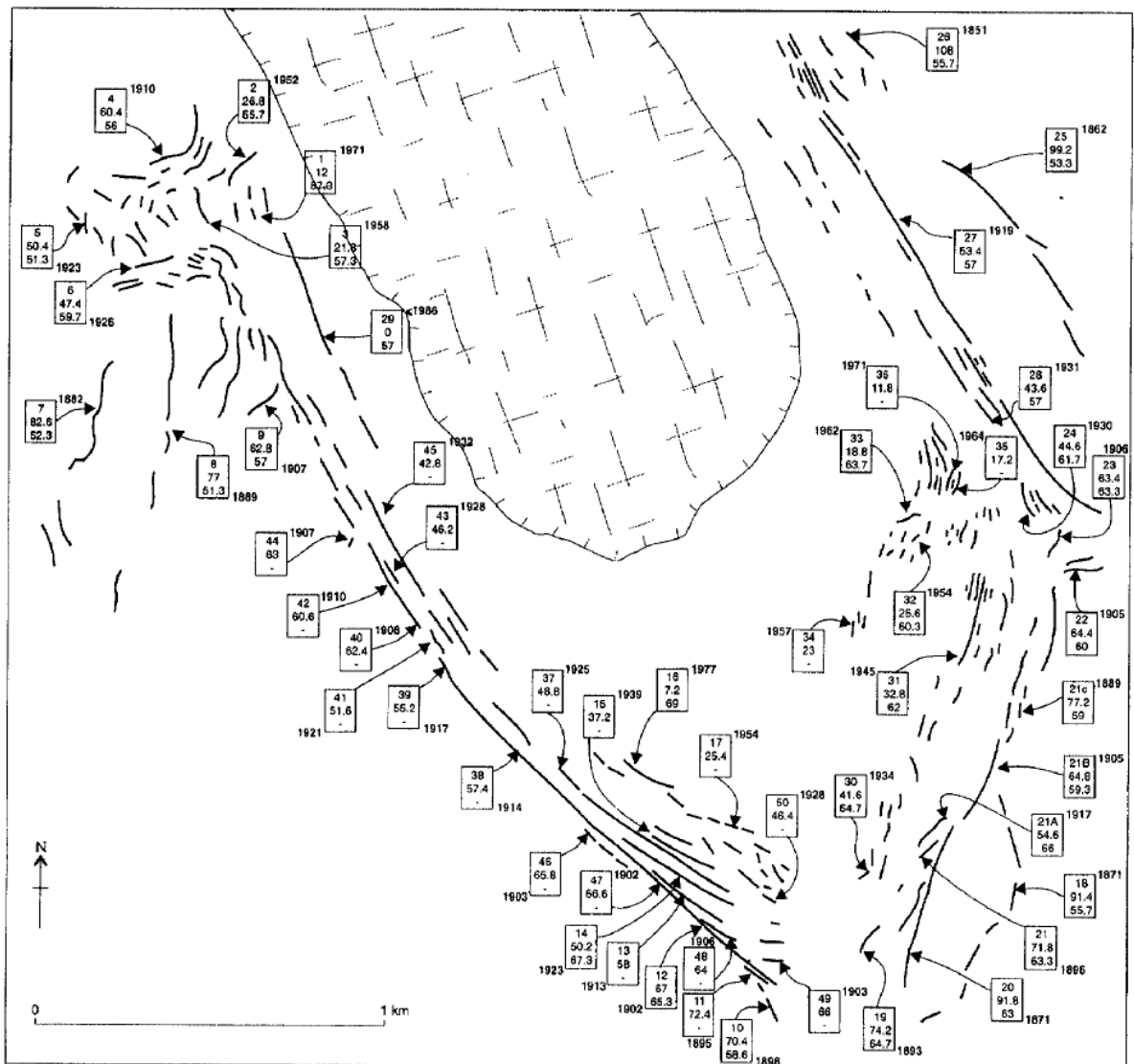
Fig 3.7 - The moraine crests of Kvíárjökull (mapped from the 1980 aerial photography) with their associated lichen sizes and R values. Numbers in each box refer to moraine number (top), average long axis of largest five lichens (middle) and Schmidt hammer R value (bottom). Ages on moraines are in years AD and are calculated using the 0.8mm a^{-1} lichen growth rate and a colonization lag time of 6.5yr (Evans et al., 1999b).

4 Methods

4.1 DEM production

4.1.1 Digital Photogrammetry

Photogrammetry is defined as the 'extraction of quantitative elevation information from stereophotography' (overlapping imagery) (Lane et al., 2000). Photogrammetry involves the reconstruction of the geometric relationship between the ground, camera and film at the time of capture for each photograph, thereby linking the two dimensional co-ordinate system of image space to the three dimensional co-ordinate system of object space. This is described mathematically using the perspective projection (Slama et al., 1980), which assumes the condition of collinearity, requiring that a point on the ground (A), the camera perspective centre (L) and the corresponding point on the image plane (a) lie on a straight line in three dimensional space (Wolf and Dewitt, 2000) (Fig 4.1).
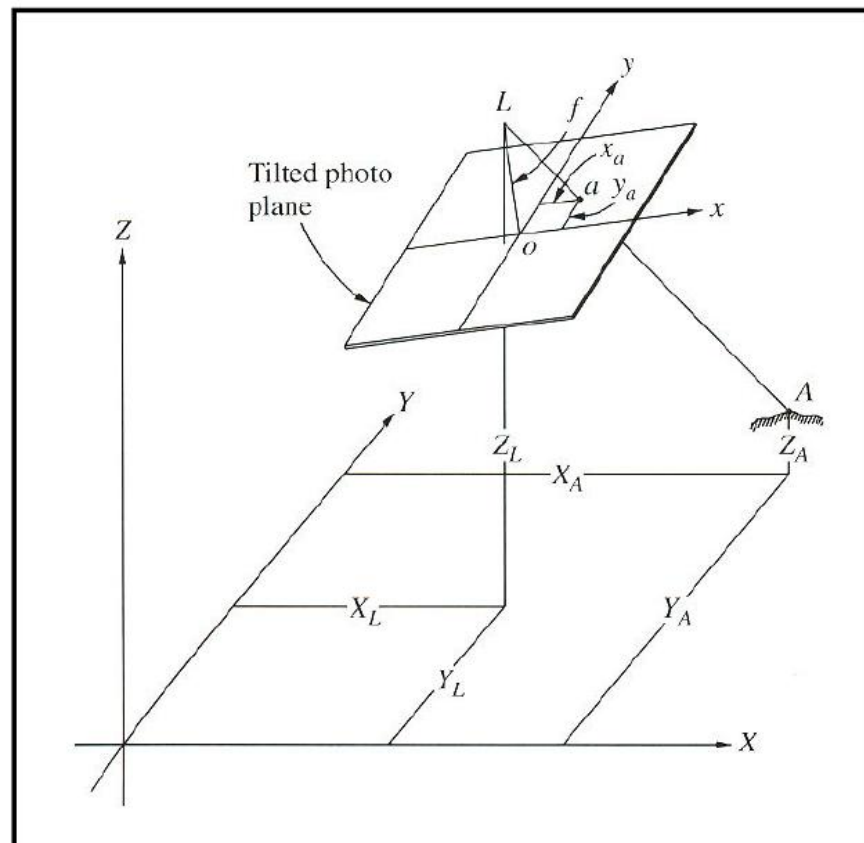
Fig 4.1 - Image geometry satisfying the collinearity condition (Wolf and Dewitt, 2000)

The relationship between the two dimensional position of *A* in image space (x_a, y_a) and its corresponding three dimensional position in object space (X_A, Y_A, Z_A), can be described by:

$$\begin{bmatrix} x_a \\ y_a \\ -f \end{bmatrix} = kM \begin{bmatrix} X_A & - & X_L \\ Y_A & - & Y_L \\ Z_A & - & Z_L \end{bmatrix}$$

[1]

Source: Ghosh, 1988

where *f* is the focal length of the camera lens; X_L, Y_L, Z_L are object space coordinates of the camera perspective centre; k is scale factor; and M is the rotation matrix such that:

$$M = \begin{bmatrix} m_{11} & m_{11} & m_{13} \\ m_{21} & m_{22} & m_{23} \\ m_{31} & m_{32} & m_{33} \end{bmatrix}$$

[2]

where m_{ij} are the elements of the rotation matrix that describe the rotation of the camera around the x, *y* and z axes ($?$, f, $?$). Equation [2] can be expanded to give the collinearity equations:

$$x_a = x_o - f \left[\frac{m_{11}(X_A - X_L) + m_{12}(Y_A - Y_L) + m_{13}(Z_A - Z_L)}{m_{31}(X_A - X_L) + m_{32}(Y_A - Y_L) + m_{33}(Z_A - Z_L)} \right]$$

[3]

$$y_a = y_o - f \left[\frac{m_{21}(X_A - X_L) + m_{22}(Y_A - Y_L) + m_{23}(Z_A - Z_L)}{m_{31}(X_A - X_L) + m_{32}(Y_A - Y_L) + m_{33}(Z_A - Z_L)} \right]$$

[4]

Source: Wolf and Dewitt (2000)

where x_o and y_o are the principle point coordinates in image space (added to correct for offset); and X_A, Y_A and Z_A are object space coordinates of A.

From Equations [3] and [4] determination of object space coordinates from image space coordinates requires knowledge of: (i) camera focal length; (ii) image coordinates of the principal point; (iii) position of the camera in object space; and (iv) rotation of the camera axes. With (i) and (ii) held as constant, (iii) and (iv) still remain unknown. These are called the *elements of exterior orientation* as they describe the altitude and position of the camera at the time each image was captured (Ghosh, 1988). The value of these parameters can be determined using the collinearity equations if the positions of at least three points for each image are known. These are known as ground control points (GCPs), stable features that are easily identifiable in the photographs.

4.1.1.1 *Block adjustment*

Distortions due to lens imperfections and atmospheric refraction can be accounted for using the process of block adjustment. The collinearity equations [3] and [4] are expanded to allow the addition of extra information to account for distortions in exterior orientation parameters (Wolf and Dewitt, 2000). Block adjustment involves a number of stages: interior orientation, exterior orientation and aero-triangulation.

4.1.1.2 *Interior orientation*

The aim of interior orientation is to reconstruct the internal geometry of the camera at the time of image capture. Camera calibration defines the interior geometry of the camera by providing precise measurements of several camera parameters that are collectively referred to as the elements of interior orientation (Thompson, 1966). These are the (i) camera focal length, (ii) the fiducial marks; (iii) principal point coordinates in image space; and (iv) radial lens distortion. These take account of distortions in the camera lenses and film and distortions resulting from atmospheric refraction and the curvature of the Earth. In this study the radial lens and film distortions are known for each image from camera calibration and fiducial point measurement, respectively, with the exception of 1945 (no camera calibration certificate) and 1980 (no fiducials). Errors due to atmosphere and curvature of the Earth are assumed to be very small for the scale of imagery used in this study.

4.1.1.3 *Exterior orientation*

The geometry of the camera relative to the ground is determined in the exterior orientation stage of photogrammetry. This requires the measurement of a sufficient number of GCPs in order to solve the elements of exterior orientation for each photograph. Overlapping images are processed simultaneously using a relatively small number of GCPs located within the overlap and the bundle adjustment process. At least two horizontal and three vertical GCPs are required to define the three dimensional coordinate system in the object space of a block of photos, regardless of the number of images (Wolf, 1983).

4.1.1.4 *Aerotriangulation*

Along with the GCPs, the information that is input from interior and exterior orientation is applied in a least squares adjustment to determine the unknown exterior orientation parameters for each image in the block. A least squares adjustment finds a best-fit solution by minimising the root mean square of the residuals. In this process, the elements of interior and exterior orientation are adjusted according to uncertainty of their measurement, as defined by the user. Overestimation of these values under-constrains the model and while it may produce a good fit of the data to the model, it may not be accurate. Underestimating these values will have the opposite effect.

4.1.1.5 *Stereomatching*

Stereomatching involves the automated detection of homologous pixel pairs in stereoscopic images within a set window size (the correlation window) in order to match pairs of photographs. There are various matching algorithms divisible into feature-based and area-based methods. Feature-based algorithms detect and match structures such as edge pixels, line segments or curves. Area-based approaches detect and match homologous pixels based on comparison of brightness values within a window whose size is defined by the user (Wolf and Dewitt, 2000). Area-based methods tend to be more suitable for natural environments due to their tendency to be well textured while lacking the sharp features typical of urban landscapes (Brockelband and Tom, 1991).

The photogrammetric method has evolved over the last century as technology has advanced. During the 1970s and 1980s, analytical methods of photogrammetry became well established and enabled geomorphologists to record topography in greater detail than traditional interpretative methods (Dixon et al., 1998). More recently, digital photogrammetry has been developed which automates the extraction of terrain models from stereophotography, greatly increasing the efficiency and ease of topographic data collection (Baily et al., 2003).

Using modern photogrammetric techniques it is possible to convert long historical archives of aerial photographs into sequential DEMs. This is known as an 'archival photogrammetric technique' (Chandler and Brunsden, 1995). A number of studies have successfully used this technique to assess change in glaciers and glacial landscapes (e.g. Etzelmüller and Sollid, 1997; Cox and March, 2004; Jordan et al., 2005; Rivera et al., 2005; Schomacker & Kjær 2007; Schiefer and Gilbert, 2007; Pope et al., 2007; Fox and Cziferszky, 2008; Racoviteanu et al., 2008).

4.1.2 **Dataset**

The dataset to be used for digital photogrammetric processing, morphometric analysis and mapping was obtained from Landmælingar Íslands and Loftmyndir ehf (Fig 4.2, Table 4.1). Aerial photograph stereo pairs from 1945, 1964, 1980 and 1998 were obtained from Landmælingar Íslands. These are all black and white images, typically at a scale of 1:30000. All photographs were scanned to a high resolution (15µm) on a photogrammetric scanner. Potential problems exist with the 1945 photographs for which there is missing calibration information. The 2003 aerial photography stereo pair was obtained from Loftmyndir ehf and are of a similar scale but are in RGB colour. 12 Ground control points were surveyed relative to a known station in the Icelandic GPS network using Leica single-frequency GPS receivers (Fig 4.3).
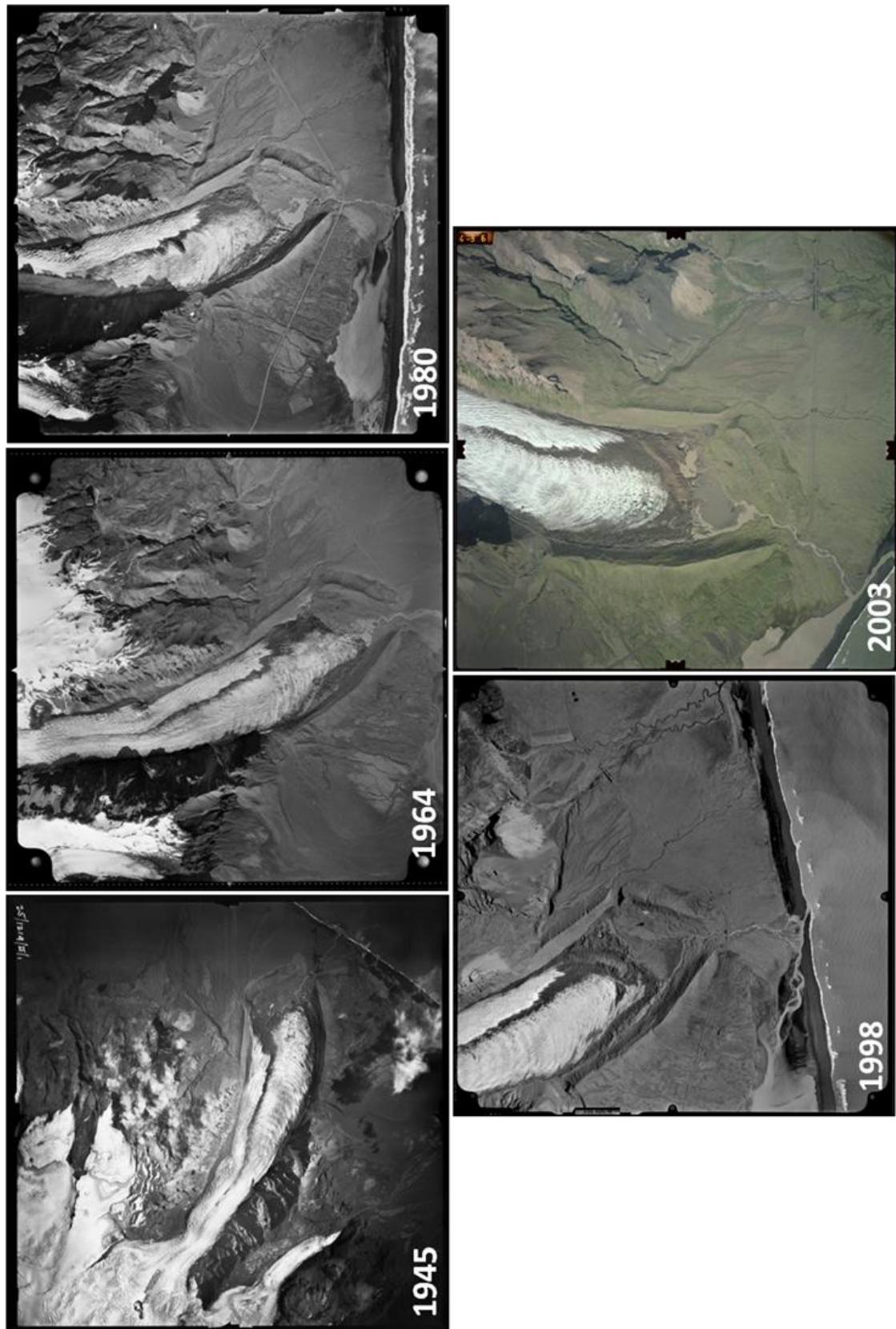
Fig 4.2 - Time series of scanned historical aerial photography used to generate DEMs. Different orientations result from different flight line directions.

Table 4.1 - Aerial photograph specifications

Photograph[a]	Nominal Scale	Camera calibration	Ground resolution
1945 BW	1:50000	Only focal length +flying height	73
1964 BW	1:50000	Complete	90
1980 BW	1:50000	No fiducials	68
1998 BW	1:30000	Complete	82
2003 BW	1:25000	Complete	51

[a] BW and C indicate panchromatic and colour photography respectively
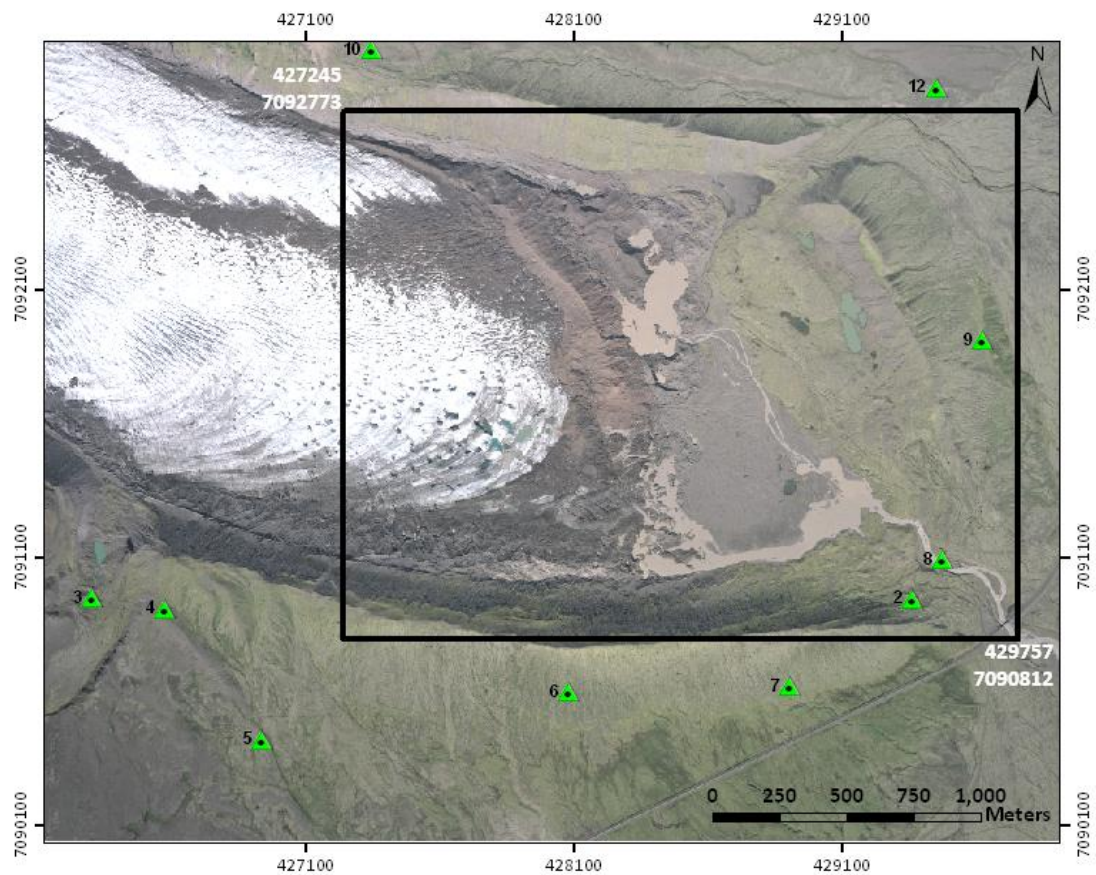
Fig 4.3 - Map showing location of GCPs (green triangles) and area of interest for DEM interpolation and subsequent morphometric analysis

4.1.3 **Data processing**

Digital photogrammetric processing of the aerial photographs was conducted in Leica Photogrammetry Suite 9.1 (LPS). LPS uses the bundle block adjustment to establish, using least squares estimation, the relationship between the positions of a set of photographs and a ground coordinate system, based on the interior and exterior parameters input into the software and the location of ground control points. Each set of photographs was processed as for a metric camera with the exception of 1945 and 1980 for which incomplete camera calibration information required processing as for a non-metric camera. The projection used was UTM, and the spheroid WGS 84 for zone 28N.

4.1.4 **DEM quality**

4.1.4.1 *Main challenges of archival photogrammetry*

Fox and Cziferszky (2008) highlight a number of potential problems associated with the use of historical aerial photography: a lack of ground control; poor photographic quality; incomplete camera calibration data; and the unavoidable use of paper prints. Whilst it is important to be aware of these problems particularly in assessments of DEM quality, they are not insurmountable as demonstrated by studies that have successfully quantified surface changes from historical imagery (e.g. Etzelmüller and Sollid, 1997; Cox and March, 2004; Fox and Cziferszky, 2008; Racoviteanu et al., 2008; Schomacker & Kjær 2007; Schiefer and Gilbert, 2007; Pope et al., 2007; Fox and Cziferszky, 2008; Racoviteanu et al., 2008). The preparation of aerial photographs and collection of adequate ground control are critical to the success of digital photogrammetry. The importance of ground control is highlighted by a study of changes in the geometry of Midre Lovenbreen in Svalbard, Norway, (Rippin et al., 2003). A lack of ground control resulted in error estimates greater than measured changes in glacier geometry. A number of studies using archival photogrammetry have overcome this lack of ground control. For example, Andreassen et al. (2002) and Fox and Cziferszky (2008) were able to apply contemporary ground control retroactively to control historical photography in their studies of volume change of glaciers in Norway and Antarctica respectively. Image quality may be maximized by scanning paper prints

on a photogrammetric scanner. Typically a photogrammetric scanner produces digital images with pixels dimensions ranging from at least 5 – 15 µm, achieving the resolution threshold of typical aerial photography.

Nonetheless, a degree of error is inherent in the multistage process of photogrammetry. Unlike controls on DEM quality associated with conventional methods of DEM collection, controls associated with automated DEM extraction are harder to quantify as many are dependent on the system used for data collection. A potential danger is to assume that accurate data are being produced simply based on the sophisticated techniques used in digital photogrammetry (Chandler, 1999). A number of studies have been criticized for not properly checking the quality of results (Pope et al., 2007), which leads to uncertainty in data derived from DEMs. Thus, any photogrammetric study, particularly one using digital collection, should involve an assessment of DEM error so as to determine the significance of any subsequent data that might be derived from the DEMs.

4.1.4.2 *Types of error*

The description and quantification of DEM errors involve consideration of the three components of quality used in surveying and terrain modelling: reliability; accuracy; and precision (Cooper and Cross, 1988; Butler *et al.*, 1998; Cooper, 1998). These three components all affect the degree to which the DEM matches the real earth surface that it represents and therefore describe the *quality* of the DEM.

Reliability refers to highly anomalous elevation values or 'blunders' (Lane et al., 2000) in the DEM surface. These are large errors that may occur for a number of reasons including incorrect surveying procedures, input errors, problems with aero triangulation, stereo-matching failures and poor image quality (diapositive imperfections and dark shadows or localized patches of glare within the photographs). If reliability is not too low these errors can usually be detected visually since they appear as spikes or holes in the data. These can then either be removed, or acknowledged within the quality assessment.

Accuracy refers to errors that are regular or repeated (Squires, 1968). These are systematic errors that may result from incorrect treatment of atmospheric and Earth curvature effects, on-screen fiducial and point measurement errors and improper camera calibration (Cooper, 1998). As their effects are cumulative, they can quickly become large if left unchecked. They are typically assessed by comparing a DEM to an independent check dataset (Wise, 1998) of greater and known accuracy for example check points collected by ground survey.

Precision refers to random errors that are inherent in the measurement process. Poor precision results from unavoidable factors such as natural variations image scale and signal-to noise ratio (SNR) of the imagery (Cooper and Cross, 1988). They can be quantified through repetition of measurement and described by the standard error of measurements.

4.1.4.3 *Quantifying error*

Typically, the DEM quality is quantified using the root mean square error (RMSE), given by:

$$RMSE = \pm\sqrt{\frac{\sum_{i=1}^{n} d_i^2}{n}}$$

[5]

Source: Lane et al. (2000)

where d_i is the difference in height at point i and n is the number of points compared.

However, RMSE does not include a term to describe the systematic error (accuracy) and as such its calculation implies the assumption that no such error exists. Li (1988) therefore recommends reporting data quality in terms of mean error (ME) and standard deviation of error (SDE) as given by:

$$ME = \frac{\sum_{i=1}^{n} d_i}{n}$$

[6]

$$SDE = \sqrt{\frac{\sum_{i=1}^{n}(d_i - ME)^2}{n}}$$

[7]

to yield an accuracy statement of the form $ME \pm SDE$. Thus, both systematic error (ME) and random error (SDE) are reported in the DEM quality statistics.

4.1.4.4 *Stereo-matching and error*

An issue influencing DEM quality that has received particular attention in the literature is the effect of the stereo-matching strategy on the quality of the resultant DEM (e.g. Gooch et al., 1999). The stereo-matching strategy is defined by a number of parameters such as search window size, correlation window size, correlation coefficient limit and a number of filters. A number of pre-defined strategies are offered by software packages. Leica Photogrammetry Suite offers strategies for different types of topography, for example: 'middle mountains', 'rolling hills' and 'steep mountains'. The strategy may alternatively be custom defined as seen fit by the user. The selection of strategy parameters was based on a visual inspection of DEMs output using different strategy parameters as time did not permit a more comprehensive assessment of the affects of strategy parameters on the automated stereo-matching process. The strategy parameters selected varied slightly for each set of photographs (Table 4.2).

A 5 x 5 correlation window size was used (Table 4.2), which resulted a different DEM resolution for each date (Table 5.1), depending on the size of a pixel in real space in the aerial photographs. For example, the size of one pixel in real space in the 2003 photographs is 51cm. The maximum DEM resolution that can be achieved using a 5x5 pixel window is 5 times this value, 2.55. Whilst a finer resolution DEM could have been generated using a smaller window size, such as 3x3, this would have resulted in greater matching errors as there is an increased likelihood that 9 pixels will match the wrong 9 pixels in the other image using a 3x3 window, than 25 pixels being wrongly matched using a 5x5 window. Therefore DEM resolution was sacrificed for the sake of better DEM quality.

Table 4.2 - Strategy parameter specifications used for each set of photographs

Year	Search window	Correlation window	Coefficient Limit	Topographic type	Object type	DTM filtering
1945	15 x 3	5 x 5	0.7	Rolling hills	Open area	moderate
1964	15 x 3	5 x 5	0.7	Rolling hills	Open area	low
1980	15 x 3	5 x 5	0.7	Rolling hills	Open area	none
1998	21 x 3	5 x 5	0.7	Rolling hills	Open area	moderate
2003	15 x 3	5 x 5	0.7	Rolling hills	Open area	none

4.1.4.5 *Error assessment*

As only 12 GCPs were available it was considered necessary to use all of these in setting up the terrain extraction model, so as to best constrain the model. However, this left no external checkpoints against which to compare the accuracy of the DEMs. As an alternative, internal checkpoints were extracted from the 2003 DEM, which had the lowest RMSE (0.39) of all the DEMs based on the GCP residuals, and therefore the highest vertical accuracy. 50 check points were extracted from the 2003 DEM from stable points around the lateral moraines, which were deemed to have not moved within the study period by visual comparison between the 1945 and 2003 orthophotos (Fig 4.4). Elevations of the checkpoints were extracted from each DEM and compared against the 2003 values.

Both the mean error and standard deviation of error were calculated, the former giving a measure of accuracy, and the latter a measure of precision. Reliability was assessed by visual inspection of the DEMs. Blunders were removed where possible by changing strategy parameters and regenerating the DEM, or otherwise acknowledged in subsequent analysis.
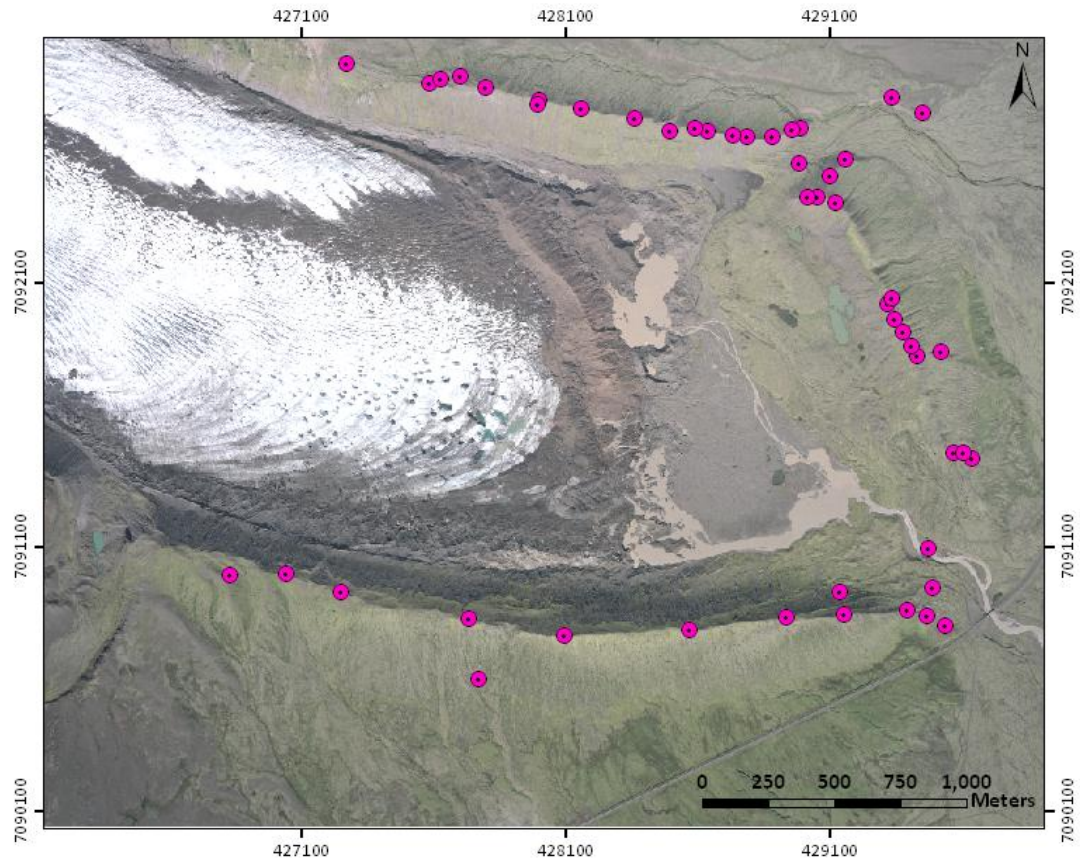
Fig 4.4 - Map of 50 checkpoints used in error assessment on 2003 orthophoto

4.1.5 **Morphometric analysis**

Morphological changes can be quantified by subtracting sequential DEMs, or sections of DEMs, extracted by photogrammetry for different snapshots in time. This approach has been widely used to reconstruct volume changes of landforms and land surfaces caused by a variety of processes including gully incision (De Rose et al., 1998; Betts et al., 2003; Schiefer and Gilbert, 2007), coastal cliff erosion (Adams and Chandler, 2002) and glacier recession (Etzelmüller and Sollid, 1997; Cox and March, 2004; Jordan et al., 2005; Riviera et al., 2005; Schiefer and Gilbert, 2007). Several other relief parameters, as well as surface elevation, may also be extracted from sequential DEM, which may be used to analyze surface changes in greater geomorphological detail (Etzelmüller and Sollid, 1997). Four relief parameters that describe surface form are: surface elevation (altitude), surface gradient (slope), exposure of the slope (aspect) and slope form (curvature). The science of geomorphometry aims to 'objectively quantify and compare landscape forms and patterns' (Etzelmüller and Sollid, 1997) based on these

parameters. These parameters are constantly changing during the retreat of a glacier and the melt of ice cores in the glacier foreland. For example, slope and curvature vary according to the driving stress and glacier velocity according to flow relationships (Paterson, 1994). Slope gradient of moraines decreases through time as a result of sediment redistribution (Sharp, 1984). These relief parameters can thus be measured from DEMs and used to analyze ice dynamics and processes of landform development.

Morphometric analysis, unless stated otherwise, was conducted in MATLAB. The extraction of five digital elevation models between 1945 and 2003 enabled the quantification of surface changes for four time periods: 1945 – 1964; 1964 – 1980; 1980 – 1998; and 1998 – 2003. Prior to morphometric analysis all DEMs were cropped to an area of interest covering the glacier snout and foreland (Fig 4.3) and interpolated to a standard 1m resolution grid. Sequential DEMs were subtracted from each other to derive difference matrixes over each interval of time on a pixel-by-pixel basis (Etzelmüller and Sollid, 1997). Elevation changes directly converted into volume changes, the area of 1 pixel being equal to 1m², enabling the quantification of volume change and de-icing rates in the glacier snout and foreland over the study period. Difference matrixes were transferred into ArcGIS for integration into a Geographic Information System (GIS) so as to visualize elevation change across the glacier snout and foreland. Calculations and visualizations of ice loss for the four time periods were used to assess spatial and temporal variation in glacier behaviour. Aspect and slope gradient DEMs were generated in ArcGIS so as to visualise changes in the parameters in relation to elevation changes. Two-dimensional profiles of various orientations were extracted in MATLAB from the DEMs across the glacier snout and foreland to assess relief change for each time period.

4.2 Geomorphological mapping

The geomorphological maps were produced from orthophotos output during the photogrammetric process. Orthophotos are essentially 'photo-maps': aerial photographs with distortion removed by resampling using elevation data produced by digital photogrammetry. Overlays of the surficial geology and geomorphological features were digitally drawn in ArcMAP using these orthophotos, aided by

stereoscopic viewing, different visualizations of the DEMs, interpretation of the aerial photographs, and by the author's knowledge of the ground from field work. A UTM grid (WGS84, 28N) was used, following the system currently used on Icelandic maps produced by Landmælingar Íslands. Contour plots of 10m intervals that accompanied the extraction of the DEMs were smoothed in ArcMAP using a smoothing algorithm. The cartographic design was based on previous maps produced by Howarth and Walsh (1969a,b) Evans and Twigg (2002) and Evans et al. (2006a, b; 2007). The final maps are plotted at 1:10000 in scale.

Several visualization methods were used to aid interpretation of the topography from the DEMs (Smith and Clark, 2005) (Fig 4.5).
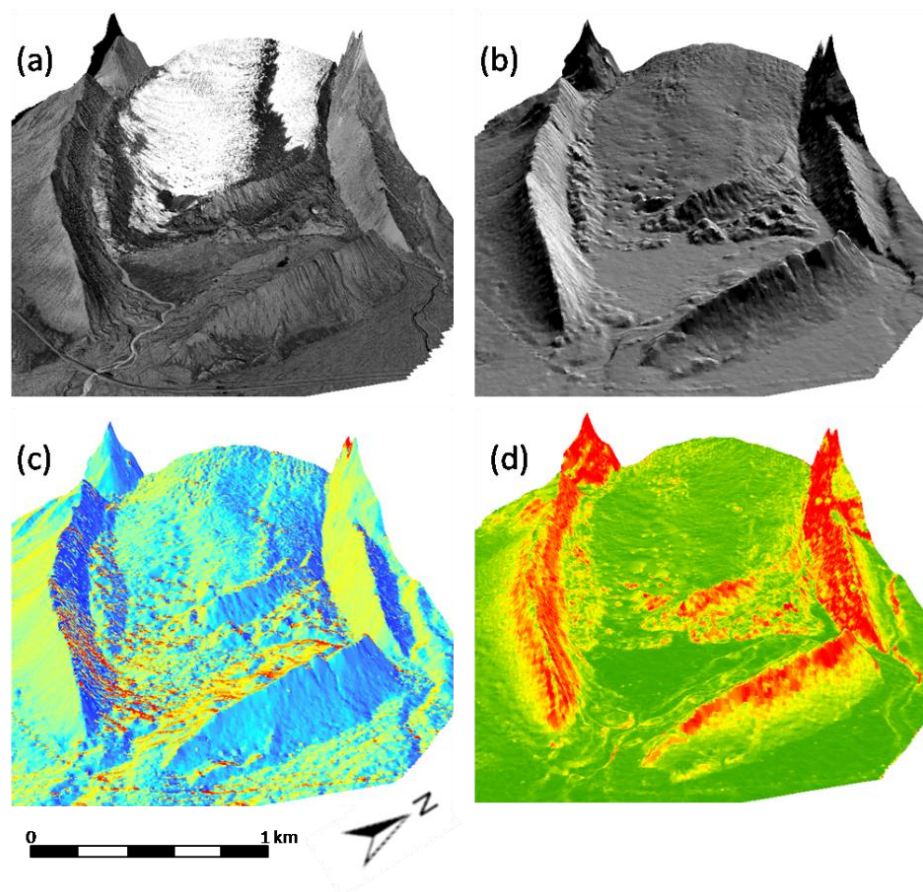
Fig 4.5 - Visualisations of 1998 DEM: (a) overlaid with orthophoto, (b) hillshaded, (c) aspect shaded, and (d) slope gradient shaded.

The default DEM output is a grey scale, grid-based plot in which the elevation of each cell is represented as a shade of grey. However subtle variations in topography are not defined in this visualization. There are several techniques that better depict these subtle variations such as relief-shading, slope-gradient and aspect-shading (Fig 4.5). Relief-shading is particularly popular and is increasingly used as standard in landform mapping (Smith and Clark, 2005). It uses a specified illumination (azimuth and elevation) to shade the topography (e.g. Pike, 1992). However Smith and Clark (2005) warn that the use of a certain direction of light introduces bias into the visualization of landforms, especially linear forms. Care was therefore used in the interpretation of features from each visualization technique.

4.3 Process-sediment-landform associations

4.3.1 Selection of moraine complexes

The length of the study period does not cover the full period of evolution of debris-covered ice into fully de-iced moraine. Therefore a number of complexes at increasingly advanced stages of development (A – D) were identified in order to try to piece together the evolutionary stages of hummocky moraine at Kvíárjökull (Fig 4.6). These areas were subjected to more detailed morphometric analysis. For each area total elevation change and average annual elevation change were calculated during the four time periods as a measure of the rate of de-icing of ice-cored landforms in the glacier foreland. A new type of cross profile was devised for visualizing relief change in moraine complexes, called a 'meshed temporal profile'. This includes time as an explicit axis (z), additional to the elevation (y) and distance (x) axes of conventional two-dimensional profiles. The major advantage of these over two-dimensional profiles is that the eye does not have to read overlapping lines of different years, as these are meshed together, making surface change visually easier to interpret. Lastly, slope gradient maps were generated for the moraine complexes to assess the impact on moraine relief of de-icing.
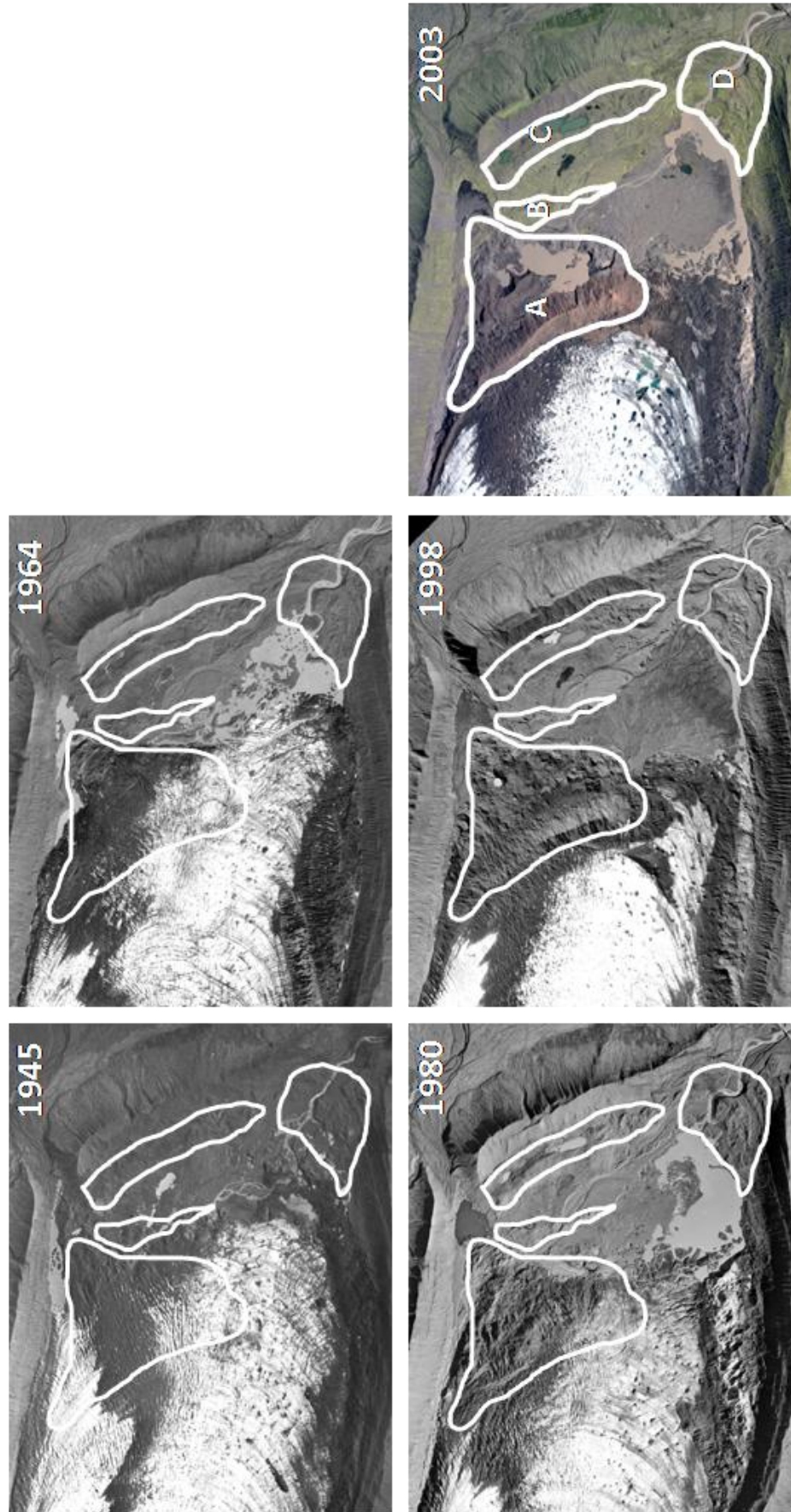
Fig 4.6 - Moraine complexes A – D located within orthophotos 1945 – 2003.

For each moraine complex morphometric analysis was combined with field mapping and data collection to identify process-sediment-landform associations involved in moraine development. A study of the structural glaciology and sedimentology within the present day debris-mantled glacier snout terminus were also conducted, as part of the holistic assessment of process-sediment-landform associations involved in moraine evolution (Evans, 2003). Three models of moraine formation were considered, outlined in Chapter 2: a push moraine model (Evans and Hiemstra, 2005) (Fig 2.5); and 2 models of controlled moraine development from englacial debris concentrations (Boulton, 1972, Fig 2.7; Bennett et al. 1998, Fig 2.8). Details of these models are outlined in Chapter 2 and further details are given in Chapter 5.

4.3.2 Structural and sedimentological mapping of the glacier terminus

Englacial sediment sources feeding supraglacial moraine ridges are exposed at melting margins and within collapsed cavities, making observations on their structure and sedimentology possible. Spedding and Evans (2002) and Swift et al. (2006) collected data on debris band spacing, thickness, clast form and sediment concentration at sites around the glacier snout. Clast form analysis is the study of pebble sized and larger clasts (Benn, 2007) so as to deduce their transport history. Clast form is defined by three properties: shape, roundness and texture, certain combinations of which are typically produced by different transport pathways. As clast form is not substantially modified by resedimentation processes (Spedding and Evans, 2002), this type of analysis is a reliable and valuable technique for distinguishing between different debris populations with different transport histories and has been used widely to aid process-based explanations of glacigenic deposits and to refine landsystems models (Matthews and Petch, 1982; Benn, 1989; Evans, 1999).This data was combined with further observations and mapping of englacial debris concentrations and supraglacial moraine ridges made during fieldwork in September 2007 and 2008 to identify four types of debris concentrations and associated supraglacial moraine ridges.

4.3.3 Structural and sedimentological study of ice-cored moraine (Complex A)

The structure and sedimentology of several ridges within ice-cored moraine complex A was assessed using cross profiles (extracted from DEMs and surveyed in the field),

photographs, field sketches, and clast form analysis. Clast form analysis was conducted for samples of 50 clasts collected at sites 1 – 6 along a surveyed profile (Fig 4.7) through the moraine as well as at an additional site (7) so as to deduce the transport history of sediment contained in moraine ridges. The a, b, and c axes of each clast was measured to define its shape, and its roundness recorded according to the roundness index of Powers (1953). Additionally, the presence of striations, indicative of transport in the basal traction zone (Boulton, 1978), was noted. Covariance analysis of clast shape and roundness was conducted on these samples by comparing the C_{40} index with the roundness angularity index (Benn and Ballantyne, 1994). The C_{40} index is the percentage of clasts with a c:a axis ratio of greater than 0.4 and the roundness angularity (RA) index is the percentage of very angular and angular clasts. There is a distinctive positive correlation between these indexes for the reason that actively transported clasts tend to be blockier and more rounded than passively transported clasts (Ben and Ballantyne, 1994; Spedding and Evans, 2002). The indexes of the samples were plotted on the clast form covariance plot devised for Kvíárjökull by Spedding and Evans (2002) (Fig 4.8) enabling the samples to be classified as one the debris populations identified within the plot.
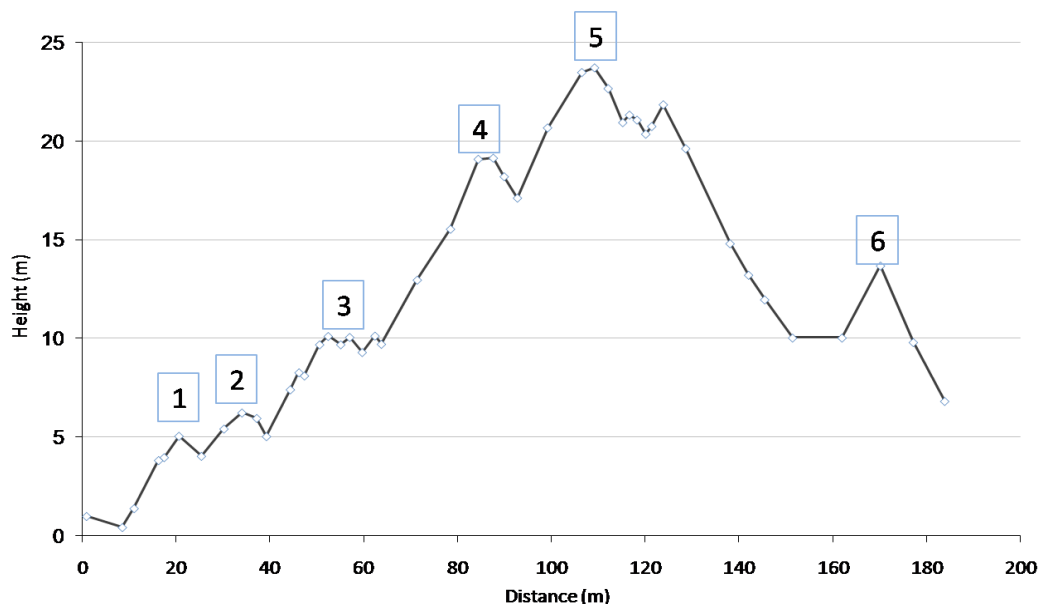
Fig 4.7 - Location of sites along cross profile through ice-cored moraine.
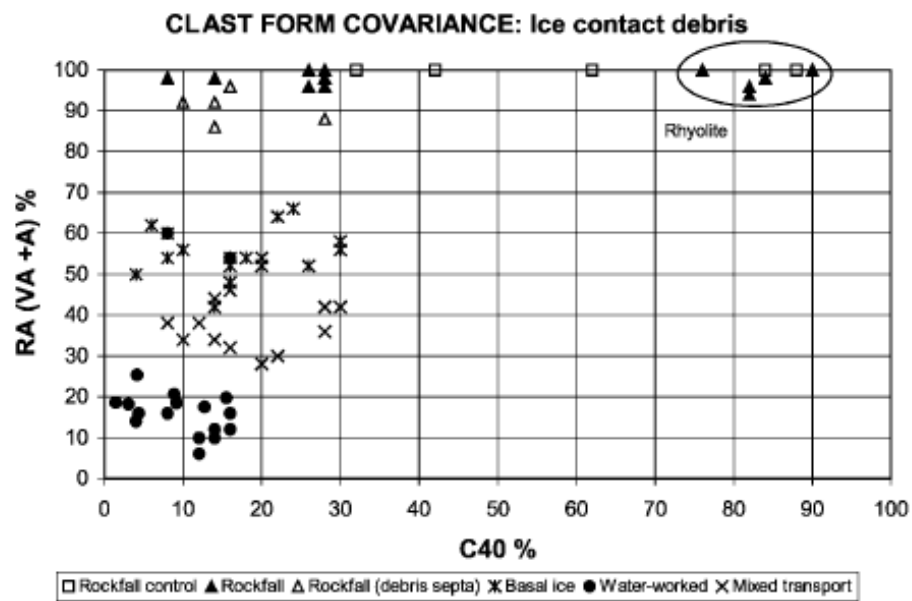
Fig 4.8 - Clast form covariance plot for ice-contact debris based on Kvíárjökull (Source: Spedding and Evans, 2002)

4.3.4 Ice disintegration and re-sedimentation processes within ice-cored moraine (complex A)

Two ablation processes are well-known: backwasting, defined as the sub-horizontal retreat of near-vertical free ice-walls, or steep ice-cored slopes; and downwasting, defined as the thinning of ice-cores by melting along the top and bottom surfaces (Kjær and Krüger, 2001) (Fig 4.9). As ice-cores disintegrate the sediment cover is reworked by a number of processes. The spatial distribution of re-sedimentation processes within an active ice-cored moraine complex still attached to the glacier snout was mapped in detail from the 2003 orthophoto, following the established methodologies of Kjær and Krüger (2000) and Kjær and Krüger, (2001). The long-term downwasting of ice-cored moraine was quantified by morphometric analysis of the DEMs. The processes of backwasting and downwasting were quantified in the short term by comparison of a profile surveyed in the field in 2008 and located using a handheld GPS (Fig 4.7), with the same profile extracted from the 2003 DEM and by comparison of the latter with the 1998 DEM. This enabled the assessment of the degree of modification and the preservation potential of controlled and pushed ridges within ice-cored moraine
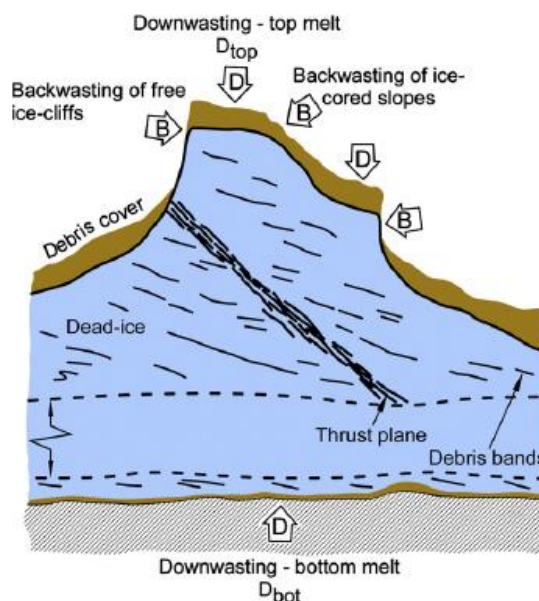
Fig 4.9 - Range of ice disintegration processes in ice-cored moraines: backwasting (B) and downwasting (D) by top melt and bottom melt. (Source: Schomacker, 2008).

4.3.5 Structure, sedimentology and morphology of older moraine complexes (B – D).

Morphometric analysis was combined with field mapping, sediment logging and clast form analysis within older moraine complexes. Sediment logging is an important tool that has been used by geomorphologists for many years to describe sediment properties, geometry and position in relation to adjacent sediments and the land surface within sub-surface exposures and out-crops (Evans and Benn, 2004). When combined with landform maps of surficial geology and geomorphology sediment logs give a three-dimensional picture of sediment assemblages (Benn and Evans, 1998, pp384-385). An exposure through a moraine ridge within moraine complex B was recorded in a two-dimensional sediment log, showing the internal sedimentology and structure of the moraine. Lithofacies were mapped using the codes of Miall (1978), Eyles et al. (1983) and Evans and Benn (2004). Clast form data collected by Spedding and Evans (2002) within hummocky moraine contained within moraine complex D was included in an assessment of the processes involved in its development.

5 Results and analysis

5.1 Digital Elevation Models

Five DEMs (Figs 5.1 and 5.2) and orthophotos (Fig 4.6) were generated from the historical aerial photography with ground resolutions from 2.5 to 4.5m, depending on the resolution of the aerial photograph (Table 5.1) and based on a 5x5 correlation window in the stereo matching process. The 1980 DEM does not provide full coverage of the study area due to incomplete aerial photograph coverage.

Table 5.1- DEM specifications

Year	Resolution of DEM	Number of GCPs used	RMSE compared to GCPs	DEM coverage of study area
1945	3.6	3	7.74	Complete
1964	4.5	8	1.03	Complete
1980	3.4	6	0.96	Top left corner missing
1998	4.1	11	0.71	Complete
2003	2.6	7	0.39	Complete

5.2 DEM error assessment

Mean error is a measure of the systematic error, or accuracy of the DEMs. The mean error, based on comparison of the DEM with the 10 GCPs, is generally less than 1m for 1964 – 2003 DEMs, but significantly larger for 1945 at 3.86m. Half of the GCPs (3 – 7) (Fig 4.3) are located on the outer slopes of the southern lateral moraine ridge, which is affected by shadowing from overhead cloud cover in the 1945 imagery. Consequently, poor image matching has resulted in poor DEM quality along this ridge. This is apparent on visual comparison of the ridge in the 1945 DEM with the ridge in the other DEMs. The ridge surface in the 1945 DEM is highly uneven compared to the smooth surface of the slope in the other four DEMs. Large errors along this ridge have increased the mean error for the 1945 DEM. DEM quality can be visually assessed by comparing temporal profiles across the lateral moraine ridges. For example, there is close correspondence across the southernmost ridge apex in profiles 1-4 (Fig 5.21) and across the frontal ridge apex in profiles 5 – 9 (Fig 5.22). The exception to this is the

1945 profile, which diverges from the ridge in several of the profiles. However, in all cases the divergence of profiles across these stable features of the landscape is minimal compared to the magnitude of the changes occurring across the glacier snout and foreland. The quality across the rest of the DEM surface is visually acceptable (Figs 5.1 and 5.2).

Both systematic and random errors (representing accuracy and precision of DEMs respectively) were evaluated by comparison of 1945 – 1998 DEMs with the 2003 DEM at points where no elevation change was expected to have occurred over the study period. Systematic errors are higher than those calculated from GCP residuals ranging from 0.75m in 1998 to -3.11m in 1945 (Table 5.2). Random error is displayed in histograms (Fig 5.3). These errors may partly reflect real elevation changes as although checkpoints were selected at apparently stable points around the lateral moraines (Fig 4.4), their stability is not certain. Apart from the 1945 data, the errors are positive compared to 2003, suggesting that this error may partly be the result of mass wasting processes reducing the elevation of the lateral moraine surface and therefore that of the checkpoints through time.

Table 5.2 - Errors based on external GCPs and internal (2003) checkpoints

	Vertical accuracy of DEMs compared to GCPs		Vertical accuracy and precision of DEMs compared to 2003 checkpoints	
Year	Mean error	RMSE	Mean error	Standard deviation of error
2003	-0.11	0.39	0	0
1998	-0.25	0.7	0.75	1.75
1980	-0.89	1.38	2.2	3.19
1964	-0.69	1.03	2.36	3.79
1945	3.86	7.74	-3.11	5.36
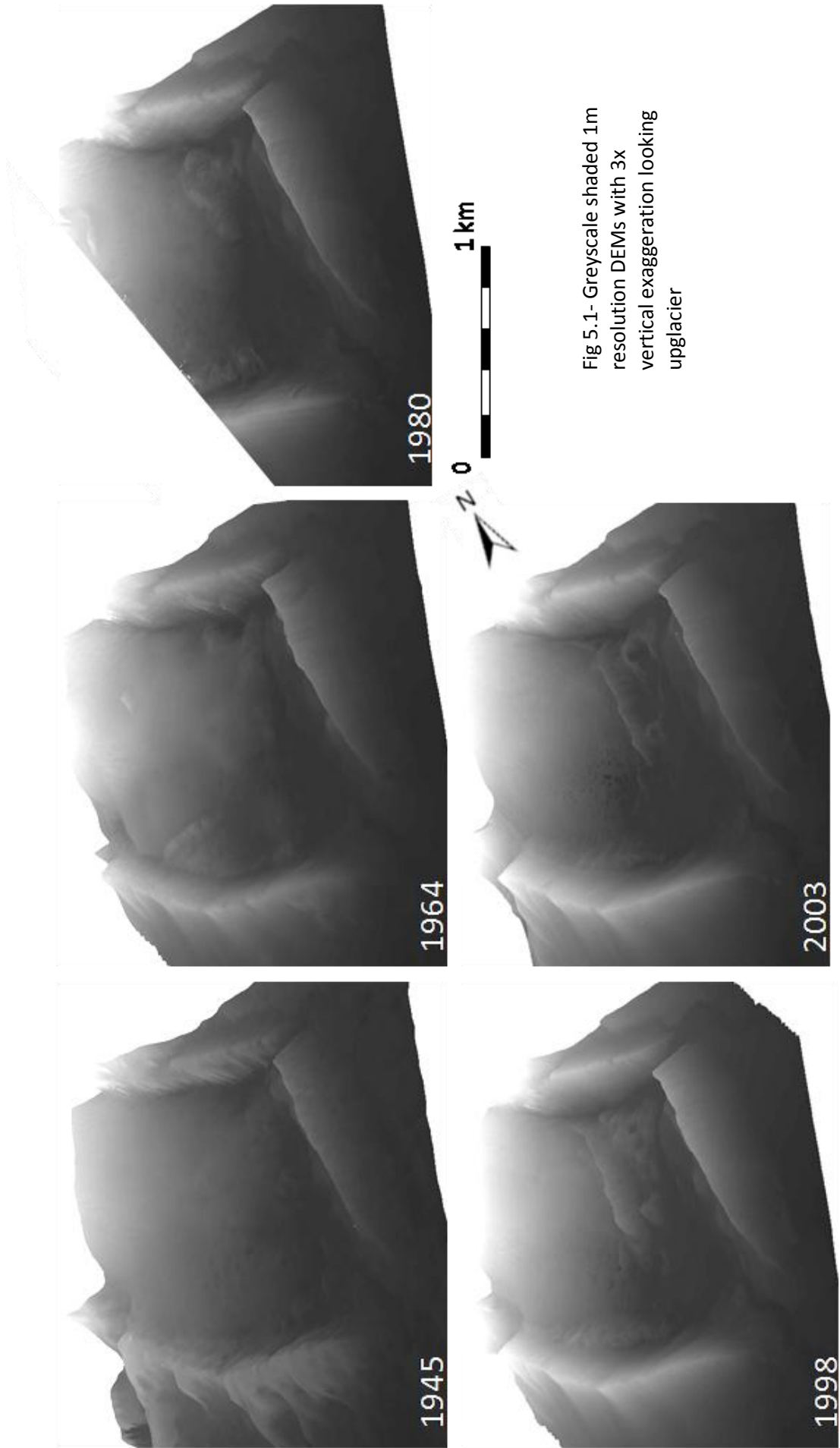
Fig 5.1- Greyscale shaded 1m
resolution DEMs with 3x
vertical exaggeration looking
upglacier

1980

1964

2003

1945

1998

1 km

0

N
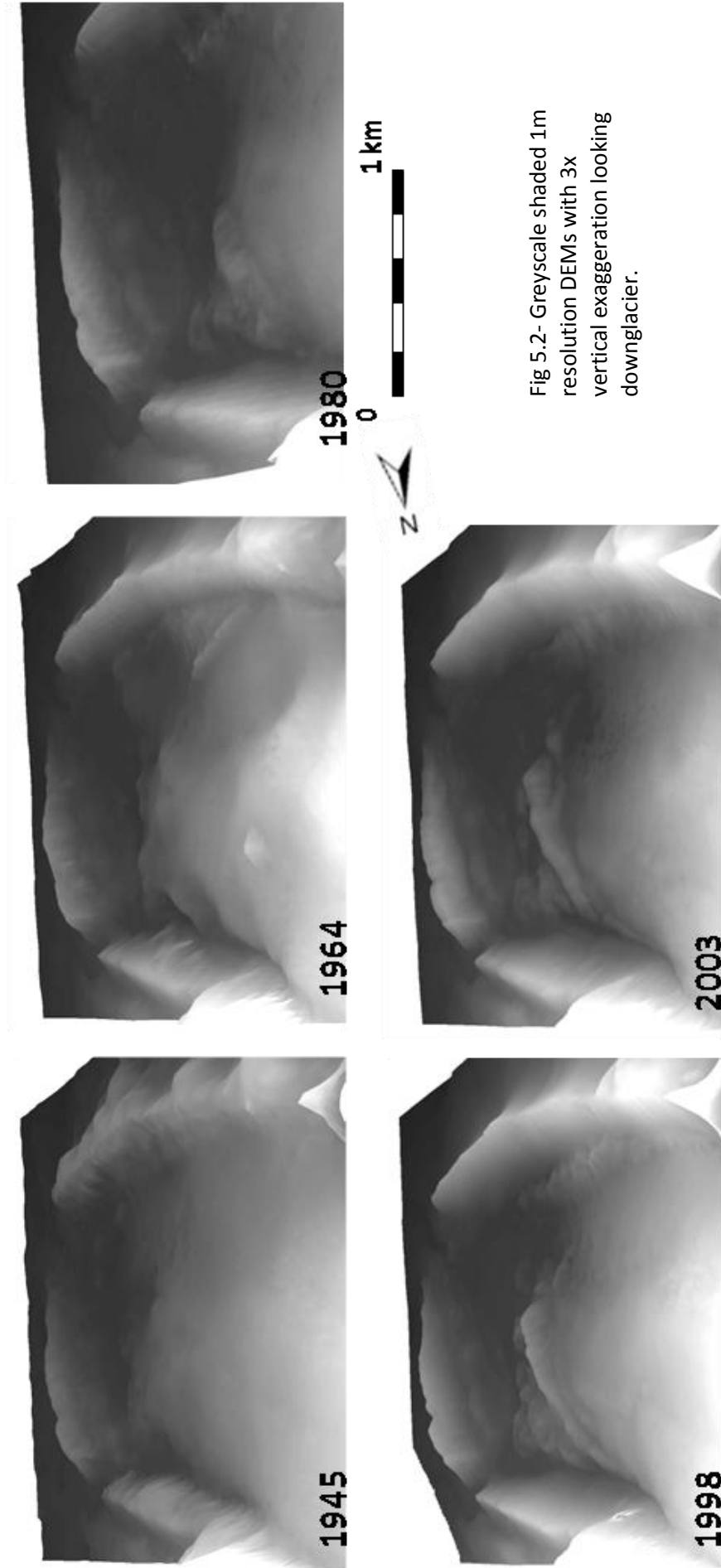
Fig 5.2- Greyscale shaded 1m resolution DEMs with 3x vertical exaggeration looking downglacier.
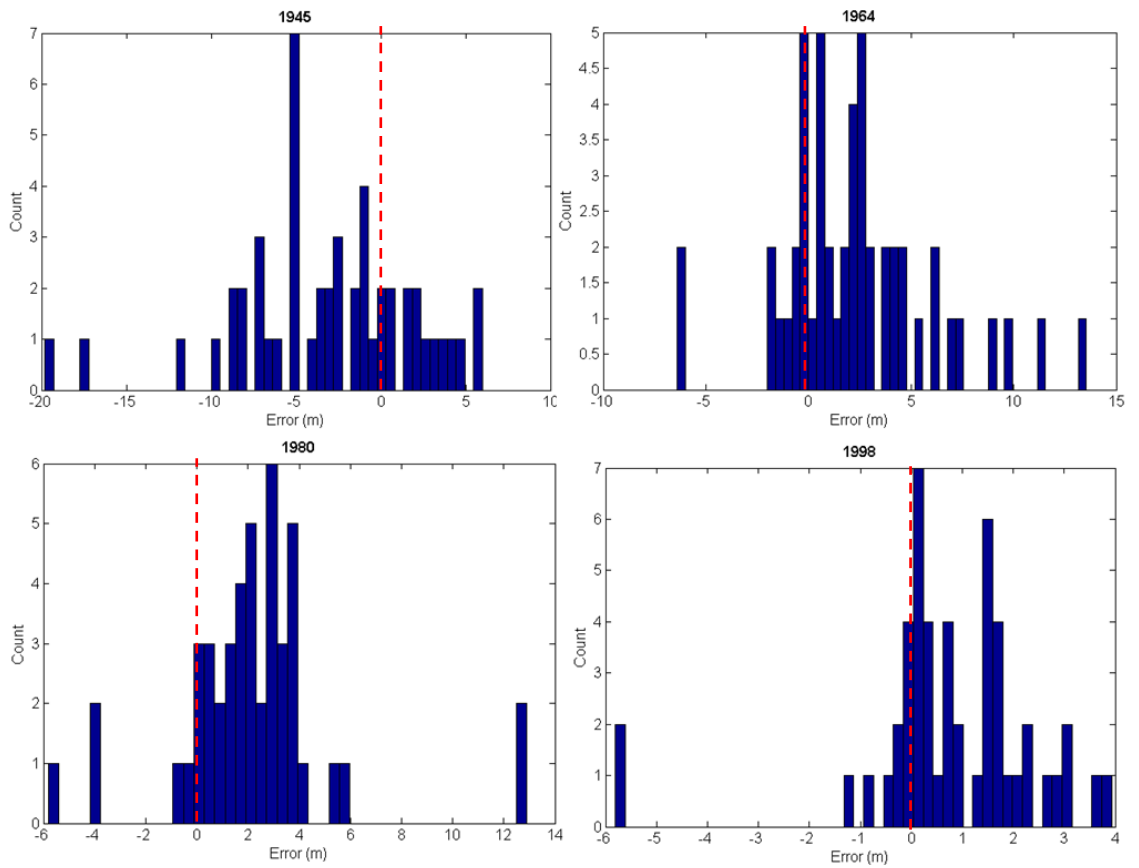
Fig 5.3 - Histograms showing the distribution of errors compared to 2003 checkpoints
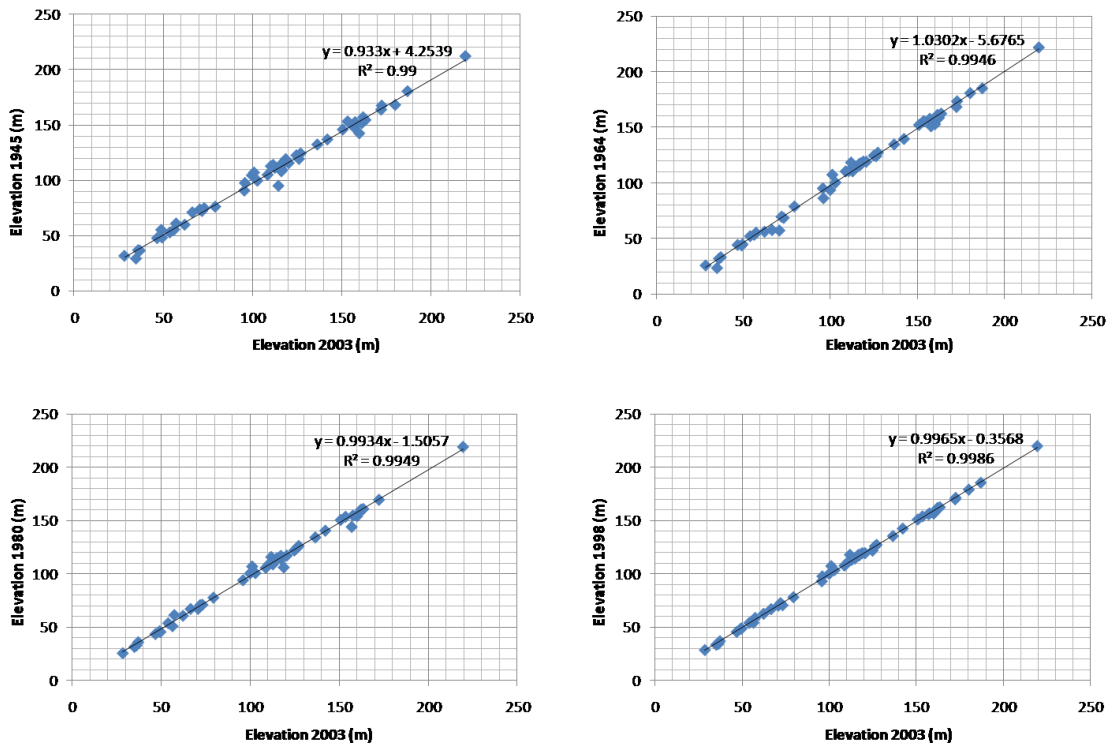
Fig 5.4 - Regression plots of checkpoint elevations for each year compared to 2003

There is generally a positive relationship between photograph age and DEM quality (Table 5.2), reflecting the limitations of using historical aerial photography for extracting high resolution DEMs. However, error estimates are considered to be conservative because image texture and therefore image matching accuracy are generally low over rock surfaces (Schiefer and Gilbert, 2007; Baily et al., 2003), where all the GCPs are located. Image texture is greater over the heavily crevassed and partly debris covered ice surface that characterizes the area of interest. Better image matching over these areas is indicated by higher reported correlation scores in DEM extraction reports. All GCPs were located along the crests and slopes of the steep lateral moraine ridges along which shadowing and illumination effects may have further reduced image matching success. Slope gradient at checkpoints may also have increased error. Schiefer and Gilbert (2007) found that DEM error was greater on steeper slopes. Image matching was particularly poor along the southern moraine ridge in the 1945 DEM due to shadows cast by overhead clouds in the aerial photography. As 10 (25%) of the checkpoints are located along this ridge this will have substantially increased the error score for the 1945 DEM.

5.3 Surficial geology and geomorphology

In addition to bedrock surfaces (blue/grey), eleven surficial geology units are mapped as polygons of various colours in the Kvíárjökull area (Figs 5.5 – 5.9) and are described below (5.3.1 - 5.3.9). Geomorphological features are mapped using symbols and these are described below in association with surficial units in which they occur. Scree and paraglacial deposits of all ages are included in one section (5.3.8).

Figs 5.5 – 5.9 on following 5 pages: Time series of maps: 1945, 1964, 1980, 1998, 2003. The 1945 and 2003 maps have greater coverage of the glacier snout than the intervening years, almost to the base of the icefall, due to the greater coverage of the aerial photography for these dates. The DEM in the southern part of the 1945 map contains significant distortion as indicated by dashed contours. The southwest corner of the 1980 map contains no contours due to incomplete image coverage.

Fig 5.5

Fig 5.6

KVÍÁRJÖKULL 1980

SCALE 1:10,000

0   250   500   750   1,000
Meters

Glacilacustrine deposits	Glacier ice
Glacifluvial deposits	Supraglacial debris cover
Jokhulaup outwash	Till - ice cored-moraine
Blockfield and residuum	Till - Post Little Ice Age
Paraglacial deposits	Till - Little Ice Age
Bedrock	Till - Pre-Little Ice Age
Scree	Lakes and Streams
Moraine ridges	Ice-walled lake plain
Boulder ridge	Kettle holes
Eskers	Proglacial meltwater channels
Kame terraces	Lateral meltwater channels
	Abandoned meltwater channels
	Fluvial terraces
	Moulins
	Ice-walled channels
	Ice cliff
	Collapsing edge
	Contours (10m intervals)
	Road

N

Fig 5.7

Fig 5.8

Fig 5.9

5.3.1 Glacier ice with supraglacial debris cover

Supraglacial debris cover forms a thin veneer of debris on the active glacier surface and is concentrated in the medial moraine and at the margins of the glacier within margin parallel strips and transverse debris bands. This unit represents the initial stage in a sequence of development of ice-cored moraine, referred to as "the young phase" by Clayton (1964) and related to active ice and transport of debris to the glacier surface. The glacier snout can be divided into two zones, north and south, based on its coverage of supraglacial debris. The southern zone is dominated by a large area of clean ice that is characterized by sets of longitudinal crevasses further upglacier, and moulins and transverse debris bands towards its frontal margin. This zone is bounded along its southern margin by supraglacial moraine and ice-cored moraine and terminates in a proglacial lake in 1964, 1980 and 2003 and in ice-cored moraine in 1945 and 1998. The supraglacial debris cover at the frontal margin is dissected by ice-walled channels (green line symbol) that are occasionally continuous with eskers (red line symbol). The northern zone is narrower than the southern zone and is dominated by the medial moraine, which descends from nunataks in the ice fall further upglacier. The medial moraine is heavily crevassed, with longitudinal crevasses appearing on all photographs during the study period. There is a thin strip of glacier ice between the medial moraine and a strip of supraglacial moraine on its northern lateral margin. Unlike the southern zone, this zone terminates in a large ice-cored moraine complex on photographs of all ages. The difference in behaviour between these two snout zones is assessed in section 5.5.3 with regards to the fluctuations of the glacier snout that occur during the study period.

5.3.2 Ice-cored moraine

This comprises ridges or mounds of debris covered ice (Fig 5.10a) (Østrem, 1964; Benn and Evans, 1998, p.247;) of greater relief than supraglacial debris cover, as a result of differential melting and the advanced development of glacier karst features such as ice walled lakes and collapsed englacial tunnels (Clayton, 1964). The unit represents the next stages of development of ice-cored moraine from that represented by supraglacial debris covered ice (Clayton, 1964; Kjær and Krüger, 2001): the "mature phase" represented by a fully ice-cored moraine; and the "final phase", represented by

partially ice-cored terrain. This unit is not necessarily completely detached from the glacier-snout, as is suggested to be necessary by Lukas et al. (2007) in order to classify it as ice-cored moraine; in such settings it is difficult to define the boundary of snout ice, which is likely to continue into the ice-cored ridges and even below the foreland. Additionally, without the direct measurements of velocity it is not possible to classify the moraine as stagnant, despite the debris cover, themokarst features and vegetation cover suggesting this is the case (Kirkbride, 1995).

At the scale of mapping it was possible to map a number of features within the ice-cored moraine that are indicative of the ice disintegration, by the backwasting and downwasting of ice cores, and associated sediment reworking that occurs in ice-cored moraine at the mature stage of development (Kjær and Krüger, 2001). **Boulder ridges** (dashed orange line symbol) are clusters of boulders that typically occur in ridges along the base of ice-cored ridge slopes due to gravitational sorting of debris cover as underlying ice-melts out (Kjær and Krüger, 2001). **Sink holes** (purple point symbol) are small depressions in the debris cover indicating the collapse of underlying ice. Meltwater filled depressions in the ice-cored moraine are mapped using the symbol for **lakes** (blue polygon with dark blue outline) are often bounded by **ice cliffs** (black line with hollow triangle), exposed by slope collapse, fluvial erosion or mass-movement induced by heavy rainfall (Krüger and Kjær, 2000). **Collapsing edges** (purple line) are distinctive fractures along which sediment collapse occurs and along which ice cliffs eventually form (Krüger and Kjær, 2000). These are mapped and described in further detail in Section 5.7.3.1. Neither collapsing edges nor ice cliffs are present in partially ice-cored moraine, in which thick debris cover prevents the exposure of ice and in which de-icing is dominated by down-wasting (Kjær and Krüger, 2001). Ice cliffs and ice-walled lakes can therefore be used to differentiate between mature and partially ice-cored moraine. Boulder ridges, sink holes and lakes are also present in partially ice-cored moraine but are more stable features in such locations. Thick debris cover in this final phase makes it difficult to distinguish from de-iced terrain meaning that moraine mapped as 'Post Little Ice Age till' may still contain small ice cores.

5.3.3 Post Little Ice Age till

This covers most of the outer glacier foreland and includes gently undulating terrain of low relief and moraine complexes composed of margin-parallel linear mounds or hummocks (Fig 5.10b). In places the surface is heavily pitted with depressions, often filled with water. Much of this till and moraine is dissected by channels containing **glacifluvial deposits**, known as ribbon sandur. Process-form relationships involved in the evolution of moraine complexes are considered in detail in Section 5.6.

5.3.4 Little Ice Age till

A 'Little Ice Age' status for the latero-frontal moraine ridges is based on observations by Thórarinsson (1956) that the glacier last filled its foreland and overtopped these ridges during the LIA, although the core of the moraines likely dates to earlier advances (Itturizaga, 2008). Inset moraine ridges (black line symbol) on the inside slopes of these moraines record the gradual retreat of the glacier from its LIA maximum (Evans et al., 1999). Therefore the latero-frontal moraines are composite features built up over the Neoglacial moraine(Thórarinsson, 1956) and much of the underlying material and perhaps the surficial deposits on the distal moraine slopes may be pre LIA.
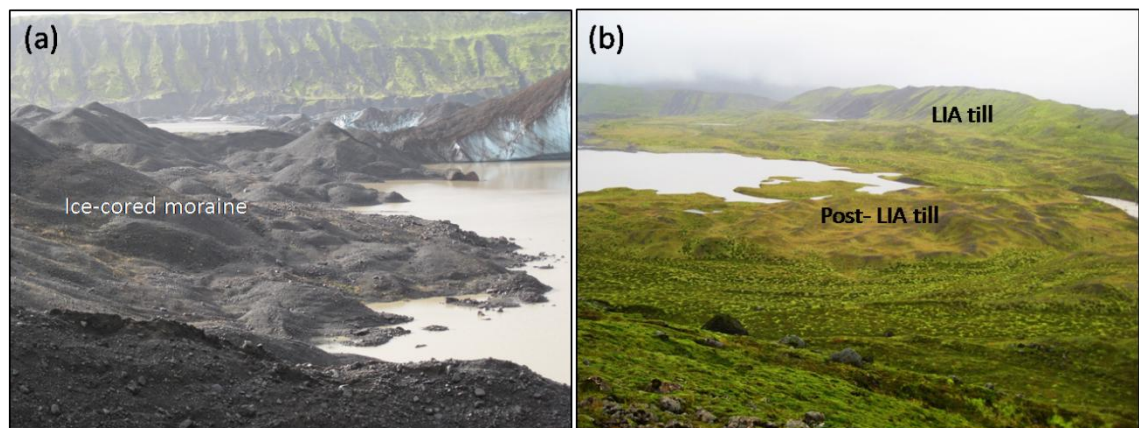
Fig 5.10 (a,b) - Till units: (a) Ice-cored moraine, (b) Post-LIA and LIA till in the outer foreland.

5.3.5 Pre-Little Ice Age till

This is contained within heavily degraded moraines at the tip of the southern lateral moraine, near to the road, and on the outer slopes of the frontal lateral moraine. Although dated at LIA by Evans et al. (1999) these are considered to be older based on the age assessments of Guðmundsson (1998).

5.3.6 Glacifluvial deposits

These are glacial outwash sands and gravels deposited by proglacial and lateral meltwater channels. In 1945 meltwater drained from the centre of the snout terminus creating a small outwash fan through the ice-cored moraine in the foreland. From 1980 onwards this fan was also fed by glacial meltwater from the northern glacier margin and formed an extensive sandur fan across most of the southern glacier foreland cross-cut by a network of **abandoned braided meltwater channels** (dashed blue line symbol).

In places outwash was pitted with **kettle holes** (small beige polygons) and small ponds of water, formed by the meltout of blocks of ice underlying the sands and gravels. Part of the sandur fan that emanates from the frontal glacier snout had collapsed and was heavily pitted with sink holes due to the meltout of underlying snout ice (Fig 5.11a). Grabens and other collapse structures seen in the field indicate that faulting and collapse continues at the edge of the outwash corridor at the northern margin (Fig 5.11b).
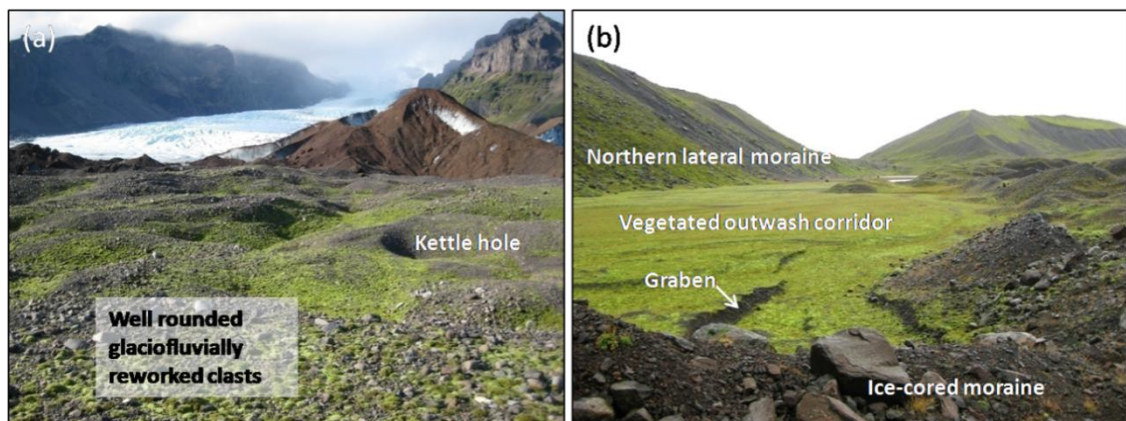
Fig 5.11(a,b) - Glacifluvial deposits: (a) collapsed ice-cored outwash near to the central margin. (b) Outwash corridor along the northern glacier margin with distinctive collapse features such as a graben.

Moraine sequences and till within the central and southern zones of the foreland have been dissected by ribbons of outwash and in places completely removed by wider trains of outwash. This network of ribbon sandur and channels was largely established by 1964 and completely established by 1980, formed by the production of meltwater from the meltout of ice within the ice-cored moraine between 1945 and 1980.

There is a strip of glacifluvial deposits along the northern snout margin, along the base of the northern lateral moraine, which comprises of a flight of **kame terraces** (Fig 5.12a,b)**.** These are steep-sided, flat-topped terraces composed of glacifluvial sand and gravel, deposited by former marginal meltwater streams between the lateral moraine and glacier margin (Benn and Evans, 1998, p487). The flight of kame terraces developed between 1945 and 2003 as a result of the gradual lowering of the glacier surface (Benn and Evans, 1998, p490). Towards the present day snout these are superimposed with red angular material, rockfall material which would have been deposited between the lateral moraine and glacier margin. (Fig 5.12b).
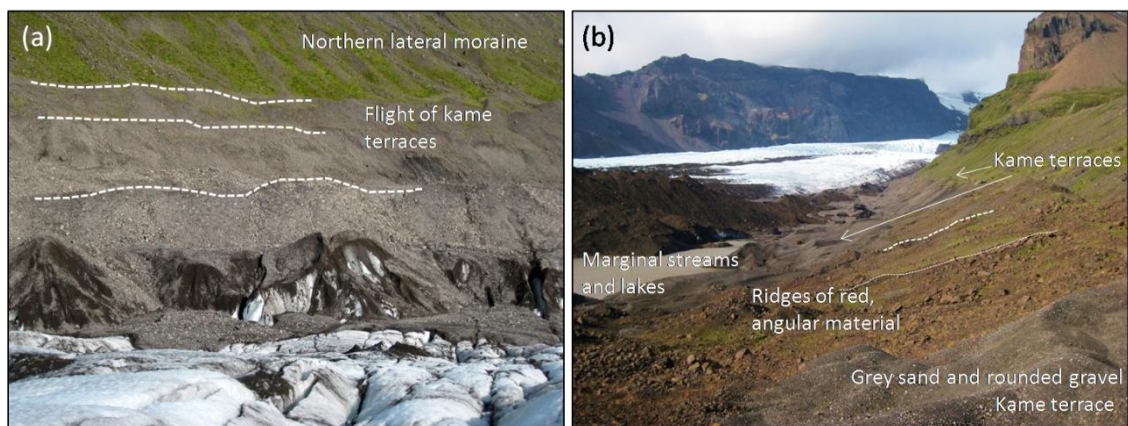
Fig 5.12(a,b) - Depositional landforms along the northern snout margin - (a) flight of kame terraces flanking the lateral moraine slope. (b) Corridor of glacifluvial outwash, lakes and streams and kame terraces and possible rockfall deposits.

Glacifluvial deposits are also contained within **eskers**: sharp crested, sinuous ridges of glacifluvial deposits that represent former meltwater streams either in subglacial or englacial tunnels, or supraglacial channels (e.g. Price, 1966). These are mainly transverse to the margin and occur within the supraglacial debris covered ice, ice-cored moraine, and on the glacier foreland.

5.3.7 Glacilacustrine deposits

These are glacial lake deposits of fine sediment that form records of past lakes in the glacier foreland. **Lakes** (mapped as blue polygons) include both proglacial lakes and supraglacial lakes. Proglacial lakes are ponded between the frontal glacier margin and topographic high points or the presence of an ice dam (e.g. Howarth and Price, 1969; Price, 1982; Benn and Evans, 1998, p105). At Kvíárjökull a small proglacial lake was present at the northern margin between 1945 and 1980, ponded between the glacier margin, the northern lateral moraine and proglacial moraine complexes. A

considerably larger proglacial lake formed periodically at the southern glacier margin, ponded behind moraine complexes and accumulations of outwash in the outer foreland. In 1964 and 1980, when the lake was at its most extensive, blocks of ice cored moraine and ice calved into the lake, forming floating blocks and ridges of ice-cored moraine, and ice-bergs. In 1998 the lakes at the northern and southern snout margins were replaced by glacilacustrine deposits.

5.3.8 Scree, paraglacial deposits and fresh paraglacial deposits

Scree is a minor component of the maps that occurs along the base of the bedrock ridges to the south of the glacier in the 1945 and 2003 maps, and to the north of the glacier in every map, as the result of frost shattering of exposed bedrock slopes. Much more prevalent are paraglacial deposits- re-worked glacial sediments along the slopes of the latero-frontal moraine ridges (Ballantyne and Benn, 1994; Ballantyne, 2002a,b). Paraglacial deposits include debris flow channels that dissect the upper slopes of the moraine, and debris cones that accumulate at the base of the slopes fed by debris flows (Fig 5.13a,b,c).
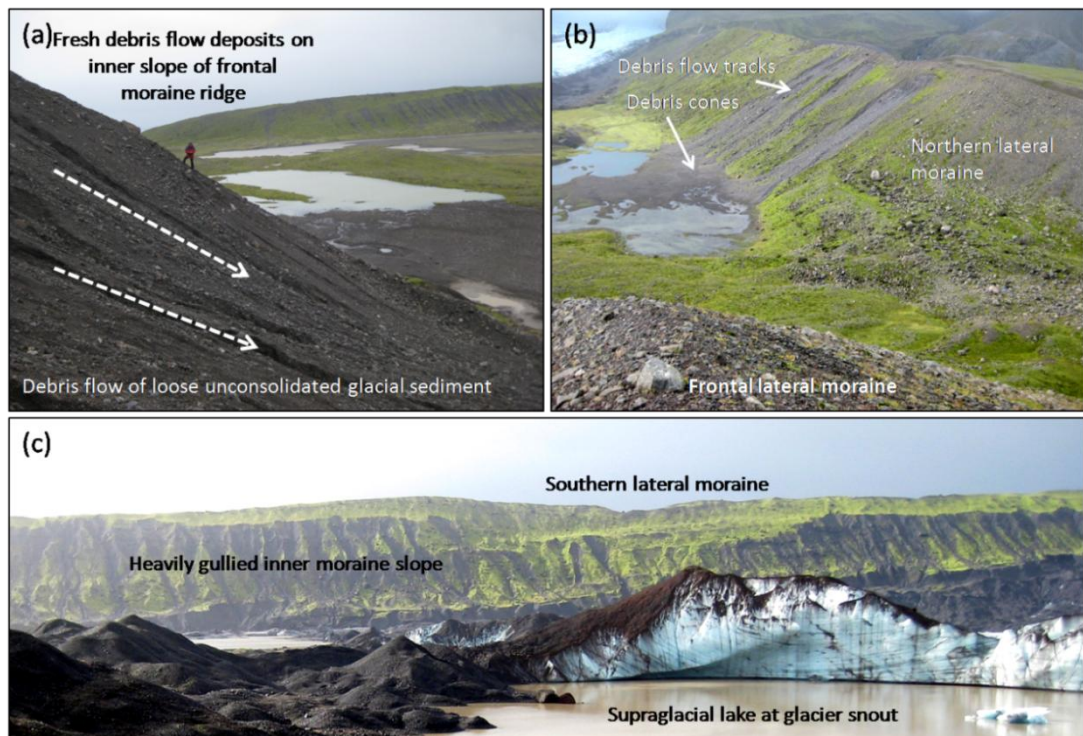
Fig 5.13 (a-c) - Paraglacial deposits. (a) Fresh debris flow deposits on the proximal slope of the latero-frontal moraine. (b) Debris flow tracks along the upper moraine slope feeding into debris cones at the slope base along the northern lateral moraine. (c) Gullied slopes along the southern lateral moraine. Note the flat terraces along the base of the slopes.

They also include older, vegetated paraglacial deposits, which continue to be modified by fluvial activity, along the outer slope of the southern lateral moraine. Paraglacial deposits are mapped in greater detail in 2003, with fresh paraglacial deposits classified separately, as a result of the greater detail of the colour photographs.

5.3.9 Jökulhlaup deposits

Jökulhlaup outwash forms a corridor outside the northern lateral moraine rampart, probably deposited during the last jökulhlaup in 1728AD (Thórarinsson, 1958). The rest of the outer foreland is covered in old, vegetated glacifluvial outwash.

5.4 Temporal variation in the spatial coverage of geomorphological units

Based on the visual assessment of Fig 5.5 - Fig 5.9 it is clear that the area of glacifluvial, glacilacustrine and paraglacial deposits all increased between 1945 and 2003. The area of post- LIA till also increased. Fig 5.14 shows quantitatively the change in the area of clear ice, debris-covered ice and ice-cored moraine over the study period. The area of debris-free ice steadily decreased between 1945 and 2003. The area of ice-cored moraine decreased between 1945 and 1980 as ice-cored moraine in the outer foreland melted to become post- LIA till. It then doubled between 1980 and 1998. The area of debris-covered ice fluctuated between 1945 and 2003. Between 1998 and 2003 the ice-cored moraine decreased in area but there was a 50% increase in the area of debris covered ice.
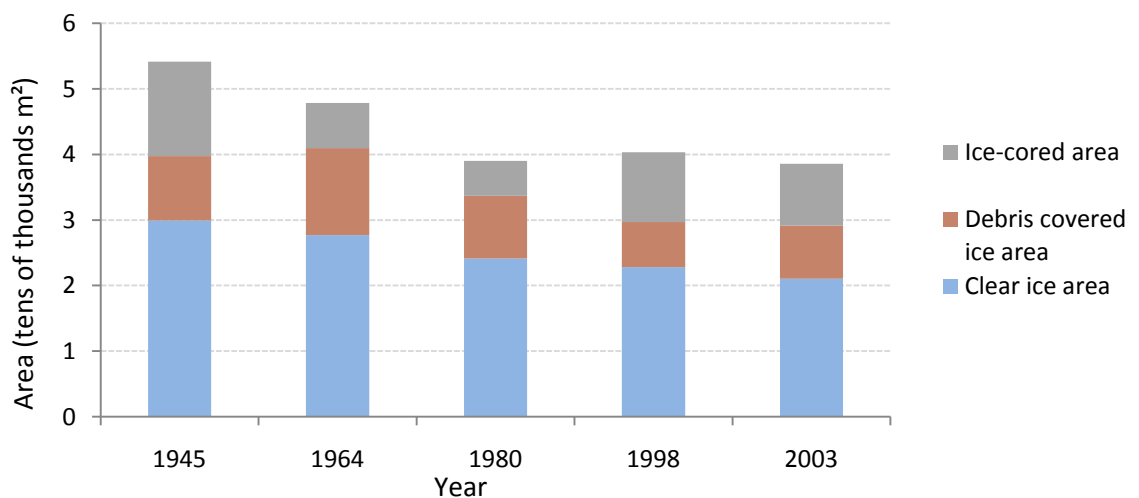
Fig 5.14 - Area of snout, debris-covered ice and ice-cored moraine, 1945 – 2003.

5.5 Morphometric changes associated with glacier retreat in the glacier snout and foreland

5.5.1 Temporal variability of ice loss

The total volume of ice lost from the glacier snout over the study period was ~138million m³, a water equivalent of 126million m³ (calculated by multiplying by the density of ice at $0.9167gcm^{3-1}$ at 0°C), or 58% of the 1945 snout volume. From 1945 – 2003 glacier snout area decreased by a total of 27.8% whilst glacier volume (within the 2003 snout area) decreased by 42%, illustrating the relative importance of thinning (volume loss) over lateral retreat (area loss) over the study period. Table 5.3 shows the annual percentage changes in snout area and volume over the study period. The rate of ice loss across the whole snout increased from 1.07% to 1.34% between the first two time periods. It then decreased to below 1% between 1980 and 1998 and then dramatically increased to more than 5% annual loss between 1998 and 2003. The differences in ice loss between the southern and northern snout zones are considered in section 5.5.3.

Table 5.3- A comparison of proportional area and volume change through time. Volume loss is based on 2003 snout area. All values are percentages are annual for each time period.

Time period	% ice loss of whole snout	% area loss/gain of whole snout	% volume loss of whole snout	% volume change of S snout	% volume change of N snout
1945 – 1964	-1.07	-0.61	-0.67	-0.78	-0.47
1964 – 1980	-1.34	-1.16	-0.59	-0.59	-0.60
1980 – 1998	-0.57	+0.19	-0.15	-0.27	+0.05
1998 – 2003	-5.04	-0.86	-4.94	-5.44	-4.14

5.5.2 The role of climate forcing

Temperature and precipitation data has been collected since 1949 at Fagurhólsmyri meteorological station (Fig 5.15), to the southwest of Kvíárjökull, enabling a comparison of these fluctuations in the rate of ice loss with fluctuations in climate over

the study period. The average summer temperature (May to September) and winter precipitation (October-April) is plotted for each time period (Figs Fig 5.16 andFig 5.17).
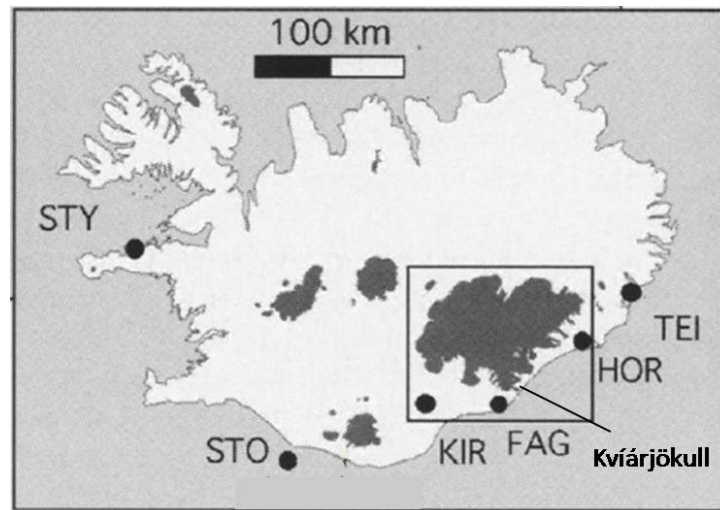
Fig 5.15 - Location of weather stations in Iceland including Fagurhólsmyri (FAG), Stykkishólmur (STY), referred to in the text. (Source: De Ruyter de Wildt et al., 2002).
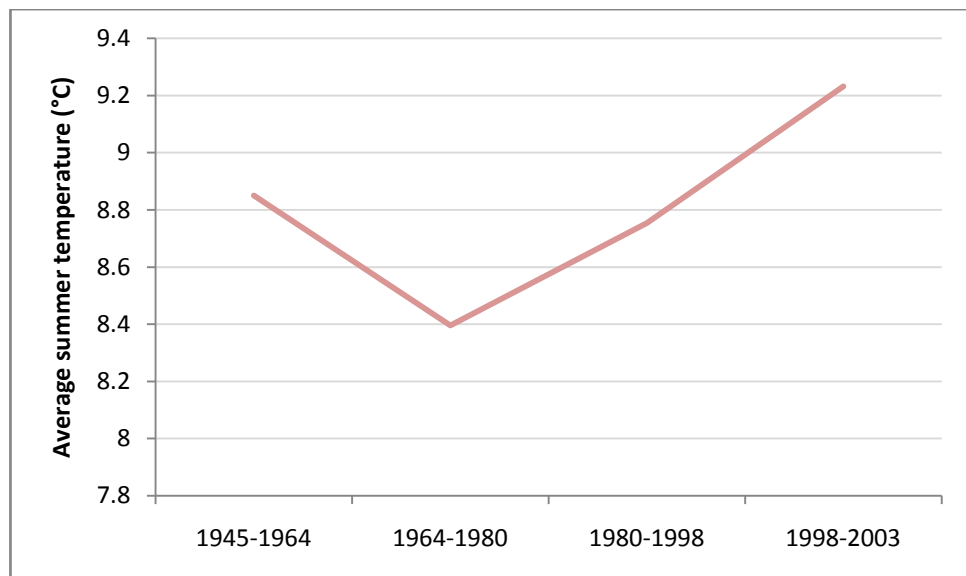
Fig 5.16 – Average summer temperature (May-September) for each time period at Fagurhólsmyri. The 1945-1964 average is based on data from 1949-1964.
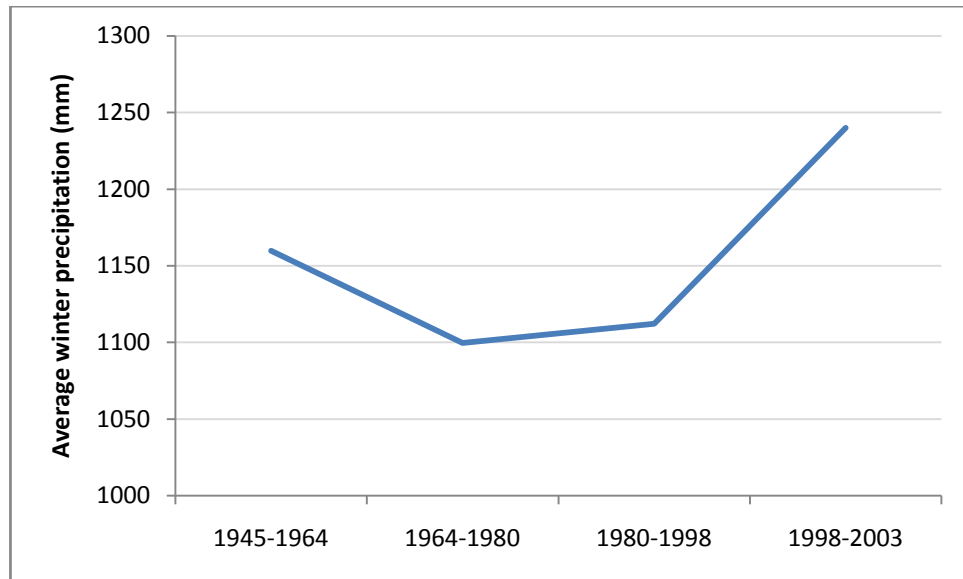
Fig 5.17 – Average winter precipitation (October – April) for each time period at Fagurhólsmyri. The 1945-1964 average is based on data from 1949-1964.

The 1945-1964 average temperature was 8.85°C, correlating with relatively high rates of ice-loss between 1945 and 1964. This is in agreement with Jóhannesson and Sigurdsson (1998) who attributed the extensive rapid glacier retreat that occurred from 1931 to 1960 across Iceland (Fig. 2.1) to high summer temperatures. However, despite a 0.2°C decrease in average temperature ice loss was greater during 1964 and 1980 than during the previous period. This increase in ice loss contrasts with most of the glaciers observed by Jóhannesson and Sigurdsson (1998), which retreated more slowly or advanced between 1965 and 1970 (Fig. 2.1). The continued retreat of the snout of Kvíárjökull over this period may be because Kvíárjökull has a longer response time than most other Icelandic glaciers due to local factors influencing ice dynamics (discussed in Chapter 6). It follows that the 1980-1998 advance of Kvíárjökull may thus be a delayed response to the decrease in average summer temperature during the previous time period. This advance may have been caused by ablation being reduced sufficiently in response to persistent low summer temperatures so that ice supply exceeded ice losses at the margin. This interpretation agrees with Jóhannesson and Sigurdsson (1998) who relate the timing of the maximum number of advancing glaciers in their sample between 1975 and 1990 to the timing of minimum summer temperature and therefore minimum ablation around 1980. Average summer temperature increased from 8.75°C to 9.2°C between 1998 and 2003, correlating with

the increase in ice-loss that occurred during this time and witnessed at glaciers throughout Iceland. However, it seems unlikely that such as small increase in temperature could result in such a dramatic increase in ice loss. Alternative interpretations are given in sections 5.5.3.4 and 5.7.3.2.

There is little correlation between rates of ice loss and average precipitation. It is anyway difficult to correlate glacier snout fluctuations with precipitation due to the delay in the transfer of mass from the accumulation zone to the snout. This lack of correlation agrees with studies by Jóhannesson and Sigurdsson (1998) and Sigurdsson et al. (2007), which both inferred trends in Icelandic glacier behaviour in the 20th century to be primarily controlled by variations in summer temperature.

De-icing rates of ice-cored moraines A-D in the glacier foreland further support the interpretation that the fluctuations of Kvíárjökull are controlled by temperature. They show the same temporal variation as those within the glacier snout (Fig 5.18) supporting the interpretation that the fluctuations of Kvíárjökull are forced by changes in air temperature rather than precipitation. These rates are in agreement with rates found elsewhere in Iceland. In particular, the lower dead-ice melting rates from 1964 – 1980 and 1980 - 1998 are in agreement with results from Schomacker and Kjær (2007) who found a lower dead-ice melting rate during the period 1964 – 1988 compared to the previous decades at Brúarjökull. Notably, de Ruyter de Wildt et al. (2003) reported low summer mass balance (and so low rates of ablation) of Vatnajökull during this period. The increase in downwasting rate from 1998 – 2003 throughout the moraine complexes also agrees with results from Schomacker and Kjær (2007) and is related to the late 20th century increase in temperature.
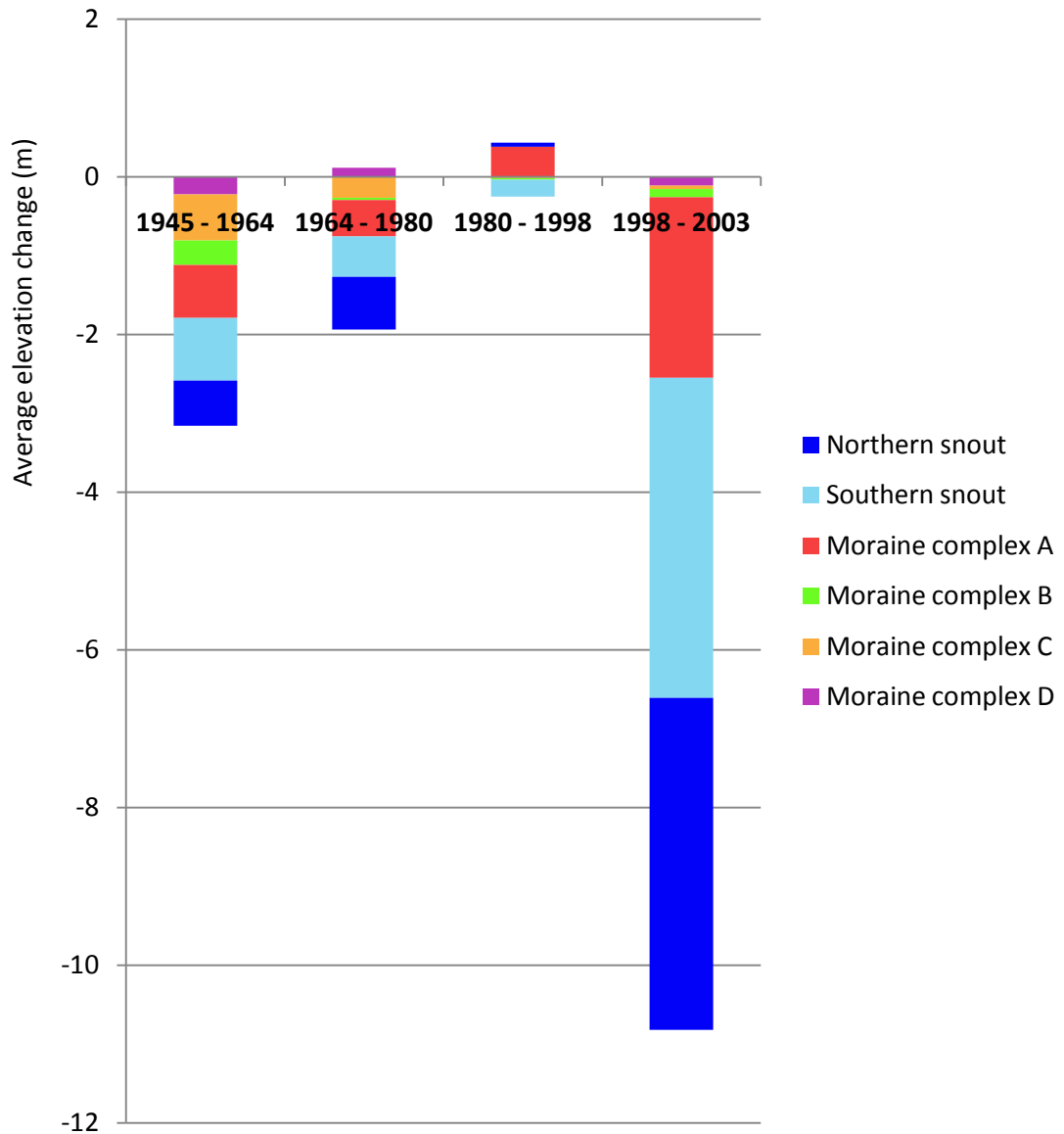
Fig 5.18 - Average annual elevation change, representing the rate of de-icing in the study area for the 4 time periods. The northern and southern snout areas relate to the 2003 snout area (as in fig.35). The moraine complexes A – D are located in figure 23 and are of increasing distance from the glacier snout and therefore age.

5.5.3 Spatial variability of ice loss

The snout of Kvíárjökull shows a differential response over the study period. Two distinctive boundaries are identified within the snout zone based on significant differences in ice loss: the first between the northern snout and the southern snout, and the second between the snout terminus and the upglacier ice. Whilst the southern snout lost 47% of its 1945 volume, the northern part of the snout lost only 34%. The map of elevation change (Fig 5.18) shows visibly the greater rate of ice loss from the

southern snout (≤75m) compared to the northern snout (~35m) over the study period. Seen in cross-profile, this difference in ice loss resulted in an increasing asymmetric transverse snout profile over the study period (Fig 5.21). Snout retreat was also greater at the southern margin (~800m) (Profile 9, Fig 5.22) than at the northern margin (~500m) (Profile 6, Fig 5.21). Furthermore, the snout retreated relatively little compared to the thinning of the glacier, as indicated by the relatively lower percentage loss in area compared to volume loss over the study period (Table 5.3).
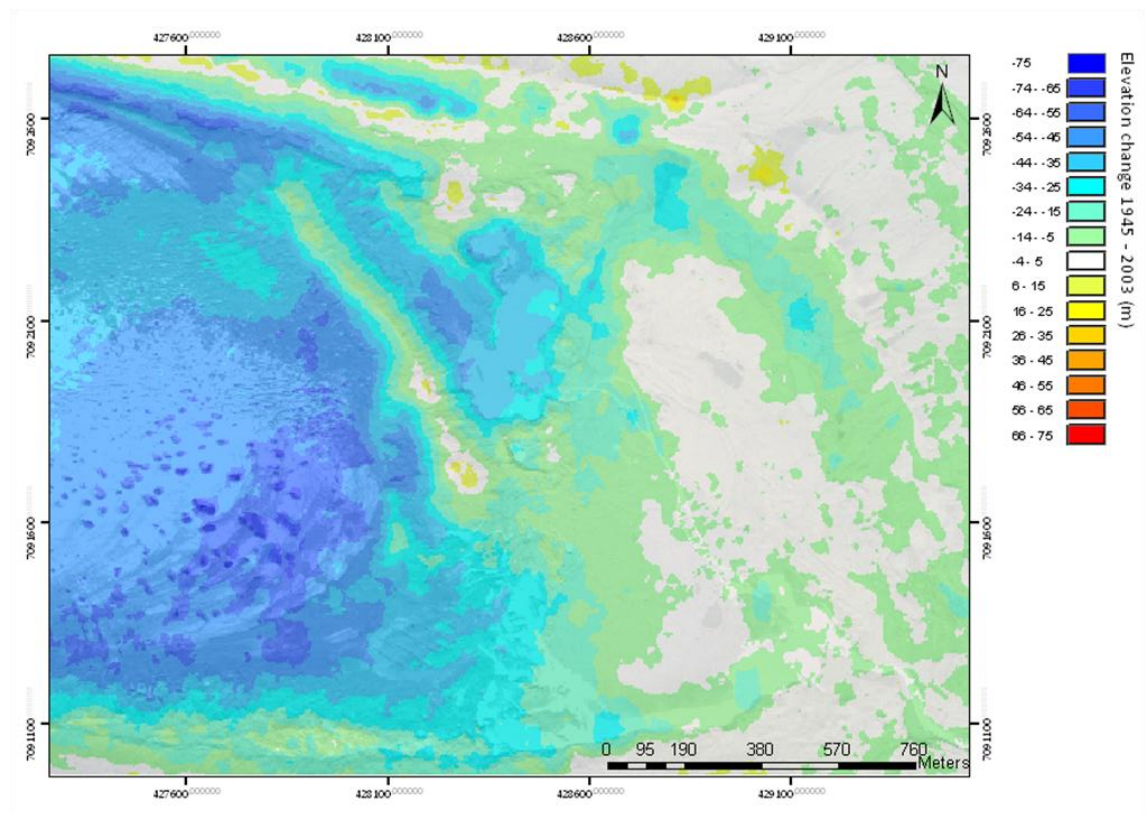
Fig 5.19- Map of elevation change across the glacier snout and foreland between 1945 and 2003
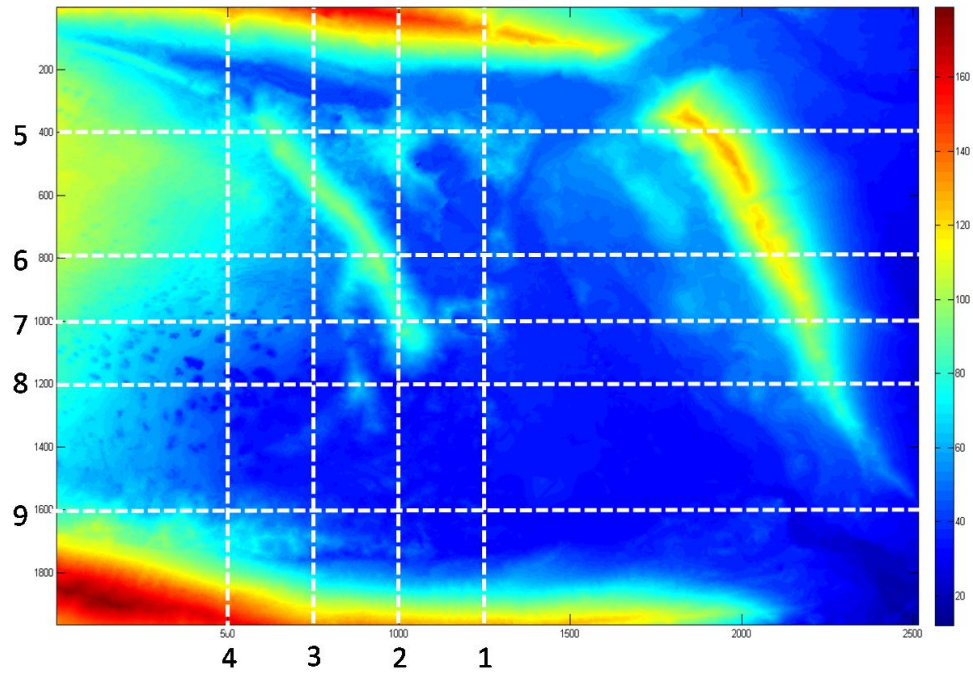
Fig 5.20 - Location of transects 1 – 9 on 2003 DEM. Colour scale from 10 – 175m
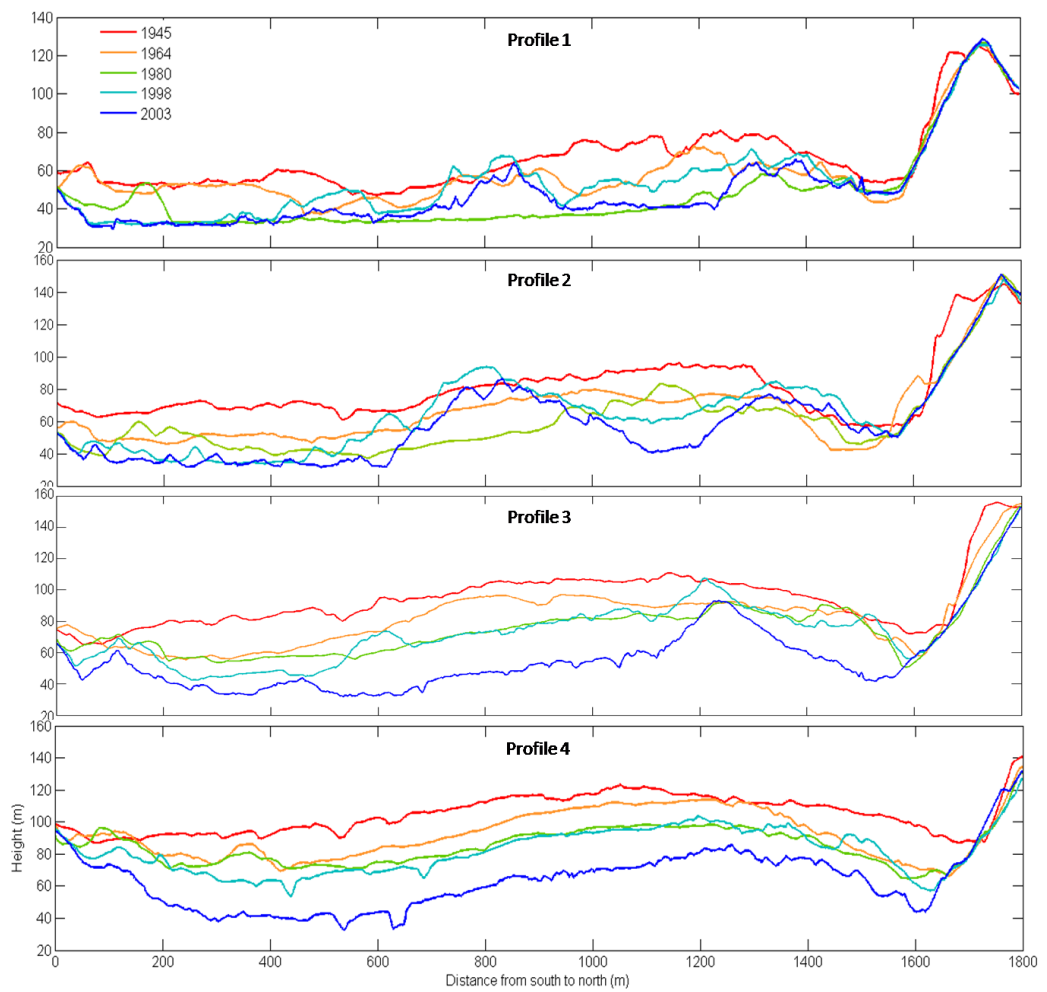
Fig 5.21 - Two-dimensional profiles transverse to the direction of ice flow.
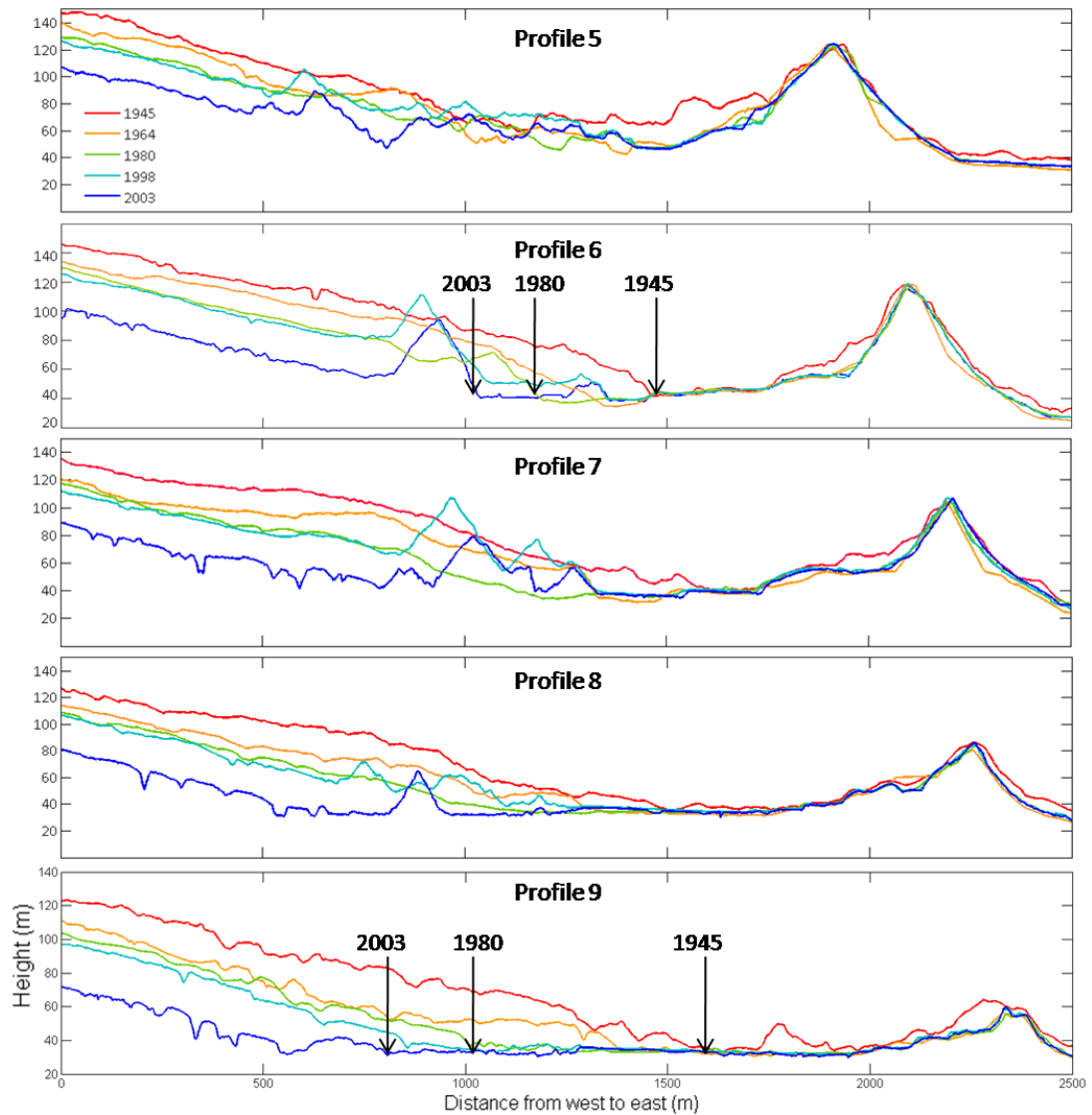
Fig 5.22 - Two dimensional profiles showing surface change in the direction of ice flow.

These spatial differences are interpreted to be largely the result of the spatial distribution of debris over the snout. The presence of a layer of debris on the glacier surface may influence ablation rates in two ways. Ablation rates may increase with thin debris cover due to decreased albedo compared to the surrounding clean ice. However, above 1 – 2cm in thickness, the debris layer may reduce ablation of underlying ice by protecting it from insolation and radiation (e.g. Benn and Evans, 1998, pp72 – 73; Kellerer-Pirklbauer et al., 2008). The lower ice loss within the northern part of the snout than within the southern part is explained by the presence

of the medial moraine. Similarly, the lower rate of retreat than the rate of thinning is explained by the presence of a thickening debris cover at the snout terminus (Fig 5.14).

However, surface elevation change within the glacier snout is a function of emergence velocity and ablation rates (Kellerer-Pirklbauer et al., 2008). Emergence velocity, the rate at which ice is replenished from upglacier, may also vary across the glacier between debris covered and debris free ice (Kellerer-Pirklbauer et al., 2008), therefore it is also necessary to consider emergence velocity in assessing spatial and temporal differences in behavior between the debris-covered northern snout and debris-free southern snout at Kvíárjökull. Without velocity data such variations may only be inferred in the following interpretation.

5.5.3.1 1945 – 1964 – meltwater erosion of the northern margin

Between 1945 and 1964 retreat rates were highest at the northern debris-covered snout margin compared to the relatively debris free southern snout margin (Table 5.3). Whilst this suggests that the debris-cover was not thick enough to insulate the underlying ice, downwasting was significantly less in the northern snout than in the southern snout from 1945-1964, indicating that debris-cover in the medial moraine was indeed thick enough to reduce ablation rates. An alternative explanation is that meltwater routed along the snout from the northern margin into the central foreland sometime during the 19 year period (Figs 5.5 and 5.6) increased backwasting rates through undercutting of the snout and thermal erosion (Etzelmüller, 2000).
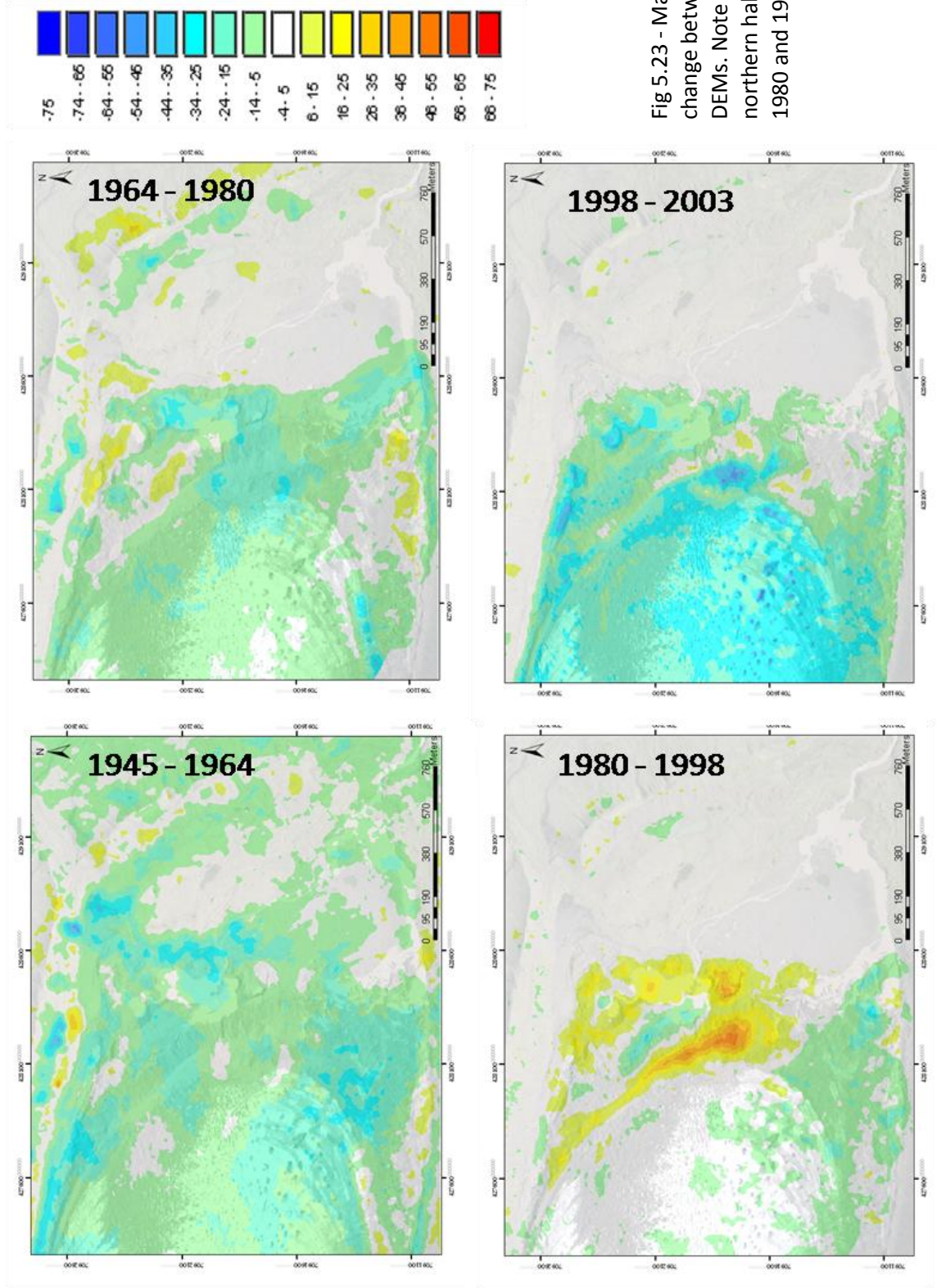
Fig 5.23 - Maps of elevation change between sequential DEMs. Note positive change in northern half of snout between 1980 and 1998

5.5.3.2 1964 – 1980 – proglacial lake development at southern margin

During the following time period, 1964 – 1980, the percentage reduction in area by backwasting was double the reduction in volume by downwasting for the snout as a whole (Table 5.3). This may be explained by the presence of a proglacial lake at the southern snout margin during this period into which the southern glacier margin broke up. Other studies have found that backwasting rates may be enhanced at a lake margin by calving, thermal undercutting and ice-wall melting (Powell, 1984; Kirkbride and Warren, 1999). The ice appears to have broken up along existing fractures within the ice, such as crevasses and englacial channels (Figs 5.6 and 5.7). The increased rate of backwasting resulted in the recession of the southern margin almost back to the position of the northern snout terminus by 1980. Proglacial lakes at the southern margin prevented the formation of terminal ice-cored moraine complexes between 1945 and 1980 by evacuating debris-covered ice and preventing its stagnation at the glacier margin. In contrast, at the northern margin, lower rates of evacuation of debris covered ice and the insulative effect of the thick debris fed from the medial moraine promoted the gradual development of an ice-cored moraine complex (A) (Profile 6, Fig 5.22).

5.5.3.3 1980 – 1998 – advance of the northern snout

Between 1980 and 1998 the northern snout increased in volume whilst the southern snout decreased (Table 5.3). The southern snout experienced significantly lower volume loss during this period relative to the previous and following periods suggesting that a climatic forcing increased the mass balance of the whole snout between 1980 and 1998. Furthermore, a number of moraine ridges formed across the snout terminus during this period (Fig 5.8), interpreted as push moraines, suggesting that the whole snout advanced in response to an increase in mass balance. The most plausible explanation for the advance of the northern snout is that the medial moraine reduced surface melting relative to that of the southern snout, particularly over the summers, so as to conserve mass, leading to the thickening of the ice, and through the increase the downvalley driving force due to gravity (Nakawo and Rana, 1999, cf. Shulmeister et al., 2009), resulting in an advance. Thus, it was a combination of climatic forcing and the insulative effect of the debris cover within the medial moraine that led to the pronounced advance of the northern snout.

5.5.3.4 1998 - 2003

Between 1998 and 2003 five times more ice was lost by downwasting than by backwasting. The significantly lower lateral retreat compared to previous periods may be explained by the increase in debris cover across the margin following the 1980-1998 advance (Figs 5.8 and 5.14). This would have insulated the margin, thus, reducing ablation at the margin. The high rates of downwasting between 1998 and 2003, by which the volume of ice lost was almost equal to that lost over the previous 53 years, may be partly explained by an increase in air temperature (section 5.5.2). The dramatic acceleration of retreat is most likely due to enhanced rates of thermo-erosion by meltwater as the glacier retreats into the water-filled overdeepening (Powell, 1984; Kirkbride and Warren, 1999) as described in section 5.5.3.2. The expansion of the lake is clear in the 2003 map (Fig 5.9).

5.6 Assessment of the process-sediment-landform associations involved in moraine evolution

5.6.1 Debris covered glacier snout: morphology and sedimentology

Supraglacial debris covers a large proportion of the snout of Kvíárjökull (between 25 and 36% during 1945-2003, (Fig 5.14), concentrated within margin parallel bands and in the medial moraine and grading into ice-cored moraine along the southern and frontal margins. Within the supraglacial debris covered zone and ice-cored moraine four distinct debris types along with their surface morphology are identified (Fig 5.24) and interpreted below. These are consistent with debris populations defined by Spedding and Evans (2002) based on their sedimentology and location (Fig 5.25). However, the 'water-worked' debris population of Spedding and Evans (2002) has been split into two separate debris types (A and B) based on their different englacial structure and debris characteristics and, therefore, morphological expression. The 'mixed' debris population defined by Spedding and Evans (2002) is not included within the supraglacial debris cover types as it is characteristic of processes of mixing within the ice-cored moraine and so is referred to in the interpretation of moraine complex A.

Type of supraglacial deposit	Distribution	Surface morphology	Thickness and spacing	Sediment concentration	Clast form of melt-out debris
A	Southern frontal margin	Transverse ridges (50cm – 5m)	Metres thick/ widely spaced	High: 50 – 80%	SR/R, matrix of sand/gravel
B	Frontal snout margin	Flow parallel lenticular deposits/sinuous ridges	NA	Very high: 100%	SR/R, matrix of sand/gravel
C	Lateral margins	Transverse ridges and sheets of debris (few cm high)	<1m thick, tightly spaced	Low: 0.6%	SA, striations, poorly sorted matrix with fines
D	Medial moraine and southern lateral margin	Series of overlapping ridges of varying size	Thin, tightly spaced	NA	SA/A

Fig 5.24 - Schematic map and table detailing the characteristics and spatial distribution of 4 different types of englacial debris concentrations and their associated morainic expressions on the supraglacial debris covered snout and within ice-cored moraine.
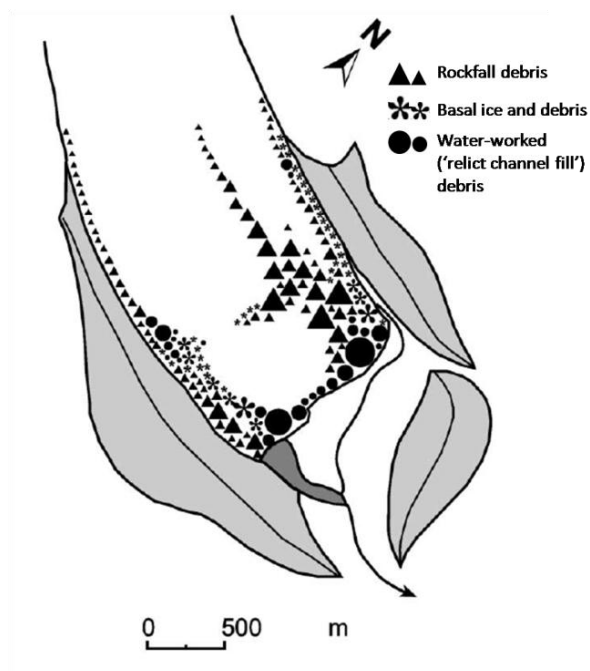
Fig 5.25- Spedding and Evans' (2002) sketch map of debris populations within the snout of Kvíárjökull.

5.6.1.1 Type A deposits:

Englacial structure and sedimentology

A number of linear ridges of sediment that vary between 50cm and a few metres in height are superimposed on the glacier surface at the frontal margin (Fig 5.26a, b and d; Fig 5.27c). Some of the results and observations included within this description (e.g. from site A of Swift et al., 2006, and a number of sites of Spedding and Evans, 2002) are from within the ice-cored moraine into which these ridges grade. These ridges are fed by transverse debris bands that dip steeply upglacier near to the lateral margins (e.g. Fig 5.26c; Fig 5.28).
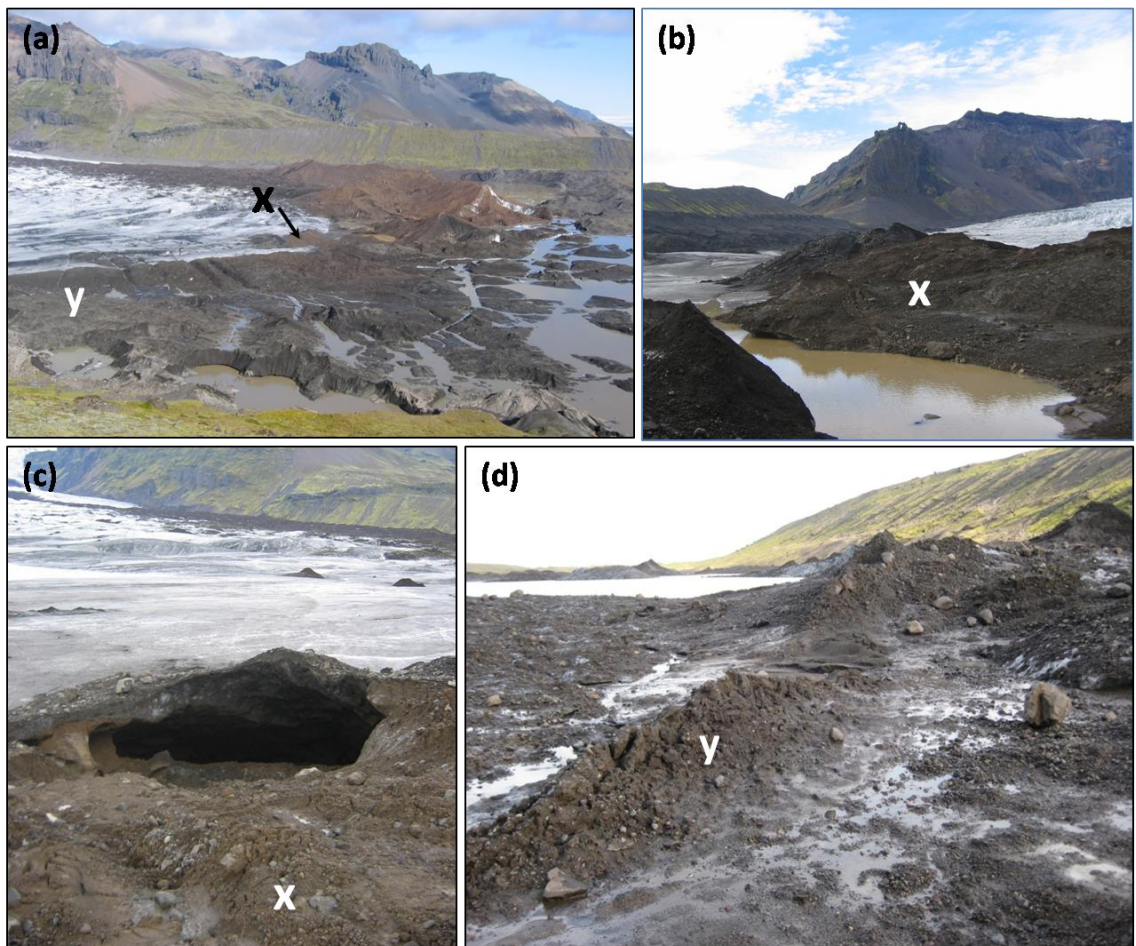
Fig 5.26 (a-d) - Type A deposits: (a) distribution of debris in wide ridges at the frontal margin (ridges at sites x and y); (b) ridge at site x, ~ 2m high and ice cored; (c) upglacier dipping 50cm thick debris band exposed within a cavity at the base of the upglacier slope of ridge x; (d) ridge at site y, ~ 50 cm high, no exposure through underlying debris band.

These bands are metres thick and separated by many metres of debris free ice. They have relatively high sediment concentrations (for example 71% by mass was measured

at site A by Swift et al. 2006, see Table 1; and Spedding and Evans, 2002 measured concentrations of 50 – 80%) and have sharp contacts with the surrounding debris free ice. Clast analysis by Spedding and Evans (2002) shows these to comprise subrounded to rounded clasts within a matrix of sand and gravel. Samples from bands cropping out towards the southerly margin, however, contain more subangular and angular clasts.

Surface morphology

A number of steep-sided ridges, or dykes (Paul and Eyles, 1990), were observed in the ice-cored moraine, directly downglacier from the outcrop of type A deposits. Fig 5.27b shows the initiation of one of these steep sided ridges: debris melting out from a debris band at a frontal margin, depositing a linear ridge of sediment on the glacier surface. This thick ridge of debris reduces the melt rate of the underlying ice relative to the melt rate of the surrounding ice so that the ridge increases in elevation relative to the surrounding topography through time, resulting in the formation of steep sided ridges (e.g. Fig 5.27c).
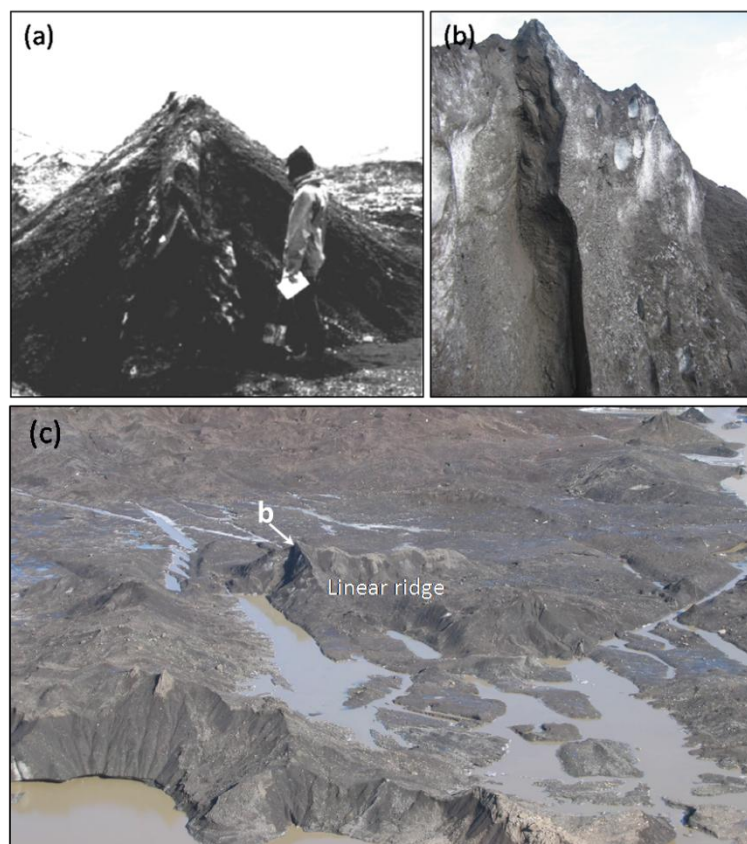
Fig 5.27 (a-c) - Vertical dykes within ice-cored moraine: (a) found by Paul and Eyles (1990); (b) found during field research within the ice cored moraine at the southern snout terminus. Debris is deposited by gravity flows down the slopes of the surrounding ice core thereby insulating the slopes and creating a steep-sided ridge, (c).

Fig 5.28 - Debris-rich ice band (behind metre rule) dipping steeply upglacier (right) from Swift et al. (2006). Note the sharp contact between the debris band and overlying debris free, englacial ice and the subrounded meltout debris.

Interpretation – Water-worked debris bands

Type A deposits are consistent in debris characteristics with the 'water-worked' class of debris identified by Spedding and Evans (2002) and are found along the frontal margin at Kvíárjökull. The high proportion of subrounded and rounded clasts and a sand/gravel matrix depleted in fines are characteristics of debris from a fluvial transport pathway. This debris is inferred by Spedding and Evans (2002) to originate from subglacial channels within the subglacial traction zone further upglacier, rather than from a supraglacial source, for the reason that the degree of rounding is indicative of a long active transport pathway. . The most likely explanation for the entrainment of water-worked debris is that it is diverted into englacial channels as a result of a switch in drainage at the base of the ice fall from subglacial to englacial. Channel growth is suppressed at the base of the icefall by glacier sliding (Walder, 1986; Kamb, 1987; cf. Spedding and Evans, 2002) resulting in sediment-rich, subglacial water forcing pathways through ice either between foliae (Kirkbride and Spedding, 1996), or through crevasse traces (Goodsell et al., 2005), and creating new englacial drainage pathways. The formation of debris bands at the margin may result from the subsequent entrainment of debris from englacial channels along shear planes or lines of foliation that intercept the channels (e.g. Swift et al., 2006, Fig 2.5b; Fig 5.34). These may subsequently be thickened by folding and compression as ice slows against the ice-cored moraine and the reverse slope of the overdeepening (Spedding and Evans,

2002; Swift et al., 2006). Evidence of marginal compression and folding of englacial channel fills into debris bands was found at the northern snout margin (Fig 5.30a,b). Debris bands may also form by drainage exploiting planar fractures within the ice (Esminger et al., 1999; Roberts et al., 2000a, b; cf. Spedding and Evans, 2002) (Fig 5.29). This process is called hydrofracture and may result in vertical dyke features seen within the ice-cored moraine (Fig 5.24).
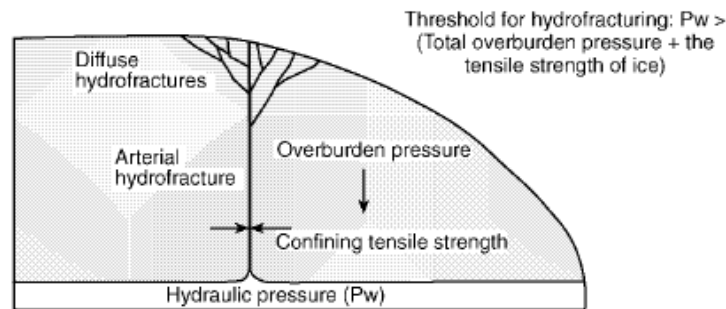
Fig 5.29- The process of hydrofracturing (Roberts et al., 2000)

5.6.1.2 Type B deposits

Englacial structure and sedimentology

Spedding and Evans (2002) observed lenticular pockets of sediment at the frontal margin of similar sedimentology to type A ridges: subrounded to rounded clasts within a matrix of sand/gravel. A number of examples were observed during fieldwork (Fig 5.30a-d). Fig 5.30d shows a 1.5m wide by 3m deep pocket of sediment comprising clasts within a sand/gravel matrix. Fig 5.30b shows a circular pocket of sediment melting out from a thin layer of overlying clean ice. Above this is a 50cm thick band of sediment that coarsens upwards from mud/clay to silt/sand (Fig 5.30c). This forms a very sharp boundary with the surrounding debris free ice and is ice free (100% sediment content). The exposed sediment and surrounding ice within this exposure contain transverse flow banding.

Surface morphology

Ridges of bedded sands and gravels are common features within the supraglacial debris covered snout and within the ice-cored moraine (Fig 5.31). These are easily distinguished morphologically and sedimentologically from ridges that form from the

other types of deposits. They are orientated in a downglacier direction rather than in a transverse direction, and contain well sorted and bedded sediment as opposed to poorly sorted sediments found in transverse ridges. They are found in proximity to meltwater features. On the glacier snout they are found near to supraglacial streams (Spedding and Evans, 2002) and to zones of upwelling. Within ice-cored moraine they are located close to supraglacial streams and tend to form along or proximal to former meltwater outlets. In 2003 they emanated from ice-walled channels on the glacier surface and formed linear islands within the proglacial lake at the southern margin (Fig 5.9). They are also found throughout the northern moraine complex in proximity to meltwater outlets.
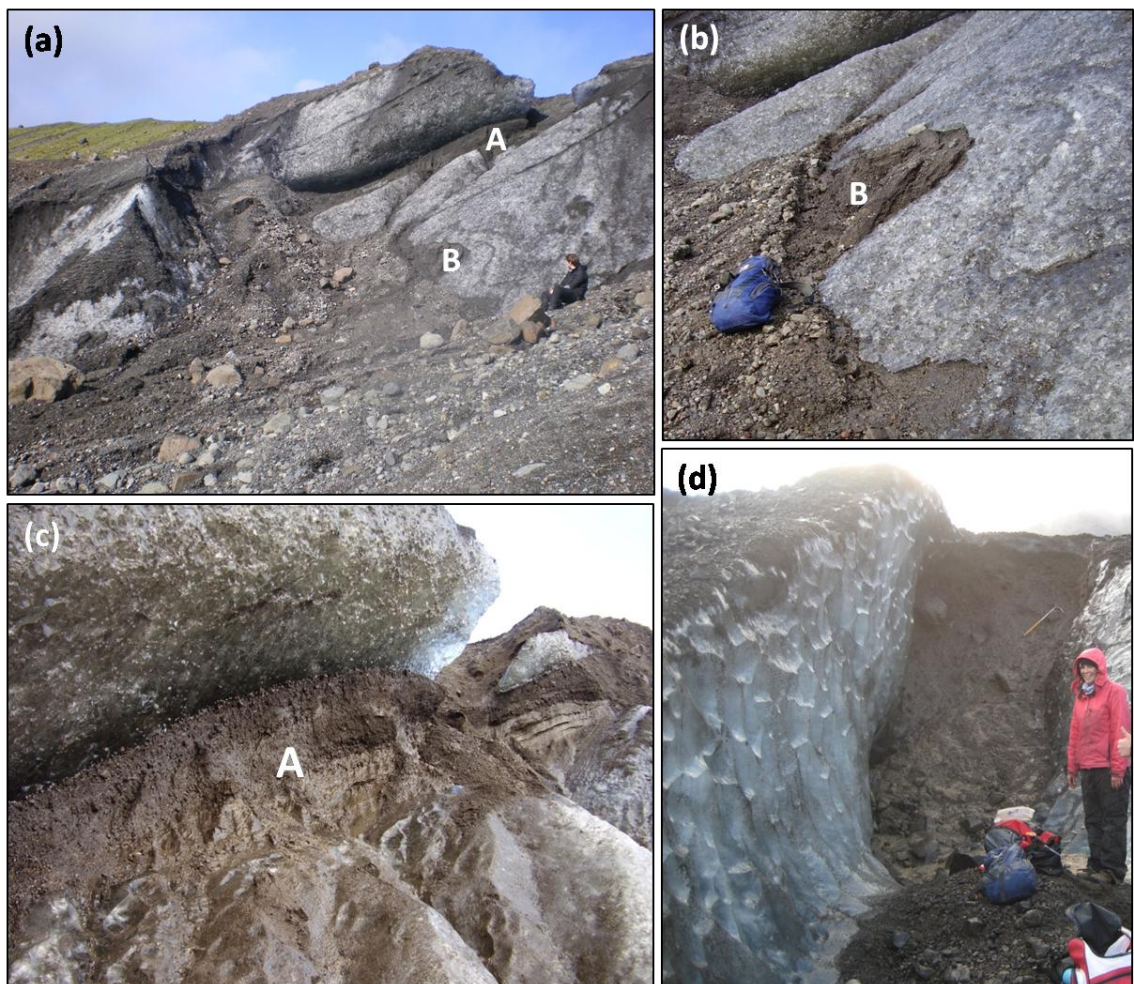
Fig 5.30(a-d). Type B deposits at frontal margin: (a) exposure of a folded band of debris, 'A', cropping out at the surface of ice-cored moraine and transverse flow banding within ice and exposed sediment, 'B'. (b) Close up of 'B', note thin covering of ice over a pod of underlying sediment and fine matrix of sand and gravel melting out. (c) Close up of 'A': note upward coarsening and unfrozen debris. (d) Trough of sediment, ~3m high, 1.5m wide.

Fig 5.31 - Supraglacial eskers at the glacier margin orientated parallel to glacier flow.

Interpretation – channel fills

Type B deposits have the same clast form characteristics as type A deposits, but differ from type A deposits in their englacial structure and surface morphology. Whilst type A deposits are typically transverse bands of debris formed by the entrainment of debris from englacial channels along lines of foliation or fractures, type B deposits are pods and troughs of debris contained within englacial channels melting out at the margin. Pods and troughs are typical of conduit-like features within englacial channel networks (e.g. Hooke and Pohjola, 1994). Fig 5.30 shows evidence of transverse and longitudinal compression of the deposits in the form of folds within the ice and an englacial channel fill that has been folded into a debris band.

5.6.1.3 Type C deposits

Englacial structure and sedimentology

A second type of debris band crops out at the lateral margins of the glacier depositing a thin covering of supraglacial debris, a few centimetres thick on the glacier surface. Vertical exposures at both the northeast and southwest glacier margins reveal many thin, closely spaced debris bands dipping steeply towards the centre of the glacier (Fig 5.32a,b). These were also observed by Spedding and Evans (2002) (Fig 5.32c) and Swift et al. (2006). In contrast to the frontal debris bands the sediment concentration of these bands is low (0.6% by mass was measured in one of these bands (site F) by Swift et al., 2006). Clast form analysis by Spedding and Evans (2002) found much of the

sediment to show distinct signs of modification in transport such as striations and faceting. Clasts are largely subangular, and within a poorly sorted matrix, rich in fine sediments (Fig 5.32d). Along the north-eastern margin Spedding and Evans (2002) observed a 1km stretch of debris-rich basal ice up to 10m thick in which debris content falls towards the glacier surface and becomes intercalated with debris free englacial ice (Fig 5.32c).

Surface morphology

The supraglacial debris derived from type C debris bands forms a thin sheet in a continuous strip along the southern margin and within transverse debris bands along the lateral margins (Fig 5.33a,b). This is continuous with type D deposits within the outer southern lateral margin.
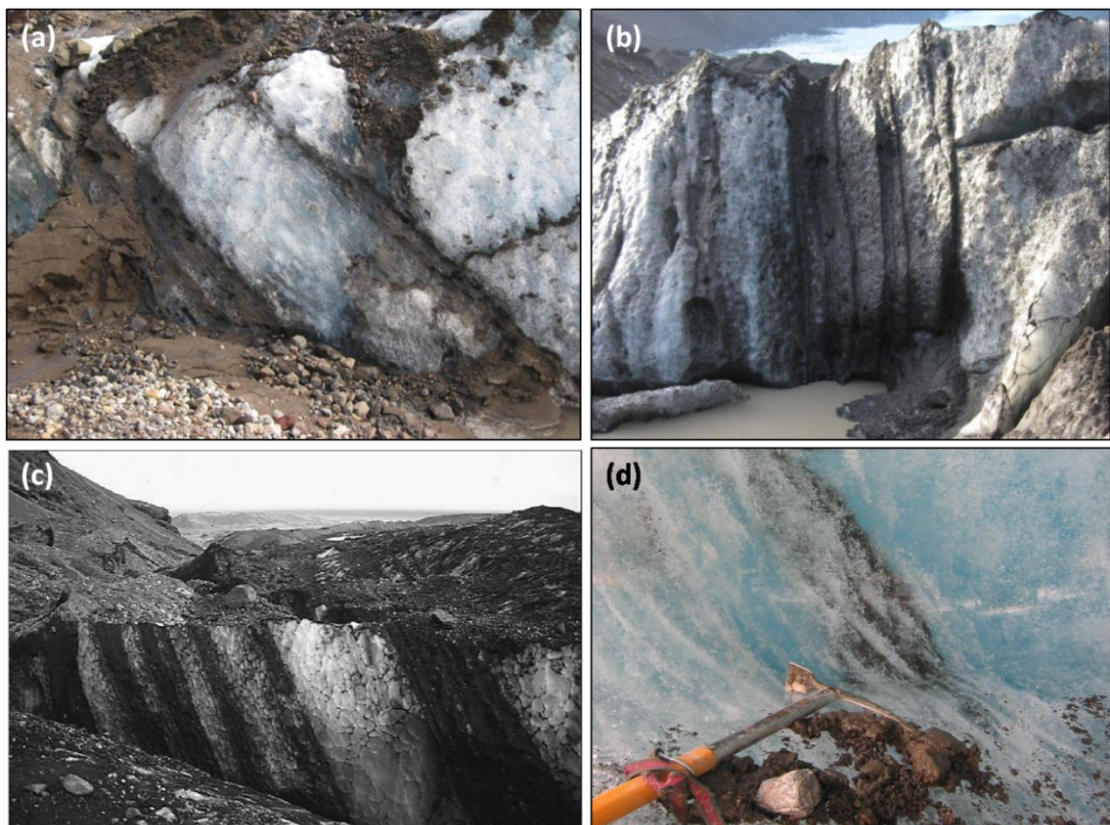
Fig 5.32 - (a-d). Type C deposits at lateral margins: (a) thin bands of debris dipping towards the centre line of the glacier exposed at the northern debris margin (note matrix of fine sediment). (b) Vertically orientated closely spaced thin debris bands melting out at the southern lateral margin. (c) Figure 8 from Spedding and Evans (2002): debris bands intercalated with crystalline, debris free englacial ice exposed at the northern margin. (d) Small clots and stringers of sediment frozen into the ice within a debris band melting out from the wall of an ice tunnel at the southern margin (note fine sediment).
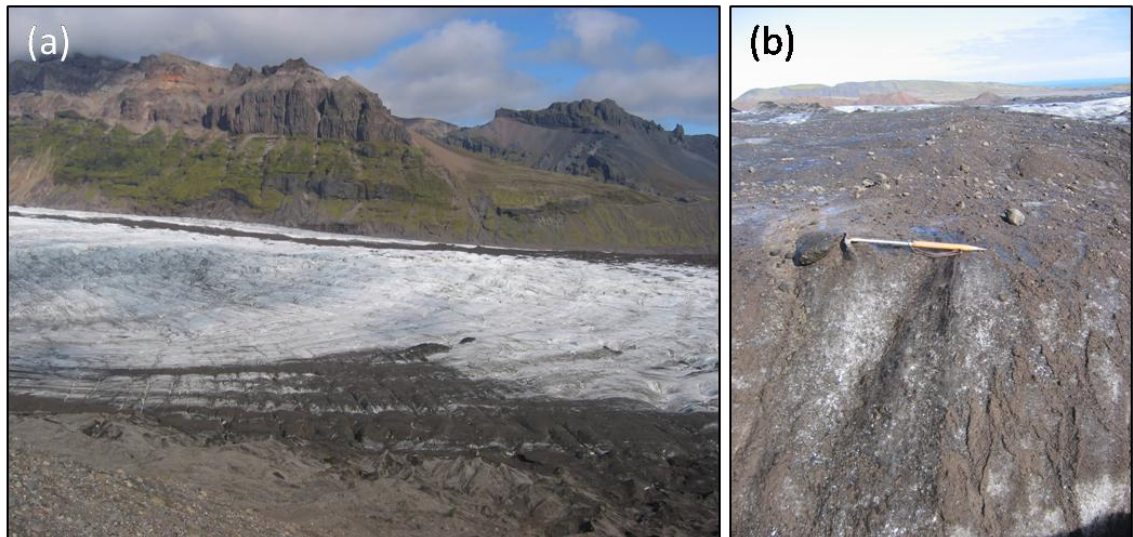
Fig 5.33 (a-b). Type C moraine deposits. (a) Transverse debris bands at the southern lateral margin. (b) Thin cover of debris derived from thin, tightly spaced debris bands.

Interpretation – Basal debris bands

Type C deposits are consistent with the basal debris class defined by Spedding and Evans (2002) in location and clast form. Subangular, slightly blocky clasts set within a poorly sorted matrix, rich in fines are properties diagnostic of transport in the subglacial traction zone. The low debris content and thinness of the debris bands is probably the result of the mechanism by which debris is entrained at the base of the glacier. The most common entrainment mechanism at a temperate glacier is by Weertman regelation, by which it is only possible to accrete a thin layer of debris. Alternatively debris may be squeezed into crevasse traces at the base of the glacier and transported to the surface along shear planes (Goodsell et al., 2002, 2005). Swift et al. (2006) invoke thrusting as the mechanism by which debris is entrained and transported to the surface (Fig 5.34). This would require the overriding of down glacier ice by up glacier ice along thrust planes (e.g. Hambrey et al., 1999; Krüger and Aber, 1998). Whilst not observed in this study, Spedding and Evans (2002) found basal debris bands to overlie thick sequences of debris-rich basal ice at the northern margin. Thick basal ice may be formed by folding of stratification as a result of compressive and converging terminal flow within the glacier snout (Hambrey et al., 1999). In this situation basal debris-rich ice may form the lower part of the fold sequence and may reach the surface along lines of intense folding offering an alternative explanation for the pattern on debris bands containing basal debris at the lateral margins.
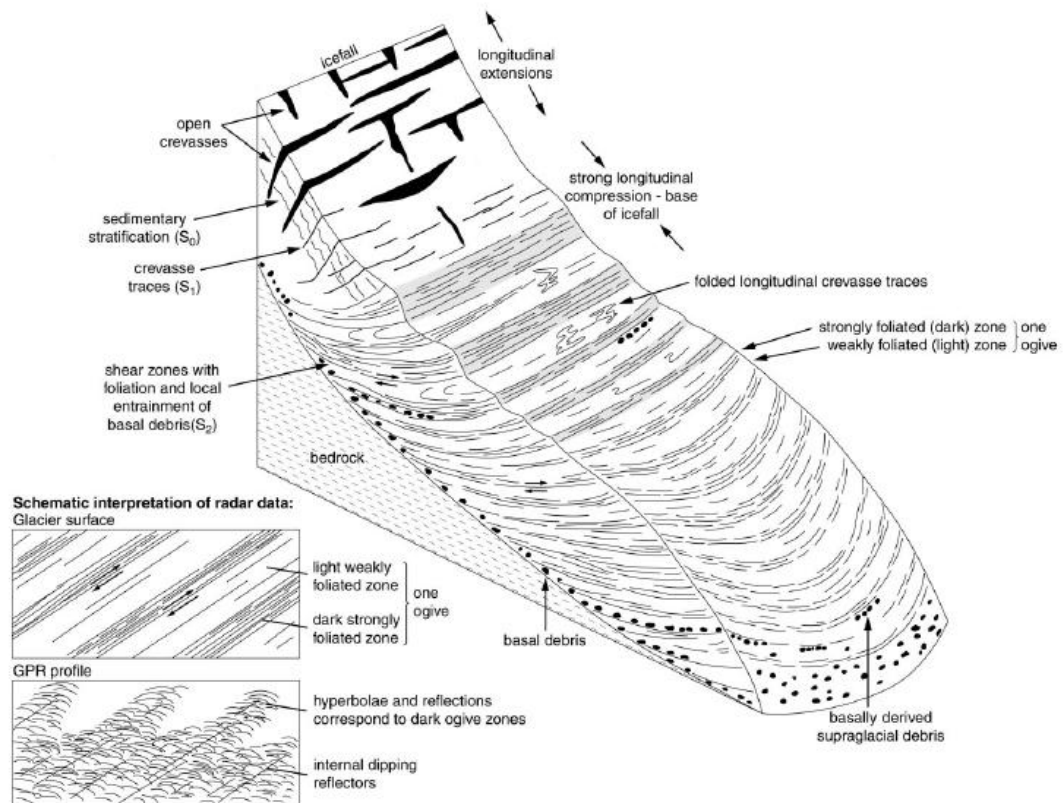
Fig 5.34 - Model developed at Haut Glacier D'Arolla of entrainment of basal debris at the base of an icefall and transport to the surface along shear planes and lines of foliation (Source: Goodsell et al., 2002).

5.6.1.1 Type D deposits

Englacial structure and sedimentology

Within the medial moraine (Fig 5.35a,b) and along the south-western glacier margin (Fig 5.35c,d) the supraglacial debris covered ice is composed of a series of overlapping ridges comprising angular to subangular sediment. Spedding and Evans (2002) distinguished between two types of debris that contribute to the debris on the glacier surface: very angular clasts sitting on the glacier surface, and subangular to angular debris emerging from debris bands. These deposits are interspersed with type C deposits along the south-western margin and with type A deposits at the frontal margin. The size of the ridges varies between low amplitude of a few centimetres high and wide (e.g. Fig 5.35a) to very large features (e.g. Fig 5.35b) particularly within the medial moraine.
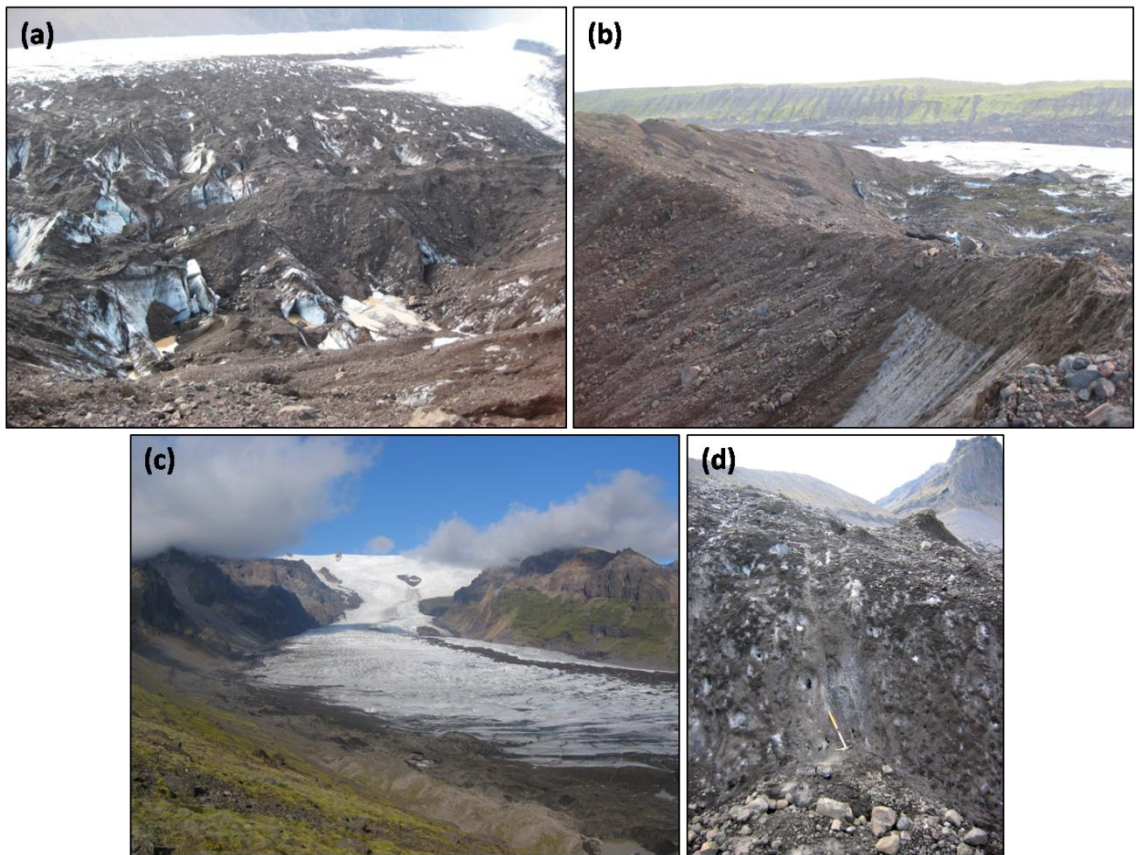
Fig 5.35(a-d) - Type D deposits - (a) view of medial moraine looking up glacier (note transverse linear ridge melting out across centre of the photo). (b) Large ridge downglacier from medial moraine covered in angular debris (note exposure of ice revealing 1m thick debris cover along ridge apex). (c) view of the southwestern lateral margin looking upglacier showing supraglacial debris cover fed directly from scree slopes). (d) Expsosure through debris band (under ice axe) within southwestern margin (note angular/subangular clasts at bottom of the exposure).

Surficial morphology

The ice-cored moraine at the northern snout terminus is dominated by a very large ice-cored ridge (visible in profile 6, Fig 5.22) with a continuous thick cover of angular debris of over 1m thick (Fig 5.35b) that was transported down the glacier in the medial moraine and is continuous with type D deposits. This ridge has become elevated through time due to differential ablation. Whilst this ridge is in itself a feature of the melt out of type D deposits, it also contains a number of features, in the form of transverse linear ridges of a few metres high along its proximal slope (Fig 5.36). One of these is near to a tongue of glacier ice that appears to be overriding the ridge.
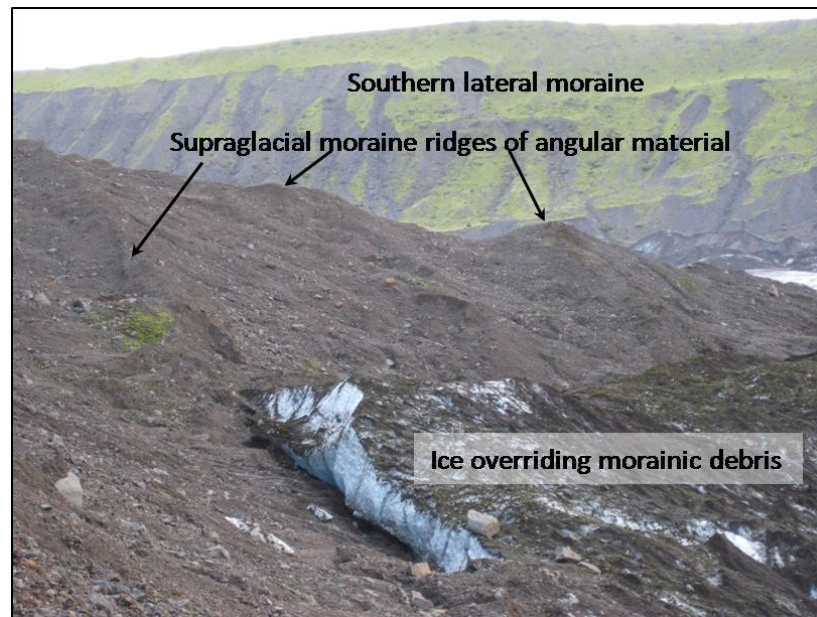
Fig 5.36 - A sequence of linear moraine ridges on the proximal slope of the very large, transverse ridge, at the end of the medial moraine (figure xb). Glacier ice appears to be overlapping the base of the ridge

Interpretation –

Type D deposits are consistent with the rockfall debris class identified by Spedding and Evans (2002), characterised by angular and very angular debris with little evidence of reworking. The rockfall debris consists of several lithologies derived from the volcanic marginal rock walls and nunataks in the icefall: basalt, palagonite and rhyolite (Fig 3.4). Rockfall debris fed onto the glacier by rockfall events of varying magnitude and frequency from a nunatak within the icefall maintains the medial moraine over the study period. There are two possible transport pathways for rockfall debris deposited on the glacier surface. Rockfall debris may either remain on the glacier surface or may be ingested by crevasses and incorporated into englacial debris bands (Spedding and Evans, 2002). Much of the rockfall debris within the medial moraine has been transported to the margin on the surface of the glacier as indicated by the presence of vegetation on the rockfall deposits, indicating that the debris has been on the surface long enough for vegetation colonisation to occur. The rockfall deposits found along the lateral margins, particularly the southern lateral margin, are partly derived from englacial debris bands, and partly surficial deposits (Spedding and Evans, 2002).

5.6.1 Evolution of supraglacial moraine

5.6.1.1 Evolution of controlled moraine from water-worked and basal debris bands

'Controlled moraine' is defined as supraglacial moraine whose linearity reflects the internal flow structure of the ice (Gravenor and Kupsch, 1959; Boulton, 1967; Benn and Evans, 1998; Fitzsimmons, 2003; Evans, 2009). Therefore only debris bands A and C may be considered to form 'controlled' moraine. The presence of transverse ice-cored ridges of similar morphology to englacial debris bands A and C at the glacier margin indicates that the initial morphology of this ice-cored moraine is 'controlled' by the distribution of the englacial debris bands within the glacier margin and therefore reflects the englacial structure of the glacier. The following interpretation concerns the controls on the size and morphology of the ice-cored ridges derived from water-worked and basal debris bands prior to their modification by proglacial and supraglacial processes.

As ice downwastes debris melts out from these bands forming a spatially heterogeneous debris mantle. Through time differential ablation increases the relief of the deposits, resulting in the formation of ice-cored ridges of various forms (Etzelmüller et al, 1996). The size and morphology of these ridges is largely dependent on the characteristics of the parent englacial debris band such as the debris concentration (Boulton, 1971; Sletten et al. 2001) and the size and dip of the debris band (Boulton, 1967), although may also be affected by reworking of the debris mantle, and thus englacial signature, by supraglacial streams (Eyles, 1979, 1983c). The debris concentration of the englacial debris band affects the thickness and density of the overlying debris mantle. Controlled moraine formation requires that the debris mantle is thick enough to insulate the underlying ice from ablation and to result in the formation of an ice-cored ridge by differential ablation.

Additionally the maximum potential slope gradient of an ice-cored ridge is affected by the size and composition of debris, which influences slope stability. Paul and Eyles (1990) found that matrix-rich sediment will become unstable on a slope of 5° or less, whereas coarse diamict will remain stable on a slope of almost 20°. Type A deposits have a high concentration of debris and melt out to form a thick mantle of coarse

debris, depleted in fines. This debris mantle protects the underlying ice-core from ablation and remains stable as slope gradient increases, resulting in the formation of large ridges within the ice-cored moraine (Figs 5.26 and 5.27). In contrast, type C deposits consist of finer sediment, which spreads as a sheet over the glacier surface (Fig 5.33). This debris is probably not sufficient to insulate underlying ice but is easily dispersed by supraglacial streams, destroying the pattern of debris bands before ridges may be formed by differential ablation. This explains why only very minor ridges with a low preservation potential are formed from basal debris bands.

Thus, only the thickest debris bands containing water-worked debris are preserved as features of positive relief at the glacier margin. The morphology of controlled moraine ridges derived from water-worked debris bands is also affected by the dip of the debris bands. Vertical dykes form steep sided elongate ridges (Fig 5.27), whereas sub-vertical debris bands form lower relief ridges, observed at the southern glacier margin (Fig 5.26). This agrees with the observation of Boulton (1967) at a glacier in Svalbard that the relief of ice-cored ridges is controlled by the dip of the englacial debris band. He found that sediment melting out from high-angle debris bands (>70°) builds up on the summit and melts out to form a steep ridge (Fig 5.37). Sediment melting out from medium-angle debris bands (30° – 70°) is deposited downglacier from the debris band and forms a more uniformly thick mantle over the ice core, which melts out to form a low relief ridge (Fig 5.38).
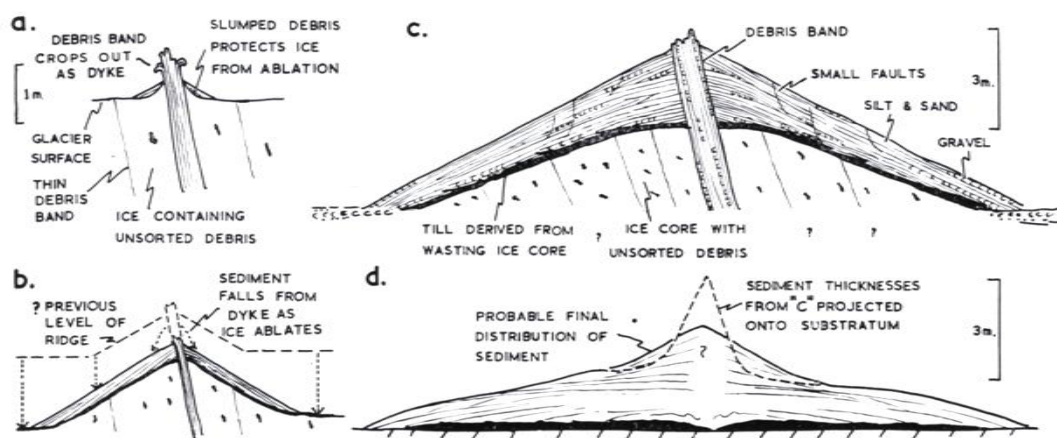
Fig 5.37 - Cross-sections illustrating the development of a controlled moraine ridge from a high-angle debris band (Boulton, 1967).
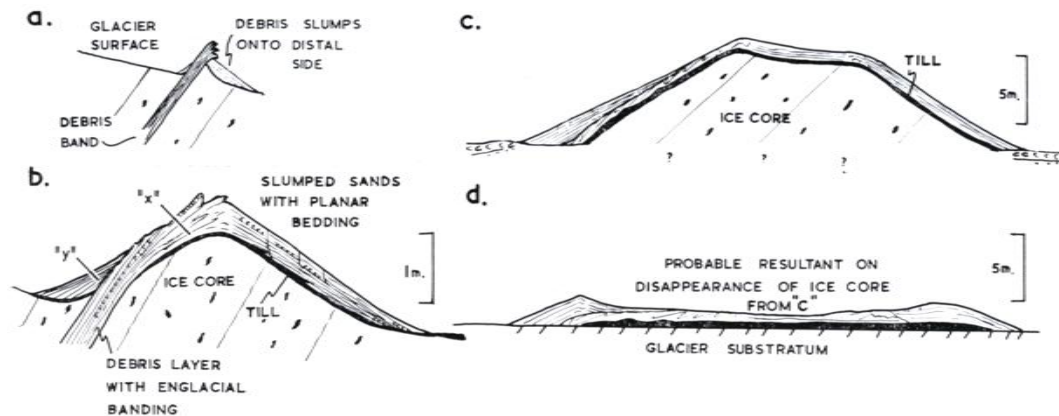
Fig 5.38 - Cross-sections illustrating the development of a controlled moraine ridge from a medium angle debris band (Boulton, 1967)

5.6.1.2 Evolution of eskers from channel fills

Type B deposits are particularly well preserved as englacial eskers containing well sorted and bedded sediment (Fig 5.31), in contrast to poorly sorted sediments found in type A ridges. Rather than melting out from ice, as in the case of debris bands, the ice walls surrounding the eskers melt out, resulting in the deposits being gradually draped onto the underlying substrate (e.g. Price, 1973). The high sand content of the deposits means that these are well drained. This fact along with the low ice content within the deposits contained within the ice-walled channels means that the deposits do not become saturated as the ice melts out from within, as is the case with type A and C deposits which are contained within pockets frozen in the ice (e.g. Fig 5.32d). As such, type B deposits maintain a low porewater pressure and therefore low susceptibility to failure on the melt out of the surrounding ice, so that their sedimentological structure may be initially preserved (Sletten et al., 2001).

However, some or all of the eskers found within the debris-covered snout and ice-cored moraine may be supraglacial eskers, which are common wherever supraglacial streams interact with supraglacial deposits (e.g. Boulton et al., 1999). Supraglacial eskers may also be formed during supraglacial 'overflow events' (Naslund and Hassinen, 1996; Spedding and Evans, 2002) resulting from the elevation of water and sediment to the surface under very high water pressure and are often found in association with hydraulic fracturing (e.g. Roberts et al., 2000). Supraglacial eskers are found close to zones of upwelling within the glacier margin (Fig 5.39), leading Spedding

and Evans (2002) to infer that some of their sediments are derived from subglacial or englacial sources during time of overflow, rather than just from supraglacial debris. Such overflow events may also result in the concentration of debris towards the margin in englacial channels (Spedding and Evans, 2002), creating the conditions for englacial esker formation on the melt out of ice.
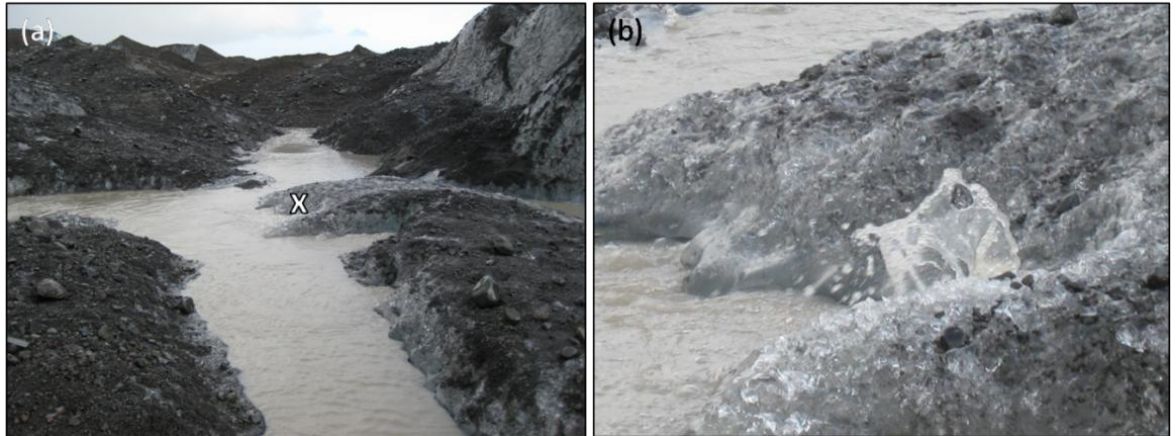
Fig 5.39 (a,b) - High pressure water emerging at the glacier margin, close to the center line of the glacier: (a) downglacier view of the channel and location of photo b marked as 'x'. (b) Water erupting out, indicating water under high pressure.

5.6.1.3 Evolution of supraglacial moraine from rockfall deposits

Supraglacial rockfall debris forms ice-cored moraine ridges along the southern lateral margin and within the medial moraine. The morphology of these ridges is determined by the shape, thickness and density of the rockfall deposit. During the study period a particularly large rockfall event occurred, resulting in the formation of a lobate deposit of angular rockfall debris within the medial moraine that was transported downglacier, reaching the glacier margin between 1980 and 1998 (Fig 5.35b, 5.36). The major distinguishing feature of large rockfalls from more frequent smaller events is the large proportion of debris from the former that remains on the glacier surface, whereas much of the latter becomes ingested into the glacier through crevasses or surface streams (Shulmeister et al., 2009). Thus, large rockfall events form a thick debris mantle on the glacier surface, protecting the underlying ice from ablation and resulting in the formation of an ice-cored ridge. Since its emplacement at the margin the rockfall deposit has evolved into a large ice-cored ridge about 40m above the glacier surface and 800m long as a result of the thick debris cover inhibiting ablation of the underlying ice relative to ablation of the surrounding glacier surface. The rockfall debris is composed of large angular clasts with a high friction angle such that the deposit can

support itself at a steeper slope (20° in 2003, Fig 5.50) (Paul and Eyles, 1990). Therefore the rockfall deposit represents a mechanism for stabilising the part of the northern margin that it impacted. This ridge is distinguished from the surrounding ice-cored moraine ridges by its monolithological appearance (reddish colour, Fig 5.44), suggesting that it originated from a single source (the rockfall event), in contrast to surrounding highly heterogeneous debris comprised of debris from many different sources within the glacier system (Shulmeister et al., 2009).

5.7 Ice-cored moraine: structure, sedimentology and morphology

All observations of ice-cored moraine in the following sections (5.7.1 - 5.7.3) are based on moraine complex A, a large ice-cored moraine complex at the frontal glacier margin (Fig 4.6). Data and observations on the sedimentology and morphology of ridges within the complex are first presented (Section 5.7.1), followed by morphometric analysis of DEMs of moraine complex A (Section 5.7.2). Finally data on recent morphological changes (1998 – 2008) associated with ice-disintegration are presented (Section 5.7.3)

5.7.1 Structure and sedimentology of moraine complex A

Sites 1 - 6

Most of the samples (Fig 5.40) along a transect surveyed through the moraine (Fig 4.7) plot within the mixed transport and water-worked clusters, defined by Spedding and Evans (2002) for debris populations at Kvíárjökull (Fig 5.41). Two samples, sites 2 and 3, plot outside these clusters and are therefore unclassified. They have a high C40 index for the low RA index meaning that the clasts are slabbier than expected for rounded clasts. This may be due to the rock type, for example rhyolite forms clasts with a very high C40 index that even if subjected to erosion and rounding may still retain some of their original slabbiness.
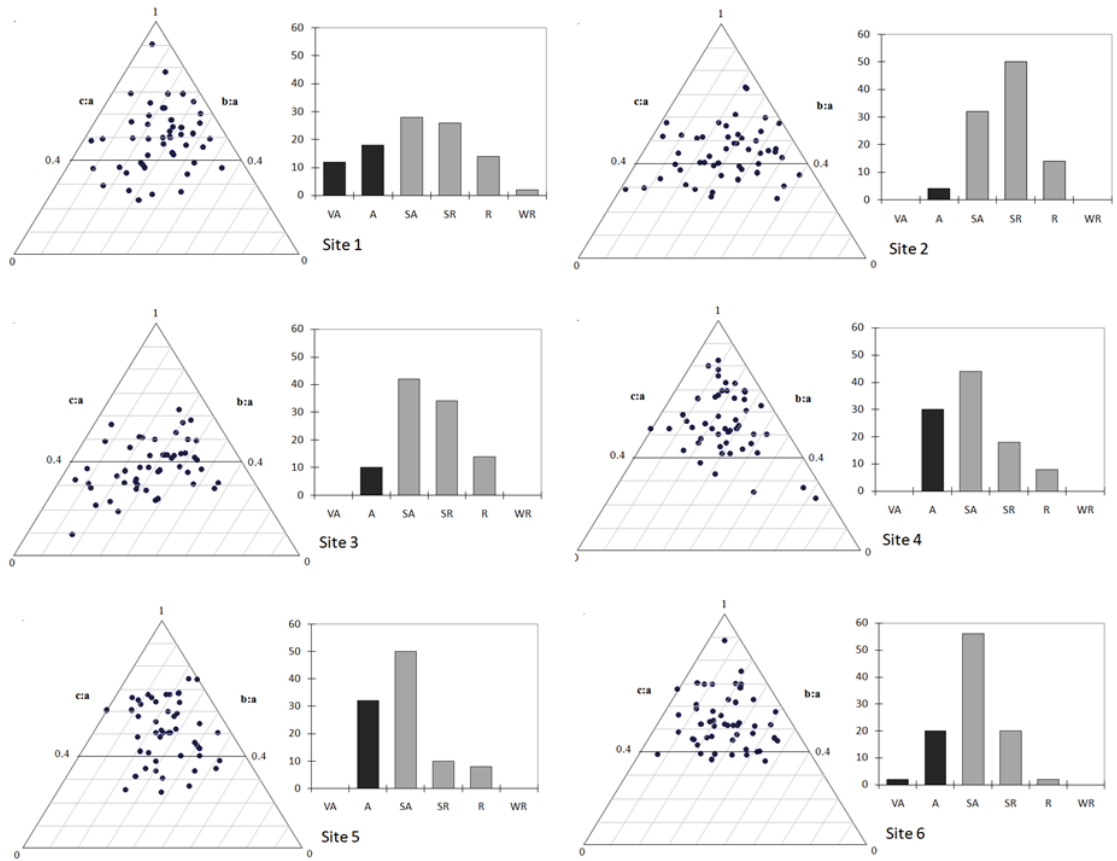
Fig 5.40 - Ternary diagrams showing clast shape data and histograms showing clast roundness distributions for each sample (1-6)
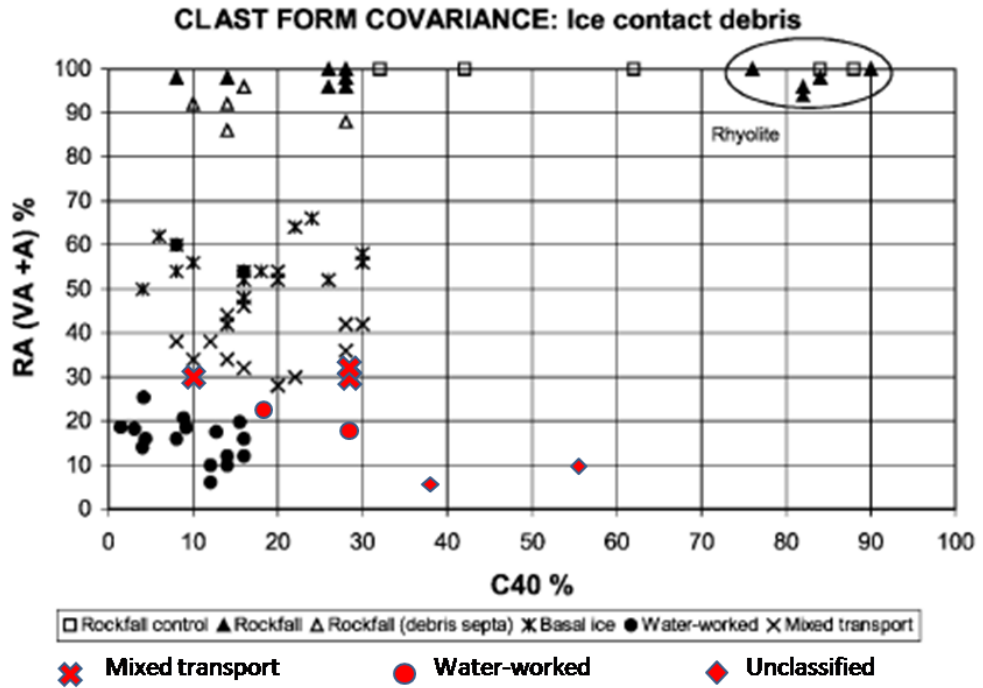
Fig 5.41 - Clast form covariance plot from Spedding and Evans (2002) with data from this study added in relevant symbols, in red. Points that are beyond transport type clusters identified in Spedding and Evans data remain unclassified.

Interpretation

The cross-profile, along which the clast form samples were taken at sites 1 - 6 within moraine complex A, traverses several ridges within a zone of ice-cored linear hummocky moraine that is situated downglacier from the large supraglacial lake (Fig 5.51a). The dark grey appearance of this zone in the 2003 colour photograph (Fig 5.44) makes it distinctive from the zone of red/brown rockfall debris upglacier from the supraglacial lake. Two samples along the cross-profile were classified as water-worked (Fig 5.41) supporting the interpretation of debris sampled within the moraine by Spedding and Evans (2002) as indicative of transport to the snout by englacial drainage networks. The influence of englacial drainage networks in the concentration of sediment at the margin is also signified by the occurrence of eskers and englacial channel fills (type B deposits) within the moraine, and the presence of collapsed cavities and englacial channels both within and proximal to the moraine complex (Fig 5.9). Three samples were classified as 'mixed' based on the debris populations identified by Spedding and Evans (2002). The difference between the water-worked and mixed debris is the latter's higher RA index (higher proportion of angular and very angular clasts). These more angular clasts may either be clasts from basal debris or rockfall debris, which are subsequently mixed with the water worked debris by the reworking of sediment.

Evans (2009) described the ice-cored moraine contained within this zone as 'controlled moraine' that has evolved from 'transverse supraglacial debris septa into ice-cored elongate mounds up to 10m high and composed of large volumes of sand and gravel', whose linearity has been 'enhanced' by ice-marginal pushing. However, prior to the 1980-1998 advance there was only a small, low relief ice-cored moraine complex with only very minor linear ridges (Fig 5.43). This complex was subsequently transformed into a complex of multiple, large, continuous linear ridges by 1998 (Fig 5.43). Therefore almost all linearity appears to have formed by pushing by a similar mechanism to that proposed by Evans and Hiemstra (2005) (Fig 2.5) during the 1980 – 1998 advance, emphasizing the morphological importance of ice-marginal pushing on moraine evolution at Kvíárjökull.

Site 7

A number of sharp crested, margin-parallel ridges found at the glacier margin do not appear to be melt out from any type of englacial debris concentration (Fig 5.42a-d). These are about 2 to 5m high and are located near to the centreline of the glacier, on the downglacier edge of the supraglacial lake, just inside the mouth of the sandur fan, at the southern end of moraine complex A. Sampling of the debris revealed the dominance of subangular clasts (Fig 5.42d) within a sandy matrix. The sample plots within the water-worked cluster of Spedding and Evans (2002) for debris populations at Kvíárjökull. Along the ridge there are numerous pockets of fine clay and silt (Fig 5.42a) as well as large striated boulders, some larger than 1m wide lodged into the proximal slopes of the ridges (Fig 5.42c).
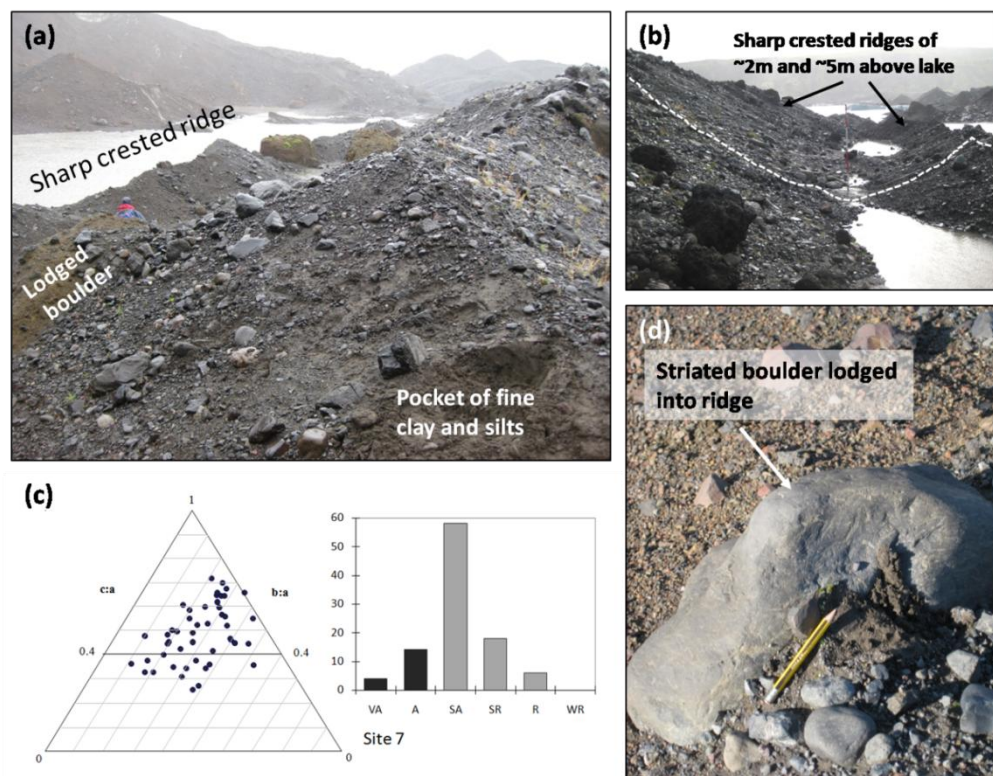
Fig 5.42 (a-d) - Sharp-crested ridges (a, b) composed of largely sub-angular clasts (c) within a sandy matrix and pockets of clay and silts, into which large boulders are lodged (d). Note the person for scale in (a) and the ranging pole in (b).

Interpretation

Sharp-crested ridges observed within the ice-cored moraine to the south of moraine complex A in 2008 are interpreted as push moraines of the small, seasonal type that

form during the winter advance of temperate glaciers (Sharp, 1984; Boulton, 1986; Bennett, 2001). The advances responsible for these moraines at Kvíárjökull are too small to be detected in morphometric analysis as they do not result in a large change in glacier volume. However, their morphology and sedimentology are both characteristic of push moraines. Their small size (2-5m high) and steep proximal slopes relative to distal slopes are morphological indicators of seasonal push moraines (Sharp, 1984). Water-worked debris and pockets of lacustrine sediments make up the ridges suggesting they were formed by the bulldozing of saturated lacustrine and outwash sediments (e.g. Hewitt, 1967; Benn and Evans, 1998, p249), which seems possible considering the location of the ridges along the distal side of a proglacial lake. Humlum (1985) identified rapid sedimentation against the ice margin as conditioning push moraine formation because of the coupling of the ice margin to the proglacial sediment that this facilitates (cf. Bennett, 2001). Sediment accumulation in the lake would have formed a supply of saturated and readily deformable sediment for push moraine formation during a glacier advance (e.g. Worsley, 1974, cf. Bennett, 2001). Bulldozing also explains the lodgement of boulders into the proximal slopes of the ridges. Many of these have indications of wear in the subglacial traction zone, suggesting that they melted out of the ice at the base of the glacier and were deposited in the lake prior to the advance.

5.7.2 Morphometric analysis

Two stages in the evolution of the present day moraine complex are identified: (1) 1945 – 1998 during which the ice-cored moraine complex expanded in area and relief; (2) 1998 – 2003 during which the moraine complex degraded in response to ice-disintegration and re-sedimentation.

5.7.2.1 Past evolution of moraine complex A

<u>1945 - 1998</u>

A few patches of higher elevation emerged at the snout between 1945 and 1964 in the northeastern corner of the complex (Figs 5.23), shown in the slope gradient change map for this period (Fig 5.46) as bands of steepening terrain, corresponding with the partly crenulated ridges mapped in the 1964 geomophological map (Fig 5.6). These

were likely formed by the pushing of ice-cored moraine during seasonal advances. Such advances are come at Icelandic glacier margins when the supply of ice exceeds ablation during the winter (Sharp, 1984; Boulton, 1986; Bennett, 2001). Similar push moraines were observed at the modern day glacier margin proximal to moraine complex A (Fig 5.42), supporting this interpretation. Between 1964 and 1980 the ridges steepened further and a large ice cored ridge (ridge x) elevated about 20m above the glacier surface emerged further uplacier, visible at 350m in profile 3 (Fig 5.45). Elevation decreased by 7m on average during this period (Fig 5.47).
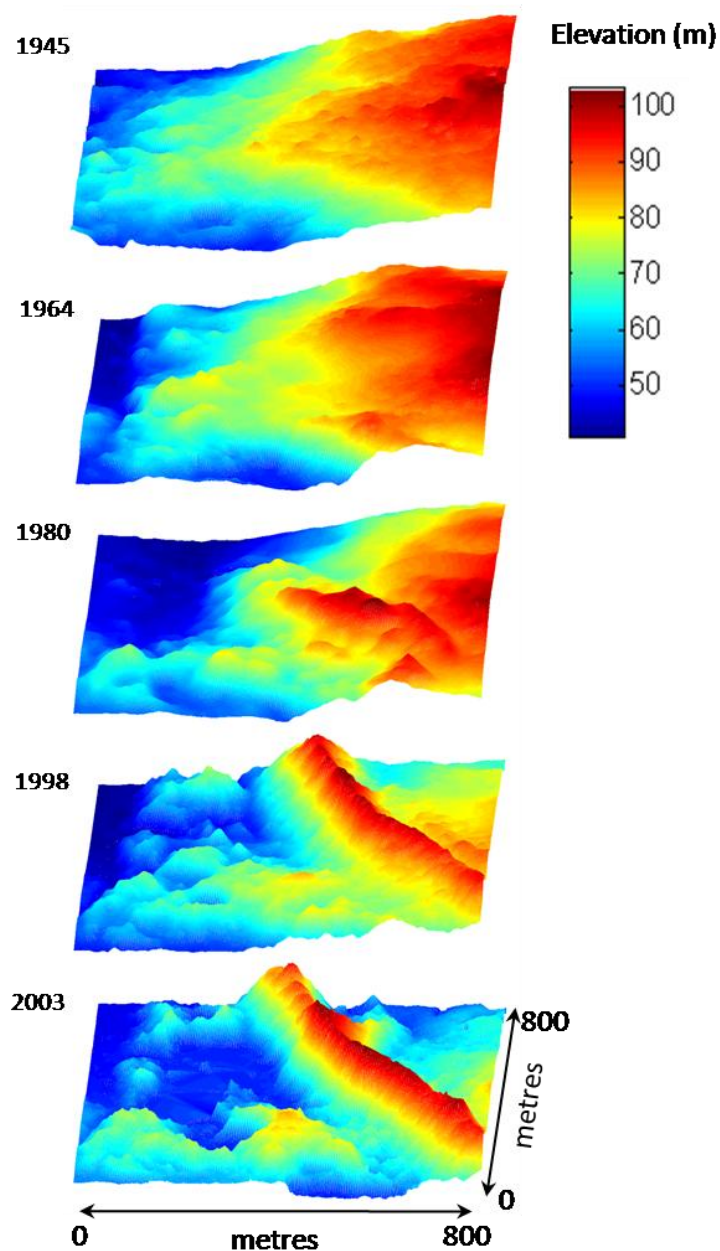
Fig 5.43 - Time series of DEMs of ice-cored moraine complex A. Note the emergence of the linear ridge and of smaller ridges in front of this between 1980 and 1998.
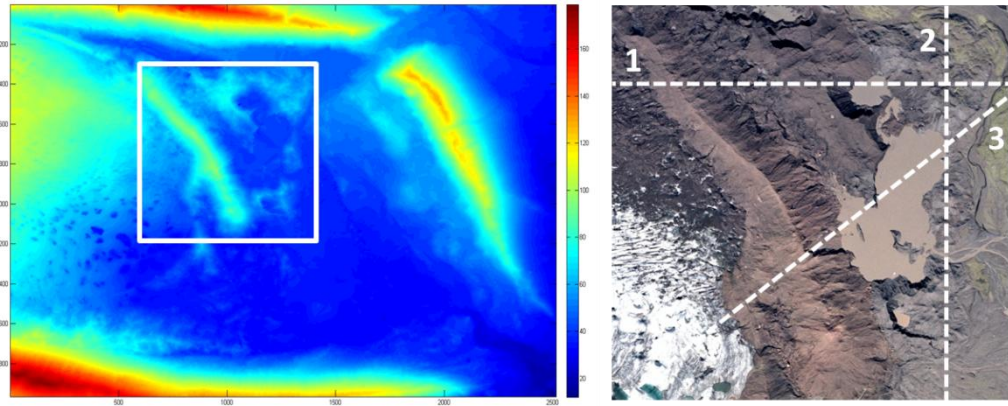
Fig 5.44 - Location of ice cored moraine complex A (white box in 2003 DEM) and locations of profiles 1 – 3 (shown on 2003 orthophoto of the boxed area).
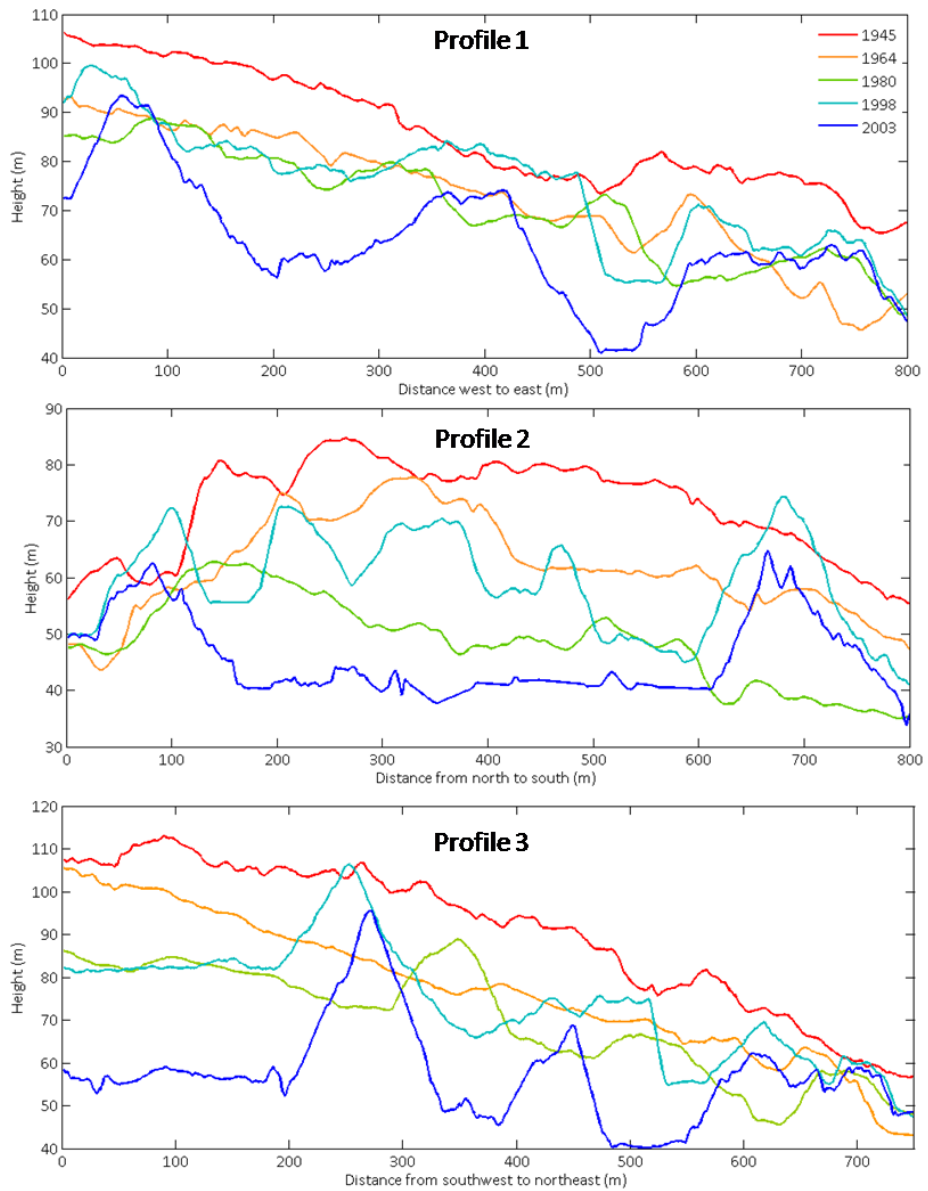
Fig 5.45 - Profiles through ice cored moraine complex (see Fig 37)

The most significant period in the construction of moraine complex A was 1980 – 1998 during the advance that occurred within the northern glacier snout. Elevation of the moraine complex increased during this period by an average of 6.5m (Fig 5.47). Ridge x moved down glacier between 1980 and 1998 by about 200m and was replaced by a 100m high, steep sided ridge, elevated above the upglacier surface by about 30m (profile 3, Figs 5.45), hereon called ridge X. Downglacier from this ridge several steep linear ridges developed along the front of the complex and in the NE corner (Fig 5.43). Notably, whilst these may have developed from ridges that have moved downglacier from 1980, they also increased in elevation by about 10m.During the advance Paul and Eyles (1990) observed ice-cored moraine being overridden, bulldozed and folded by active ice. These processes explain the elevation of moraine ridges present within 1980 by up to 10m by 1998 as well as the movement of these downglacier (profile 3, Fig 5.45). This ice also extended to the northeast corner of the complex, where it overrode the existing push moraine ridges present in 1980.
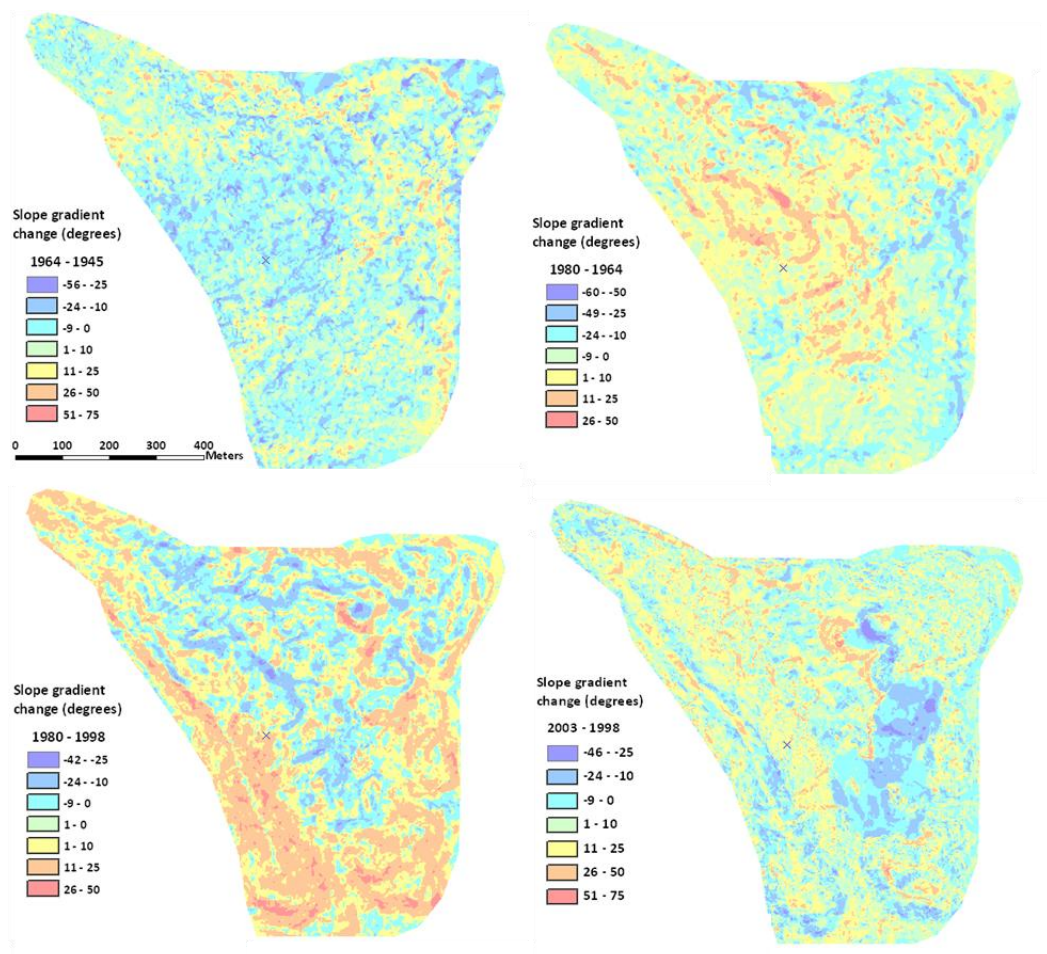
Fig 5.46 - Slope gradient change maps for each period in time. Red shows an increase and blue a decrease in slope gradient
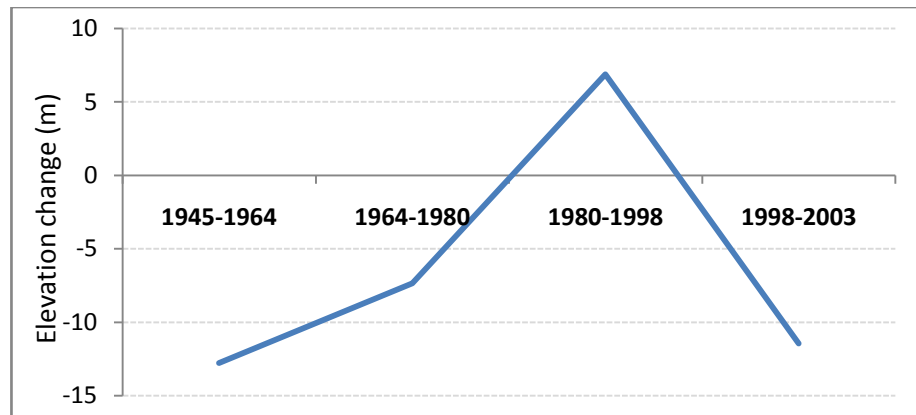
Fig 5.47- Elevation change within moraine complex A.

1998 - 2003

Between 1998 and 2003 a glacier karst landscape developed, as indicated by features of ice-disintegration and re-sedimentation present in 2003 (Fig 5.48). The present day complex is dominated by a large sharp crested ridge of about 150m wide and 100m high, that stretches more than 800m across the northern and central glacier snout (Fig 5.44) (ridge X). Upglacier from this ridge is the medial moraine and down glacier is a pitted complex of mounds of up to 75m high surrounding a large ice-walled lake.

5.7.3 Development of glacier karst from 1998 - 2008

The sediment-process-form relationships involved in the recent evolution of moraine complex A are described below based on detailed geomorphological mapping of surface features and processes (Section 5.7.3.1) and the quantification of de-icing by backwasting and downwasting (Section 5.7.3.2).

5.7.3.1 Features of re-sedimentation

Ice disintegration results in a number of processes of sediment reworking within moraine complex A (Fig 5.48). These can be categorized into those associated with either backwasting or downwasting of ice cores (Fig 4.9, see Section 4.3.4 for definitions).
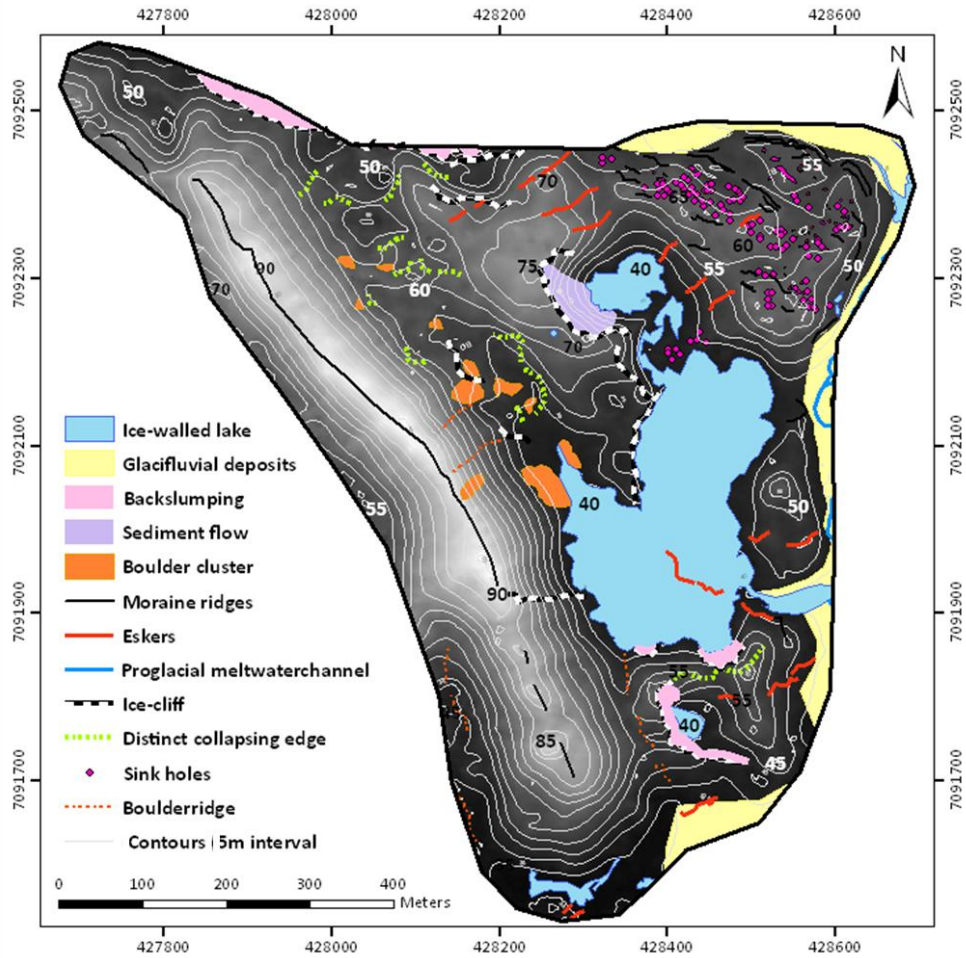
Fig 5.48 - .Distribution of ice-disintegration features and re-sedimentation processes in moraine complex A draped over a greyscale shaded DEM with contours at 5m intervals

Backwasting

The most dominant features are large supraglacial lakes surrounded by ice-cliffs. The largest of these stretches along the base of the distal slope of the large moraine ridge to the east of the complex (Fig 5.51a). The lakes are likely formed by the thermoerosion of englacial cavities and channels by meltwater (Etzelmüller, 2000). This is supported by the proximity of the lakes to eskers and proglacial meltwater channels. Continual backwasting of ice cliffs is facilitated by the de-stabilization of the cliffs by

Fig 5.49 - Blocks of ice in ice-walled lake following large rainfall event.

undercutting by lake water, evidenced by the notches along the base of the ice cliff in Fig 5.51a. The combination of thermal undercutting and backwasting results in the steepening of moraine ridges within the moraine complex (Fig 5.46), which by 2003 are as steep as 90° (Fig 5.50). Backwasting is enhanced by heavy precipitation, during which large blocks of ice fall off the ice walls, along planes of weakness. A large rainfall event during fieldwork resulted in the deposition of many large blocks of ice in the supraglacial lake (Fig 5.49) contributing to backwasting of the ice cliff.

Several smaller ice-exposures were observed throughout the ice-cored moraine. The dominant process of ice disintegration at these exposures is backwasting. Ice exposure 'b' is eroded at its base by a meltwater stream, contributing to both downwasting (by bottom melt) and backwasting by oversteepening of the ice wall (Fig 5.51d). Sediment cover of the ice cores at these exposures forms a heterogeneous and irregularly distributed mantle up to 3m thick (Fig 5.51c). The dominant processes of sediment redeposition from the top of these exposures are backslumping (Fig 5.51c) and sediment flows. Less dominant features of backwasting are ridges and clusters of boulders that accumulate at the base of the large moraine ridge as a result of gravitational fall sorting of sediment off the ridge.
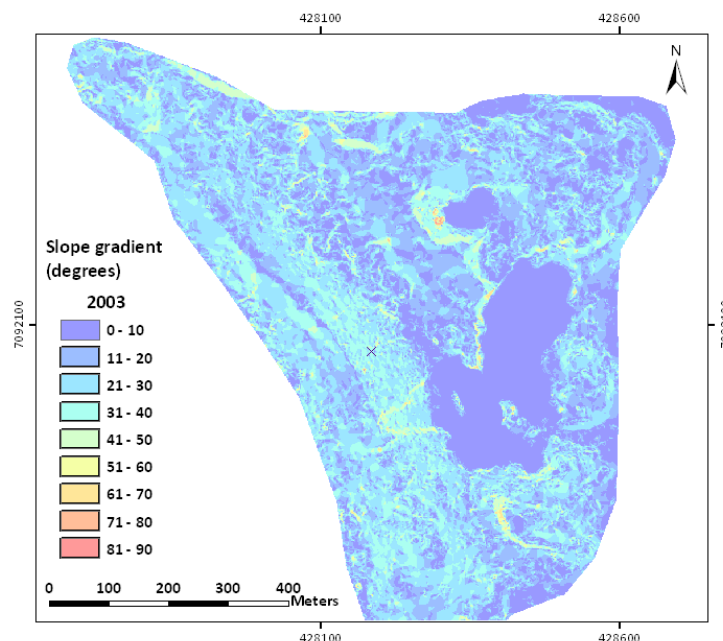
Fig 5.50 - 2003 slope gradient map of moraine complex A. Ice cliffs are highlighted in yellow – red colours and the lake and troughs are highlighted in dark blue.
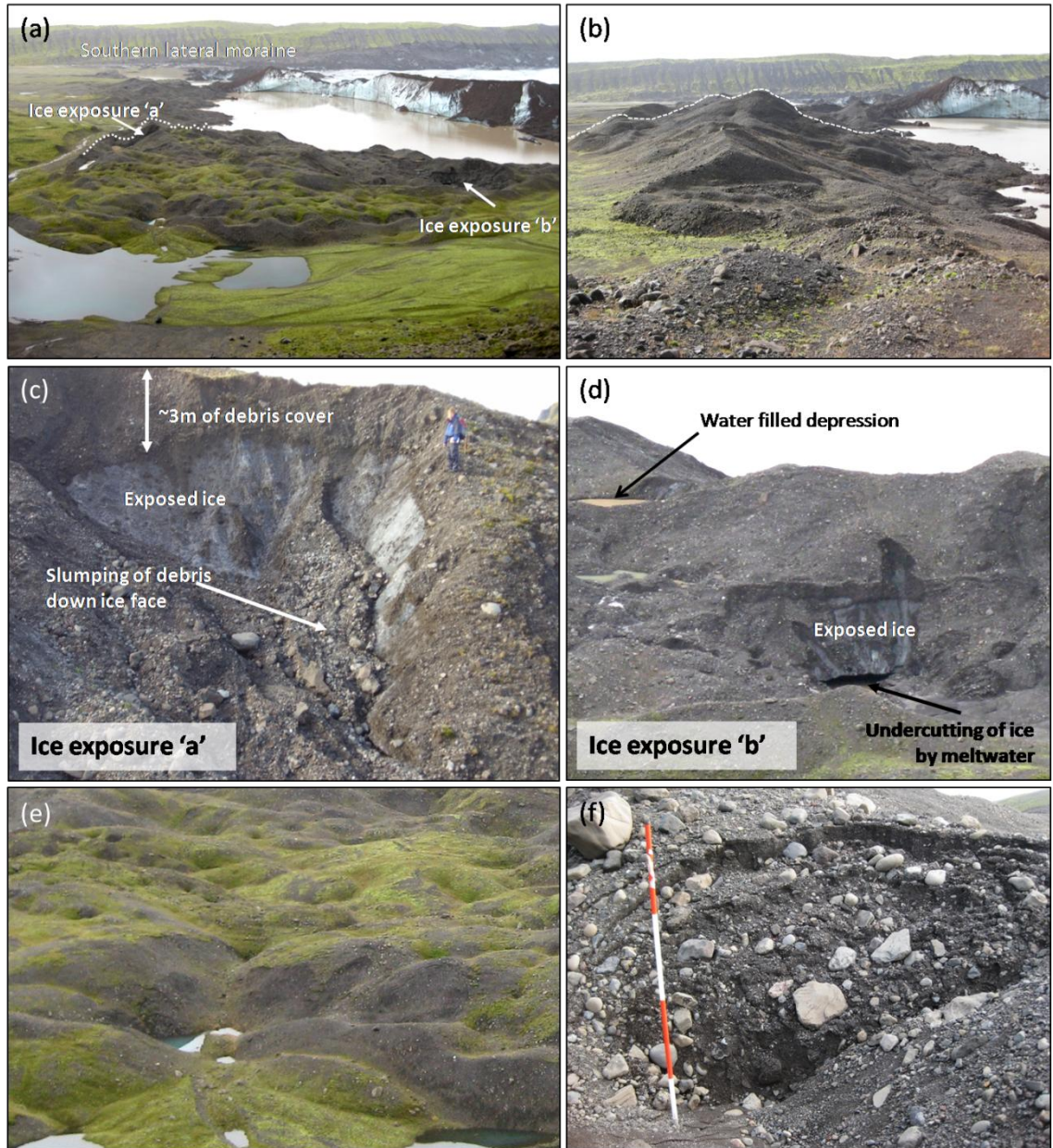
Fig 5.51 (a-f) - Photographs of moraine complex A - (a) oblique view of ice-cored moraine showing locations of ice-exposures 'a' and 'b' and of cross profile surveyed in 2008 (white dotted line) (Fig 5.52). Note the exposed vertical ice-wall on the far side of the ice-cored lake and the transition of ice cored moraine from non-vegetated into vegetated away from the lake edge. (b) Profile view of ice-cored moraine near to ice-exposure 'a'. Note the variable debris cover and the linearity in some of the ridges. (c) The slumping of debris down the exposed ice face at ice-exposure 'a'. (d) Prevalence of meltwater throughout ice-cored moraine in underlying streams and surface ponds demonstrated at ice exposure 'b'. (e) Partially ice-cored moraine in the north-eastern corner of the moraine complex. Ice-cores are cannot be seen due to a thick, partially vegetated debris mantle but their presence is evident from collapse features such as slump scars surrounding sink holes. (f) Arcuate slump scars on an ice-cored slope within mature ice-cored moraine, resulting from the slipping of sediment along slip planes associated with the melting of underlying ice.

Downwasting

Distinct collapsing edges occur throughout the moraine as tension cracks form around zones of sinking (Fig 5.51f) caused by high rates of localized downwasting, into which surrounding sediment collapses (Schomacker and Kjær, 2007). The north-eastern corner of the moraine complex displays unique surface features. This corner is the oldest ice-cored moraine within the complex having been formed by 1964. It is dominated by sink holes (Fig 5.51e), which indicate collapse due to the decay of deeply buried ice and are typical features in the final stage of ice-cored moraine development (Kjær and Krüger, 2001). A number of these sink holes are filled with water derived from the melting of underlying ice. A thick, partially vegetated debris mantle of heterogenous sediments completely covers the ice-core, suggesting that ice-disintegration is at a more advanced stage. Continued downwasting is also evident from slumping features such as slump scars around sink holes. There is apparent linearity in the topography that has been mapped as moraine ridges. Throughout the moraine are many examples of linear ridges highlighted by the collection of water in pools within the intervening troughs.

5.7.3.2 Quantification of short term dead ice melting

1998 – 2003

Between 1998 and 2003 the ice-cored moraine complex downwasted rapidly by about 12m (Fig 5.47), or $2.4ma^{-1}$. However, ridge X downwasted very little (10m in total) compared to downwasting of up to 34m upglacier and 45m in the downglacier moraine complex (Fig 5.43). The ridge was therefore further elevated above the glacier surface at about 45m in 2003 and, thus, well preserved. In the centre of the moraine complex, particularly high rates of downwasting occurred, associated with the growth of a number of supraglacial lakes. The ice walled banks of these lakes steepened by up to 75° in places as a result of backwasting. The area of the lakes increased from $100m^2$ to $125000m^2$ (calculated from Figs 5.8 and 5.9). The height of the ice walls surrounding the lake are about 20m, meaning that backwasting of the ice walls from 1998 to 2003 resulted in the loss of 2.5million m^3, contributing to 13% of the total ice volume lost between 1998 and 2003.

2003 - 2008

The cross profile surveyed in the field was extracted from the most recent DEM from 2003 in order to quantify the rate of backwasting and downwasting in the intervening time period of five years (Fig 5.52). The following rates represent the minimum values for backwasting and downwasting as there may have been some movement considering that the moraine complex is still attached to the glacier snout. The steepest southwest facing slope backwasted by a total of 20m, giving a rate of 4m a^{-1}. This is comparable with rates of backwasting recorded at Kötlujökull by Kjær and Krüger (2001) of 7.1m a^{-1}. The rate of backwasting on northeast facing slopes was about half the rate of southwest facing slopes. The maximum amount of downwasting along the profile was about 7m, giving an annual rate of 1.4m a^{-1}. The rate of downwasting was lowest over site 5, at which the debris mantle is thickest (3m), and highest between sites 3 and 4, where the debris mantle is much thinner (~0.35m). As a result of high rates of backwasting, about 30m laterally of high ground is lost between 2003 and 2008 but there is little change in elevation as a result of low rates of downwasting and a lack of topographic inversion.
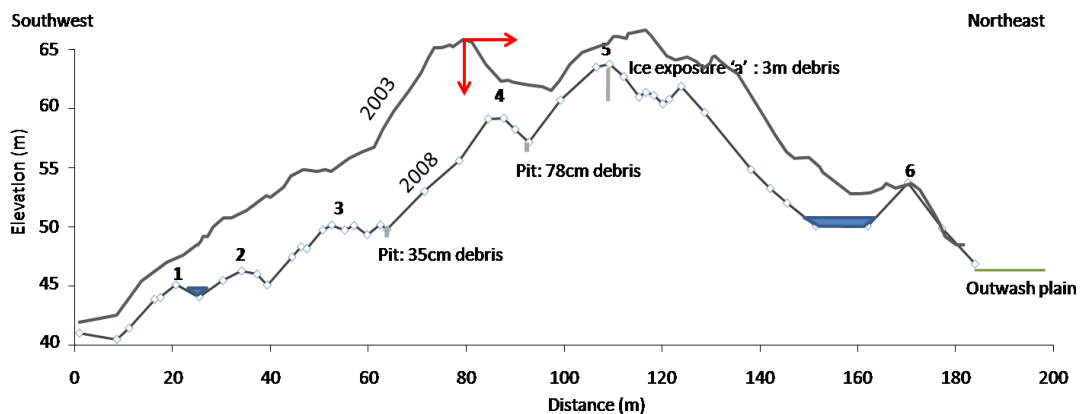
Fig 5.52 - Cross profile through moraine complex A (located in Fig 5.51(a)+(b)) extracted from 2003 DEM and surveyed in the field in 2008 for comparison. Locations of sites 1 – 6 at which clast form analysis was conducted are marked on the 2008 profile as well as depths of debris cover at three points along the profile and ponded water.

Backwasting rates along the profile through moraine complex A between 2003 and 2008 were more than 3 times higher than downwasting rates (Fig 5.52) indicating that backwasting rates are particularly important in ice-disintegration within mature ice-cored moraine at Kvíárjökull. As well as high air temperatures, high precipitation and

subglacial meltwater production enhance backwasting of ice cliffs by promoting mass movement processes and thus preventing the build up of an insulating debris mantle (Krüger and Kjær, 2000). High backwasting rates, assisted by thermal undercutting of ice cliffs by ponded water, were responsible for the rapid retreat of ice walls exposed by the collapse of englacial conduits and thus the enlargement of supraglacial lakes within the moraine. It was the enlargement of these lakes that made the most rapid contribution to the surface lowering of moraine complex A during mature karst development (Pickard, 1983). Between 1998 and 2003 38% of moraine complex A was lowered by the enlargement of supraglacial lakes by backwasting of ice-walls.

Effect of climate on rates of backwasting and downwasting

Annual de-icing rates within moraine complexes A, B, C and D for 1998 – 2003, were higher than those in the previous period (Fig 5.18). There was an increase in air temperatures over this period which would have promoted higher rates of both downwasting and backwasting within moraine complex A and downwasting in debris-covered moraine complexes B, C and D. Other studies have found a strong correlation between air temperature and de-icing rates (Schomacker and Kjær, 2007; Schomacker, 2008). In a comparison of backwasting rates from dead-ice areas under different climate conditions Schomacker (2008) identified that the highest rates occur in the warm maritime climate of the Tasman Glacier, New Zealand.

Effects of meltwater on rates of backwasting and downwasting

Whilst it was not possible to quantitatively assess the relative importance of top and bottom melt in downwasting at Kvíárjökull, bottom melt is probably more important considering the prevalence of meltwater streams within and around the ice cored moraine, the geothermal heat flux at Kvíárjökull related to its volcanic setting, and the melting of ice beneath lakes, all of which enhance bottom melt (Driscoll, 1980). Welch (1967) found that at Breiðamerkurjökull ice wastage by bottom melt was double that by top melt under 50cm of gravel. Bottom melt results in the enlargement of cavities into which debris is deposited and washed away by meltwater (Fig 5.51d) thus reducing the thickness of the overlying debris mantle and enhancing the rate of ice melt.

Melting may have been enhanced following the 1980-1998 advance of the glacier, related to an increase in meltwater activity accompanying the advance. Kruger (1994) found that at Kötlujökull the melt-out of ice in front of the advancing glacier in the 1980s proceeded much faster due to the increased meltwater discharged during the glacier advance causing an increase in thermo-erosion at the base of ice cores (Etzelmüller, 2000). This would also explain the increase in the melting rate of moraine complex B during this period (Fig 5.56), around which meltwater was routed after 1964 (Fig 5.6). Most meltwater discharged from the northern part of the snout was channelled away from the margin and along the edge of the sandur fan throughout the study period, meaning that its affect on ice-core melting was restricted to ice-cored moraine at the edge of the channels. In contrast, meltwater discharged from the southern snout margin was periodically ponded within the overdeepening between the glacier snout and higher relief within the outer foreland, which acts as a reservoir for englacial drainage.

Between 2003 and 2008 the proglacial lake has expanded across the foreland. In just one melt season several collapsed englacial channels that dissect the ice-cored moraine at the southern margin in 2007 (Fig 5.53a) coalesced, consuming much of the ice-cored moraine and leaving only a few ice-cored ridges as islands in the lake (Fig 5.53b).
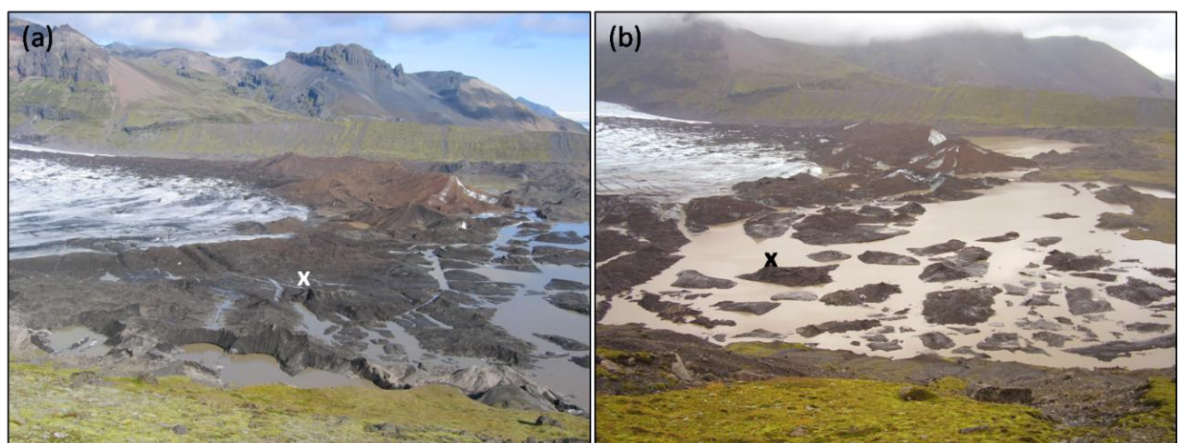
Fig 5.53(a,b) - The growth of a proglacial lake at the glacier margin between 2007 (a) and 2008 (b). 'x' marks the location of the vertical dyke structure in figure x.

Although air temperature definitely exerted control over the rate of glacier retreat over the study period, the recent accelerated retreat of Kvíárjökull between 1998 and 2003 exceeds the increase in temperature. The increase in meltwater erosion related to lake expansion within the overdeepening seems the most likely explanation for the accelerated rate of retreat between 1998 and 2003. Lake expansion is geomorphologically very significant at Kvíárjökull as it effectively 'drowns' the proglacial area and destroys other landform signatures below the water level.

5.7.3.3 Topographic evolution of the moraine complex (1945 – 2003)

The dynamic nature of change within the ice-cored moraine is illustrated by the meshed temporal profile and corresponding temporal bar (Fig 5.54b,c), that cross cuts the moraine complex along part of Profile 3 (Fig 5.54a). In the meshed temporal profile time is an additional axis (z) along with distance (x) and elevation (y). The profiles are meshed together along the z axis, through time, such that elevation changes are more explicit than in the equivalent overlapping two-dimensional profiles. The temporal bar chart shows bars of elevation variation in colour along the profile for each date alongside each other, aiding the interpretation of the meshed profiles. There are several instances of relief inversion through time. For example, at 100m along the profile, elevation decreases from over 100m in 1945 to about 80m in 1964, then increases in 1980 back to almost 100m, and decreases again in 1998 and 2003. At 200m along the profile, elevation decreases between 1945 and 1980, increases in 1998 and decreases in 2003. Relief becomes more complex within the profile between 1945 and 2003. In 1945 there is a graduation from high elevation to low elevation (dark red to blue in the temporal bar chart) along the profile with minor fluctuations in elevation of less than 10m. In 1964 the graduation is even smoother, with minor fluctuations of around 10m after 300m along the profile. In 1980 there are much larger elevation fluctuations of about 20m along the profile. For example, there are ridges of higher elevation at 50m, 250m and 350m. In 1998 there are more fluctuations along the profile with ridges of higher elevation at 140m, 200m, 300m and 450m. In 2003 these fluctuations are larger (~30m) but fewer and many of the ridges of high elevation in 1998 are replaced by troughs of lower elevation, for example between 60 and 160m and 240 – 380m.
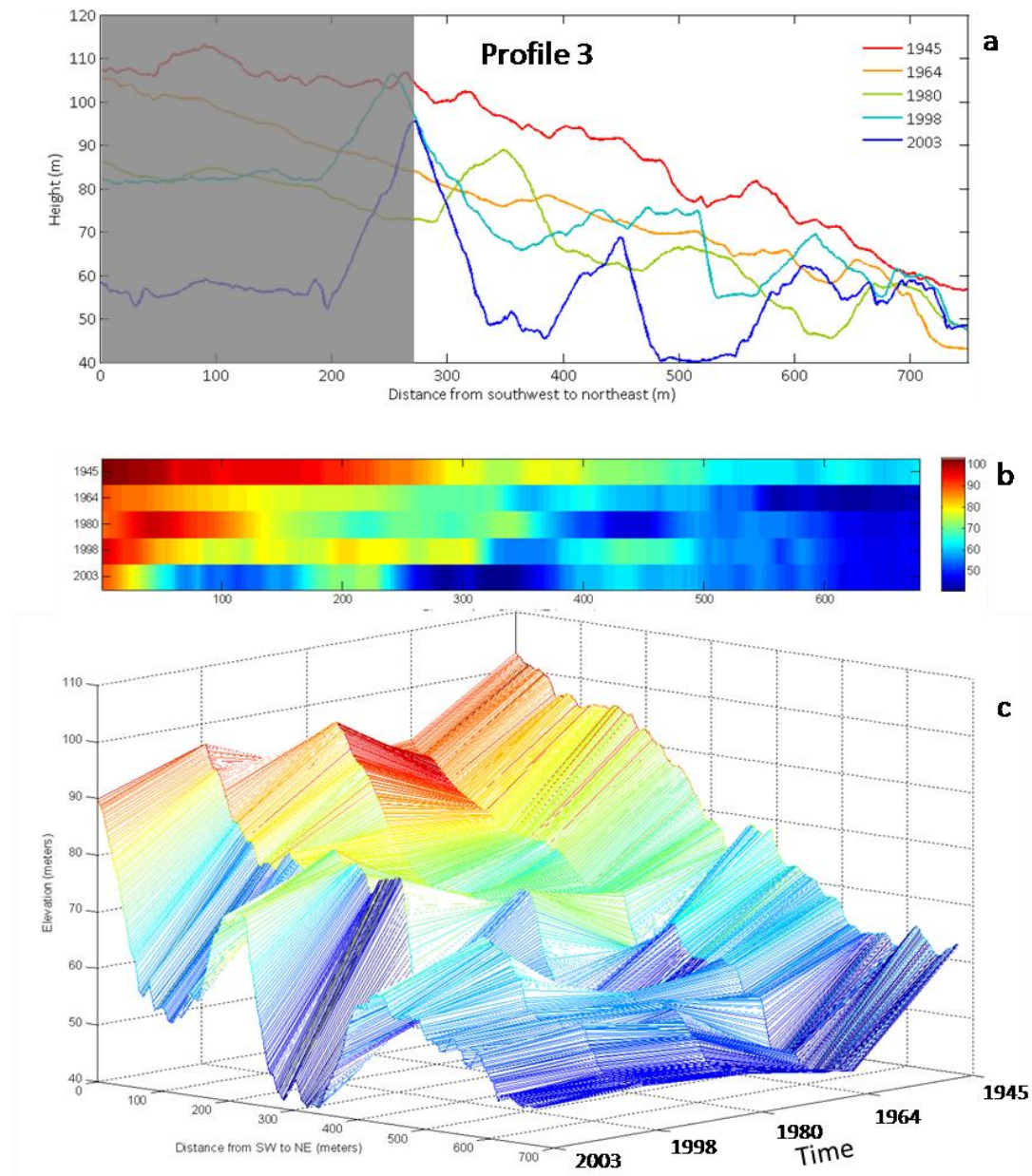
Fig 5.54 (a-c) - Visualizing elevation change in the ice-cored moraine complex: (a) corresponding two dimensional profile 3 (Fig 5.45) covered by the meshed temporal profile (section not covered is greyed out); (b) bar chart in which each bar shows elevation in colour along the profile that year; (c) meshed temporal profile in which temporal profiles through the moraine are meshed together along the time (z) axis, thus visualizing elevation change in three dimensions.

5.8 Structure, sedimentology and morphology of older moraine complexes (B – D)

5.8.1 Moraine compex B

5.8.1.1 Results

<u>*Geomorphology*</u>

Moraine complex B (Fig 5.55) forms a 40852m² strip of largely de-iced moraine (mapped as post-LIA till) that evolved from ice-cored moraine between 1980 and 1998. It emerged in 1964 as a collection of discontinuous, sawtooth shaped ridges (Fig 5.6) and was isolated from the snout by 1980 by glacifluvial meltwater emanating from the northern snout margin.

Fig 5.55 - Hummocky moraine of moraine complex B. X marks the location of the exposure shown in Fig 5.57.

The ridges are interspersed with water filled depressions of varying sizes that signify past collapse due to the melt out of ice. A sawtooth pattern is still recognisable in the moraine ridges despite re-sedimentation and degradation of the moraine complex. This pattern is highlighted by the location and orientation of the water filled depressions on either side of these ridges.

<u>*Morphometric analysis*</u>

The de-icing progression of the moraine complex was interrupted by an increase in elevation of 0.5m between 1964 and 1980 (Fig 5.56), although this may represent DEM error, especially as the 1964 DEM typically underestimates elevation elsewhere in the

foreland. Whilst mapped as post LIA till from 1998 onwards (Figs 5.8 and 5.9), the complex is evidently still partially ice-cored, because elevation continued to decrease by about 0.5m between 1998 and 2003. The irregular shape of the ridges is also shown on the slope gradient map as strips of higher slope gradient (Fig 5.56). In comparison to moraine complex A (Fig 5.50), the predominant slope gradient in moraine complex B is much lower: 0 - 10°, compared to 21 - 30°. The highest slope gradient is 60° compared to 90° in moraine complex A.
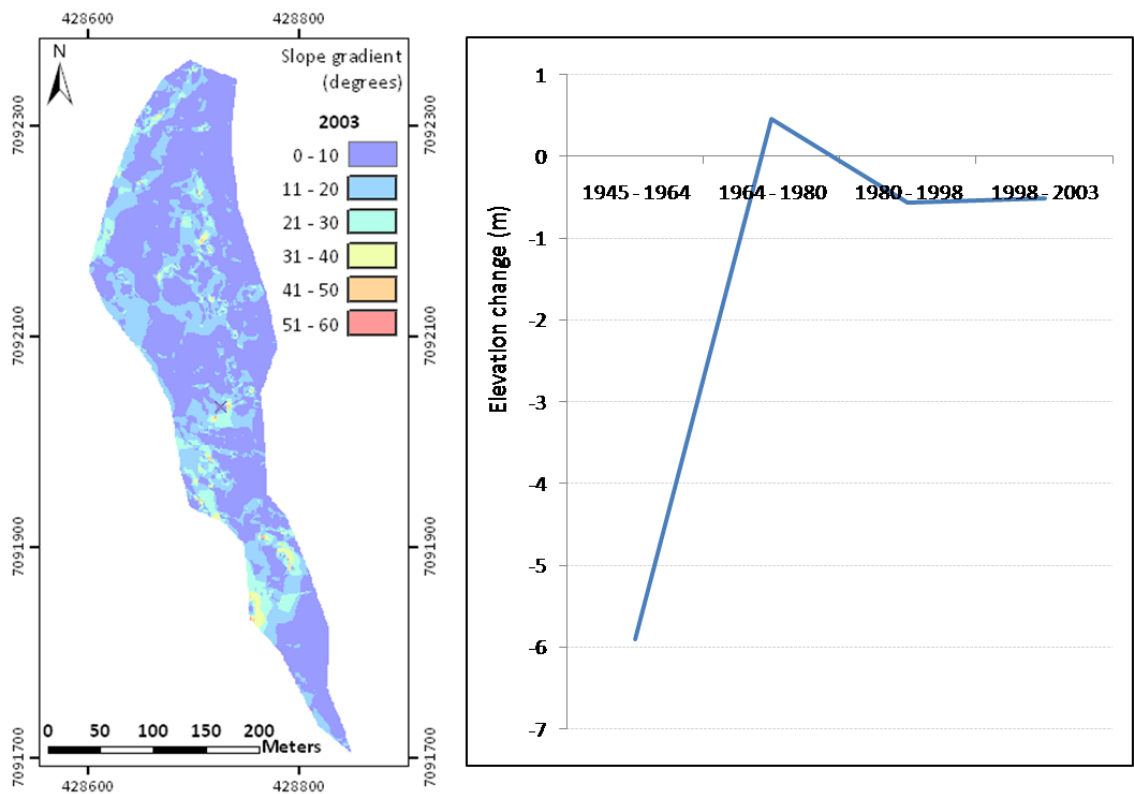
Fig 5.56 - Moraine complex B: left: 2003 slope gradient map; right: elevation change

Sediment log

Fig 5.57 was drawn from a photograph taken by Dr D.J.A. Evans in 1992. The exposure has since been degraded so that the structures are no longer visible. The moraine ridge is about 10m high and has a symmetrical planform profile. It consists of a core of deformed sediment with a surface of re-worked gravels. There is evidence of gravitational sorting on the proximal slope, with an accumulation of larger gravel clasts at the base of the slope. The base of the exposure above the river is concealed by about 30cm of gravel. There is no evidence of a remnant ice-core in the ridge.
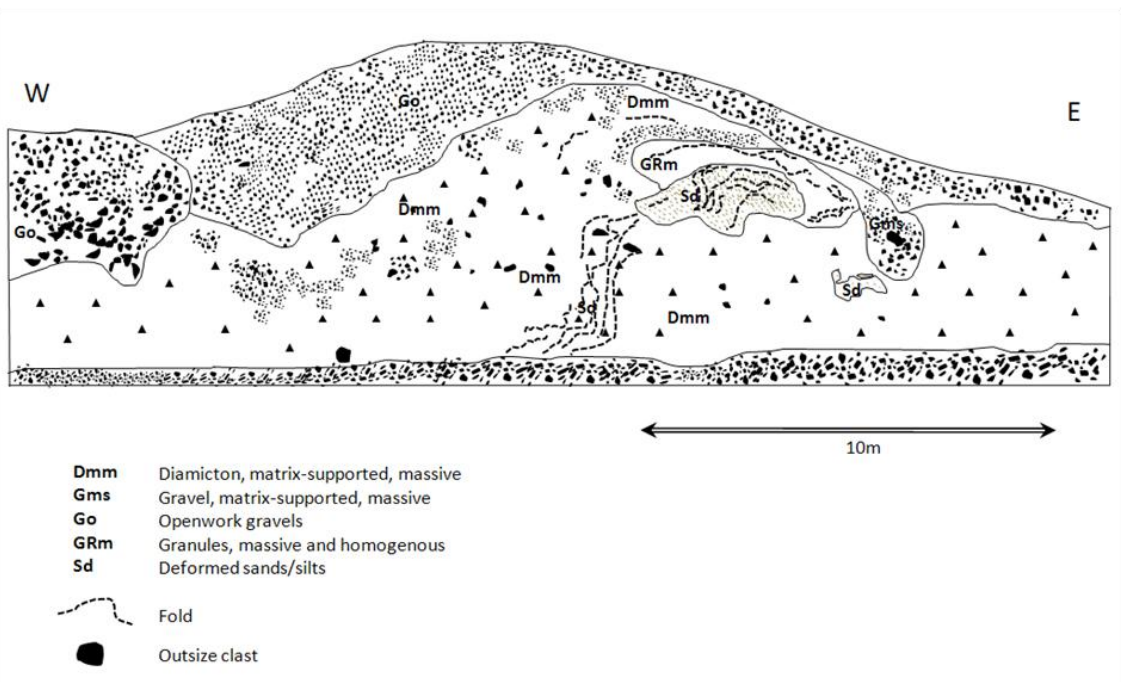
Fig 5.57 - Top: Exposure through moraine ridge in moraine complex B (X in Fig 5.55). Bottom: Diagram of exposure through moraine ridge shown in figure x. Facies codes are those Evans and Benn (2004).

The core is composed mainly of diamicton, through the middle of which is a sequence of folded and contorted sands and granules. Towards the base of the core the fold axes dip upglacier by ~45°. On the upglacier side of this sequence there are several outsized clasts and minor deformation structures such as small folds. Towards the top of the core the dip of the fold axes decreases and reverses towards the eastern end of the core. Together the folds form a large overfold (Benn and Evans, 1998, p255). The diamicton unit that lies below these contorted sediments contains small stringers of fine sediment.

5.8.1.2 Interpretation

The folded and contorted sediments within Fig 5.57 are clear indications of a post-depositional ductile deformation during ice-marginal bulldozing (Benn and Evans, 1998). An increase in elevation between 1945 and 1964 at several points along this moraine (Fig 5.23) give credence to the interpretation that the glacier pushed up glacial sediment along this slope. The moraine section exposed is part of a crenulated moraine that formed at the glacier margin by 1964 (Fig 5.6).

The sequence of folded sands, granules and gravels is suggestive of an ice advance into outwash sediments. This outwash sediment was likely dumped into crevasses as part of an apron covering the glacier snout prior to bulldozing. The longitudinal crevasses at the 1945 margin are buried in an apron of supraglacial debris, supporting this interpretation. Humlum (1985) identified rapid glacifluvial sedimentation against ice margins as conditioning push moraine formation because of the coupling of the ice margin to the proglacial sediment that this facilitates (cf. Bennett, 2001). The sequence of folds would have been formed by compression and shortening during ice marginal advance. The orientation of the main axis of the folded sequence indicates that the direction of pushing was west to east, similar to the axes of folds in Fig 5.58.
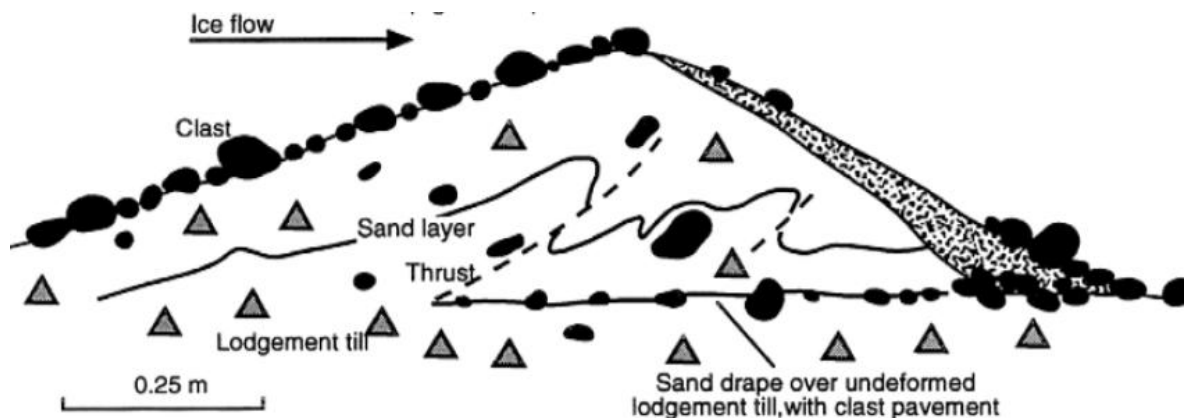
Fig 5.58 - Section through a ridge formed in the winter 1978/1979 in front of Sléttjökull (modified from Krüger, 1994). (Source: Bennett, 2001).

5.8.2 Moraine complex C

5.8.2.1 Results

<u>Geomorphology</u>

Moraine complex C forms a 150,594 m² strip of largely de-iced hummocky moraine (mapped as post LIA till) along the base of the latero-frontal moraine (Fig 5.59a-d) that evolved from ice-cored moraine between 1964 and 1980. It is separated from moraine complex B by a flat area of lower elevation (Fig 5.59c), in which there has been little elevation change during the study period. On its uplacier side there is a long chain of hummocks (Fig 5.59b), with many subtle linear features (Fig 5.59c), not depicted in the DEMs but visible in the higher resolution orthophoto. Along the base of the slopes there is a wide channel filled with lakes and slope deposits (debris cones and alluvial fans) (Fig 5.59b). At the southern end of the complex there are a number of sinuous ridges of several meters in length and up to two metres high that descend from the slopes of the lateral moraine onto the foreland. They are orientated almost perpendicular to the chain of hummocks (Fig 5.59d). There are also a number of abandoned meltwater channels with the same orientation that cut down through the chain of hummocks into the middle foreland.

<u>Morphometric analysis</u>

Rates of de-icing between 1945 and 1964 averaged 0.6m yr⁻¹ with a total reduction in elevation of 11m (Fig 5.60). Annual de-icing rate was halved to about 0.3m between 1964 and 1980 with a total reduction in elevation of 4.5m. The rate decreased further to 1.5cm each year from 1980 to 1998. It then increased to 4.4cm per year between 1998 and 2003. The predominant slope gradient is 0-10° and maximum slope gradient is 50° (Fig 5.60).
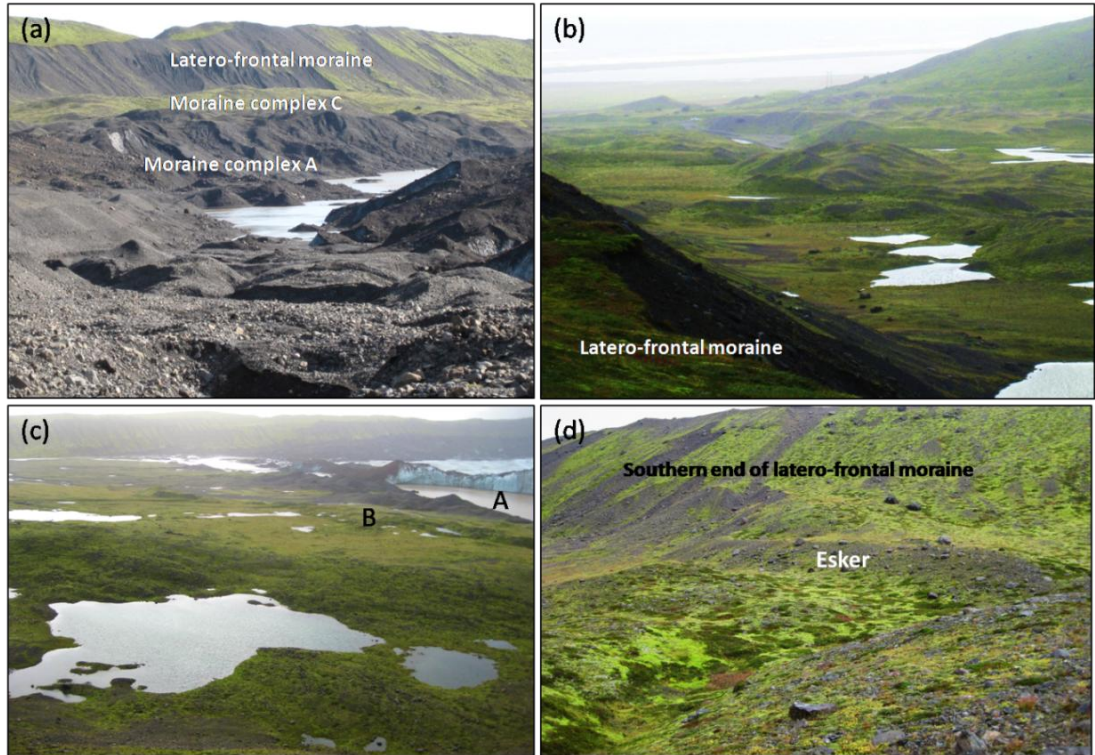
Fig 5.59 (a-d) - Moraine complex C. (a) View of complex C, beyond complex A, viewed from upglacier. (b) View from latero-frontal moraine, showing band of hummocky moraine in complex C separated from the base of the lateral moraine by a corridor filled with lakes and alluvial fan deposits. (c) View across the northern end of the complex. Note the fine linear ridges and boulder ridges on either side of the small lake. (d) A sinuous ridge descending from the base of the lateral moraine and interpreted as a valley esker.
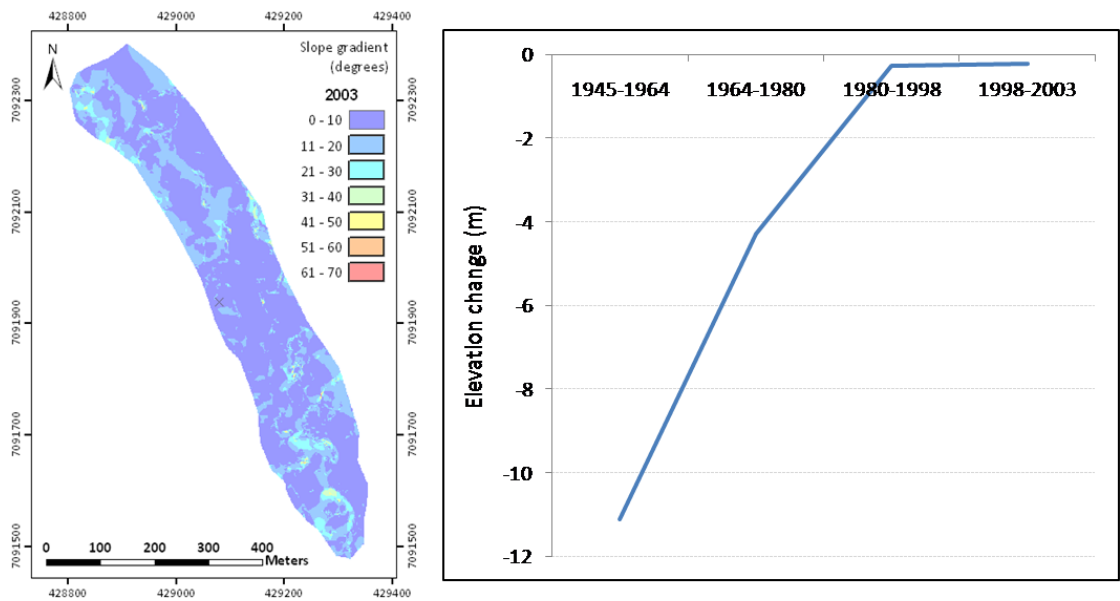
Fig 5.60 - Moraine complex C: left: 2003 slope gradient map; right: elevation change.

5.8.2.2 Interpretation

<u>Geomorphology</u>

Moraine complex C is situated downglacier from the medial moraine, and moraine complexes A and B. As indicated by morphometric analysis most ice-melted out between 1945 and 1964 (Fig 5.60), and consequently most morphometric change related to ice melt-out would have occurred during this time. These changes are not captured at the temporal resolution of the aerial photographs used. With no exposures or sedimentological data available, the origin of moraine ridges within moraine complex C is uncertain, however, considering its location downglacier from moraine complexes A and B (Fig 5.59a) it is reasonable to assume that similar processes were responsible for its current morphology.

Using the moraine complexes A and B as analogues for moraine complex C, several processes may be responsible for the features that developed within the complex on the melt out of ice between 1945 and 1964. The large transverse ridge along the downglacier edge of the complex (Fig 5.59c) is unlikely to be a deposit from a large rockfall event, as there is no indication of a large ice-cored ridge in 1945 similar to that at the present day glacier margin (Fig 5.5). Considering the subtle transverse and partly crenulated ridges along its distal slope, it could be a large push moraine complex, formed by an advance between 1945 and 1964. Similar multiple-crested complexes have been observed to form at modern day glacier margins (e.g. Boulton et al., 1976). Considering the scale of morphometric change induced by the 1980-1998 advance at the northern margin during which sufficient stresses were propagated into the foreland to elevate moraine ridges by up to 10m, this interpretation does not seem unreasonable. Furthermore, a number of glaciers in Iceland started to advance at the end of the 1940s (Fig 2.1) corresponding with a drop in summer air temperature. Alternatively, the ridge may be an existing feature within the foreland, either a bedrock ridge or a sandur train which has resisted deformation. Boulton (1986, 1987) reported that remnants of pre-advance sandur fans up to 2.5km long still survive in the proglacial area at Breiðamerkurjökull. Breiðamerkursandur is a 20km wide, 5km long sandur fan composed of many smaller sandur fans of only a few hundred meters wide. These fans are effectively thick ramps of sediment that are difficult for later proglacial

meltwater to rework. Meltwater is diverted around them resulting in the development of channelized, terraced outwash trains with ribbon lakes in the depressions between them.

Between the ridge and the latero-frontal moraine, several lakes were formed between 1945 and 1964. These were likely formed by the enlargement of collapsed cavities within the ice-cored moraine by backwasting. Sinuous ridges within the southern end of the complex are interpreted as valley eskers. These are distinctive along the southern glacier margin as downslope-orientated sinuous ridges, superimposed on terraces of rockfall debris. Valley eskers form from tunnels within thin marginal ice in which water flow follows the local slope rather than the ice surface gradient (Benn and Evans, 1998: 451; Bird, 1967), explaining the downslope alignment of the complex C eskers at the base of the slope of the latero-frontal moraine.

De-icing progression

Rates of de-icing during the fully ice-cored stage of complex C (1945 – 1964) are less that those within moraine complex A between 1998 and 2003 but may have been higher during the first five years of de-icing (1945 – 1950). This is because free ice faces would have promoted high rates of backwasting, leading to rapid surface lowering, as observed in moraine complex A more recently. The redistribution of sediment from topographic highs to topographic lows would have decreased debris cover on ridges, leading to their rapid downwasting. Bottom melt would have also been high as a result of meltwater produced by melting and routed underneath the moraine complex from marginal meltwater production. The combination of these processes led to an annual lowering of almost 0.6m between 1945 and 1964 and a total lowering of 11m (Fig 5.60). Between 1964 and 1980 the annual rate of lowering was reduced to about 0.3m. This agrees with the rate of surface lowering at partially ice-cored moraine at Kötlujökull (Kjær and Krüger, 2000). This reduction would have been the result of the thickening debris cover associated with surface lowering, debris melt out and re-sedimentation during melt out of the fully ice-cored moraine (Kjær and Krüger, 2000). Vegetation and the reduction of meltwater may also have reduced the melting rate within partially ice-cored moraine. These findings suggest that it takes about 20 years

for a fully ice-cored moraine to evolve into partially ice-cored moraine, agreeing with the calculation of Kjær and Krüger (2000) based on Kötlujökull.

5.8.3 Moraine complex D

Geomorphology

Moraine complex D is a 171,317m² area in the outer southern foreland, on the banks of the proglacial lake (Fig 5.61a,b). It is composed of several inset, linear chains of hummocks, 5 – 10m high, separated by several abandoned meltwater channels and pitted with a variety of water filled and dry depressions.
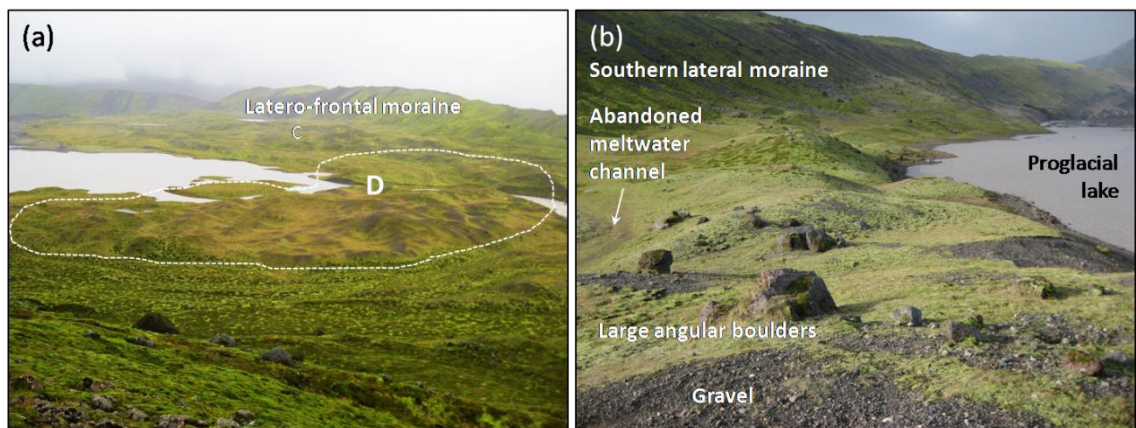
Fig 5.61 - Moraine complex D: (a) Overview of complex; (b) Surface characteristics of moraine, showing vegetated chains of hummocks composed of gravel with overlying angular boulders. The complex is dissected by abandoned meltwater channels.

Morphometric analysis

The moraine complex downwasted between 1945 and 1964, with a reduction in elevation of 4m (Fig 5.62). The increase in elevation between 1964 and 1980 is likely due to particularly high DEM error around the lake, over which matching is difficult as a result of the smooth reflective surface. Between 1980 and 1998 there was negligible elevation change, and between 1998 and 2003 there was a reduction in elevation of about 0.6m. Slope gradients range from 0 to 70° (Fig 5.62). The highest slope gradients occur along the banks of the river Kvíár, which winds through the centre of the complex from northwest to southeast. The predominant slope gradient on either side of these banks is 0 - 10°. Continuous strips of higher slope gradient highlight the courses of abandoned meltwater channels feeding into the river Kvíár.
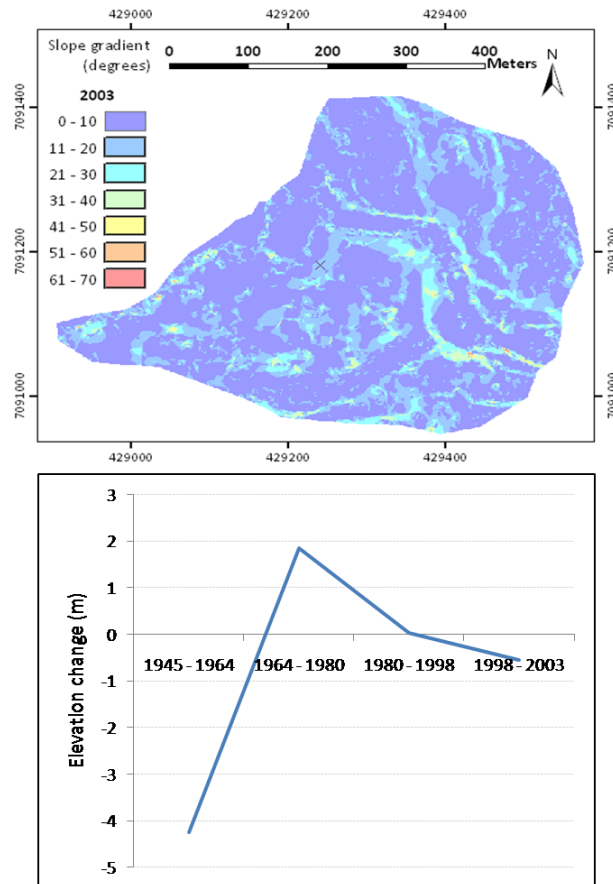
Fig 5.62 - Moraine complex D: top: slope gradient map from 2003 DEM of moraine complex D; bottom: elevation change.

Two meshed temporal Profiles, 1 and 2 (Fig 5.64), located on either side of the river Kvíár (Fig 5.63) show morphometric changes during the study period within the moraine complex. In both profiles there is a large reduction in elevation along the length of the profile from 1945 and 1964, particularly at either end of the profiles. The lowering of the northwest end corresponds to the formation of the proglacial lake by 1964 (Fig 5.6). The lowering and flattening of the southeast end corresponds to the formation of trains of glacifluvial outwash in areas of previously ice-cored moraine. The lower elevation of the 1964 profiles compared to 1980 - 2003 is due to the underestimation of elevation within the 1964 DEM. In the middle of the profiles there is less of a reduction in elevation, and ridges present within the 1945 profile are preserved through to 2003. For example there are distinct sharp peaked ridges in Profile 1 at 280m, 500m and 580m. In Profile 2 there ridges are preserved at 400m, 480m and 560m.
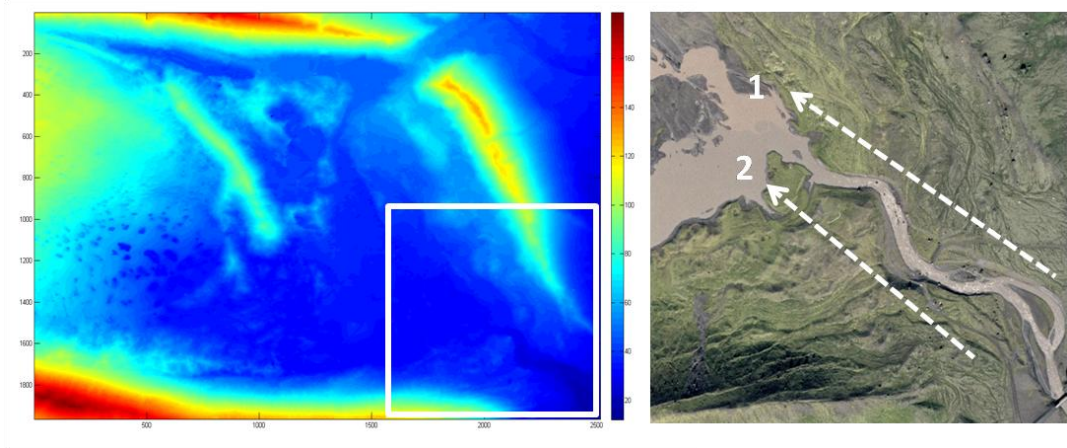
Fig 5.63 - Location of moraine complex D (white box in 2003 DEM) and locations of meshed temporal profiles 1 and 2 within the 2003 orthophoto.
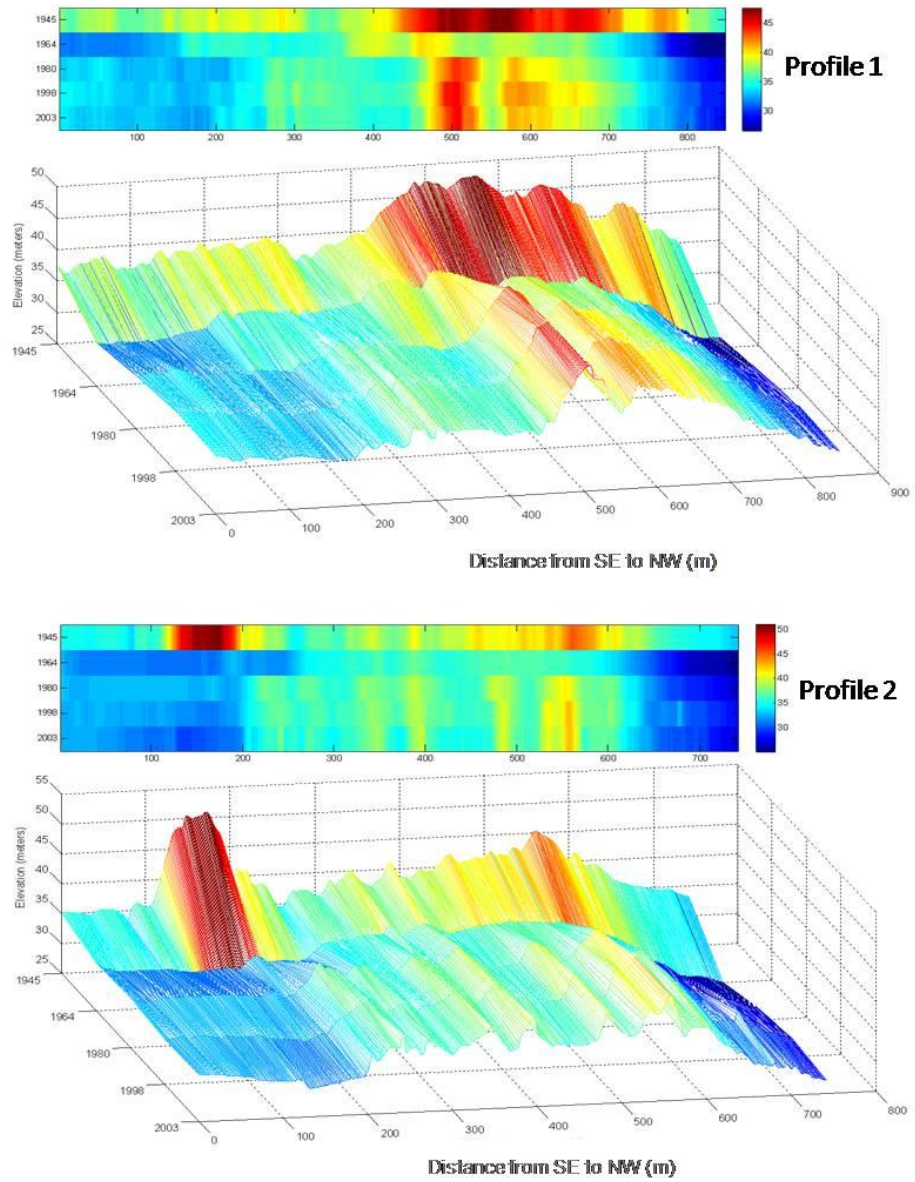
Fig 5.64 - Meshed temporal profiles 1 and 2 with corresponding bar charts, showing preservation of structure within outer moraine ridges.

Moraine complex D is situated downglacier from a large complex of ice-cored moraine along the southern glacier margin and the proglacial lake. In 1945 it was on the downglacier edge of an ice-cored moraine complex at the glacier snout. The long linear ridges within the outer section of the moraine complex are continuous with terraces along the inner slope of the lateral moraine (Fig 5.65).

Fig 5.65 - 2003 orthophoto with terraces deposited over the study period preserved along the base of the inner slope of the southern lateral moraine marked in white dashed lines with ages deduced from aerial photographs.

These terraces form by the dumping of debris off the lateral margins of the glacier. As the ice downwastes, debris contained within the upper layers of the ice is let down as crevasses fills, supraglacial eskers and valley eskers. Supraglacial eskers and crevasses fills form from the infilling of surface streams and crevasses respectively by rockfall debris, and may have various orientations depending on the orientations of the crevasses and streams. Debris also avalanches off the ice-margin to form dump moraines and terraces along the southern lateral margin.

The material appears to be predominantly supraglacial, derived from the paraglacial reworking of the inner slope of the lateral moraine (Ballantyne and Benn, 1994). Material is removed from the upper slopes by gullying and redeposited at the base of the slope in debris cones which accumulate on the surface of the glacier. Debris sampled from the distal end of the lateral moraine was found to be characteristic of active transport processes (Fig 5.66, Spedding and Evans, 2002). Therefore, debris re-sedimented from these moraines onto the lateral margin would inherit these characteristics, whilst still being derived from a supraglacial source. Linearity of these terrace features has been significantly enhanced by meltwater channels that would have been fed by the melting of ice-cores at a more fully ice-cored stage and drained

into the river Kvíár. These created steep sided banks through the moraine complex and are now recorded as abandoned meltwater channels (Fig 5.9).

Further into the glacier foreland is a zone of more discontinuous linear hummocks composed of gravel (Fig 5.61b). Roundness values of debris sampled from these hummocks by Spedding and Evans (2002) (Fig 5.66) are similar to water-worked debris at the modern day glacier margin. Elevation decreased within the complex between 1945 and 1964 and there is no evidence of pushing at the southern margin during this period from the DEMs (whilst it did occur at the northern margin forming moraine complex B and possibly C). Small meltwater channels within this zone do not appear to have enhanced linearity significantly but rather meltwater seems to have been routed around the complex, between the long linear terraces described above. It is reasonable to assume that linearity therefore reflects the preservation of controlled moraine ridges derived from water-worked debris bands, like those seen within the modern day southern margin.
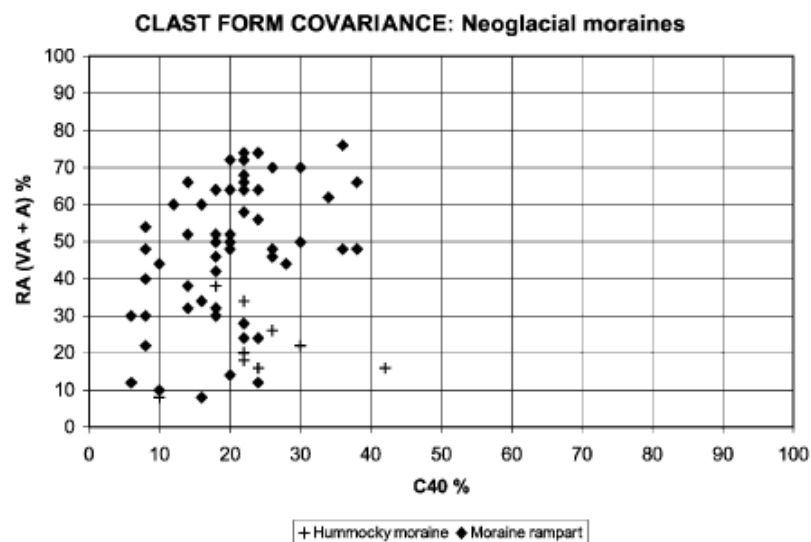
Fig 5.66 - Clast form covariance plots of debris from Neoglacial moraines and hummocky moraines (within moraine complex D) (Spedding and Evans, 2002).

6 Discussion

6.1 The impact of climate fluctuations on the snout behaviour and landform evolution at a 'debris-charged' glacier

Whilst several studies have found that an extensive and thick supraglacial debris cover may reduce, delay or retard the response of a glacier to fluctuations in climate (e.g. Kirkbride and Warren, 1999; Thomsen et al., 2000), the synchronicity of marginal fluctuations of Kvíárjökull between 1945 and 2003 with fluctuations of other Icelandic glaciers (Fig 2.1) (reflecting regional climatic forcing) suggests that the debris cover was not sufficient to mask the mass balance signal from the accumulation zone, as is the case at true debris-covered glaciers (Evans, 2009). This is not surprising considering that the debris cover on the snout of Kvíárjökull is confined to the outer 100m (apart from in the medial moraine), and in places is only thin. Additionally, push moraines at the present day glacier margin, interpreted as seasonal push moraines, suggest that Kvíárjökull has a seasonal climatic response, similar to the temperate outlet lobes of Vatnajökull (Boulton, 1986; Kruger, 1993, 1995, 1996; Evans and Twigg, 2002; Evans and Hiemstra, 2005).

However, the response of Kvíárjökull is delayed slightly compared to other Icelandic glaciers. For example, the rate of retreat of Kvíárjökull increased between 1945-1964 and 1964-1980, whilst other Icelandic glaciers were retreating more slowly, or even advancing in response to a drop in temperature during this period (Jóhannesson and Sigurdsson (1998) (Figs 2.1 andFig 6.1). Kvíárjökull advanced between 1980 and 1998 in delayed response to this drop in temperature. This suggests that Kvíárjökull may have a longer response time.

The response time is of fundamental importance when interpreting past glacier variations in terms of historical climate change (Jóhannesson et al., 1989). Response time depends on a number of different parameters related to topographic and climatic setting, unique to each glacier. Haeberli (1995) defines 3 types of glacier, differentiated according to their size and thus responsiveness to climate forcing:

(1) The smallest, somewhat static, low-shear-stress glaciers (e.g. cirque glaciers) reflect yearly changes in climate and mass balance almost without delay

(2) Larger dynamic, high-stress glaciers (mountain glaciers) react dynamically to decadal variations in climatic and mass balance forcing with an enhanced amplitude after a delay of several years

(3) The largest valley glaciers give strong and most efficiently smoothed signals of secular trends with a delay of several decades.

However, response time can be calculated more precisely as a function of climate and glacier geometry (Jóhannesson et al., 1989; Raper et al., 1996, Bahr et al., 1998; Oerlemans, 2001). For example, according to Jóhannesson (1989) response time (T_J) is given by:

$$T_J = h/ - b_t \qquad [8]$$

where h approximates maximum glacier thickness and b_t is the mass balance or scale of ablation at the glacier terminus.
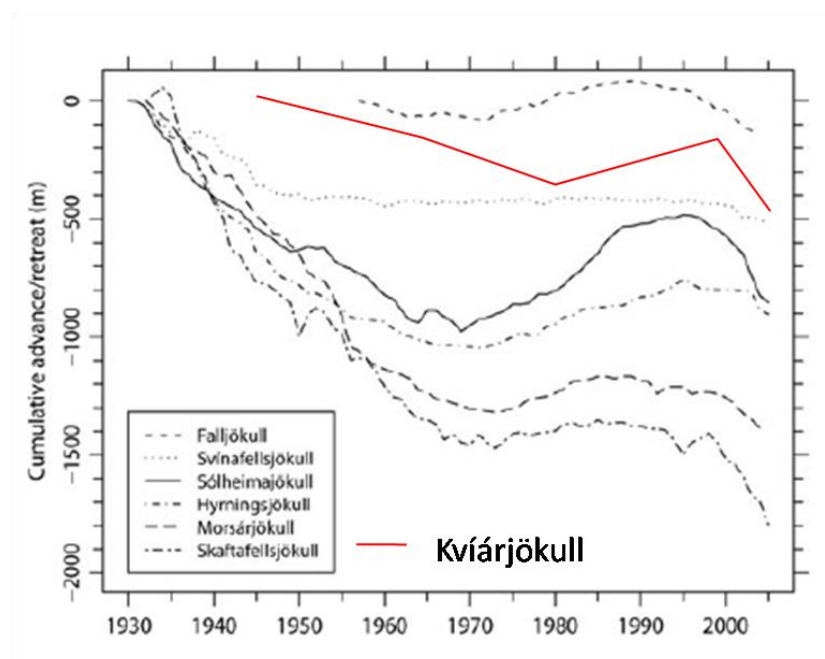
Fig 6.1 - Cumulative variations of the termini of seven non-surge type glaciers during the period 1930 – 2005 (modified from Sigurdsson et al. 2007).

Therefore the thicker the glacier, the longer the response time of the glacier to climate change. Whilst this does not account for the mass balance-elevation feedback associated with both the area reduction across the whole glacier (Raper and Braithwaite, 2009) it can be used to differentiate between glaciers according to their topography.

The icefall over which Kvíárjökull descends may increase its response time because of the time taken to transfer mass between the upper and lower parts of the glacier. Oerlemans (1989) demonstrated that a valley glacier with an icefall has a 50 year longer response time than a valley glacier with a constant slope because the ice-fall causes the glacier to thicken at its base, increasing its response time according to equation [8] (Jóhannesson et al., 1989). An additional topographic feature that causes the glacier to thicken at the base of the ice fall at Kvíárjökull is a 50m deep overdeepening (Fig 3.3), identified in a field survey by Spedding and Evans (2002). This would have been carved out during greater glacier extent during the LIA, when the most active outlet glaciers in this region typically excavated their beds down to hard surfaces 200 – 300m below sea level (Björnsson and Pálsson, 2008).

The response time of Kvíárjökull may also be affected by volcanic activity for the reason that it descends from the caldera of Öræfajökull, Iceland's largest active stratovolcano (Thórarinsson 1958). Volcanic ash melts out along lines of foliation within the snout at Kvíárjökull (Fig 6.2) and may therefore enhance ablation rates within the snout, although it is difficult to quantify by how much. Eruptions of Öræfajökull in 1362 and 1727-28 were accompanied by large jökulhlaups that were routed down Kvíárjökull. However, this is not the typical hydrological regime of Kvíárjökull as it is at other Icelandic glaciers such as Kötlujökull (Spedding and Evans, 2002). Geothermal melting at the base of the glacier may enhance melt at the base of the glacier and therefore enhance sliding, thus facilitating the transfer of ice from the accumulation zone to the snout and decreasing the response time.

Fig 6.2 - Volcanic ash melting out within the ablation zone at Kvíárjökull.

Several studies have also demonstrated that the climatic response of adjacent clean and debris-covered zones of a glacier may differ (e.g. Pelto, 2000; Takaeuchi et al., 2000; Thomsen et al., 2000; Kellerer-Pirklbauer et al., 2008). This is also the case at Kvíárjökull, where the debris covered northern snout behaves differently to the debris-free southern snout. The possible links between a large rockfall, increasing debris-cover of the northern snout at Kvíárjökull, and the 1980-1998 advance is discussed below (Section 6.1.1). There are indications that a recent increase in debris-cover associated with the aforementioned rockfall, as well as increased rates of ablation and debris melt-out, is now reducing the rate of lateral retreat of the glacier terminus. This is discussed in Section 6.1.2.

6.1.1 A possible connection between a large rockfall and the 1980 – 1998 advance of Kvíárjökull

Large rockfall events contribute large volumes of material to the glacier surface and may therefore affect glacier behaviour by increasing the thickness, density and spatial extent of the debris cover and reducing ablation (e.g. Gardner and Hewitt, 1990; D'Agata and Zanutta, 2005; Hewitt, 2009). At Kvíárjökull the advance of the northern snout in 1980 – 1998 corresponded with a large rockfall event from the nunatak in the ice fall feeding the medial moraine. A number of researchers have found a connection between large rockfall events and glacier advances or surges (Gardner and Hewitt, 1990; Hewitt, 2009; Shulmeister et al., 2009). Shulmeister et al. (2009) define a large rock avalanche deposit as $\sim 10^7$ m³ or more in volume and find that an average depth of 1m is adequate to significantly reduce ablation. An exposure through the rockfall deposit (Fig 5.35b) demonstrates that the rockfall debris is more than a meter in thickness. If the average thickness is taken as 1.5m across the deposit, with the area of the deposit covering roughly 200,000m², the volume of the rockfall deposit is 300,000m³, about 2 orders of magnitude below the threshold for a large rock avalanche deposit. Therefore, it is debatable whether the rockfall deposit was of significant magnitude to result in a glacier advance.

There are three mechanisms by which the rockfall deposit could have resulted in the advance of part of the glacier snout (Shulmeister et al., 2009):

1. The rockfall event would have increased the thickness of the debris cover within the medial moraine, enhancing the insulating effect of the medial moraine on this part of the glacier snout, and reducing ablation sufficiently below ice-replenishment to result in the thickening of the ice, increasing the downvalley driving force due to gravity (Nakawo and Rana, 1999, cf. Shulmeister et al., 2009).

2. Increased weight of rock fall debris, increasing the downvalley force.

3. An increase in the quantity of rock debris within the glacial drainage system or at the glacier base may increase basal water pressure and sliding velocity (Davies and Smart, 2007).

Considering the relatively small size of the rockfall deposit, mechanism (2) is viewed as unlikely. Mechanism (3) is possible based on observations of debris choked englacial channels (Fig 6.3a-c). Davies and Smart (2007) found that basal water pressures of the glacier may significantly increase as a result of the restriction of subglacial drainage by sediment, resulting in increasing sliding velocity.
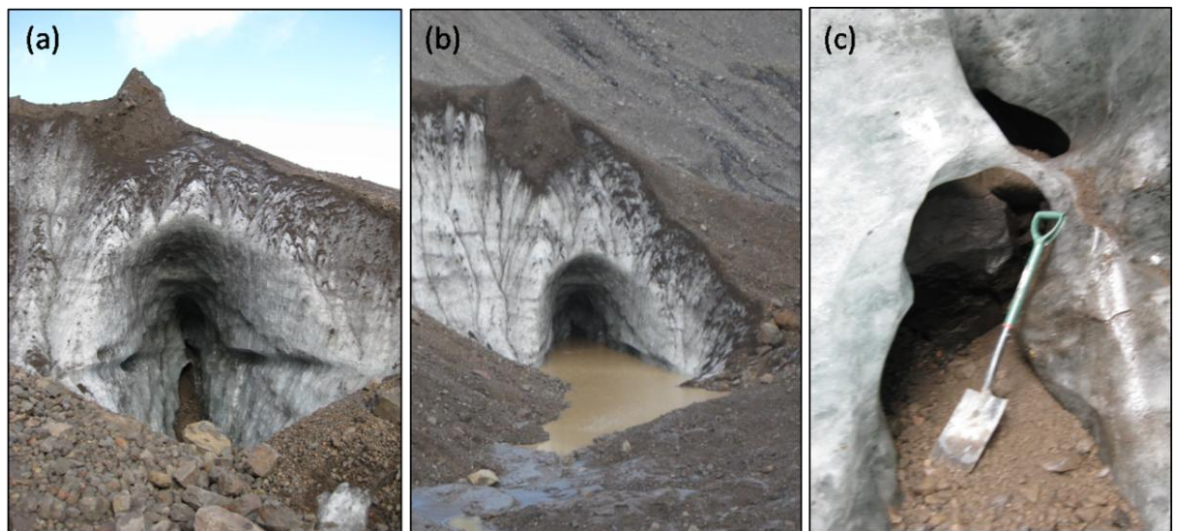
Fig 6.3(a-c) - Englacial channel melting out within the rockfall deposit ice-cored ridge. (a) Tunnel with scalloped ice walls and tide-water mark created by thermo-erosion. (b) Tunnel entrance filled with water after a large rainfall event suggesting that the tunnel is closed. (c) Large angular rockfall boulder blocking the tunnel.

Mechanism (1) is the most plausible considering the effect of the debris cover within the medial moraine on reducing ice loss in the northern snout relative to ice loss in the southern snout over the study period. There was an average thickening of 0.9m over

the northern part of the snout during 1980 and 1998. The southern snout experienced significantly lower volume loss over the same period relative to the previous and following periods, suggesting that a climatic forcing increased the mass balance of the whole snout between 1980 and 1998, and therefore was the primary control in resulting in the glacier advance within the northern snout. However, the rockfall may have amplified the advance within the northern part of the snout by mechanism (1).

6.1.2 The effects of increasing debris-cover on glacier snout behaviour and ice-cored moraine production

Prior to 1998 the debris cover at the margin was not extensive enough to affect terminus fluctuations at Kvíárjökull. However, following the advance of 1980 – 1998 there was very little lateral retreat of the snout terminus compared to the ice lost by thinning, which was 6 times higher than that lost by lateral retreat (Table 5.3). This switch in glacier snout behaviour appears to be related to an increase in the spatial extent and thickness of marginal debris cover. The deposition of rockfall deposits at the northern margin increased between 1964 and 1998, culminating in the deposition of the large ice-cored rockfall deposit at the margin during the 1980 – 1998 glacier advance. Hewitt (2009) found that although a rock avalanche lasts only a minute or two '...its legacy can persist as a morphogenetic influence for millennia or tens of millennia through disturbance of other processes'. Supraglacial debris cover spread upglacier between 1998 and 2003 as a result of increased ablation. This corresponds to Kirkbride's model for debris-cover expansion (Kirkbride, 2000): *'in periods of positive mass balance, faster ice flow and lower bare-ice ablation ('transport dominant' conditions) cause the cover to contract towards the terminus; under negative balance, reduced flow and increased ablation ('ablation-dominant' conditions) favour the upstream spread of the debris cover'* (cf. Deline, 2005).

The upglacier spread of debris at Kvíárjökull resulted in the formation of an 'extended' ablation zone (Kirkbride and Warren, 1999), in which more ice is lost by the downwasting of the upglacier clean ice than at the snout, which is protected by a thickening debris mantle. Lateral retreat of the glacier snout between 1998 and 2003 was therefore reduced. This is similar to observations at other debris-covered glaciers, where ice wastage occurs by thickening and thinning rather than by lateral advance

and retreat. For example, Thomsen et al. (2000) compared the long term behaviour of the partially debris-covered Miage Glacier in the Italian Alps with neighbouring clean glaciers and found that whilst both show a broadly synchronous response to positive mass balance, during periods of negative mass balance, the terminus retreat of uncovered glaciers is more pronounced than the retreat of the Miage.

Over a period of years this pattern of ice loss results in the formation, stagnation and detachment of terminal ice-cored moraine complexes (Kirkbride and Warren, 1999) as exemplified at Kvíárjökull by moraine complex A. An increasingly concave downglacier profile following deposition of rockfall deposits at the margin, resulted in the reduction in ice surface gradient towards the margin, which in turn would have resulted in a reduction in downglacier driving force and therefore velocity upglacier from complex A. The combination of decreased ablation and surface velocity towards the margin would have decreased the sensitivity of the debris-covered zone to ice-discharge variations towards the margin, allowing the complex A to melt-out in situ (Kirkbride and Warren, 1999). Moraine complex A may thus represent the formation of an arc of moraine during the incremental stagnation model of Eyles (1979) (Fig 6.6).

The fluctuations of the glacier snout correlate with temperature, with a time lag. However, the recent accelerated retreat exceeds the observed increase in temperature. Temperature increased by less than 0.5°C, whilst the wastage of the snout accelerated rapidly, with nearly half the total ice loss over the study period lost between 1998 and 2003. The accelerated retreat may be explained by increased glacier sensitivity. Mass balance sensitivity refers to the immediate change in mass balance caused by a climatic change. Glacier sensitivity is often measured as the annual-balance sensitivity to temperature ($\partial b/\partial T$), where b is the annual mass balance and T is the air temperature in °C (Dyurgerov, 2006). Dyurgerov (2006) suggests that accelerated glacier retreat worldwide is the result of increasing mass balance sensitivity in response to global warming.

There are two mechanisms by which a large increase in air temperature may lead to an increase in glacier sensitivity. Firstly, Oerlemans (1989) states that as during the ablation season the temperature of the glacier surface is at melting point, any extra

radiation will be used entirely for additional melting. Furthermore, because the glacier temperature cannot increase, extra radiation creates a greater temperature gradient between the glacier and its surroundings. This causes an 'oasis effect' in which there is a large flux of heat towards the glacier tongue. This mechanism is particularly effective when the glacier tongue is narrow and may result in the doubling of melting rate and acceleration of glacier wastage. Haeberli (2006) suggests that for glaciers in Patagonia that adjust to climate warming by downwasting, rather than area loss, that an important mass balance/altitude feedback occurs. A cumulative surface lowering of about 50 – 100m within a century could increase the mass-balance sensitivity by a factor of two, doubling the rate of surface lowering and leading to a runaway effect.

Kvíárjökull meets the conditions for both of these mechanisms. It has a narrow tongue, hemmed in by the steep rock walls and lateral moraines, and responds to climate warming predominantly by downwasting. Whilst snout area decreased by 27.8% over the study period, glacier volume decreased by 42%. Much of the surface of the glacier snout has lowered by over 50m over the study period, and probably significantly more over the past century considering that temperatures reached a peak in the 1930s. This suggests that Kvíárjökull is highly unstable and that accelerated retreat may continue in response to global warming.

The other factor that enhances retreat rates at the margin of Kvíárjökull is the expansion of proglacial and supraglacial lakes. Both are common features of karst development at debris-covered glaciers, for example at the Tasman Glacier in New Zealand (Kirkbride and Warren, 1999) and at the Ngozumpa Glacier (Benn et al., 2000) and Imja Glacier (Watanabe et al., 1994), both in Nepal, and have been found to be major contributors to ablation of these glacier snouts. Similarly, the growth of a proglacial lake at the southern margin of Kvíárjökull between 1964 and 1980 was thought to be responsible for its greater rate of retreat compared to the northern margin (section 5.5.4.2). The expansion of both a proglacial lake at the southern margin and a supraglacial lake within moraine complex A between 1998 and 2003 provides the most likely explanation for the accelerated retreat of the margin over this period (section 5.5.4.4). Higher rates of lake growth were found at Kvíárjökull than in previous studies. Previous studies have found that the transition from small

supraglacial ponds into a large moraine-dammed lake may occur within 2–3 decades (e.g. Ageta et al., 2000). However, this study finds that this transition may occur within a decade. For example within moraine complex A, between 1998 and 2003 the area of the lakes increased by four orders of magnitude, from 100m³ to 125,000m³.

The most common process by which lakes increase retreat rates is by calving (Powell, 1984; Kirkbride and Warren, 1999). Blocks of ice within the proglacial lake in 1980, and 2003 are indicative of this process. A large calving event was observed within the supraglacial lake in moraine complex A during field work in 2008 (Fig. 5.49). Calving occurs when sufficient stresses are generated to initiate fracturing of the ice at the lake margins. These stresses may be generated by the following mechanisms (Benn and Evans, in press):

1. Longitudinal stretching associated with large-scale velocity gradients:

Ice velocities typically increase towards the terminus at the edge of a proglacial lake because faster sliding is encouraged by diminishing basal drag as the glacier approaches flotation. This downstream increase in velocity stretches the ice, potentially opening surface crevasses transverse to flow, and if net tensile stresses are large enough, crevasses will propagate through the ice and trigger calving.

2. Ice-cliff undercutting by melting at or below the waterlevel

Melt rates at or below the waterlevel usually exceed subaerial melt rates, due to efficient transfer of energy from warm, circulating water. Melting is commonly focused close to the waterlevel, due to the presence of a buoyant layer of warmer water, but in volcanic settings meltwater erosion can occur at greater depths as a result of geothermal heating. Melting at the water line cuts notches at the base of ice cliffs, as observed at the base of ridge X in moraine complex A. Calving can then occur by outward toppling of undercut pillars, collapse of melt-notch roofs along fractures, and other processes.

Deepening water encourages calving retreat by mechanisms 1 and 2. Water deepening may increase velocity, stresses and fracturing via mechanism 1. It may also increase calving rates by encouraging the circulation of warm water, thus, enhancing melt rates

at the base of ice cliffs, and because of the submergence of ice, meaning that more ice faces are brought into contact with water, whereupon undercutting by thermo-erosional notching occurs. Benn et al. (2000) found that water deepening and calving retreat form a positive feedback cycle, together leading to the rapid growth of the lake and further water deepening. This positive feedback may accelerate margin retreat. At Breidamerkurjökull to the east of Kvíárjökull, the retreat of the glacier into the overdeepened basin has encouraged rapid retreat of part of the margin as a result of increasing water depth, and calving rates by the above mechanisms (Benn and Evans, in press). Similarly, the retreat of Kviarjokull into its overdeepening, as indicated by the growth and coalescence of lakes across the margin by 2008, appears to be accelerating the rate of retreat due to deepening water and increased calving rates via mechanisms 1 and 2.

6.2 De-icing progression of ice-cored landforms

Krüger and Kjær (2000) developed a model for the de-icing progression of ice-cored moraine in a maritime climate (Fig 6.4) based on measurements of dead-ice melting collected from dead-ice fields of different ages in the glacier foreland of Kötlujökull over one decade. This research tests this model based on de-icing rates within a single moraine complex (C) measured over almost 6 decades (Fig 6.5). Kjær and Krüger (2000) suggest a period of 50 years for the completion of de-icing based on an ice-core of 40m in thickness and a debris mantle of 0.2m – 1m thickness. Moraine complex C has decreased in elevation by an average of 15m over the study period and had a melt rate of 0.8m between 1945 and 1964. This suggests that the stage of most rapid de-icing occurred prior to the start of the study period in 1945. If an initial melt rate of 2.5m yr^{-1}, based on the initial melt rate within Kruger and Kjaers's (2000) model, is applied to moraine complex C for a period of 10 years, this gives an estimated initial ice thickness of 40m within moraine complex C, making its de-icing progression comparable with Krüger and Kjær's (2000) model.

The melt rate of moraine complex C between 1945 and 1964 agrees with the melt-rate of 0.8m for the second stage of ice-melt within their model, but continues at this rate for longer. The transition from fully ice-cored into partially ice-cored occurs at 29 years at Kvíárjökull, 9 years later than at Kötlujökull. The melt-rate between 1964 and 1980

agrees with the melt-rate of 0.3m yr⁻¹ within partially ice-cored moraine at Kötlujökull. Krüger and Kjær (2000) suggest that based on a steady melt rate of 0.3m during the final stage of de-icing, a further 30 years would be required to entirely melt out a 10m thickness of ice cores. However, at Kvíárjökull there is another stage of ice-melt beyond the 50 year period specified for the completion of de-icing by Krüger and Kjær. After 1980 the melt rate continues to decrease within moraine complex C below 0.3m yr⁻¹, to 1.5cm yr⁻¹ from 1980 – 1998. It then increases slightly to 4.4cm yr⁻¹ between 1998 and 2003, but remains well below 0.3m.

The ice-core thickness in 2003 is estimated at 0.6m. Based on a melt rate of 0.04m yr⁻¹ it would take a further 15 years to completely melt out the ice-core. Therefore this research suggests a period of 83 years for the completion of de-icing based on an ice-core of similar thickness. As both glaciers have a similar climate, this may be because of a greater thickness of debris cover at Kvíárjökull compared to Kötlujökull. For example, Driscoll (1980) determined from Klutan Glacier in the Yukon Territory that a 950 year period was required to melt down 180m of ice with a 1% debris content, but this increased to 1200 years with a 1.5% debris content due to the development of a thicker debris cover (Krüger and Kjær, 2000).
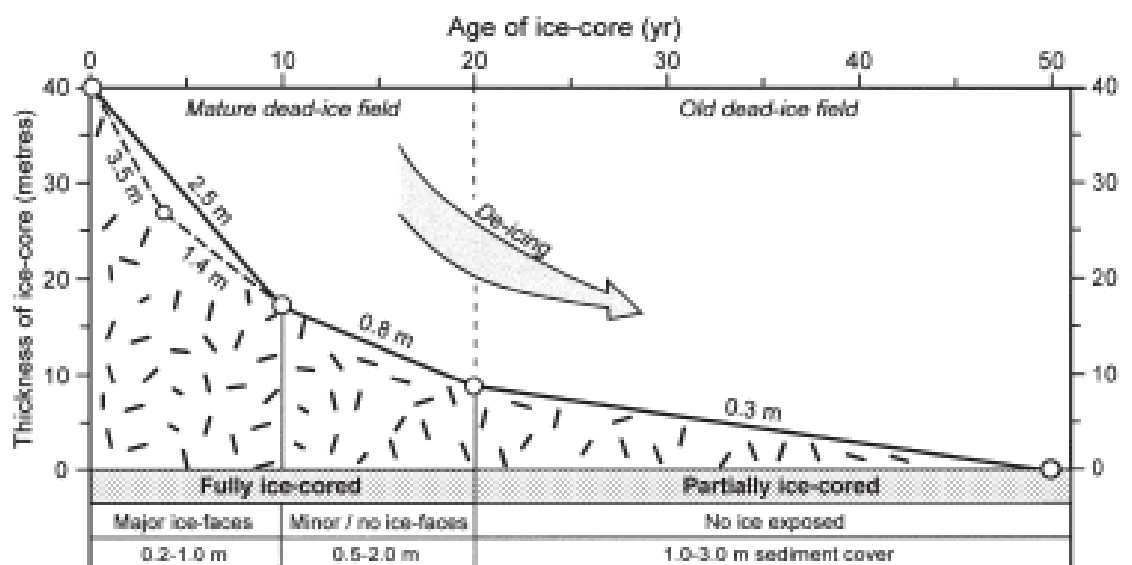
Fig 6.4 - De-icing progression of ice-cored terrain in a maritime climate, the Kötlujökull terminus region. (Source: Krüger and Kjær, 2000)
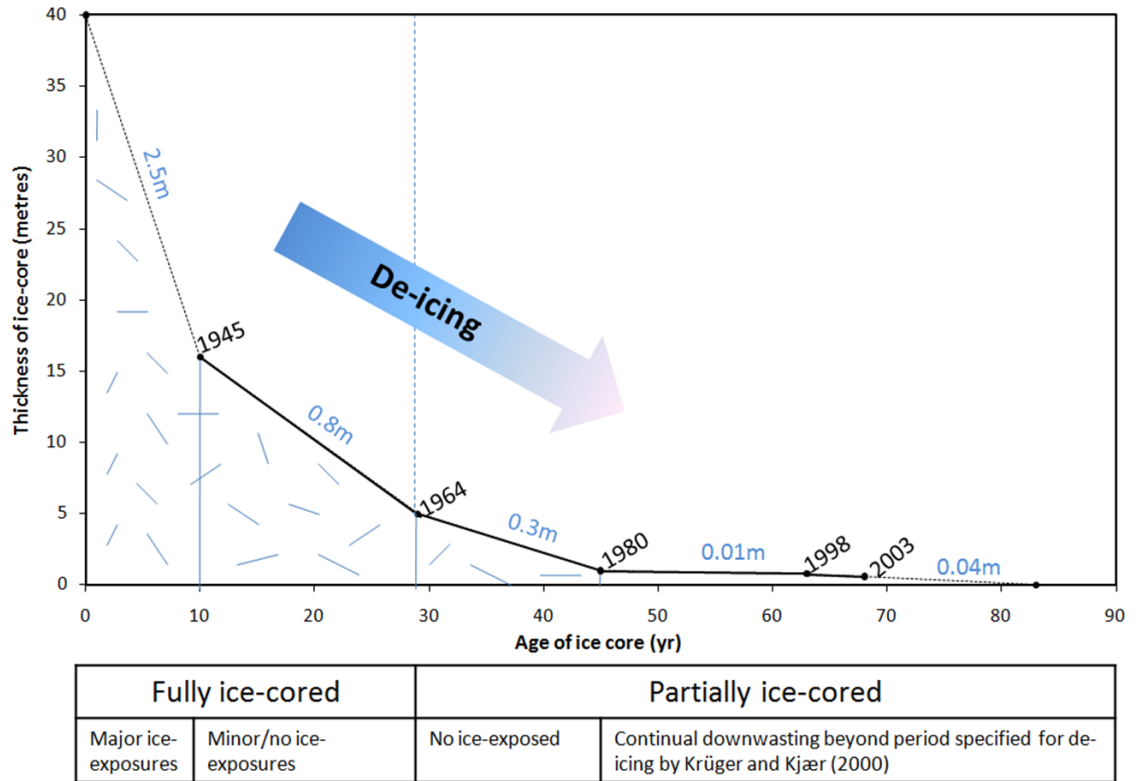
Fig 6.5 - New model for de-icing progression of ice-cored terrain in a maritime climate based on a moraine complex within the foreland of Kvíárjökull.

6.3 Process-form relationships in the genesis of hummocky moraine complexes

Two different models of moraine formation exist for Kvíárjökull both of which describe the moraine within the foreland as 'hummocky moraine'. Eyles (1979) originally described and interpreted the hummocky moraine of Kvíárjökull as a landscape formed by the melting of stagnant ice-cored moraine detached from the glacier during incremental retreat (Fig 6.6A-C). Linearity within the final landscape was ascribed to the bulldozing of ice-cored moraine by the glacier during active retreat. Spedding and Evans (2002) and Evans (2009) later interpreted it as a landscape of linearity primarily inherited from englacial debris concentrations within the parent ice and enhanced by ice marginal pushing (Fig 2.9). Both models of moraine formation at Kvíárjökull were developed based on the use of ergodic principles, whereby moraines of different ages are used to analyse long term landform development. This is problematic when ice dynamics may have changed over time, therefore changing sediment-process-form relationships involved in moraine formation. This study demonstrates the spatial and temporal variability in moraine formation at Kvíárjökull over a 58 year period of

changing climate and style of retreat and offers fresh insights into the relative importance of control imparted englacial debris concentrations, ice marginal pushing and re-sedimentation processes in moraine formation at Kvíárjökull. Two research questions are answered: (1) what is the preservation potential of controlled moraine? (2) What is the role of ice-marginal pushing in moraine linearity?

6.3.1 Supraglacial debris cover: debris provenance and transport

Contrary to the model advocated by Eyles (1979), in which hummocky moraine comprises three facies of supraglacial debris (Fig 6.6D), the evidence presented demonstrates that 'hummocky moraine' contains a variety of debris types, mainly well-rounded debris derived from fluvio-glacial transport pathways, as well as more angular debris from supraglacial sources (Spedding and Evans, 2002). Well-rounded debris tends to dominate in proglacial foreland, associated with the outcrop of water-worked debris bands, eskers and outwash sediments at the frontal margin. Moraine containing rockfall sediment occurs along the lateral margin in terraces, crevasse fills and valley eskers, associated with the deposition of rockfall debris along the lateral margins from the surrounding rock walls.
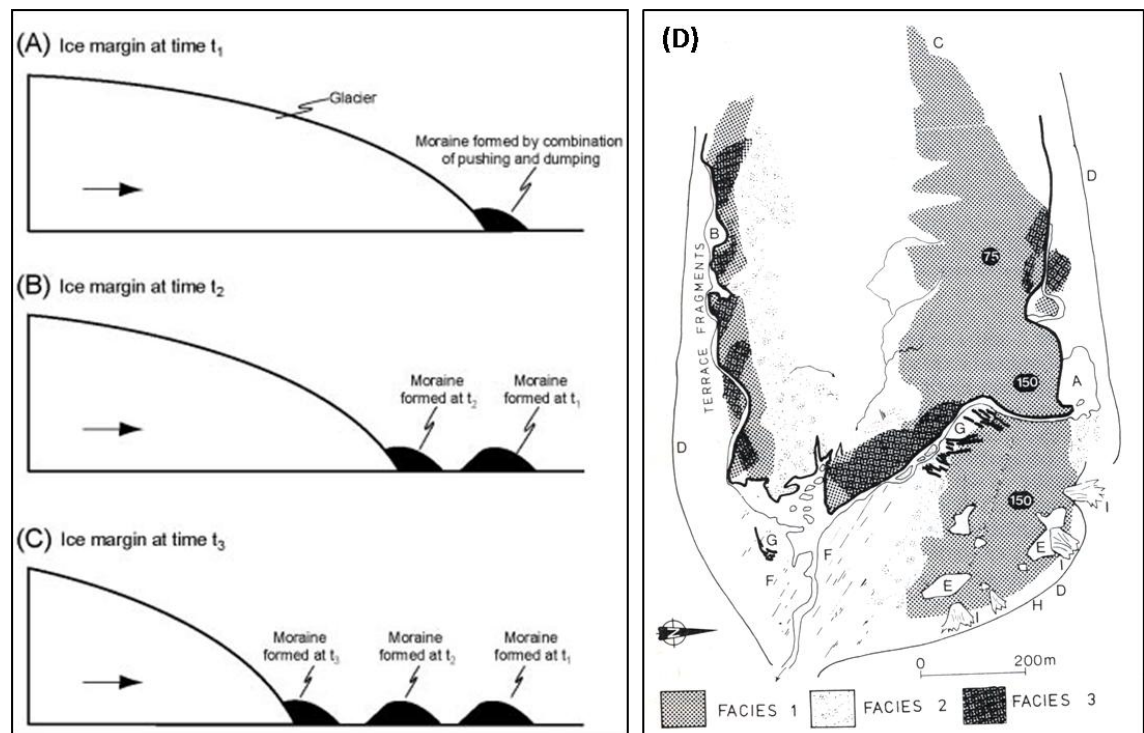
Fig 6.6 A-D. A-C: Conceptual sketch of moraine formation according to the incremental 'active' retreat model without incorporation of dead ice bodies or significant stagnation (Lukas, 2005).

D: Facies of supraglacial morainic till at Kvíárjökull. (A) Proglacial lake, (B) marginal meltwater stream. (C) medial moraine, which extends into the foreland as Facies 1 (D) latero-frontal moraine ridges (E) Thaw lakes in ice-cored moraine (F) fluted lodgement till surface (G) push moraine ridges and (G) boulder veneer of facies 2 (I) mudflows through marginal terraces. Numbers refer to depth of till in centimetres. (Eyles, 1979)

This study has combined the findings of Spedding and Evans (2002) on the debris types at Kvíárjökull and of Swift et al. (2006) on the structural geology of debris concentrations with observations on the morphological expression of different debris concentrations to identify four types of debris concentration, along with their contribution to final moraine morphology. These four debris concentrations are: debris bands containing water-worked debris, channel fills, basal debris bands and rockfall deposits (Fig 6.7). The preservation potential of basal debris bands is low because of their low debris content and spatial distribution at the lateral margins where marginal meltwater activity prevents the build up of a thick debris mantle. Rockfall debris and channel fills that are not folded into debris bands are not technically 'controlled' as the former does not reflect the internal structure of the glacier and the later are well known as 'eskers'. Thus, the following discussion concerning the origin and preservation of controlled moraine refers to the debris bands of water-worked debris that crop out at the margin.

6.3.2 Evolution of icecored moraine from debris-covered ice

The evolution of moraine complex A into a mature glacier karst system following the formation of the complex between 1980 and 1998 was rapid, taking just 5 years to develop characteristic karst features such as supraglacial lakes and ice cliffs (Fig 5.48) (Clayton, 1964). Between 1998 and 2003 ridge X along the upglacier edge of the moraine complex continued to move downglacier (profile 3, Fig 5.54), indicating that the ice-cored moraine remained active, even during the accelerated downwasting that occurred across the snout during this period. Whilst processes of ice-cored moraine disintegration suggest a stagnant ice margin (e.g. Eyles, 1979) this is not a necessary condition for karst development. For example, Kirkbride (1995b) found that the Tasman Glacier was still moving at its terminus even during advanced karst development.

Benn and Evans (1998:239) state that karst development may be maintained on actively moving glacier snouts if overall ablation rates are high. The well developed internal drainage network within the snout of Kvíárjökull results in the presence of many collapsed tunnels around which ice disintegration occurs, providing the conditions for rapid karst development (Kirkbride, 1993; Benn and Evans, 1998). Furthermore, the creation of relief during controlled moraine production, and during ice-marginal pushing, results in debris reworking and the exposure of ice cores to increased rates of ablation, providing the conditions for ice collapse.

6.3.3 Controlled moraine: origins and preservation potential

6.3.3.1 Origins of controlled moraine

Transverse water-worked debris bands that crop out at the margin of Kvíárjökull control the pattern of differential ablation on the glacier surface to produce 'controlled' ice-cored linear ridges (Evans, 2009). The origin of these transverse water-worked ridges is ambiguous but almost certainly involves sustained transport within the englacial drainage system (Spedding and Evans, 2002). The debris bands may either form by the folding of channel fills into bands, or the incorporation of debris from channel fills along lines of foliation within the ice that are subsequently thickened under compressive flow at the base of the ice fall and within the overdeepening. Compression is a vital process in the concentration of debris at the glacier snout and subsequent formation of controlled moraine. Whilst at Kvíárjökull it occurs against the reverse slope of the overdeepening, at polythermal glaciers it occurs at the glacier-permafrost interface (e.g. Clayton and Moran, 1974, cf. Evans, 2009). High water pressure likelyresults in the formation of vertical debris bands, or dykes, by hydrofracture. Controlled moraine formation at Kvíárjökull therefore reflects the importance of both hydrological conditions and ice dynamics associated with an overdeepening. It is, however, difficult to attribute controlled moraine development to a specific process (Evans, 2009).

6.3.3.2 What is the preservation potential of controlled moraine?

Spedding and Evans (2002), in their observation that the hummocky moraine at Kvíárjökull retains 'distinct elements' of linearity on the melt out of 'controlled moraine' despite reworking by mass movements and ice-marginal streams, imply the

preservation of controlled moraine and therefore englacial structure within the final moraine morphology. In contrast, whilst Eyles (1983b) also recognized 'controlled' moraine as features that are *'aligned transverse to ice flow'* within the glacier snout, he describes the final landform signature as *'an irregular topography consisting of steep-sided bouldery mounds and ridges and dead ice hollows'*, implying low preservation potential of controlled moraine. The preservation of controlled moraine, and thus englacial structure, primarily relies of the preservation of ice-cored moraine at the glacier snout. Where ice-cored moraine is preserved, the preservation of controlled moraine relies on the stability of the debris mantle on the melt out of the underlying ice (e.g. Paul and Eyles, 1990).

Two zones of preservation of ice-cored moraine are identified within the foreland (Fig 6.7), which agrees with zones of moraine formation identified by Eyles (1979) along the line of the medial moraine and along the lateral margins. These zones of preservation contain moraine complexes A, B, C and D. Between these zones of preservation is a zone of low moraine preservation in which ice-cored moraine is destroyed by glacifluvial reworking and proglacial lake development. Between 1945 and 1980 supraglacial debris-covered ice at the southern margin broke up into proglacial lake, and existing ice-cored moraine was buried. A surviving transverse ridge that formed a promontory into the lake at the southern lake margin was subsequently removed by glacifluvial reworking by 1998. Another ice-cored moraine complex developed at the southern margin during the 1980-1998 advance. By 2003 ridges within this complex survived only as islands within the lake. Moraine formation between 2003 and 2007 was dominated by the emergence of ridges and dykes of water worked debris and eskers as documented by photographs taken in 2007 (e.g. Fig 5.27). However, by 2008 most of these were submerged in the growing proglacial lake (Fig 6.13). The preservation of controlled moraine at the southern margin over the study period is therefore low. Moraine complex D survives in the outer foreland beyond the limits of proglacial lake formation at the southern margin. A small complex of discontinuous linear ridges on the edge of the lake within moraine complex D, where Spedding and Evans (2002) based their interpretation of linearity within hummocky moraine as 'controlled', may therefore represent the final landform signature of controlled moraine. This is possible considering that this area would have

been adjacent to the site of controlled moraine production at the present day snout prior to 1945.

Fig 6.7 - Schematic map showing the evolution of different types of supraglacial moraine into moraine complexes in the outer foreland.

Preservation of controlled moraine within ice-cored moraine relies on the stability of ice-cores as they downwaste. Much of the previous literature on the melting of ice-cored terrain has noted the role of topographic inversion cycles in lowering the terrain surface (Clayton, 1964; Boulton, 1967, 1972; Clayton and Moran, 1974; Watson, 1980; Paul, 1983; Benn and Evans, 1998). The creation of relief through differential ablation results in the redistribution of debris from topographic ridges into topographic lows. In time the thickening of debris cover in basins and thinning of debris cover on the moraine ridges reverses the spatial pattern of differential ablation responsible for the initial creation of topographic highs, causing them to become topographic lows. Topographical inversions are repeated until all ice has wasted. This would result in the preservation of linearity within the final de-iced moraine, as illustrated by Boulton's (1972) process-form model of hummocky moraine evolution from englacial debris concentrations (Fig 2.7).

However, whilst it is recognized that topographic inversion may occur within the early stages of ice-cored moraine development (although not captured at the spatial and temporal resolution of this study) topographic inversion did not occur during mature ice-cored moraine evolution as represented by moraine complex A. Within moraine

complex A minor ridges developed at the base of ice-cored slopes between 1998 and 2003, as a result of sediment accumulation and reduced ablation of ice cores beneath a thicker sediment cover, but the intervening ridges did not downwaste sufficiently so as to result in topographic inversion. Instead, the ridges steepened and narrowed between 1998 and 2003 by backwasting.

The lack of topographic inversion is therefore explained by the rate of backwasting relative to downwasting as quantified in this study and recognized by Eyles (1979). Whilst backwasting and downwasting re-distribute sediment into topographic lows, which in theory would subsequently evolve into topographic highs through differential ablation, they do not because backwasting consumes high ground, causing the flattening of the terrain before topographic inversion can occur (Kjær and Krüger, 2001). Sediments are thus shifted laterally as backwasting results in the re-location of topographic highs. Over time this results in a stepwise lowering of the ice-cored moraine (Kjær and Krüger, 2001), the burial of ice-cores by a thick debris mantle and reduction in slope gradient, as seen within moraine complexes A - D. The importance of backwasting therefore prohibits the preservation of englacial debris bands. Eyles (1983c) described this as 'karstic destruction' of englacial melt out tills.

Another factor that prevents the preservation of englacial debris is the relative importance of bottom melt as a result of the wet based regime and geothermal heat flux at Kvíárjökull, typical of many Icelandic glaciers. Bottom melt results in the enlargement of cavities, into which englacial debris is deposited and washed away by meltwater streams. This inhibits the accumulation of melt-out debris in troughs, as illustrated in stage (c) of Boulton's (1972) model (Fig 2.7), which both enhances backwasting by preventing the build up of an insulative debris mantle, and prevents topographic inversions. This can be contrasted with the supraglacial environment at a polar/ sub-polar glacier, where the slow top or bottom melt of debris-rich ice ensures that linearity controlled by the pattern of englacial debris is preserved (Boulton, 1972; Shaw, 1977, cf. Eyles, 1983c).

This study therefore concurs with the importance given to resedimentation processes during deposition, such as slides, flows, meltwater erosion, and glacifluvial and

lacustrine sediments within the final hummocky landform by Eyles (1983c). As ice-cores gradually diminish, the most recent re-sedimentation overprints the results of previous events (Kjær and Krüger, 2001) (Fig 6.8A-C). The morphology of the largely ice-free terrain is the product of sinkhole formation and backslumping that dominate in partially ice cored terrain (Fig 6.8C).
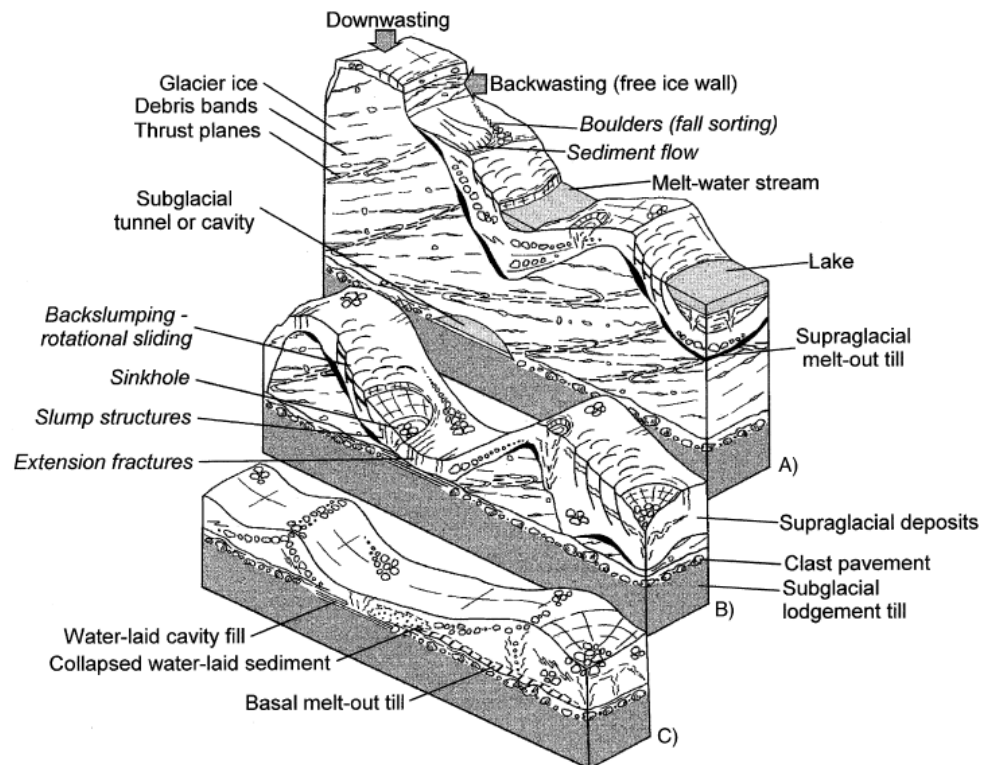
Fig 6.8A-C - Sedimentological model showing different phases of de-icing of ice-cored features and the formation of dead-ice moraine (A) fully ice-cored moraine. (B) Partially ice-cored moraine. (C) Dead-ice moraine. (Source Kjær and Krüger, 2001)

There are some features that record re-sedimentation processes that occur in fully ice-cored moraine. Lakes within moraine complex C record the position of past ice-walled lakes (described as 'thaw lakes' by Eyles (1979) in Fig 6.6D). Meltwater channels also have a high preservation potential and are responsible for much of the linearity within hummocky moraine, particularly surrounding the river Kvíár. Both moraine complexes C and D are dissected by ribbon sandur and abandoned meltwater channels. One particular area of moraine beyond moraine complex B is so heavily channelized by the evacuation of meltwater from moraine complex B that it is within the zone designated as having low preservation potential within the foreland of Kvíárjökull. Other abundant

features are chains and clusters of boulders, which represent the accumulation of boulders along the base of ridges and within troughs within the former ice-cored moraine.

6.3.4 What is the role of ice-marginal pushing?

Both models of moraine formation at Kvíárjökull recognized the role of ice-marginal pushing in enhancing moraine linearity (Eyles, 1979; Spedding and Evans, 2002). Eyles (1983c) observed that repeated incremental marginal stagnation forms transversely lineated ice-cored moraine as a result of bulldozing by faster flowing ice upglacier. He compared the topography to surging glaciers, where ice-cored moraine complexes are repeatedly bulldozed during surges (Wright, 1980, cf. Eyles, 1983c). However, Eyles (1983c) regarded the preservation potential of this linearity to be low due to the extent of deformation by re-sedimentation processes such that the final landform '*is one of uncontrolled stagnation topography*'. Spedding and Evans (2002) noted small scale glacitectonic structures within moraines as representative of ice-marginal pushing, leading them to suggest that ice-marginal pushing contributes to moraine linearity. This study provides previously lacking morphological and sedimentological evidence for ice-marginal pushing, which demonstrates that ice-marginal pushing is more important in the final landform signature than previously thought.

Moraine complex A demonstrates the occurrence and morphological implications of ice-marginal bulldozing during the sustained advance that occurred between 1980 and 1998. Moraine complex A contains both large bulldozed ice-cored moraines such as those through which the cross-profile was taken, and smaller push moraines formed by the bulldozing of outwash and lacustrine sediments in between the margin and the ice-cored moraine complex during this advance. Evans (2009) described the ice-cored moraine through which the cross-profile was surveyed in moraine complex A as 'controlled moraine' that has evolved from *'transverse supraglacial debris septa into ice-cored elongate mounds up to 10m high and composed of large volumes of sand and gravel'*, whose linearity has been 'enhanced' by ice-marginal pushing. These are re-interpreted as push moraines rather than 'controlled moraine' based on morphometric analysis and the time-series of geomorphological maps. Prior to the 1980-1998 advance there was only a small, low relief ice-cored moraine complex (Fig 5.7)

containing only very minor linear ridges in between many features of ice-disintegration, such as ice-walled lakes. This complex was subsequently transformed into a complex of multiple, large, continuous linear ridges by 1998 (Figs 5.8 and 5.43). Therefore, almost all linearity appears to have formed by bulldozing during the 1980 – 1998 advance. Ice-marginal pushing did not just 'enhance' existing linearity of controlled moraine, but completely reworked and remoulded ice-cored moraine into push moraine ridges. Thus, ice-marginal pushing is also a major process responsible for the low preservation potential of controlled moraine, along with processes of ice-wastage and resedimentation.

Morphometric analysis also reveals a push moraine origin for many of the ridges mapped within moraine complex A and the foreland of Kvíárjökull, including those in the north-eastern corner of moraine complex A, formed between 1964 and 1980, and those within moraine complex B, formed between 1945 and 1964. The heavily contorted and folded sequence of sediments is evidence of compression during ice-marginal bulldozing. The deformation of proglacial sediments requires that the transmitted stress from the glacier exceeds the sediment creep strength (Etzelmüller et al., 1996) and therefore may result from the bulldozing of outwash sediments alone (e.g. Humlum, 1985). However, another factor that may increase compressive forces, and therefore influence the style of deformation, is the presence of the reverse slope of an area of higher topography on the downglacier end of the moraine complex, separating moraine complexes B and C. This area is interpreted as a possible palaeo ice-contact fan that has resisted erosion, deposition or deformation, such as those reported by Boulton (1986) in the proglacial area at Breiðamerkurjökull. This would have formed an obstruction that would have increased compressive stresses within the proglacial sediments between the slope and the glacier margin (e.g. Humlum, 1985; Boulton, 1986).

Ice-cored push moraines within moraine complex A are subject to re-working on the melt out of ice-cores just as controlled moraine ridges at the present day southern margin are. Similar ice-cored push ridges are formed at the neighbouring debris-rich glacier snout of Fjallsjökull (Eyles, 1979; Evans, 2009b). Many of these surround lakes and are degraded by the lateral migration of these lakes by backwasting (Eyles, 1979).

Similarly, at Kvíárjökull the ice-cored pushed ridges with moraine complex A are being eroded by backwasting on the edge of the supraglacial lake and by the exposure of ice-cores by mass wasting processes, promoted by meltwater and frequent rainfall. Despite these processes, push moraines have a high preservation potential at Kvíárjökull, as demonstrated by moraine complexes B, C and the north-eastern corner of A.

The north-eastern corner of moraine complex A represents a push moraine complex that survived overriding of ice in the 1980-1998 advance. In contrast to the rest of moraine complex A, the north-eastern corner contains no features of backwasting, such as ice-walled lakes or ice exposures, despite the fact that it was also overridden by ice in the 1980-1998 advance. The sink holes are evidence of the collapse of underlying ice by downwasting, commonly associated with partially ice-cored moraine (Kjær and Krüger, 2001). Between 1998 and 2003 linearity that was well defined in 1980, in the form of crenulated push moraines (Fig 5.7), partly re-emerged within the north-eastern corner of moraine complex A, as ice that overrode the complex in the advance melted out. Although the surface expression of the 1980 push moraine ridges was subsequently reduced, or in some places completely extinguished by a partially vegetated debris mantle deposited on the melt out of the ice overlying the push moraine, elements of linearity still survive. The fact that the existing moraines resisted deformation in the advance of 1980-1998 demonstrates the preservation potential of push moraines within the foreland of Kvíárjökull.

Moraine complex B also demonstrates the preservation potential of push moraine ridges within the foreland of Kvíárjökull. Whilst sink holes and water filled depressions pit the surface of the moraine ridges, these only enhance the crenulated planform appearance of the moraine complex formed during bulldozing. There is no indication of backwasting processes having occurred such as larger lakes or boulder ridges. The preservation of these push moraines following de-icing is most likely due to the relatively low ice-content of push moraine ridges which are formed by the bulldozing of proglacial and partially ice-cored moraine. This is in contrast to controlled moraine ridges which have large ice-cores protected by a relatively thin debris mantle. Thus, contrary to Eyle's (1983b) model of chaotic hummocky moraine formation in which

push moraines have a low preservation potential, the evidence suggests a high preservation potential of push moraines.

6.3.5 Rockfall signal within the landform record

Eyles (1979) cited rockfall debris as the dominant source of debris in moraine construction at Kvíárjökull, carried along supraglacially in a 'conveyor belt' fashion and dumped at the margin. Whilst other types of debris have since been identified within the debris-charged glacier snout and within moraines (Spedding and Evans, 2002), rockfall debris may occasionally dominate glacial sedimentation, glacier behaviour and, thus, moraine formation at Kvíárjökull. Rockfall debris dominates moraine construction along the southern lateral margin, where rockfall debris is dumped as crevasse fills, valley eskers, and terraces between the bedrock ridges/ lateral moraines and the glacier margin. However, more significantly, large rockfall events may contribute to linearity within moraine complexes in the foreland.

Rockfall deposits from high magnitude rockfall events form large ice-cored ridges within the medial moraine because of the high proportion of debris that remains on the glacier surface (Shulmeister et al., 2009) and protects the underlying ice from ablation. Since its emplacement at the margin, a particularly large, lobate rockfall deposit has evolved into ridge X, an ice-cored ridge that is elevated by ~40m above the glacier surface and is 800m long. The slopes of this moraine have remained relatively stable, whilst the upglacier ice and downglacier ice-cored moraine have downwasted. If the debris mantle continues to be stable on the downwasting of the ice-core it is a possibility that this rockfall event will have a lasting morphological expression within the de-iced landscape and contribute linearity in the landform record. For example, Hewitt (1999) and Porter (2000) re-interpreted a large number of moraines in the Karakoram and Southern Alps of New Zealand respectively as deposits of large rock avalanches (cf. Shulmeister et al., 2009).

6.3.6 Temporal and spatial variability in moraine production

Processes of moraine formation are closely linked to ice dynamics and the style of glacier retreat, which may vary over time in relation to fluctuations in climate and localized factors such as debris-cover. Between 1945 and 1980 the glacier retreated by

an average of 500m up the foreland punctuated by periods of standstill and advances that produced moraine complexes such as moraine complex B and the north-eastern corner of moraine complex A. These moraines were formed by the bulldozing of partially ice-cored moraine and marginal outwash and lacustrine sediments, deposited during periods of standstill. The southern snout was completely free of debris during this time and wasted into a proglacial lake so that moraines did not form along this part of the glacier terminus. Between 1980 and 1998 the snout experienced a sustained advance, resulting in the bulldozing of ice-cored moraine, the overriding of push moraines in the north-eastern corner of moraine complex A, and the bulldozing of proglacial sediments across the snout.

However, between 1998 and 2003 the snout retreated little, especially at the northern snout margin and instead the ice upglacier from moraine complex A downwasted leading to the ice-cored moraine complex being partially detached from the glacier, as in the incremental stagnation model of Eyles (1979). Kvíárjökull is thus a good example of the model of 'incremental active retreat' (Eyles, 1983c), which results in the production of arcs of moraine which represent ice margin positions during periods of stagnation and their subsequent bulldozing by active ice (Dyke and Evans, 2003). Moraine complexes A, B and C represent such arcs of moraine within the northern part of the foreland. The feedback between increasing debris cover, associated with 'ablation dominant' conditions (Kirkbride, 2000) and the marginal emplacement of deposits from large rockfall events, and decreased marginal ice velocity in leading to the stagnation of the debris covered snout and the in-situ downwasting of ice-cored moraine is exemplified by the evolution of moraine complex A (Section 6.1.2).

Process-form relationships responsible for linearity within moraine complexes are spatially variable, influenced by the quantity and type of marginal debris cover and proglacial processes. Moraine complexes that form along the lateral margins, as represented by the outer sections of moraine complexes C and D, form by the dumping of supraglacial debris, predominantly rockfall debris, in kame terraces, crevasse fills and eskers as the glacier downwastes. Meltwater channels channelled between the glacier margin and outer lateral moraines are particularly important in enhancing linearity within the moraine complexes. Linearity within the moraine

complexes at the northern snout is formed by ice-marginal pushing of ice-cored moraine (which may or may not contain controlled moraine) and proglacial outwash and lacustrine sediments. The magnitude of pushing means that any pre-existing controlled moraine is destroyed. Whilst controlled moraine is clearly produced at the southern snout it is rapidly submerged by the proglacial lake or incorporated into outwash sediments. Moraine complex D is the only complex where linearity may be partially derived from controlled moraine and, thus, reflect englacial structure.

6.4 Synthesis: The 'debris-charged landsystem'

6.4.1 A Debris-charged landsystem model

Spedding and Evans (2002) and Evans (2005) proposed the 'debris-charged glacier landsystem' based on the variety of sediment transport and moraine formation processes found at Kvíárjökull. Several characteristics of the debris-charged landsystem were proposed that distinguish it from pre-existing landsystems: moderate relief, a high debris turnover, a terminal overdeepening and the impact of this on hydrology and sediment transport. A preliminary landform record was proposed related to the distinctive topographic and glaciological characteristics, consisting of kame terraces, latero-frontal moraine loops, hummocky moraine, and heavily re-worked ice-contact glacifluvial sediment accumulations (such as terraced and kettled sandur and kame terraces), along with glacilacustrine deposits.

From the evidence presented it is evident that 'hummocky moraine' at Kvíárjökull is polygenetic. Three principle sediment-process-landform associations (1-3) can be recognised based on the morphology and orientation of their ridges relative to glacier flow and their sedimentology. These are associated with other landforms (a – q), detailed below, and together comprise a landform assemblage characteristic of the 'debris-charged glacier landsystem' (Fig 6.9 - Fig 6.11). The three associations are: **(1)** chaotic hummocky moraine with minor elements of linearity resulting from the stagnation of controlled moraine (a); **(2)** push moraine complexes, which may still be ice-cored, comprising transverse and often crenulated push moraine ridges resulting from the bulldozing of proglacial outwash sediments (b), lacustrine sediments (c), deposited by proglacial lakes (d), and ice-cored moraine (e) during glacier advances; **(3)**

heavily channelized moraine complexes within the outer foreland containing linear chains of hummocks interspersed with ribbon sandur (f) resulting from the reworking of marginal deposits, that may include terraces of supraglacial material (g), kame terraces (h) and valley eskers (i), by meltwater channels (j). At the base of lateral moraine slopes these deposits are also incorporated with paraglacial slope deposits (k). Features of ice-core disintegration: thaw lakes (l), sink holes (m) and kettle holes (n), are prevalent throughout the foreland, as are englacial eskers (o). Lastly, it is possible that a large ice-cored rockfall deposit at the modern day glacier margin (p) within the medial moraine (q) may have a future landsystem signature.

It should be noted that ice is still present throughout most of the glacier foreland as indicated by the continued downwasting of moraine complexes C and D between 1998 and 2003. Everest and Bradwell (2003) describe this phenomenon of the melt out of buried ice following initial 'primary' deglaciation as 'secondary' deglaciation. Secondary deglaciation is only complete when the ice cores have melted and no further surface lowering takes place. Only when secondary deglaciation is complete is the landscape stable and can the landform record be used as an accurate analogue for ancient deglaciated terrain.

6.4.1 Comparison with other landsystems

Spedding and Evans (2002) first questioned the suitability of classifying Kvíárjökull alongside alpine glaciers such as the Brenva or Tsidjiore Nouve Glaciers as a 'glaciated valley landsystem' as defined by Eyles (1979, 1983a,b,c) and expanded by Benn et al. (2003), citing major differences in sediment transport pathways and process-form relationships involved in landform production. Kvíárjökull has distinct differences to these and many other alpine glaciers since classified as 'glaciated valley landsystems'. These glaciers are bounded by steep rock walls along their length, including their accumulation zones, whereas Kvíárjökull descends from a plateau icefield (Rea and Evans, 2003) and is bounded by steep rock walls only in its ablation zone. The volume of supraglacial debris on the glacier surface is primarily a function of the rock wall area surrounding the glacier (Eyles, 1979), and therefore the debris-cover of true alpine glaciers such as Brenva is much more extensive than that on Kvíárjökull.
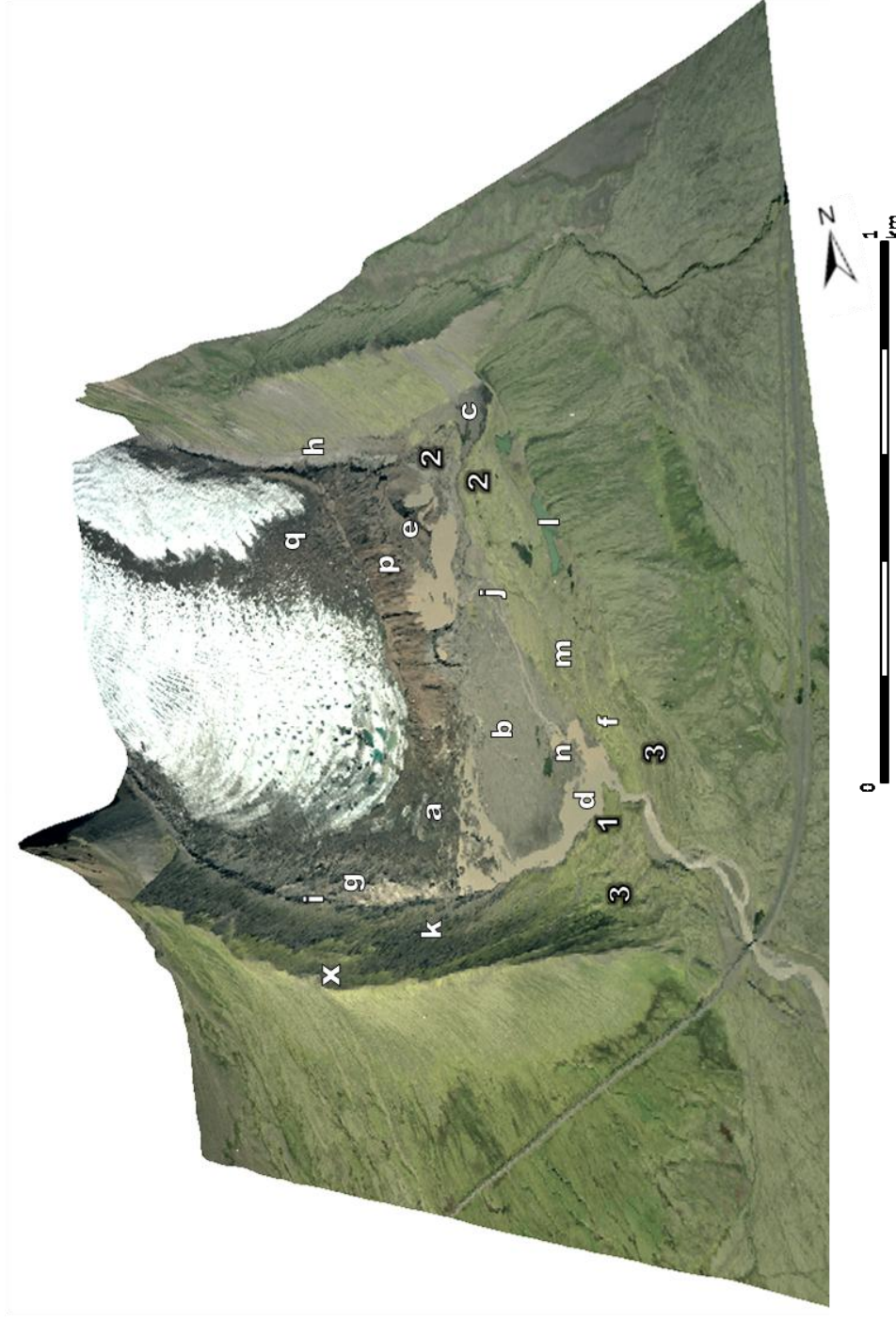
Fig 6.9 – The 'debris-charged glacier landsystem' of Kvíárjökull shown on the 2003 orphophoto draped over the DEM. 1 – 3 and a – q and are described within Fig.7.12. x is referred to in Fig. 7.13. 1 = Chaotic hummocky moraine; 2 = Push moraine complex; 3 = Heavily channelized hummocky moraine; a = Controlled moraine; b = Glacifluvial outwash sediments; c = Lacustrine sediments; d = Proglacial lakes; e = Ice-cored moraine; f = Ribbon sandur; g = Terraces of supraglacial debris; h = Kame terraces; i = valley eskers; j = meltwater channels; k = paraglacial slope deposits; l = thaw lakes; m = sink holes; n = kettle holes; o = englacial eskers; p = ice-cored rockfall deposit; q = medial moraine

Fig 6.10 – Oblique photograph taken from point x in Fig 7.11 towards the northeast in 2007, showing some of the features of the 'debris-charged landsystem'. 1 = Chaotic hummocky moraine; 2 = Push moraine complex; 3 = Heavily channelized hummocky moraine; a = Controlled moraine; b = Glacifluvial outwash sediments; c = Lacustrine sediments; d = Proglacial lakes; e = Ice-cored moraine; f = Ribbon sandur; g = Terraces of supraglacial debris; h = Kame terraces; i = valley eskers; j = meltwater channels; k = paraglacial slope deposits; l = thaw lakes; m = sink holes; n = kettle holes; o = englacial eskers; p = ice-cored rockfall deposit; q = medial moraine
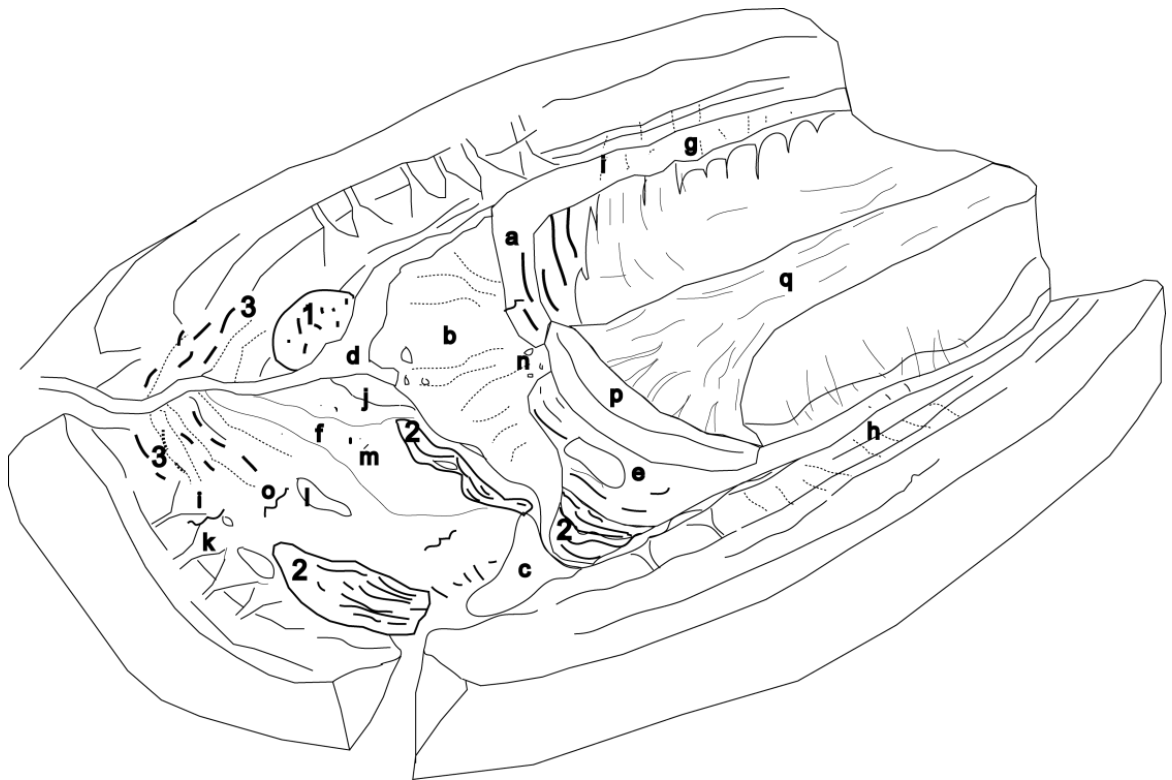
Fig 6.11 - Schematic model of the 'Debris-charged glacier landsystem' based on Kvíárjökull. 1 = Chaotic hummocky moraine; 2 = Push moraine complex; 3 = Heavily channelized hummocky moraine; a = Controlled moraine; b = Glacifluvial outwash sediments; c = Lacustrine sediments; d = Proglacial lakes; e = Ice-cored moraine; f = Ribbon sandur; g = Terraces of supraglacial debris; h = Kame terraces; i = valley eskers; j = meltwater channels; k = paraglacial slope deposits; l = thaw lakes; m = sink holes; n = kettle holes; o = englacial eskers; p = ice-cored rockfall deposit; q = medial moraine

Eyles emphasized the importance of rockfall debris in the sediment budget of a glaciated valley glacier, transported passively as 'supraglacial morainic till' (Boulton and Eyles, 1979; Eyles, 1979). However, Spedding and Evans (2002), Swift et al., (2006) and this study have demonstrated the diversity of debris types that make up the debris cover, and the dominance of actively transported debris in the sediment budget, rather than passively transported rockfall debris. In particular this research emphasizes the importance of water-worked debris transported along glacio-fluvial pathways within the glacial system in landform production. Eyles treated glacio-fluvial processes as proglacial processes that influenced moraine formation only at and beyond the snout terminus, whereas Spedding and Evans (2002) recognize ice and water as *'parallel components of a single, integrated system of subglacial and englacial sediment transfer'*.

The differences in sediment transport processes in landform production between Kvíárjökull and alpine glaciers are demonstrated by the lateral moraines. Whilst large lateral moraines are features common to the debris-charged glacier landsystem and the 'glaciated valley landsystem', the process-form relationships involved in their formation differs. At alpine glaciers lateral moraine construction involves the deposition of rockfall debris in troughs between the glacier margins and valley walls (Boulton and Eyles, 1979). However, at Kvíárjökull the lateral moraines contain an increasing proportion of water-worked debris towards their distal ends reflecting the dominance of water-worked debris discharged from Kvíárjökull in moraine construction. Spedding and Evans (2002) attribute the size of these moraines to enhanced delivery of actively transported debris to the glacier margin at times of maximum ice extent during the Neoglacial, related to a steeper surface slope relative to the adverse bed slope, and therefore a greater rate of subglacial erosion and increased elevation of debris along glacio-fluvial pathways. However, considering the importance of ice-marginal bulldozing at the modern day glacier margin demonstrated by this study it is likely this process would have contributed significantly to the size and steepness of these moraines.

The difference in the spatial extent of debris-cover between Kvíárjökull and an alpine glacier results in differences in glacial dynamics and ultimately moraine production. Whilst true debris-covered glaciers in a glaciated valley setting have a muted or non-existent response to climatic fluctuations (e.g. Thomsen et al., 2000), the partial debris-cover of Kvíárjökull is not sufficient to disrupt the climatic signal as demonstrated by this study. The style of retreat at Kvíárjökull is one of incremental retreat punctuated by climatically forced advances in contrast to the style of retreat at glaciated valley landsystems of more gradual retreat or stagnation (Kirkbride and Warren, 1999). As such, whilst the morphology of hummocky moraine at the terminus of debris-covered glaciers is governed by the distribution of reworking processes within in situ downwasting ice-cored moraine complexes, at the terminus of the debris-charged landsystem it is governed mainly by ice-marginal bulldozing.

It is the quantity of debris produced at a debris-charged glacier such as Kvíárjökull that differentiates it from the typical Icelandic active temperate glacier (e.g.

Breiðamerkurjökull and Sandfellsjökull). Most lowland plateau outlet glaciers of Iceland generally transport relatively small quantities of supraglacial and ice-marginal debris and as such do not form latero-frontal moraines and hummocky moraine (Evans, 2005). An exception is Kötlujökull where a debris-mantled snout is formed by thrusting of debris-rich ice (Krüger and Kjær, 2000). It is also differentiated by its topography. Whereas a typical active temperate glacier spreads out into a piedmont lobe, Kvíárjökull is confined by its lateral moraines and rock walls. The confinement of the glacier snout at Kvíárjökull and the presence of the overdeepening both amplify compressional forces within the snout, leading to tectonic thickening of debris-rich basal ice (Spedding and Evans, 2002) and folding and thickening of debris bands towards the frontal margin, and are thus critical in 'charging' the snout with debris.

Because of the large volume of supraglacial and englacial debris deposited by a debris-charged glacier, subglacial landforms such as flutings and minor push moraines, characteristic of active temperate landsystems are not visible within the landform signature. The most conspicuous landforms shared by these landsystems are proglacial moraine complexes. Spedding and Evans (2002) differentiated between those at Kvíárjökull, which they suggested evolved from controlled moraine produced by the melt out of englacial debris bands (although they recognized a degree of ice-marginal pushing), and those at an active temperate glacier, which are formed by the bulldozing of pre-existing till and outwash deposits during advances (Howarth, 1968; Price, 1970; Kruger, 1985). However, this research has demonstrated that the significance of ice-marginal bulldozing in moraine construction at Kvíárjökull has been previously underestimated. Whilst push moraines at Kvíárjökull are also shaped by de-icing processes following bulldozing of ice-cored sediments, there are greater similarities in process-form relationships responsible for moraine complexes at the debris-charged and active-temperate landsystems than previously realised.

Spedding and Evans (2002) also differentiate Kvíárjökull from active temperate glacier landsystem based on its lack of *'meltwater channels, eskers and outwash fans'*, which they attribute to the lack of *'large subglacial drainage channels and the distributed nature of englacial drainage in its terminal lobe'*. However, the time-series of maps show the development of all three of these features within the foreland of Kvíárjökull

over the study period. It is the spatial organisation of the features that differs from those within an unconfined foreland of an active temperate glacier. Glacifluvial outwash deposition is partly controlled by large hummocky moraine complexes and is confined by the latero-frontal moraine loop and, therefore, forms heavily reworked ice-contact glacifluvial sediment accumulations, such as terraced and kettled sandur and kame terraces, along with glacilacustrine deposits in between hummocky moraine complexes.

Kvíárjökull has several similarities to the debris-rich landsystem of Kötlujökull (Krüger, 1994; Naslund and Hassinen, 1996; Krüger and Aber, 1999; Krüger and Kjær, 2000; Kjær and Krüger, 2001). Both glaciers drain volcanic icecaps (Kvíárjökull drains the ice cap over Oræfi and Kötlujökull drains that over Katla). The maritime climate and geothermal heat flux common to both glaciers promotes the initial rapid lateral retreat and lowering of terminal ice-cored moraine complexes by backwasting and the eventual formation of a low relief hummocky moraine surface characterised by linear mounds and ridges, as illustrated in the model of ice-cored moraine evolution by Kjær and Krüger (2001) (Fig 6.8). However, whereas at Kötlujökull ice-cored moraines melt out undisturbed and therefore both the sedimentary architecture and geomorphological imprint in the final landform are governed by the final reworking processes (Schomacker and Kjær, 2007), at Kvíárjökull glacier ice repeatedly overrides and bulldozes mature ice-cored moraine so that the final geomorphological imprint is more linear.

Considering the frequent advances that punctuated glacier retreat at Kvíárjökull over the study period, ice-cored moraine development has more in common with that in the forelands of the surging glacier landsystem such as Brúarjökull (e.g. Schomacker and Kjær, 2007), where mature dead-ice is repeatedly overridden during surges producing multiple generations of ice-cored landforms. Overriding of ice-cored moraines at Brúarjökull during glacial surges disrupts the melt-out of ice-cored moraines and increases the time taken for complete de-icing to occur. Dead ice may also be incorporated into new ice-cored landforms such as ice-cored drumlins and ice-cored outwash plains. Advances of Kvíárjökull are smaller however, resulting in ice-cored moraine being pushed from behind. Only the 1980-1998 advance was extensive

enough to result in the overriding and reincorporation of ice-cored moraine at the northern margin to form moraine complex A. Another similarity between the debris-charged landsystem and the surging glacier landsystem (e.g. Eyjabakkajökull and Brúarjökull) is high water pressure, associated with the overdeepening and a well developed drainage system at Kvíárjökull, and generated during surges at surging glaciers. Englacial eskers associated with the deposition of debris in terminal drainage channels during high water flow are therefore common features of both landsystems (Spedding and Evans, 2002).

6.4.2 Implications for palaeoglaciological reconstructions

Well established process-form models exist for the evolution of ice-cored moraine around glacier snouts in which ice-cored moraine melts out to form hummocky moraine with only a weak impression of former englacial structure (e.g. Boulton, 1972). Much research has highlighted the extensive reworking that occurs at downwasting debris-rich glacier snouts and the resulting complexity of sedimentary signatures (e.g. Boulton 1972; Eyles, 1983; Krüger, 1994; Kjær and Krüger, 2001; Schomacker et al., 2006). Observations at modern day glacier margins have been applied to interpretations of till-stratigraphies and glacifluvial sequences in ancient glaciated landscapes (e.g. Boulton, 1977; McCarroll and Harris, 1992; Thomas et al., 1985).

Despite the establishment of these process-form relationships and models, which imply the low preservation potential of englacial structure, much recent research has focused on identifying englacial structure in ancient landform signatures, in recognition that apparently 'chaotic' hummocky moraine within ancient glaciated landscapes contains transverse linearity. This shift in thinking is exemplified by the Scottish Younger Dryas hummocky moraine. Sissons (1967, 1974, and 1979) initially interpreted tracts of hummocky moraine as representing widespread ice-stagnation at the end of the Younger Dryas. These moraine complexes have since been re-interpreted as representing incremental 'active' ice retreat on the basis of linearity within the moraine complexes (Eyles, 1983c). Following this reinterpretation a debate concerning the origin of linearity within the hummocky moraine has arisen. Several studies have proposed a push moraine origin (Bennett and Glasser, 1991; Benn, 1992;

Bennett and Boulton, 1993a, b; Lukas, 2003, 2005), whilst other studies have proposed a controlled moraine origin for linearity in this moraine (Hambrey et al., 1997; Bennett et al., 1998) based on modern analogues.

Evans (2009) states that *'it is the preservation potential of the controlled moraine, irrespective of its origins, that remains crucial to progress in palaeoglaciological reconstructions. Only if preservation is possible can we speculate about the palaeoglaciological implications of a controlled versus push origin and then, more specifically, the processes involved in controlled ridge construction on ancient glaciers'*. This research offers insights into the preservation potential of controlled moraine (regardless of its origins e.g. thrusting, supercooling, tectonic thickening) and therefore whether it is feasible to attribute linearity in ancient glaciated landform signatures to processes of controlled moraine formation. It also offers insights into the role of ice-marginal pushing in moraine linearity at a temperate actively retreating glacier margin and whether ice-marginal pushing may be a more likely origin for the linearity in Scottish hummocky moraine.

In Bennett et al.'s (1998) conceptual process-form model of hummocky moraine formation from englacial debris bands, linearity within hummocky moraine reflects the stacking of moraines derived from englacial and proglacial thrusting, therefore implying a high preservation potential of controlled moraine within the de-iced landscape (Fig 2.8). The model is based on observations at polythermal surging and non-surging glaciers on Svalbard and applied to the Scottish Younger Dryas moraine to propose a thrusting origin for several moraine complexes (Hambrey et al., 1997; Bennett et al. 1998). The proponents of the model argue that moraine-mound complexes in Svalbard therefore provide more suitable analogues for the transverse linearity within Scottish Younger Dryas moraine than temperate glaciers, such as in Iceland, and that by implication some of the British Younger Dryas glaciers had a polythermal character and a colder climate than previously thought (e.g. Payne & Sugden, 1990). The main problem with this model is that it involves the uninterrupted lowering of debris bands onto the subglacial surface (Evans, 2009) and therefore ignores the widespread research that highlights the extensive reworking that occurs at

downwasting debris-rich glacier snouts. Furthermore, in the model outwash is deposited only after melt-out is complete.

At Kvíárjökull the low preservation potential of controlled moraine is largely attributed to the high rate of backwasting that occurs during the fully-ice cored stage of moraine evolution. Whilst Kvíárjökull has a different climate and thermal regime to Svalbard glaciers, backwasting processes have been shown to be weakly correlated to climate by Schomacker (2008), who found that backwasting is more effective than downwasting in ice wastage at glaciers in Svalbard as well as Iceland. Furthermore, he found that at Holmströmbreen, Svalbard, the rate of backwasting is higher than at Kötlujökull, even though the climate is cooler at Holmströmbreen. This is because the presence of an impermeable layer of permafrost at the base of ice-cored moraine at Svalbard glaciers prevents the evacuation of meltwater, which therefore promotes mass movement processes and prevents the build up of an insulative debris mantle (Schomacker, 2008). Therefore the findings at Kvíárjökull concerning the low preservation of controlled moraine may be plausibly applied to Svalbard in suggesting that the simple lowering of debris bands within Bennett et al.'s (1998) model is unfeasible. Another problem with the model is that it is based on moraines that still contain ice-cores (Evans, 2009), which therefore do not represent the final landform signature and should not be used in palaeoglaciological reconstructions. This research has demonstrated the length of the period of 'secondary deglaciation' at a temperate glacier with a maritime climate. The completion of de-icing is likely to take much longer at Svalbard glaciers, under a cooler climate.

A number of studies have proposed a push origin for the Scottish hummocky moraine (e.g. Bennett and Glasser, 1991; Benn, 1992; Bennett and Boulton, 1993a, b; Lukas, 2003, 2005). Whilst this research has demonstrated the significance of ice-marginal pushing in moraine construction at an actively retreating glacier, as well as the preservation potential of push moraines, therefore supporting a push moraine origin over a controlled moraine origin for hummocky moraine complexes in Scotland, it has also highlighted problems with specific aspects of these models, notably with the model proposed by Lukas (2005).

Lukas (2005) proposes a model of hummocky moraine formation for the Scottish hummocky moraine in which hummocky moraine represents a continuum of undeformed to completely overridden and glacitectonized terrestrial ice-contact fans formed during oscillatory retreat (Fig 6.12).
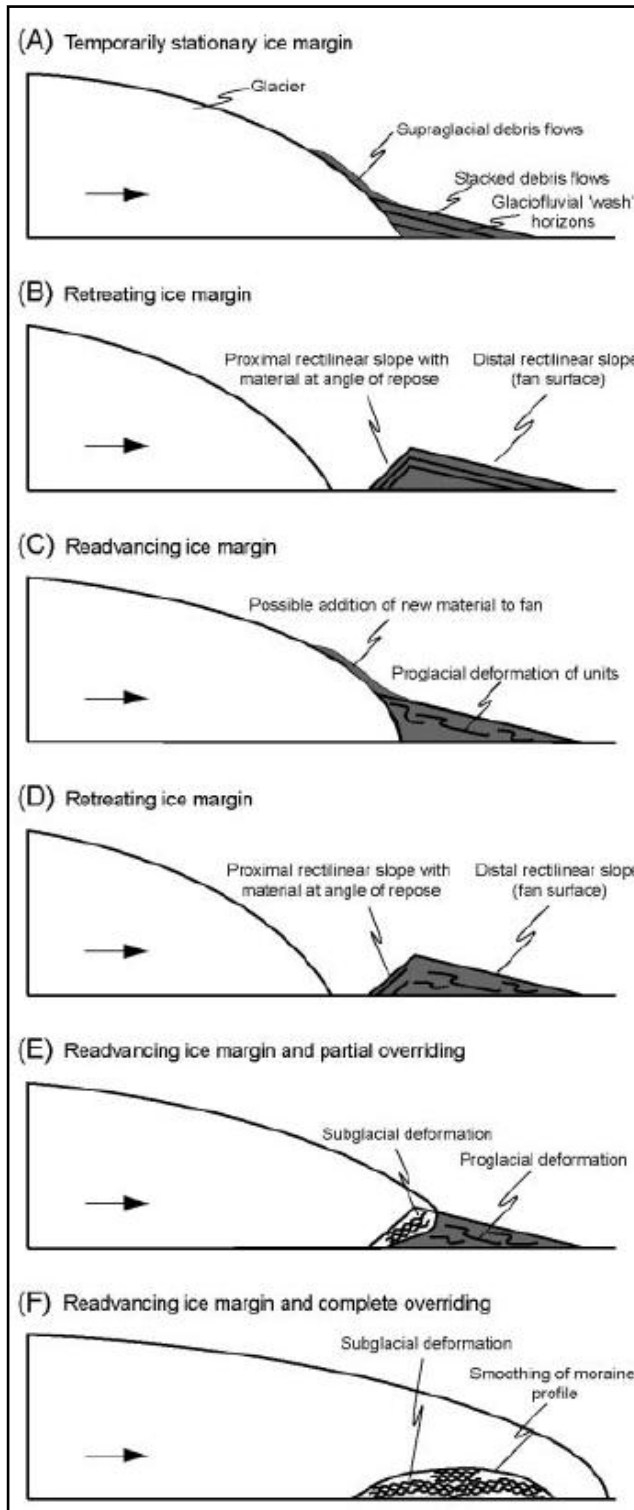
Fig 6.12 - Model of hummocky moraine formation by ice-contact fan formation. A. Fan formation along a temporarily stationary ice margin by stacking of supraglacial debris flows and glacifluvial sediments. B. Formation of the rectilinear ice-contact face where material is at the angle of repose as a result of partial collapse following withdrawal of ice support. C. Short-lived readvance of the ice margin (with a possible annual signature in some areas) causing widespread deformation within the fan and occasionally the addition of new material. D. Formation of a new ice-contact face and abandonment of the fan. E. Partial overriding of the proximal part of a moraine leading to partial glacitectonization. F. Larger-scale overriding leading to smoothing and alteration of the original moraine asymmetry and complete glacitectonization.

(Lukas, 2005)

Like Bennett et al.'s (1998) englacial thrusting model, the processes of deformation inherent on the melt out of ice-cores are discounted based on the absence of any disturbance caused by melt-out of potential dead ice cores within the moraines. However, as cautioned by Casely and Dugmore (2004) it is not wise to accept *'absence of evidence'* as *'evidence of absence'*. The absence of evidence of re-sedimentation is interpreted as an indication of a temperate glacier that responded quickly enough to climate change to not leave stagnant ice bodies cut off from supply upglacier (Lukas, 2005). However, ice-contact fan accumulation and subsequent preservation would involve large quantities of sediment accumulating at the glacier snout which would inevitably bury the glacier terminus, as shown in stages A and C of Lukas's model, and as seen at the margin of Kvíárjökull. As demonstrated at Kvíárjökull where a thick debris cover insulates the ice, the accumulation of debris at the snout would inevitably result in the incorporation of ice. It is therefore argued that the exclusion of melt out processes in the final sedimentology and morphology of hummocky moraine based on the absence of evidence for ice-melt out is unlikely.

There are two major criticisms that apply to both the thrusting model and ice-contact fan accumulation model. Firstly both attempt to fit a landform assemblage ('hummocky moraine') that is by nature polygenetic (Benn, 1992) to a single set of processes. Secondly, both take a small scale landform approach, therefore, not considering the associated landforms and landsystem beyond the moraine complexes they attempt to represent. Arguably a better approach to interpreting the Scottish Younger Dryas moraines is that taken by Benn (1992), who does not attempt to apply a single model to the moraine complexes, but rather presents evidence for three sediment-process-landform associations that together make up hummocky moraine complexes. These sediment-landform associations are: 'recessional moraine' produced by ice-marginal pushing, 'chaotic moraine' resulting from stagnation of ice-cored moraine, and 'drumlins and fluted moraines' formed subglacially.

Benn's (1992) interpretation of the Scottish moraine as polygenetic is supported by this study, which has demonstrated the spatial and temporal variability of sediment-process-form relationships in moraine construction. Landform associations at Kvíárjökull are similar to those within the valleys of the Scottish Highlands. Three

sediment-process-landform associations are identified at Kvíárjökull, making up the 'debris-charged glacier landsystem': **(1)** chaotic hummocky moraine with minor elements of linearity resulting from the stagnation of controlled moraine; **(2)** push moraine complexes, which may still be ice-cored, comprising transverse and often crenulated push moraine ridges resulting from the pushing of proglacial outwash sediments, lacustrine sediment and ice-cored moraine during glacier advances; **(3)** heavily channelized moraine complexes within the outer foreland containing linear chains of hummocks interspersed with ribbon sandur resulting from the reworking of marginal deposits, that may include terraces of supraglacial material, kame terraces and valley eskers, by meltwater channels. Kvíárjökull lacks a subglacial signature in the form of 'drumlins and fluted moraines' identified by Benn (1992) in Scotland, as this either destroyed by lake expansion, ice-marginal pushing, or hidden by englacial and supraglacial sediment deposition. However, assemblages (1) and (2) correspond with the 'chaotic moraine' and 'recessional moraine' associations respectively, identified by Benn (1992) in Scotland. Additionally, the ice-marginal kame terraces, meltwater channels, ice-contact fans and esker fragments that comprise assemblage (3) at Kvíárjökull all occur in close association with moraine complexes in valleys in Scotland (Bennett and Boulton, 1993a,b). Therefore it is concluded that the debris-charged landsystem provides a suitable analogue for the Scottish Younger Dryas moraines.

7 Conclusions

DEMs at five epochs between 1945 and 2003 with a range of resolutions from 2.6m (2003) - 4.5m (1964) were generated from stereopairs of large to medium scale, vertical aerial photographs using digital photogrammetry. Morphometric analysis using the DEMs has been effectively combined with field measurements and geomorphological mapping in an advanced quantitative ergodic approach to draw the following conclusions.

7.1 Glacier-climate interactions, glacier retreat and de-icing rates

Kvíárjökull advanced several times between 1945 and 1998. Most advances that occurred prior to 1980 were too small to be detected in morphometric analysis at the temporal resolution of this study but are indicated by push moraines within the foreland such as moraine complex B. The 1980 - 1998 advance was detected in morphometric analysis and resulted in the pushing of terminal ice-cored moraine and sediments.

The fluctuations of Kvíárjökull correlate with air temperature on a decadal scale with a delay of about 10 years compared to other Icelandic glaciers. The longer response time of Kvíárjökull is explained by two main factors: the thickness of the glacier snout within the overdeepening, which increases the time taken for the transfer of ice to the snout; and the debris-cover, which insulates the glacier snout from ablation. Spatial differences in ice loss across the snout over the study period are explained by the distribution of the supraglacial debris. Debris cover within the medial moraine insulated the northern snout over the study period, reducing ice loss compared to the southern snout. It also amplified the 1980-1998 advance of the northern part of the snout by reducing ablation over the preceding years so as to result in the conservation of ice and enhanced thickening in response to an increase in the supply of ice to the margin.

Between 1998 and 2003 ice loss accelerated, with 25% of total ice loss (1945-2003) occurring lost over only <10% of the study period. This accelerated rate of ice loss exceeds the rate of air temperature rise, suggesting that Kvíárjökull may have become

sensitive to increasing air temperatures. However, a more likely explanation for the accelerated retreat is the growth of proglacial and supraglacial lakes between 1998 and 2003 and the associated increase in rates of calving and thermoerosion.

Whereas ice loss occurred by both lateral retreat and thinning relatively equally between 1945 and 1998, between 1998 and 2003, ice loss by thinning was ~6 times that lost by lateral retreat. This change in the style of retreat has implications for moraine production. Whilst between 1945 and 1998 moraines formed by ice marginal pushing of terminal ice-cored moraine and sediments, between 1998 and 2003 moraine was formed by the stagnation of the debris-covered glacier retreat related to a complex feedback loop between increased ablation, the upglacier spread of debris-cover, and ice dynamics at the margin.

7.2 De-icing progression of ice-cored landforms in a temperate, maritime climate

This study has used an advanced quantitative ergodic approach to revise the model of de-icing progression for a temperate, maritime climate developed by Krüger and Kjær (2000) using an ergodic approach at Kötlujökull. In their model they suggest a period of 50 years for the completion of de-icing that relied on the assumption that hummocky moraine in the outer foreland was completely de-iced. Morphometric analysis at Kvíárjökull has revealed that ice-cores may survive for much longer than 50 years. A period of 83 years is estimated for the completion of de-icing based on an ice core of 40m in thickness.

As the study period was not long enough to observe the full evolution of ice-cored moraine into hummocky moraine, this new model of de-icing progression combines two moraine complexes of different ages (A and C). To validate this model, measurement of de-icing rates within these moraine complexes should continue. However, it demonstrates with relative certainty that ice-cores remain in the landscape for the length of the study period, 58 years, which is already 8 years longer that the period of time suggested by Krüger and Kjær (2000). Furthermore, by observing a single moraine complex over a number of decades of changing climate, this study has demonstrated the effect of changing climate on the rate of de-icing

within the proglacial landscape. The de-icing rate increased in all four moraine complexes observed between 1998 and 2003 as a result of increasing air temperature.

7.3 Sediment-process-form relationships in the genesis of hummocky moraine complexes

This study has combined sedimentological data with DEM and field measurements of morphometric change to refine process-sediment-form models for hummocky moraine formation. Four debris concentrations combine to 'charge' the glacier snout with debris: water-worked debris bands, channel fills, basal debris bands and rockfall deposits. Basal debris bands are found to have very low preservation potential and therefore little contribution to hummocky moraine development, via controlled moraine formation. Transverse water-worked debris bands crop out at the margin and control the pattern of differential ablation as a result of their thickness and high debris content, to produce 'controlled moraine'. This has diverse origins involving sustained debris transport within the englacial drainage system and thickening and folding of debris bands under compressive flow at the base of the ice fall and within the overdeepening, as well as elevation of debris under high water pressure.

The preservation of controlled moraine within the final landform signature is prohibited in much of the foreland by marginal meltwater activity and development of proglacial and supraglacial lakes. Previous studies have found that the transition from small supraglacial ponds into a large moraine-dammed lake may occur within 2–3 decades (e.g. Ageta et al., 2000). However, this study finds that this transition may occur within a decade. For example, within moraine complex A between 1998 and 2003, the area of the lakes increased by four orders of magnitude, from 100m³ to 125,000m³.

Where controlled moraine survives its preservation is prohibited by high rates of backwasting of ice-cores. DEMs were effectively combined with field measurements to quantify rates of backwasting and downwasting within an ice-cored moraine complex, thus utilizing the approach was pioneered by Schomacker and Kjær (2007). Backwasting rates of 5m/yr were measured, compared to a downwasting rate of 1.4m/yr. High rates of backwasting at Kvíárjökull are promoted by high air

temperatures, precipitation, meltwater production and supraglacial lake formation. Backwasting consumes high ground before topographic inversion can occur, thus destroying controlled moraine ridges.

Another process responsible for the low preservation potential of controlled moraine is ice-marginal pushing. Morphometric analysis revealed the elevation of ice-cored moraine ridges by ~10m during the 1980-1998 advance. It also revealed a push moraine origin for many of the ridges mapped within the foreland, supported by sedimentological evidence of post-depositional deformation. Push moraines were found to have a high preservation potential, and it is therefore concluded that ice-marginal pushing of ice-cored and proglacial outwash sediments during climatically forced glacial advances makes a greater contribution to linearity in the final landform signature than previously thought.

The styles of retreat changed from active retreat between 1945 and 1998 to stagnation between 1998 and 2003, associated with 'ablation dominant' conditions as defined by Kirkbride (2000), resulting in the in situ downwasting and karst development of terminal ice-cored moraine. Observations in the field in 2008 suggest that this stagnation continues. Kvíárjökull is thus a good example of the model of 'incremental active retreat', in which arcs of moraine are produced during periods of stagnation and are subsequently bulldozed by active ice during periods of active retreat.

7.4 The debris-charged landsystem

Through the geomorphological mapping of the glacier foreland, the refinement of process-sediment-form relationships involved in hummocky moraine formation at Kvíárjökull, and the identification of a climatic signal within the landform signature, the landsystem classifications previously applied to Kvíárjökull have been reassessed. This study supports the conclusion of Spedding and Evans (2002) that the 'glaciated valley landsystem' model of Eyles (1979, 1983a,b,c) previously proposed for Kvíárjökull is unsuitable. Instead a landsystem model for the 'debris-charged landsystem', originally outlined by Spedding and Evans (2002) and Evans (2005), has been developed. Three principle sediment-process-landform associations are recognised: (1) chaotic

hummocky moraine with minor elements of linearity resulting from the stagnation of controlled moraine; (2) push moraine complexes, comprising transverse and often crenulated ridges; (3) heavily channelized moraine complexes containing chains of hummocks dissected by outwash trains and eskers.

7.5 Implications of this research

7.5.1 For the quantification of change within glacial environments

This study has demonstrated the potential to convert a long archive of aerial photographs into a time-series of high-resolution DEMs in an automated and repeatable fashion using digital photogrammetry, and to use these DEMs to quantify morphometric change within a glacier snout and foreland. The glacial and proglacial environment is well suited to this type of analysis because of the magnitude of geomorphic change as well as the highly textured surface of both the debris-covered and crevassed snout and the recently exposed glacial deposits. For many glaciated regions of the world aerial photographs have been collected for over half a century, providing accurately dated records of ice volume change and landform evolution that could be used to extend the record of glacier mass balance measurements, to constrain models of de-icing progression, and to improve understanding of landform evolution.

7.5.2 For palaeoglaciological reconstructions

Evans (2009) stated that 'only if preservation (of controlled moraine) is possible can we speculate about the palaeoglaciological implications of a controlled versus push origin, and then, more specifically, the processes involved in controlled ridge construction on ancient glaciers.' In demonstrating the low preservation potential of controlled moraine and the morphological significance of ice-marginal pushing in moraine construction in the foreland of Kvíárjökull, this study questions the viability of a controlled moraine origin for ancient hummocky moraine such as the Scottish Younger Dryas moraine. Whereas hummocky moraine has previously been interpreted as the morphological end product of glacier stagnation and dead-ice melting, this research

demonstrates that hummocky moraine in ancient glaciated terrain may contain a climatic signal in the form of pushed moraine ridges.

The new model of de-icing progression of ice-cored landforms in a temperate, maritime climate has implications for the use of apparently de-iced glacier forelands as analogues for ancient glaciated terrain. The model suggests that 'secondary' deglaciation may last as long as 83 years. Only when secondary deglaciation is complete is the landscape stable and can the landform record be used as an accurate analogue for ancient deglaciated terrain.

7.6 Limitations and further work

7.6.1 DEM Quality

A first quality analysis, internal to each DEM, was performed by comparing the predicted DEM elevations to the observed check point elevations. This analysis revealed that systematic error in the DEMs compared to GCPs was generally less than or around 1m apart from in the 1945 DEM (7.74m). This error increases with age largely because image quality reduces with age associated with poorer quality acquisition and an increased number of diapositive imperfections. The especially high mean error in the 1945 DEM is thought to be a consequence of shadow cast by clouds along the southern lateral moraine during image acquisition, a large number of scratches on the scanned diapositives as well as a lack of interior orientation parameters.

A second quality analysis was performed by comparing the DEMs over 50 stable check points, extracted from the 2003 DEM, selected as the highest internal quality DEM (0.39m). Systematic error in the DEMs based on this analysis was higher than that calculated in the internal analysis at 0.75 - -3.11m. The random error in the DEMs ranged from 1.75 - 5.36m but may reflect the limitation of this method of error analysis, which involved checking the quality of the DEMs with a DEM whose quality was not checked externally.

Overall these quality analyses revealed that the errors were generally an order of magnitude less than the observed changes. It was therefore concluded that the results

of this work are generally significant and reliable. However, localised random errors were found to be significant when mapping smaller scale landforms (e.g. fig 5.52).

7.6.2 Use of ground based data collection

It was not possible at the temporal and spatial resolution of the DEMs to capture topographic inversion in the early stages of ice-cored moraine development or to follow the morphological evolution of features smaller than 4.5m (the resolution of the coarsest DEM). Better understanding of the rapid changes involved in the evolution of controlled moraine could be achieved by using Terrestrial Laser Scanning, by which it is possible to generate very high resolution DEMs.

Furthermore, the field testing of specific debris mantle characteristics may further understanding of the controls on the style of failure of moraine slopes and therefore the preservation potential of controlled moraine. The dependency of morphological change within ice-cored land forms on the characteristics of the debris mantle, such as pore water pressure and shear strength (e.g. Paul and Eyles, 1990), was considered in this study based on observations of material characteristics such as colour, size and thickness. For example, the low preservation potential of basal debris bands was attributed to the fine and thin debris mantle that these produce. Within ice-cored moraine it is the style of failure of moraine slopes that acts to either reinforce the linearity of features, or to conversely lead to degradation or a loss of structure. For example, within moraine complex A extensive backslumping of the debris mantle exposes ice cores to backwasting resulting in the destruction of linearity, on which basis the preservation potential of controlled moraine was inferred to be low (Fig 5.41). Detailed field testing of debris mantle characteristics such as pore water pressure and shear strength, combined with higher spatial and temporal resolution topographical data would help to further refine process-sediment-form relationships involved in the evolution of controlled moraine into hummocky moraine.

7.6.3 Automated classification of topography and surface geomorphology

Geomorphological mapping was based on visual interpretation of the DEMs and aerial photographs, and was verified in an extensive field survey. Slope, aspect and shaded

relief DEMs were generated from the DEMs to aid interpretation of the topography for geomorphological mapping. However, the generation of maps for 5 epochs using visual classification was time-consuming. The accuracy and efficiency of mapping could have been improved by applying automated classification techniques to classify terrain according to morphometric parameters, such as curvature, slope gradient and aspect (e.g. Giles and Franklin, 1998; Aderdiran et al., 2004), and spectral parameters, such as surface reflectance and texture (e.g. Giles, 1998). Geomorphological signatures, that describe landforms numerically according to these variables, may be generated for specific landforms and may subsequently be used to generate a classified map of a wider area (e.g. Giles, 1998). For example, Mackay et al. (1992) identified glacial troughs and cirques by applying rules about the known form of such features. In the same way such signatures could have been generated for landforms within the foreland of Kvíárjökull and used to generate maps for each epoch automatically. Additionally, these signatures may be applied to future aerial photographs to automatically update the time series maps of Kvíárjökull (e.g. van Asselen and Seijmonsbergen, 2006).

7.6.4 Integration of aerial photographs with other types of remotely sensed data

This study has used 5 epochs of aerial photography over a period of 58 years. Whilst a comprehensive archive, this may be enhanced further by converting the full archive of aerial photographs available for Kvíárjökull into DEMs. Additional photographs are available for 1954 and 1988 and would improve the temporal resolution of change in what is a dynamic landscape. Including a 1988 DEM in morphometric analysis would improve understanding of the timing and magnitude of the advance that occurred between 1980 and 1998. An even higher temporal resolution could be achieved by combining DEMs produced from aerial photographs with optical satellite imagery (e.g. Kaab, 2002). Medium-resolution satellite data (10 – 90m) became available for cryospheric studies from the early 1970s with the launch of new satellite-based sensors: Landsat Multispectral Scanner (MSS), Landsat Thematic Mapper (TM) and Enhanced Thematic Mapper Plus (ETM+), 'System Pour l'Observation de la Terre' (SPOT) and Terra ASTER, to name just a few. The major advantages of these data over aerial photographs are its higher temporal resolution. For example, ASTER imagery is

available for every 16 days. The stereoviewing capability of ASTER enables the creation of DEMs to complement those produced from aerial photography (Massom and Lubin, 2006). With a wider spatial coverage that aerial photographs, satellite imagery could be used to measure the mass balance of the whole glacier, rather than just the glacier snout as was the case in this study. However, these have a maximum resolution of 15m, meaning that, whilst ASTER is valuable for monitoring glacier mass balance at a high temporal resolution (e.g. Kaab, 2002), it cannot be used to monitor changes of smaller magnitude within the proglacial landscape.

Another way in which satellite data may be combined with DEMs generated from aerial photographs is in automated mapping. For example, in a study by Giles (1998) SPOT data was used to classify the terrain according to spectral properties such as reflectance and texture, and DEMs were used to obtain morphometric parameters. These were combined to develop geomorphological signatures, discussed in section 8.6.1, that were used in generating maps of the study area. Significantly, the multispectral thermal imaging bands of ASTER provide the potential for distinguishing debris-cover on glaciers (Taschner et al., 2002), making it useful for the study of debris-covered glaciers such as Kvíárjökull.

Bibliography

Adams, J.C., Chandler, J.H. 2002. Evaluation of Lidar and medium scale photogrammetry for detecting soft-cliff coastal change. *Photogrammetric Record*, 17: 405–418.

Adediran, A.O., Parcharidis, I., Poscolieri, M., Pavlopoulos, K. 2004. Computer-assisted discrimination of morphological units on northcentral Crete (Greece) by applying multivariate statistics to local relief gradients. *Geomorphology*, 58: 357–370.

Alley, R.B., Cuffey, K.M., Evenson, E.B., Strasser, J.C., Lawson, D.E., Larson, G.J. 1997. How glaciers entrain and transport basal sediment: physical constraints. *Quaternary Science Reviews* 16: 1017-1038.

Alley, R.B., Lawson, D.E., Evenson, E.B., Strasser, J.C., Larson, G.J. 1998. Glaciohydraulic supercooling: a freeze-on mechanism to create stratified, debris-rich basal ice. II. Theory. *Journal of Glaciology*, 44,: 563-569.

Alley, R.B., Clark, P.U., Huybrechts, P., Joughin, I. 2005. Ice-sheet and sea-level changes. *Science*, 310: 456–460.

Andreassen, L.M., Elvehøy, H., Kjøllmoen, B. 2002. Using aerial photography to study glacier changes in Norway. *Annals of Glaciology*, 34: 343–348.

Bahr, D.B., Pfeffer, W. T., Sassolas, C., Meier, M. F. 1998. Response time of glaciers as a function of size and mass balance: 1. Theory. *Journal of Geophysical Research*, 103: 9777-9782.

Baily, B., Collier, P., Farres, P., Inkpen, R. and Pearson, A. 2003. Comparative assessment of analytical and digital photogrammetric methods in the construction of DEMs of geomorphological forms. *Earth Surface Processes and Landforms*, 28: 307-320.

Ballantyne, C.K., Benn, D.I. 1994. Paraglacial slope adjustment and resedimentation following glacier retreat, Fåbergstølsdalen, Norway. *Arctic and Alpine Research*, 26: 255-269.

Ballantyne, C.K. 2002a. A general model of paraglacial landscape response. *The Holocene*, 12: 371-376.

Ballantyne, C.K. 2002b. Paraglacial geomorphology. *Quaternary Science Reviews*, 18/19: 1935-2017.

Baltsavias, E.P., Favey, E., Bauder, A., Bosch, H., Pateraki, M. 2001. Digital surface modelling by airborne laser scanning and digital photogrammetry for glacier monitoring. *Photogrammetric Record*, 17: 243-273.

Bamber, J., Krabill, W., Raper, V., Dowdeswell, J. 2005. Interpretation of elevation changes on Svalbard glaciers and ice caps from airborne lidar data. *Annals of Glaciology*, 42: 202-208.

Benn, D.I. 1989. Debris transport by Loch Lomond Readvance glaciers in northern Scotland, basin form and the within-valley asymmetry of lateral moraines. *Journal of Quaternary Science*, 4: 243-254.

Benn, D.I. 1992. The genesis and significance of 'hummocky moraine': evidence from the Isle of Skye, Scotland. *Quaternary Science Reviews*, 11: 781-799.

Benn, D.I., Ballantyne, C.K. 1994. Reconstructing the transport history of glacigenic sediments: a new approach based on the covariance of clast-form indices. *Sedimentary Geology*, 91: 215–227.

Benn, D.I., Evans, D.J.A. 1998. *Glaciers and glaciation*. Edward Arnold: London, 734 pp.

Benn, D.I., Evans, D.J.A. in press. *Glaciers and glaciation*. 2nd Edition

Benn, D.I., Wiseman, S., Warren, 2000. C.R. Rapid growth of a supraglacial lake, Ngozumpa Glacier, Khumbu Himal, Nepal. In: Nakawo, M., Raymond, C.F., Fountain, A. (Eds.) *Debris-Covered Glaciers*. IAHS Publication no. 264 pp. 177-186.

Benn, D.I., Kirkbride, M.P., Owen, L.A. and Brazier, V. 2003. Glaciated Valley Landsystems. In: Evans, D.J.A. (Ed.) *Glacial Landsystems*. Arnold: London pp. 372-405.

Benn, D.I., Evans, D.J.A. 2004. *A Practical Guide to the Study of Glacial Sediments*. Arnold:

Bennett, M.R., Glasser, N.F. 1991. The glacial landforms of Glen Geusachan, Cairngorms: a reinterpretation. *Scottish Geographical Magazine*, 107: 116–123.

Bennett, M.R., Boulton, G.S. 1993a. A reinterpretation of Scottish 'hummocky moraine' and its significance for the deglaciation of the Scottish Highlands during the Younger Dryas or Loch Lomond Stadial. *Geological Magazine*, 130: 301-318.

Bennett, M.R., Boulton G.S. 1993b. The deglaciation of the Younger Dryas or Loch Lomond Stadial ice-field in the northern highlands, Scotland. *Journal of Quaternary Science*, 8: 133-146.

Bennett, M.R., Huddart, D., Glasser, N.F.,Hambrey,M.J. 2000. Resedimentation of debris on an ice-cored lateral moraine in the high-Arctic (Kongsvegen, Svalbard). *Geomorphology*, 35: 21–40.

Bennett, M.R. 2001. The morphology, structural evolution and significance of push moraines. *Earth Science Reviews*, 53: 197 - 236.

Bennett M.R., H.M.J., Huddart D., Glasser N.F. 1998. Glacial thrusting and moraine-mound formation in Svalbard and Britain: the example of Coire a' Cheudchnoic (Valley of a Hundred Hills). *Quaternary Proceedings*, 6: 17-34.

Betts, H.D., Trustrum, N.A., De Rose, R.C. 2003. Geomorphic changes in a complex gully system measured from sequential digital elevation models, and implications for management. *Earth Surface Processes and Landforms*, 28: 1043–1058.

Bird, J.B. 1967. *The Physiography of Arctic Canada*. John Hopkins University Press: Baltimore,

Björnsson, H., Pálsson, F. 2008. Icelandic glaciers. *Jökull*, 58: 365-386.

Boulton, G.S. 1967. The development of a complex supraglacial moraine at the margin of Sorbreen, Ny. Friesland, Vestspitsbergen. *Journal of Glaciology*, 6: 717–736.

Boulton, G.S. 1972. Modern Arctic glaciers as depositional models for former ice sheets. *Journal of the Geological Society, London*, 128: 361-393.

Boulton, G.S. 1977. A multiple till sequence formed by a Late Devensian Welsh ice-cap: Glanllynnau, Gwynedd. *Cambria*, 4: 10-31.

Boulton, G.S., Paul, M.A. 1976. The influence of genetic processes on some geotechnical properties of tills. *Journal of Engineering Geology*, 9: 159-194.

Boulton, G.S., Dickson, J.H., Nichols, H., Nichols, M. Short, S.K. 1976. Late Holocene glacier fluctuations and vegetation changes at Maktak Fiord, Baffin Island, N.W.T. Canada. *Arctic and Alpine Research*, 8: 343 - 356.

Boulton, G.S. 1978. Boulder shapes and grain size distributions as indicators of transport paths through a glacier and till genesis. *Sedimentology*, 25: 773– 799.

Boulton, G.S., Eyles, N. 1979. Sedimentation by valley glaciers: a model and genetic classification. In: Schluchter, C. (Ed.) *Moraines and Varves*. Balkema: Rotterdam, pp. 11-23.

Boulton, G.S. 1986. Push moraines and glacier contact fans in marine and terrestrial environments. *Sedimentology*, 33: 677-698.

Bradwell, T., Dugmore, A.J., Sugden, D.E. 2006. The Little Ice Age glacier maximum in Iceland and the North Atlantic Oscillation: evidence from Lambatungnajökull, southeast Iceland. *Boreas*, 35: 61-80.

Brockelband, D.C., Tom, A. 1991. Stereo elevation determination technique for SPOT imagery. *Photogrammetric Engineering and Remote Sensing*, 57: 1065-1073.

Butler, J.B., Lane, S.N. and Chandler, J.H. 1998. Assessment of DEM quality for characterizing surface roughness using close range digital photogrammetry. *Photogrammetric Record*, 16(92): 271-291.

Casely, A.F., Dugmore, A.J. 2004. Climate change and "anomalous" glacier fluctuations: the southwest outlets of Mýrdalsjökull, Iceland. *Boreas*, 33: 108-122.

Cattle, H., and Thomson, J.F. 1993. The Arctic response to CO2-induced warming in a coupled atmosphere-ocean general circulation model. In: Peltier, W.R. (Ed.) *Ice in the Climate System*. Springer-Verlag: Berlin, pp. 579-596.

Chandler, J.H., Brunsden, D. 1995. Steady state behaviour of the Black Ven mudslide: the application of archival analytical photogrammetry to studies of landform change. *Earth Surface Processes and Landforms*, 20: 255-275

Chandler, J.H. 1999. Effective application of automated digital photogrammetry for geomorphological research. *Earth Surface Processes and Landforms*, 24: 51-63.

Chinn, T., Winkler, S., Salinger, MJ and Haakensen, N. 2005. Recent glacier advances in Norway and New Zealand: a comparison of their glaciological and meteorological causes. *Geografiska Annaler*, 87A: 141-157.

Chorley, R.J. 1972. *Spatial Analysis in Geomorphology*. Methuen and Co Ltd: UK, 393pp

Clague, J.J., Evans, S.G. 2000. A review of catastrophic drainage of moraine-dammed lakes in British Columbia. *Quaternary Science Reviews*, 19: 1763–1783.

Clayton, L. 1964. Karst topography on stagnant glaciers. *Journal of Glaciology*, 5: 107–112.

Clayton, L., Moran, S.L. 1974. A glacial process-form model. In: Coates, D.R. (Ed.) *Glacial Geomorphology*. State University of New York: Binghamton, pp. 89-119.

Collin, R.L., Chisholm, N.W.T. 1991. Geomorphological photogrammetry. *Photogrammetric Record*, 13: 845-854.

Cook, S.J., Waller, R.I. and Knight, P.G. 2006. Glaciohydraulic supercooling: the process and its significance. *Progress in Physical Geography*, 30: 577-588.

Cook, S.J., Waller, R.I., Knight, P.G. 2006. Glaciohydraulic supercooling: the process and its significance. *Progress in Physical Geography*, 30: 577–588.

Cooper, M.A.R. 1998. Datums, coordinates and differences. In: S.N. Lane, K.S. Richards and J.H. Chandler (Editors), *Landform Monitoring, Modelling and Analysis*. Wiley, Chichester, pp. 454.

Cooper, M.A.R. and Cross, P.A. 1988. Statistical concepts and their application in photogrammetry and surveying. *Photogrammetric Record*, 12(71): 637-663.

Cox, L.H., March, R.S. 2004. Comparison of geodetic and glaciological mass-balance techniques, Gulkana Glacier, Alaska, U.S.A. *Journal of Glaciology*, 50: 363-370.

Crochet, P., Jóhannesson, T., Jónsson, T., Sigurdsson, O., Björnsson, H., Pálsson, F., Barstad, I. 2007. Estimating the Spatial Distribution of Precipitation in Iceland Using a Linear Model of Orographic Precipitation. *Journal of Hydrometeorology*, 8: 1285-1306.

D'Agata, C.A., Zagutta, A. 2007. Reconstruction of the recent changes of a debris-covered glacier (Brenva Glacier, Mont Blanc Massif, Italy) using indirect sources: Methods, results and validation. *Global and Planetary Change*, 56: 57-68.

Davies, T.R., Smart, C.C. 2007. Obstruction of subglacial conduits by bedload sediment – implications for alpine glacier motion. *Journal of Hydrology (New Zealand)*, 46: 51-62.

De Rose, R.C., Gomez, B., Marden, M., Trustrum, N.A. 1998. Gully erosion in Mangatu Forest, New Zealand, estimated from digital elevation models. *Earth Surface Processes and Landforms*, 23: 1045–1053.

De Ruyter de Wildt, M.S., Klok, E.J., Oerlemans, J. 2002. Reconstruction of the mean specific mass balance of Vatnajökull (Iceland) with a Seasonal Sensitivity Characteristic. *Geografiska Annaler*, 85A: 57-72.

De Ruyter de Wildt, M.S., Oerlemans, J., Björnsson, H. 2003. A calibrated mass balance model for Vatnajökull, Iceland. *Jökull*, 52: 1 - 20.

Deline, P. 2005. Change in surface debris cover on Mont Blanc massif glaciers after the 'Little Ice Age' termination. *The Holocene*, 15: 302-309.

Dixon, L.F.J., Barker, R., Bray, M., Farres, P., Hooke, J., Inkpen, R., Merel, A., Payne, D., Shelford, A. 1998. Analytical photogrammetry for geomorphological research. In: Lane, S.N., Richards, K.S., Chandler, J.H. (Eds.) *Landform Monitoring, Modelling and Analysis*. Wiley: Chichester, pp. 63-94.

Dowdeswell, J.A. 1995. Glaciers in the High Arctic and recent environmental change. *Philosophical Transactions of the Royal Society, London, Series A*, 352: 321-334.

Dowdeswell, J.A., Hagen, J.O., Björnsson, H., Glazovsky, A.F., Harrison, W.D., Holmlund, P., Jania, J., Koerner, R.M., Lefauconnier, B., Ommanney, C.S.L., Thomas, R.H. 1997. The mass balance of circum-Arctic glaciers and recent climate change. *Quaternary Research*, 48: 1-14.

Dyke, A.S., Evans, D.J.A. 2003. Ice-Marginal Terrestrial Landsystems: Northern Laurentide and Innuitian Ice Sheet Margins. In: Evans, D.J.A. (Ed.) *Glacial Landsystems*. Arnold: London, pp. 143 - 163.

Dyurgerov, M.B., Meier, M.F. 1997. Mass balance of mountain and subpolar glaciers: a new global assessment for 1961-1990. *Arctic and Alpine Research*, 29: 379-391.

Etzelmüller, B., Sollid, J.L. 1997. Glacier geomorphometry- an approach for analyzing long-term glacier surface changes using grid-based digital elevation models. *Annals of Glaciology*, 24: 135-141.

Etzelmüller, B. 2000. Quantification of thermo-erosion in pro-glacial areas – examples from Svalbard. *Zeitschrift für Geomorphology*, 44: 343-361.

Etzelmüller, B., Hagen, J. O., Vatne, G., Ødegård, R. Sollid, J. L. 1996. Glacier debris accumulation and sediment deformation influenced by permafrost, examples from Svalbard. . *Annals of Glaciology*, 22: 53-62.

Etzelmüller B., Ø.R.S., Vatne G., Mysterud R.S., Tonning T. & Sollid J.L. 2000. Glacier characteristics and sediment transfer system of Longyearbreen and Larsbreen, western Spitsbergen. *Norsk Geografisk Tidsskrift* 154: 157-168.

Evans, D.J.A., Lemmen, D.S. and Rea, B.R. 1999a. Glacial landsystems of the southwest Laurentide Ice Sheet: modern Icelandic analogues. *Journal of Quaternary Science*, 14: 673-691.

Evans, D.J.A., Archer, S., Wilson, D.J.J. 1999b. A comparison of the lichenometric and Schmidt hammer dating techniques based on data from the proglacial areas of some Icelandic glaciers. *Quaternary Science Reviews*, 18: 13-41.

Evans, D.J.A., Rea, B.R. 1999. Geomorphology and sedimentology of surging glaciers: a landsystems approach. *Annals of Glaciology*, 28: 75-82.

Evans, D.J.A. 1999. Glacial debris transport and moraine deposition: a case study of the Jardalen cirque complex, Sogn-og-Fjordane, western Norway. *Zeitschrift für Geomorphologie*, 43: 203– 234.

Evans, D.J.A., Twigg, D.R. 2002. The active temperate glacial landsystem: a model based on Breiðamerkurjökull and Fjallsjökull, Iceland. *Quaternary Science Reviews*, 21: 2143-2177.

Evans, D.J.A. 2003. *Glacial Landsystems*. Hodder Arnold: London,

Evans, D.J.A., Benn, D.I. 2004. Facies description and the logging of sedimentary exposures. In: Benn, D.I., Evans, D.J.A. (Eds.) *A Practical Guide to the Study of Glacial Sediments*. Arnold, pp. 11-51.

Evans, D.J.A. 2005. The Glacier-marginal landsystems of Iceland. In: Caseldine, C. J., Russel, A.J., Hardardottir, J. & Knudsen, O. (Eds.) *Iceland - Modern Processes and Past Environments.* Elsevier: Amsterdam, pp. 93-126.

Evans, D.J.A., Hiemstra, J.F. 2005. Till deposition by glacier submarginal, incremental thickening. *Earth Surface Processes and Landforms*, 30: 1633–1662.

Evans, D.J.A., Twigg, D.R., Rea, B.R. 2006a. Surging glacier landsystem of Tungnaárjökull, Iceland. Durham University: 1:25000 scale map poster.

Evans, D.J.A., Twigg, D.R., Shand, M. 2006b. Surficial geology and geomorphology of the þórisjökull plateau icefield, west-central Iceland. *Journal of Maps*, 2006: 17-29.

Evans, D.J.A., Twigg, D.R., Rea, B.R., Shand, M. 2007. Surficial geology and geomorphology of the Brúarjökull surging glacier landsystem. *Journal of Maps*, 2007: 349-367.

Evans, D.J.A. 2009. Controlled moraines: origins, characteristics and palaeoglaciological implications *Quaternary Science Reviews*, 28: 183-208

Evenson, E.B., Lawson, D.E., Strasser, J.C., Larson, G.J., Alley, R.B., Ensminger, S.L., Stevenson, W.E. 1999. Field evidence for the recognition of glaciohydraulic supercooling. In: Mickelson, D.M., Attig, J.W. (Eds.) *Glacial Processes Past and Present. Geological Society of America, Special Paper*. Geological Society of America: Boulder, Colorado, pp. 23–35.

Everest, J., Bradwell, T. 2003. Buried glacier ice in southern Iceland and its wider significance. *Geomorphology*, 52: 347-358.

Eyles, N. 1979. Facies of supraglacial sedimentation on Icelandic and Alpine temperate glaciers. *Canadian Journal of Earth Science*, 16: 1341–1361.

Eyles, N. 1983a. Glacial geology: a landsystems approach. In: Eyles, N. (Ed.) *Glacial geology*. Pergamon: Oxford, pp. 1-18.

Eyles, N. 1983b. The glaciated valley landsystem. In: Eyles, N. (Ed.) *Glacial geology*. Pergamon: Oxford, pp. 91-110.

Eyles, N. 1983c. Modern Icelandic glaciers as depositional models for "hummocky moraine" in the Scottish Highlands. In: Evenson, E.B., Schlüchter, C., Rabassa, J. (Eds.) *Tills and Related Deposits*. Balkema: Rotterdam, pp. 47–60.

Findsterwalder, R. 1954. Photogrammetry and glacier research with special reference to glacier retreat in the eastern Alps. *Journal of Glaciology*, 2: 306-315.

Fitzsimons, S.J. 2003. Ice-marginal terrestrial landsystems: polar continental glacier margins. In: Evans., D.J.A. (Ed.) *Glacial Landsystems*. Arnold: London pp. 89-110.

Fox, A.J., Cziferszky, A. 2008. Unlocking the time capsule of historic aerial photography to measure changes in Antarctic Peninsula glaciers. *The Photogrammetric Record*, 23: 51-68.

Gardner, J.S., Hewitt, K. 1990. A surge of Bualtar Glacier, Karakoram Range, Pakistan: a possible landslide trigger. *Journal of Glaciology*, 36: 159–162.

Ghosh, S.K. 1988. *Analytical Photogrammetry*. Pergamon Press: Oxford, 308 pp.

Giles, P.T., Franklin, S.E. 1998. An automated approach to the classification of the slope units using digital data. *Geomorphology*, 21: 251–264.

Giles, P.T. 1998. Geomorphological signatures: classification of aggregated slope unit objects from digital elevation and remote sensing data. *Earth Surface Processes and Landforms*, 23: 581–594.

Glasser, N.F., Hambrey, M.J. 2002. Sedimentary facies and landform genesis at a temperate outlet glacier: Soler Glacier, North Patagonian Icefield. *Sedimentology*, 49: 43–64.

Glasser, N.F., Hambrey, M.J., Etienne, J.L., Jansson, P., Pettersson, R. 2003. The origin and significance of debris-charged ridges at the surface of Storglaciaren, northern Sweden. *Geografiska Annaler*, 85A: 127-147.

Gooch, M.J., Chandler, J.J., Stojic, M. 1999. Accuracy assessment of digital elevation models generated using the Erdas Imagine Orthomax digital photogrammetric system. *The Photogrammetric Record*, 16: 519-531.

Goodsell, B., Hambrey, M.J., Glasser, N.F. 2002. Formation of band ogives and associated structures at Bas Glacier d' Arolla, Valais, Switzerland. *Journal of Glaciology*, 48: 287–300.

Goodsell, B., Hambrey, M.J., Glasser, N.F. 2005. Debris transport in a temperate valley glacier: Haut Glacier d'Arolla, Valais, Switzerland. *Journal of Glaciology*, 51: 139-146.

Gravenor, C.P., Kupsch, W.O. 1959. Ice disintegration features in western Canada. *Journal of Geology*, 67: 48–64.

Grove, J.M. 1988. *The Little Ice Age*. Routledge: London, 498 pp

Guðmundsson, H.J. 1998. *Holocene glacier fluctuations and tephrochronology of the Öræfi district, Iceland.* Unpublished PhD thesis, University of Edinburgh, Scotland.

Guðmundsson, H.J. 2000. Mass balance and precipitation on the summit plateau of Öræfajökull. *Jökull*, 48: 49 - 54.

Guðmundsson S., Björnsson H., Pálsson F., Haraldsson H.H. 2006. Energy balance of Brúarjökull and circumstances leading to the August 2004 floods in the river Jökla, N-Vatnajökull. *Jökull,* 55.

Haeberli, W. 1995. Glacier fluctuations and climate change detection — operational elements of a worldwide monitoring strategy. *World Meteorological Organisation Bulletin*, 44: 23-31.

Haeberli, W. 2006. Integrated perception of glacier changes: a challenge of historical dimensions. In: Knight, P.G. (Ed.) *Glacier Science and Environmental Change*. Blackwell, pp. 423-430.

Hambrey, M.J., Muller, F. 1978. Structures and ice deformation in White Glacier, Axel Heiberg Island, NWT, Canada. *Journal of Glaciology*, 20: 41-67.

Hambrey, M.J., M.R. Bennett, J.A. Dowdeswell, N.F. Glasser and D. Huddart. 1999. Debris entrainment and transfer in polythermal valley glaciers. *Journal of Glaciology*, 45: 69–86.

Hambrey M.J., H.D., Bennett M.R., Glasser N.F. 1997. Genesis of 'hummocky moraine' by thrusting in glacier ice: evidence from Svalbard and Britain. *Journal of the Geological Society, London*, 154: 623-632.

Hanna, E., Jónsson, T., Box, J. E. 2004. An analysis of Icelandic climate since the nineteenth century. *International Journal of Climatology*, 24: 1193 - 1210.

Hart, C.A., 1948. *Air Photography Applied to Surveying*. Longmans, London. 366 pp.

Henry, J.-B., Malet, J.-P., Maquaire, O., Grussenmeyer, P. 2002. The use of small-format and low-altitude aerial photos for the realization of high-resolution DEMs in mountainous areas: application to the Super-Sauze Earthflow (Alpe-De-Haute-Provence, France). *Earth Surface Processes and Landforms*, 27: 1339-1350.

Hewitt, K.J. 1967. Ice-front deposition and the seasonal effect, a Himalayan example. *Transactions of the Institute of British Geographers*, 42: 93 - 106.

Hewitt, K. 1999. Quaternary moraines versus catastrophic rock avalanches in the Karakorum Himalaya, northern Pakistan. *Quaternary Research*, 51: 220-237.

Hewitt, K. 2009. Rock avalanches that travel onto glaciers and related developments, Karakoram Himalaya, Inner Asia. *Geomorphology*, 103: 66–79.

Hooke, R.L., Pohjola, V.A. 1994. Hydrology of a segment of a glacier situated in an overdeepening, Storglaciären, Sweden. *Journal of Glaciology*, 40: 140 - 148.

Houghton, J.T., Meiria Filho, L.G., Callander, B.A., Harris, N., Kattenberg, A., Maskell, K. (Eds.). 1996. *Climate Change 1995: the Science of Climate Change*.

Cambridge University Press (Published for Intergovernmental Panel on Climate Change): Cambridge and New York, 572 pp.

Howarth, P.J. 1968. *Geomorphological and Glaciological Studies, Eastern Breidamerkurjokull, Iceland.* Unpublished PhD Thesis, University of Glasgow.

Howarth, P.J., Price, R.J. 1969. The proglacial lakes of Breiðamerkurjökull and Fjallsjökull, Iceland. *Geographical Journal*, 135: 573-581.

Howarth, P.J., Welch, R. 1969a. Breiðamerkurjökull, South-east Iceland, August 1945. University of Glasgow: 1:30000 map.

Howarth, P.J., Welch, R. 1969b. Breiðamerkurjökull, South-east Iceland, August 1965. University of Glasgow: 1:30000 map.

Humlum, O. 1985. Genesis of an imbricate push moraine, Höfdabrekkujökull, Iceland. *Journal of Geology*, 93: 185 -195.

Hurrell, J.W. 1995. Decadal Trends in the North Atlantic Oscillation: Regional Temperatures and Precipitation. *Science*, 269: 676-679.

Iturrizaga, L. 2008. Post-sedimentary transformation of lateral moraines- the tributary tongue basins of the Kvíárjökull (Iceland). *Journal of Mountain Science*, 5: 1-16.

James, T.D., Murray, T., Barrand, N.E., Barr, S.L. 2006. Extracting photogrammetric ground control from lidar DEMs for change detection. *The Photogrammetric Record*, 21: 312-328.

Jóhannesson, T., C. Raymond, Waddington, E.,. 1989. Time-scale for adjustment of glaciers to changes in mass balance. *Journal of Glaciology*, 35: 355–369.

Jóhannesson, T., Sigurdsson., O. 1998. Interpretation of glacier variations in Iceland 1930-1995. *Jökull*, 45: 27-33.

Johnson, P.G. 1975. Recent crevasse fillings at the terminus of the Donjek Glacier, St. Elias Mountains, Yukon Territory. *Quaestiones Geographicae*, 2: 53-59.

Johnson, M.D., Clayton, L. 2003. Supraglacial landsystems in lowland terrain. In: Evans, D.J.A. (Ed.) *Glacial Landsystems*. Arnold: London, pp. 228–258.

Jordan, E., Ungercchts, L., Caceres, B., Penafiel, A., Francou, B. 2005. Estimation by photogrammetry of the glacier recession on the Cotopaxi Volcano (Ecuador) between 1956 and 1997. *Hydrological Sciences Journal*, 50: 949-961.

Kääb, A. 2002. Monitoring high-mountain terrain deformation from repeated air- and spaceborne optical data: examples using digital aerial imagery and ASTER data. *ISPRS Journal of Photogrammetry & Remote Sensing*, 57: 39-52.

Kasser, M., Egels, Y. 2002. *Digital Photogrammetry*. Taylor and Francis: London, 349 pp.

Kellerer-Pirklbauer, A., Lieb, G.K., Avian, M. and Gspurning, J. 2008. The response of partially debris-covered valley glaciers to climate change: the example of the Pasterze Glacier (Austria) in the period 1964 to 2006. *Geografiska Annaler: Series A, Physical geography*, 90: 269-285.

Kirkbride, M.P. 1993. The temporal significance of transitions from melting to calving termini at glaciers in the central Southern Alps of New Zealand. *The Holocene*, 3: 232-240.

Kirkbride, M.P. 1995. Ice flow vectors on the debris-mantled Tasman Glacier, 1957-1986. *Geografiska Annaler*, 77A: 147-157.

Kirkbride, M., Spedding, N. 1996. The influence of englacial drainage on sediment transport pathways and till texture of temperate valley glaciers. *Annals of Glaciology*, 22: 160–166.

Kirkbride, M.P., Warren, R.C. 1999. Tasman Glacier, New Zealand: 20th-century thinning and predicted calving retreat. *Global and Planetary Change*, 22: 11-28.

Kirkbride, M.P., 2002. Icelandic climate and glacier fluctuations through the terminus of the 'Little Ice Age'. *Polar Geography*, 26: 116-133.

Kirkbride, M.P., Dugmore, A.J. 2008. Two millennia of glacier advances from southern Iceland dated by tephrochronology. *Quaternary Research*, 70: 398–411.

Kjær, K.H., Krüger, J. 2001. The final phase of dead-ice moraine development: processes and sediment architecture, Kötlujökull, Iceland. *Sedimentology*, 48: 935-952.

Knight, P.G. 1989. Stacking of basal debris layers without bulk freezing on: isotopic evidence from west Greenland. *Journal of Glaciology*, 35: 214-216.

Knight, P.G. 1999. *Glaciers*. Stanley Thornes: Cheltenham, 261 pp.

Knudsen, O., Roberts, M.J., Tweed, F.S., Russell, A.J., Lawson, D.E., Larson, G.J., Evenson, E.B., Björnsson, H. 2002. Five 'supercool' Icelandic glaciers. In: Jónsson, S. (Ed.) *25th Nordic Geological Winter Meeting (Abstract volume)*. Reykjavik, Iceland.

Krüger, J. 1985. Formation of a push moraine at the margin of Hofdabrekkujökull, south Iceland. *Geografiska Annaler*, 67A: 199-212.

Krüger, J. 1993. Moraine-ridge formation along a stationary ice front in Iceland. *Boreas*, 22: 101–109.

Krüger, J. 1994. Glacial processes, sediments, landforms, and stratigraphy in the terminus region of Mýrdalsjökull, Iceland. *Folia Geographica Danica*, 21: 1-233.

Krüger, J. 1995. Origin, chronology and climatological significance of annual-moraine ridges at Mýrdalsjökull, Iceland. *The Holocene*, 5: 420–427.

Krüger, J. 1996. Moraine ridges formed from subglacial frozen-on sediment slabs and their differentiation from push moraines. *Boreas*, 25: 57–63.

Krüger, J., Aber, J.S. 1999. Formation of supraglacial sediment accumulations on Kötlujökull, Iceland. *Journal of Glaciology* 45: 400- 402.

Krüger, J., Kjær, K.H. 2000. De-icing progression of ice-cored moraines in a humid, subpolar climate, Kötlujökull, Iceland. *The Holocene*, 10: 737–747.

Lane, S.N., Richards, K.S., and Chandler, J.H. 1993. Developments in photogrammetry; the geomorphological potential. *Progress in Physical Geography*, 17: 306-328.

Lane, S.N., Richards, K.S., and Chandler, J.H. 1998. *Landform Monitoring, Modelling and Analysis*, British Geomorphological Research Group Symposia Series. Wiley: 453 pp.

Lane, S.N., James, T.D. and Crowell, M.D. 2000. Application of digital photogrammetry to complex topography for geomorphological research. *Photogrammetric Record*, 16: 793-821.

Larsen, G. 2000. Holocene eruptions within the Katla volcanic system, South Iceland: Characteristics and environmental impact. *Jökull*, 49: 1-28.

Lawson, D.E., Strasser, J.C., Evenson, E.B., Alley, R.B., Larson, G.J., Arcone, S.A. 1998. Glaciohydraulic supercooling: a freeze-on mechanism to create stratified, debris-rich basal ice. I. Field evidence. *Journal of Glaciology*, 44: 547–562.

Li, Z. 1988. On the measure of digital terrain model accuracy. *Photogrammetric Record*, 12(72): 873-877.

Lichti, D., Pfeifer, N., Maas, H-G. 2007. ISPRS Journal of Photogrammetry and Remote Sensing theme issue "Terrestrial Laser Scanning" (Editorial). *ISPRS Journal of Photogrammetry and Remote Sensing* 63: 1-3.

Lim, M., Petley, D.N., Rosser N.J., Allison, R.J., Long, A.J., Pybus, D. 2005. Combined digital photogrammetry and time of-flight laser monitoring for cliff evolution. *Photogrammetric Record*, 20: 109–129.

Lønne, I., Lauritsen, T. 1996. The architecture of a modern push moraine at Svalbard as inferred from ground penetrating radar measurements. *Arctic and Alpine Research*, 28: 488–495.

Lukas, S. 2003. Scottish Landform Example 31: the moraines around the Pass of Drumochter. *Scottish Geographical Journal*, 119: 383–393.

Lukas, S. 2005. A test of the englacial thrusting hypothesis of 'hummocky' moraine formation - case studies from the north-west Highlands, Scotland. *Boreas* 34: 287-307.

Lukas, S., Nicholson, L.I., Ross, F.H., Humlum, O. 2005. Formation, meltout processes and landscape alteration of high-arctic ice-cored moraines - examples from Nordenskiöld Land, central Spitsbergen. *Polar Geography*, 29: 157-187.

Lukas, S., Nicholson, L.I., Humlum, O. 2007. Comment on Lønne and Lyså (2005):"Deglaciation dynamics following the Little Ice Age on Svalbard: implications for shaping of landscapes at high latitudes". *Geomorphology*, 72: 300-319.

Lyså, A., Lønne, I. 2001. Moraine development at a small High-Arctic valley glacier: Rieperbreen, Svalbard. *Journal of Quaternary Science*, 16: 519-529.

Mackay, D.S., Robinson, V. B. and Band, L. E. 1992. Classification of higher order topographic objects on digital terrain data. *Computers, Environment and Urban Systems*, 16: 473–496.

Mackintosh, A., Dugmore, A. J., Hubbard, A. L. 2002. Holocene climatic changes in Iceland: evidence from modelling glacier length fluctuations at Sólheimajökull. *Quaternary International* 91: 39-52.

Maizels, J.K. 1995. Sediments and landforms of modern proglacial terrestrial environments. In: Menzies, J. (Ed.) *Modern Glacial Environments*. Butterworth-Heinemann: Oxford, pp. 365-416.

Massom, R., Lubin, D. 2006. *Polar Remote Sensing, Volume 2: Ice Sheets*. Springer-Praxis, Chichester, 426 pp.

Matthews, J.A., Petch, J.R. 1982. Within-valley asymmetry and related problems of Neoglacial moraine development at certain Jotunheim glaciers, southern Norway. *Boreas*, 11: 225– 247.

Mattson, L.E., Gardner, J.S., Young, G.J. 1993. Ablation on debris covered glaciers: an example from the Rakhiot Glacier, Punjab, Himalaya. In: Young, G.J. (Ed.) *Snow and Glacier Hydrology. Proceedings of the Kathmandu Symposium, November 1992*. IAHS Publication, pp. 289–296.

McCarroll, D., Harris, C. 1992. The glacigenic deposits of western Lleyn, north Wales: terrestrial or marine? *Journal of Quaternary Science*, 7: 19–29.

Meier, M.F. 1984. Contribution of Small Glaciers to Global Sea Level. *Science* 226: 1418.

Nakawo, M., Rana, B. 1999. Estimate of ablation rate of glacier ice under a supraglacial debris layer. *Geografiska Annaler*, 81A: 695 - 701.

Nakawo, M., Fountain A. and Raymond C. 2000. Debris-covered glaciers. *IAHS Publication* 264:

Näslund, J.-O., Hassinen, S. 1996. Supraglacial sediment accumulations and large englacial water conduits at high elevations in Mýrdalsjökull, Iceland. *Journal of Glaciology*, 42: 190–192.

Nesje, A., Lie, Ø., Dahl, S. O. 2000. Is the North Atlantic Oscillation reflected in Scandinavian glacier mass balance records? *Journal of Quaternary Science*, 15: 587-601.

Nye, J.F. 1965. The frequency response of glaciers. *Journal of Glaciology*, 5: 567-587.

Oerlemans, J., Reichert, B. K. 2000. Relating glacier mass balance to meteorological data by using a seasonal sensitivity characteristic. . *Journal of Glaciology*, 46: 1521–1526.

Oerlemans, J. 2001. *Glaciers and climate change*. Swets and Zeitlinger BV: Lisse, 156 p

Østrem, G. 1959. Ice melting under a thin layer of moraine and the existence of ice cores in moraine ridges. *Geografiska Annaler*, 41: 228–230.

Østrem, G. 1964. Ice-cored moraines in Scandinavia. *Geografiska Annaler*, 46A: 282 - 337.

Paine, A.D.M. 1985. Ergodic reasoning in geomorphology: time for a review of the term? *Progress in Physical Geography*, 9: 1-15.

Pálsson, F., Guðmundsson, S., Björnsson, H. 2007. *The impact of volcanic and geothermal activity on the mass balance of Vatnajökull*. Extended abstract in conference proceedings for The Dynamics and Mass Budget of Arctic Glaciers, Workshop and Glaciodyn (IPY) meeting, 2007, Pontresina, Switzerland, pp. 80-84

Paparoditis, N., Polidori, L. 2002. Overview of digital surface models. In: Kasser, M., Egels., Y. (Eds.) *Digital Photogrammetry*. Taylor and Francis: London, pp. 159-167.

Paterson, W.S.B. 1994. *The physics of glaciers* (Third Edn). Elsevier: Oxford, 480 pp

Paul, M.A. 1983. The supraglacial landsystem. In: Eyles, N. (Ed.) *Glacial Geology*. Pergamon Press: New York, pp. 71-90.

Paul, M.A., Eyles, N. 1990. Constraints on the preservation of diamict facies (melt-out tills) at the margins of stagnant glaciers. *Quaternary Science Reviews*, 9: 51–69.

Payne, A.J., Sugden, D.E. 1990. Topography and ice sheet growth. *Earth Surface Processes and Landforms*, 15: 625-639.

Pickard, J. 1983. Surface lowering of ice-cored moraine by wandering lakes. *Journal of Glaciology*, 29: 338–342.

Pickard, J. 1984. Retreat of ice scarps on an ice-cored moraine, Vestfold Hills, Antarctica. *Zeitschrift für Geomorphologie*, 28: 443–453.

Pike, R. 1992. Machine visualization of synoptic topography by digital image processing. *US Geological Survey Bulletin*, 2016: B1-B12.

Pike, R.J. 1995. Geomorphometry - progress, practice and prospect. *Zeitschrift für Geomorphologie Supplementband*, 101: 221-238.

Pope, A., Murray, T., Luckman, A. 2007. DEM quality assessment for quantification of glacier surface change. *Annals of Glaciology*, 46: 189-194.

Porter, S.C. 2000. Onset of neoglaciation in the Southern Hemisphere. *Journal of Quaternary Science*, 15: 395-408.

Powell, R.D. 1984. Glacimarine processes and inductive lithofacies modelling of ice shelf and tidewater glacier sediments based on Quaternary examples. *Marine Geology*, 57: 1-52.

Powers, M.C. 1953. A new roundness scale for sedimentary particles. *Journal of Sedimentary Petrology*, 23: 117– 119.

Preusser, H. 1976. *The landscapes of Iceland, types and regions*. W. Junk B. V. Publishers: The Hague, The Netherlands, 363 pp.

Price, R.J. 1966. Eskers near the Casement Glacier, Alaska. *Geografiska Annaler*, 48: 111-125.

Price, R.J. 1970. Moraines at Fjallsjökull, Iceland. *Arctic and Alpine Research*, 2: 27-42.

Price, R.J. 1973. *Glacial and Fluvioglacial Landforms*. Oliver and Boyd: Edinburgh,

Price, R.J. 1982. Changes in the proglacial area of Breiðamerkurjökull, southeastern Iceland: 1890-1980. *Jökull*, 32: 29-35.

Racoviteanu, A.E., Manley, W.F, Arnaud, Y, Williams, M.W. 2007. Evaluating digital elevation models for glaciologic applications: An example from Nevado Coropuna, Peruvian Andes. *Global and Planetary Change*, 59: 110-125.

Raper, S.C.B., Wigley, T. M. L., Warrick, R. A. 1996. Global sea-level rise: Past and future. In: Milliman, J.D., Haq, B. U. (Ed.) *Sea-Level Rise and Coastal Subsidence*. Kluwer Academic, pp. 11-46.

Raper, S.C., Braithwaite, R.J. 2009. Glacier volume response time and its links to climate and topography based on a conceptual model of glacier hypsometry. *The Cryosphere Discussions*, 3: 243-275.

Rea, B.R., Evans., D.J.A. 2003. Plateau Icefield Landsystem. In: Evans, D.J.A. (Ed.) *Glacial Landsystems*. Arnold: London, pp. 407-431.

Rentsch, H. 1990. Digital terrain models as a tool for glacier studies. *Journal of Glaciology*, 36: 273-278.

Rippin, D., Willis, I., Arnold, N., Hodson, A., Moore, J., Kohler, J. and Bjørnsson, H. 2003. Changes in geometry and subglacial drainage of Midre Lovénbreen, Svalbard, determined from digital elevation models. *Earth Surface Processes and Landforms*, 28: 273–298.

Rivera, A., Casassa, G., Bamber, J., Kaab, A. 2005. Ice-elevation changes of Glacier Chico, southern Patagonia, using ASTER DEMs, aerial photographs and GPS data. *Journal of Glaciology*, 51: 105-112.

Roberts, M.J., Russell, A.J., Tweed, F.S., Knudsen, Ó. 2000. Controls on englacial sediment deposition during the November 1996 jökulhlaup, Skeiðarárjökull, Iceland. *Earth Surface Processes and Landforms*, 26: 935–952.

Roberts, M.J., Tweed, F.S., Russell, A.J., Knudsen, O., Lawson, D.E., Larson, G.J., Evenson, E.B. and Bjornsson, H. 2002. Glaciohydraulic supercooling in Iceland. *Geology* 30: 439-442.

Roberts, D.H., Yde, J.C., Knudsen, N.T., Long, A.J., Lloyd, J.M. 2009. Ice marginal dynamics during surge activity, Kuannersuit Glacier, Disko Island, West Greenland *Quaternary Science Reviews*, 28: 209–222.

Salinger, M.J., Mullan, A.B. 1999. New Zealand climate: temperature and precipitation variations and their link with atmospheric circulation 1930-1994. *International Journal of Climatology*, 19: 1049-1071.

Scheifer, E., Gilbert, R. 2007. Reconstructing morphometric change in a proglacial landscape using historical aerial photography and automated DEM generation. *Geomorphology*, 88: 167-178.

Schomacker, A., Kruger, J., Kjær, K.H. 2006. Ice-cored drumlins at the surge-type glacier Bruarjokull, Iceland: a transitional-state landform. *Journal of Quaternary Science*, 21: 85-93.

Schomacker, A., and Kjær, K.H. 2007. Origin and de-icing of multiple generations of ice-cored moraines at Brúarjökull, Iceland. *Boreas*, 36: 411 - 425.

Schomacker, A., Kjær, K.H. 2007. Origin and de-icing of multiple generations of ice-cored moraines at Brúarjökull, Iceland. *Boreas*, 36: 411–425.

Schomacker, A. 2008. What controls dead-ice melting under different climate conditions? A discussion. *Earth Science Reviews*, 90: 103-113.

Sharp, M.J. 1984. Annual moraine ridges at Skalafellsjökull, south-east Iceland. *Journal of Glaciology*, 30: 82-93.

Shaw, J. 1977. Till body morphology and structure related to glacier flow. *Boreas*, 6: 189- 201.

Shroder, J.F., Bishop, M.P., Copland, L. and Sloan, V.F. 2000. Debris-covered glaciers and rock glaciers in the Nanga Parbat Himalaya, Pakistan. *Geografiska Annaler*, 82A: 17-31.

Shulmeister, J., Davies, T.R, Evans, D.J.A., Hyatt, O.M. and Tovar, D.S. 2009. Catastrophic landslides, glacier behaviour and moraine formation – A view from an active plate margin. *Quaternary Science Reviews*, 28: 1085-1096.

Sigurdsson, O., Jónsson, T. and Jóhannesson, T. 2007. Relation between glacier-termini variations and summer temperature in Iceland since 1930. *Annals of Glaciology*, 46: 170-176.

Sissons, J.B. 1967. *The Evolution of Scotland's Scenery*. Oliver and Boyd: Edinburgh,

Sissons, J.B. 1974a. A lateglacial ice cap in the central Grampians. *Transactions of the Institute of British Geographers*, 62: 95-114.

Sissons, J.B. 1974b. The Quaternary in Scotland: a review. *Scottish Journal of Geology*, 10: 311–337.

Sissons, J.B. 1977. The Loch Lomond Readvance in the northern mainland of Scotland. In: Gray, J.M., Lowe, J.J. (Ed.) *Studies in the Scottish Lateglacial environment*. Pergamon: Oxford, pp. 44-59

Sissons, J.B. 1979. The Loch Lomond Stadial in the British Isles. *Nature*, 280: 199–203.

Slama, C.C. 1980. *Manual of Photogrammetry* (Fourth Edn). American Society of Photogrammetry, Falls Church, Virginia, 1056 pp

Sletten, K., Lyså, A. and Lønne, I. 2001. Formation and disintegration of a high-arctic ice-cored moraine complex, Scott Turnerbreen, Svalbard. *Boreas*, 30: 272-284.

Smith, M.J., Clark, C.D. 2005. Methods for the visualization of digital elevation models for landform mapping. *Earth Surface Processes and Landforms*, 30: 885-900.

Spedding, N., Evans, D.J.A. 2002. Sediments and landforms at Kvíárjökull, southeast Iceland: a reappraisal of the glaciated valley landsystem. *Sedimentary Geology*, 149: 21–42.

Squires, G.L. 1968. *Practical Physics*. McGraw Hill, London, 224 pp.

Stevenson, A.J., McGarvie, D.W., Smellie, J.L., Gilbert, J.S. 2006. Subglacial and ice-contact volcanism at the Öræfajökull stratovolcano, Iceland. *Bulletin of Volcanology*, 68: 737-752.

Strasser, J.C., Lawson, D.E., Larson, G.J., Evenson, E.B., Alley, R.B. 1996. Preliminary results of tritium analyses in basal ice, Matanuska Glacier, Alaska, USA: evidence for subglacial ice accretion. *Annals of Glaciology*, 22: 126– 133.

Sturm, M., Hall, D.K., Benson, C.S., Field, W.O. 1991. Non-climatic control of glacier-terminus fluctuations in the Wrangell and Chugach Mountains, Alaska, U.S.A. *Journal of Glaciology*, 37: 348-356.

Swift, D.A., Evans, D.J.A., Fallick, A.E. 2006. Transverse englacial debris-rich ice bands at Kvíárjökull, southeast Iceland. *Quaternary Science Reviews*, 25: 1708-1718.

Takeuchi, Y., Kayastha, R.B. and Nakawo, M. 2000. Characteristics of ablation and heat balance in debris-free and debris-covered areas of Khumbu Glacier, Nepal Himalayas, in the pre-monsoon season. In: Nakawo, M., Raymond, C. and Fountain, A. (Eds.) *Debris-Covered Glaciers. IAHS Publication 264*, pp. 53–61.

Taschner, S., Ranzi, R. 2002. Landsat-TM and ASTER data for monitoring a debris covered glacier in the Italian Alps with the GLIMS project. *Proceedings of the International Geoscience and Remote Sensing Symposium*, 4: 1044-1046.

Thomas, G.S.P., Connaughton, M., Dackombe, R.V. 1985. Facies variation in a late Pleistocene supraglacial outwash sandur from the Isle of Man. *Geological Journal*, 20: 193–213.

Thomas, R., Rignot, E., Casassa, G., Kanagaratnam, P., Acuna, C., Akins, T., Brecher, H., Frederick, E., Gogineni, P., Krabill, W., Manizade, S., Ramamoorthy, H., Rivera, A., Russell, R., Sonntag, J., Swift, R., Yungel, J., Zwally, J. 2004. Accelerated sea-level rise from West Antarctica. *Science*, 306: 255-258.

Thomson, M.H., Kirkbride, M.P. and Brock, B.W. 2000. Twentieth-century surface elevation change of the Miage Glacier, Italian Alps. In: Nakawo, M., Raymond, C. and Fountain, A. (Eds.) *Debris-Covered Glaciers. IAHS Publication 264*, pp. 219–225.

Thórarinsson, S. 1956. On the variations of Svínafellsjökull, Skaftafellsjökull and Kvíárjökull in Öræfi (Ágrip). *Jökull*, 6: 1-15.

Thórarinsson, S. 1958. The Öræfajökull eruption of 1362. *Acta Naturalia Islandica*, 2: 5-99.

Todtmann, E. 1960. *Gletscherforschungen auf Island (Vatnajökull)*. Cram, de Gruyter &Co.: 95 pp.

Van Asselen, S., Seijmonsbergen, A.C. 2006. Expert-driven semi-automated geomorphological mapping for a mountainous area using a laser DTM. *Geomorphology*, 78: 309-320.

Waller, R.I., Tuckwell, G.W. 2005. Glacier–permafrost interactions and glaciotectonic landform generation at the margin of the Leverett Glacier, West Greenland. In: Harris, C., Murton, J.B (Eds.) *Cryospheric Systems: Glaciers and Permafrost*. Geological Society, Special Publications: London, pp. 39–50.

Washington, W.M., and Meehl, G.A. 1989. Climate sensitivity due to increased CO2: Experiments with a coupled atmosphere and ocean general circulation model. *Climate Dynamics*, 4: 1-38.

Watanabe, T., Ives, J.D., Hammond, J.E., 1994. Rapid growth of a glacial lake in Khumbu Himal, Himalaya: prospects for a catastrophic flood. *Mountain Research Development*, 14: 329-340

Watson, R.A. 1980. Landform development on moraines of the Klutan Glacier, Yukon Territory, Canada. *Quaternary Research*, 14: 50-59.

Winkler, S., Haakensen, N., Nesje, A., Rye, N. 1997. Glaziale Dynamik in Westnorwegen – Ablauf und Ursachen des aktuellen Gletschervorstoßes am Jostedalsbreen. *Petermanns Geographische Mitteilungen*, 141: 43-63.

Wise, S.M. 1998. The effects of GIS interpolation errors on the use of digital elevation models in geomorphology. In: S.N. Lane, K.S. Richards and J.H. Chandler (Editors), *Landform Monitoring, Modelling and Analysis*. Wiley, Chichester, pp. 139-164.

Wolf, P.R. 1983. *Elements of Photogrammetry* (Second Edn). McGraw-Hill: Singapore.

Wolf, P.R., Dewitt, B.A. 2000. *Elements of Photogrammetry with Applications in GIS*. McGraw-Hill: New York, 608 pp.

Wright, H.E. 1980. Surge moraines of the Klutan Glacier, Yukon Territory, Canada: origin, wastage, vegetation, succession, lake development, and application to the Late Glacial of Minnesota. *Quaternary Research*, 14: 2-17.

Yde, J.C., Knudsen, N.T., Larsen, N.K., Kronborg, C., Nielsen, O.B., Heinemeier, J., Olsen, J. 2005. The presence of thrust-block naled after a major surge event: Kuannersuit Glacier, West Greenland. *Annals of Glaciology*, 42: 145–150.

Zwally, H.J., Giovinetto, M.B., Li, J., Cornejo, H.G., Beckley, M.A., Brenner, A.C., Saba, J.L., Yi, D.H. 2005. Mass changes of the Greenland and Antarctic ice sheets and shelves and contributions to sea-level rise: 1992–2002. *Journal of Glaciology*, 51: 509-527.